

**BULETINUL
INSTITUTULUI
POLITEHNIC
DIN IASI**

Publicat de

UNIVERSITATEA TEHNICĂ "GH. ASACHI", IAȘI

Tomul LII (LVI)

Fasc. 2

Secția

ȘTIINȚA ȘI INGINERIA MATERIALELOR

2006

MATERIALS SCIENCE AND ENGINEERING

CONTENT	
VOICU, M., WELCOME ADRESS	I
ZAHARIA, L., COMĂNECI, R., CHELARU, R., CHICHIRĂU, M., THE STUDY OF FLOW AND THE EVALUATION OF STRAIN BY EQUAL CHANNEL ANGULAR PRESSING	1
VIDA-SIMITI, I., JUMĂTATE, N., HARD LAYERS OBTAINED BY COATING WITH NICKEL BASE SUPERALLOYS	7
PRISACARIU, C., SCORTANU, E., PRISACARIU, VA., CHARACTERIZATION OF SOME POLYURETHANE ELASTOMERS WITH 1,4-BUTANEDIOL CHAIN EXTENDER AND DIBENZYL DERIVATIVES	13
PREDESCU, C., CALEA, GG, NICOLAE, A., SOCIAL ENGINEERING - A NEW INSTRUMENT FOR ENGINEERS TO MAKE OPERATIONAL THE CONCEPT OF SUSTAINABLE DEVELOPMENT	19
PRISACARIU, C., SCORTANU, E., MODIFICATIONS INDUCED BY STATIC TENSILE TESTINGS IN THERMOPLASTIC POLYURETHANIC FILMS	23
NICOLAE, M., SOHACIU, M., PARPALA, D., NICOLAE, A., FOREVER YOUNG AND GREEN, STEEL WILL BE IN THE FUTURE A SUSTAINABLE MATERIAL	27
NEJNERU, C., , BERNEVIG, M., CARABET, R., HOPULELE, I., STUDIES ABOUT THE COOLING CHARACTERISTICS OF THE POWDER BACKING IN FLUIDIZED BED TIP SALT, FERRO-MANGANESE PARTICLES, CAST-IRON SPLINTERS BARBOTAGED WITH AIR	31
GEAMĂN, V., JIMAN, V., WORKED EXAMPLES IN THE FIELD OF HOT ISOSTATIC PRESSING	37
CIOBANU, I., MUNTEANU, S.I., CRISAN, A., RESEARCHES CONCERNING THE ANALYSIS OF CASTING SOLIDIFICATION USING THE REAL SOLIDIFICATION MODULE	41
NEJNERU, C., ACHIȚEI, D., CARABET, R., CIMPOEȘU, N., HOPULELE, I., STUDIES ABOUT THE SIZE OF PRECIPITATES IN PARTIAL SOLUTION QUENCHING OF SOME ALUMINUM ALLOYS	47
BACIU, M., ALEXANDRU, I., BACIU, C., ALEXANDRU, A., IMPLICATIONS OF THE THERMAL AND THERMO-CHEMICAL TREATMENTS IN ELECTROLYTIC PLASMA IN THE PHYSICAL STRUCTURE OF THE STEELS OLC15 AND 21MoMnCr12	53
VARGA, B., FINISHING OF THE STRUCTURE OF SILUMINS BY MEANS OF RAPID COOLING	61
BRABIE, G., ALBUT, A., SIMULATION OF THE RESIDUAL STRESS DISTRIBUTION IN THE CASE OF DRAW PARTS MADE FROM HOMOGENEOUS AND HETEROGENEOUS METAL SHEETS	69

CÂNDEA, V. , LĂPUȘAN, S., POPA, A., ZLATE, I., CHENDE, R., ASPECTS CONCERNING THE PRESSING AND REPRESSING BEHAVIOUR OF A NI-BASE SUPERALLOY	75
CIUCESCU, E.P., CIUCESCU, D., A METHOD TO DETERMINE THE DISTRIBUTION OF TEMPERATURE IN CUTTING TOOLS OF GIVEN CONFIGURATION	81
ANTON, A.D., SLĂTINEANU, L., ONOFREI, R., CALCULATIONAL MODEL OF ENERGETIC BALANCE-SHEETS IN THE CASE OF PROCESSING THROUGH ELECTRIC EROSION	87
DIMA, A., MINEA, AA., SUSTAINABLE INDUSTRIAL DEVELOPMENT, THE ONLY WAY FOR EUROPEAN INTEGRATION OF ROMANIA	91
BURCEA, C.O., MINEA, A.A., DIMA, M I, IBN OMER MOHAMED ABDALLA MOHAMED ABUGUSSAISSA, ASPECTS REGARDING MICRO ALIED STEELS BEHAVIOR AT HOT FORGING	95
DIMA, A., MINEA, A.A., DIMA, MI., IBN OMER MOHAMED ABDALLA MOHAMED ABUGUSSAISSA, MATERIALS SCIENCE AND ENGINEERING, AN IMPORTANT AREA OF A SUSTAINABLE DEVELOPMENT	99
PITICESCU , RR., TECHNOLOGY TRANSFER IN ADVANCED MATERIALS IN ROMANIA: A KEY ISSUE FOR SUSTAINABLE DEVELOPMENT	103
TIMOFTE, N., NICOLAU, B., THE STUDY OF SANDS FROM THE REGION VĂLENI THE VALLEY FÂNTÂNELE (HUȘI)	109
PITICESCU, R. M., PITICESCU, R.R., VASILE, E., HYDROTHERMAL PROCEDURES: A NEW METHOD IN THE ENVIRONMENTAL DEVELOPMENT OF NANOMATERIALS	117
SPOREA,I., MANDEK,FR., BORDEASU,I., STOICAN, I., SPOREA,M., STUDIES REFFERING TO THE EFFECT OF THERMIC TREATMENT, OF CLASSIFICATION THROUGH THE PRECIPITATION OF ALUMINIUM ALLOYS THAT ARE CAST IN THE PISTONS OF TERMIC MOTORS	125
SUSAN, M., ILIESCU, V., DUMITRAȘ, P., CHANGES OF THE MECHANICAL CHARACTERISTICS OF HIGH RESISTANCE WIRES DRAWN IN ULTRASONIC FIELD	131
OMER MOHAMED ABBALLA MOHAMED, DIMA, A., CONSIDERATIONS CONCERNING THE METAL-PLUG CONTACT FRICTION AT THE PIPES DRAWING WITH ULTRASONIC VIBRATIONS	137
ONOFREI, RI., NEGURA, C., CONSIDERATION CONCERNING THE OUTPUT PARAMETERS OF THE CO₂ LASER	143
ALEXANDRU, M., BADARAU, G., RUSU, L., MIRON, V., MANEA, R., MODERNISATION TRENDS IN THE COLD ROLLING AND CONSIDERATIONS CONCERNING THE DETERMINATION OF THE OPTIMUM COLD ROLLING FORCE	151
DIA, V., ALEXANDRU, M., COJOCARA, M., HINCU, D., BADARAU, G., IDENTIFICATION AND MEASUREMENT OF QUALITY PARAMETERS FROM RESIDUAL WATER, WHO ARE SPECIFIED TO TECHNOLOGICAL PROCESS OF THERMAL ZINC PLATING, FOR SOLVE BY EFFICIENCY WAY, THE CHEMICAL (SEWAGE) TREATMENT PROCESS, WITH STRAIGHT IMPLICATION TO THE ENVIRONMENT.	155
MIRON, V., HINCU, D., ALEXANDRU, C., DIA, V., COJOCARU, M., RESEARCHES ABOUT THE SUSTAINABLE DEVELOPMENT AND HOT – DIP GALVANIZING	163

MNERIE, D., ANGHEL, GV., SOME ADVANCED MATERIALS AND TECHNOLOGIES FOR ELECTRONICS	171
ALEXANDRU, I., ALEXANDRU, A., IACOB STRUGARIU, S., BACIU, M., THE STUDY OF DEGRADATION THROUGH AGEING OF THE THERMORESISTENT STEELS 13CRMO4-5 USED IN THE TUBULATURE OF THE LIVE STEAM IN THERMO-ELECTRIC POWER STATIONS	179
ALEXANDRU, A., IACOB STRUGARU, S., ALEXANDRU, I., GHEORGHIAN, M., THE EFFECT OF COOLING BELOW 0°C ON STRUCTURE AND HARDNESS OF BEARING STEELS	185
BACIU, C., ALEXANDRU, I., GEORGESCU, S., DÉVELOPPEMENT DURABLE DES SYSTÈMES DE PRODUCTION. L'INTÉGRATION DE L'ERGONOMIE ET DE LA PREVENTION DANS UN PROJET DE CONCEPTION D'UNE ALUMINERIE	191
BRABIE, G., CHIRITA, B., CHIRILA, C., APPLICATION OF THE RULE OF MIXTURE, PARALLEL TENSILE TEST AND IMAGE ANALYSIS METHOD FOR DETERMINATION OF THE WELD METAL PROPERTIES IN THE CASE OF TAILOR WELDED BLANKS	197
CORĂBIERU, A., ALEXANDRU, I., VELICU, S., CORĂBIERU, P., VRABIE, I., BUTNARU, S., SUPERFICIAL HARDENING OF TOOLS THROUGH SUCCESSIVE ALLOYING	203
CORĂBIERU, P., PREDESCU, C., CORĂBIERU, A., BUTNARU, S., EXPERIMENTS REGARDING THE CASTING OF BIMETALLIC CYLINDERS WITH SMOOTH BARREL ROLL	211
DRUGESCU, E., BALINT, L., BALINT, S., CO-FeTi COMPOSITE MATERIAL WITH SOFT MAGNETIC PROPERTIES	217
MIHAI, D., STEFAN, M., BADARAU, G., THE CREEP BEHAVIOUR AT 500°C FOR THE STEEL 41MoCr11	225
VIZUREANU, P., EXPERIMENTAL PROGRAMMING IN MATERIALS SCIENCE	239
PAPADATU, CP., SOME ASPECTS REGARDING THE INFLUENCE OF THE THERMOMAGNETIC TREATMENTS ON THE HARDNESS NUMBER OF STEELS AND THE SUPERFICIAL LAYERS NITRIDED EVOLUTION DURING WEAR PROCESS	243

ȘTIINȚA ȘI INGINERIA MATERIALELOR

CUPRINS	
VOICU, M., CUVANT DE DESCHIDERE	I
ZAHARIA, L., COMĂNECI, R., CHELARU, R., CHICHIRĂU, M., STUDIUL CURGERII ȘI EVALUAREA DEFORMĂRII LA PRESAREA UNGHIULARĂ ÎN CANALE EGALE	1
VIDA-SIMITI, I., JUMĂTATE, N., STRATURI DURE OBTINUTE PRIN ACOPERIRE CU SUPEALIAJE PE BAZĂ DE NICHEL	7
PRISACARIU, C., SCORTANU, E., PRISACARIU, VA., CARACTERIZAREA UNOR ELASTOMERI POLIURETANICI PE BAZĂ DE ALUNGITORUL DE LANȚ 1,4 - BUTANDIOL ȘI DERIVAȚI DIBENZILICI	13
PREDESCU, C., CALEA, GG, NICOLAE, A., "INGINERIA SOCIALĂ-NOU INSTRUMENT DE OPERAȚIONALIZARE DE CĂTRE INGINERIA CONCEPTULUI DE DEZVOLTARE DURABILĂ"	19
PRISACARIU, C., SCORTANU, E., MODIFICĂRI INDUSE DE SOLICITĂRI DE ÎNTINDERE STATICĂ ÎN FILME POLIURETANICE TERMOPLASTE	23
NICOLAE, M., SOHACIU, M., PARPALA, D., NICOLAE, A., "ÎNTOTDEAUNA TÂNĂR ȘI VERDE, OȚELUL VA FI ÎN VIITOR UN MATERIAL DURABIL."	27
NEJNERU, C., BERNEVIG, M., CARABET, R., HOPULELE, I., STUDII PRIVIND CARACTERISTICILE DE RĂCIRE ÎN PAT FLUIDIZAT A MEDIILOR PULVERULENTE TIP SARE, FEROMANGAN, SPAN DE FONTA BARBOTAT CU AER	31
GEAMĂN, V., JIMAN, V., APLICAȚII PRACTICE CU EXEMPLIFICĂRI ÎN DOMENIUL COMPACTĂRII IZOSTATICE LA CALD	37
CIOBANU, I., MUNTEANU, S.I., CRISAN, A., CERCETĂRI PRIVIND ANALIZA SOLIDIFICĂRII PIESELOR TURNATE PRIN METODA MODULULUI DE SOLIDIFICARE REAL	41
NEJNERU, C., ACHIȚEI, D., CARABET, R., CIMPOEȘU, N., HOPULELE, I., STUDII PRIVIND MARIMEA PRECIPITATELOR LA CALIREA DE PUNERE IN SOLUTIE PARTIALA A UNOR ALIAJE PE BAZA DE ALUMINIU	47
BACIU, M., ALEXANDRU, I., BACIU, C., ALEXANDRU, A., IMPLICAȚIILE TRATAMENTELOR TERMICE ȘI TERMOCHIMICE ÎN PLASMĂ ELECTROLITICĂ ASUPRA COMPOZIȚIEI FAZICE A OȚELURILOR OLC15 ȘI 21 MOMNCR12	53
VARGA, B., FINISAREA STRUCTURII SILUMINURILOR PRIN APLICAREA UNOR VITEZE MARI DE RĂCIRE	61
BRABIE, G., ALBUT, A., SIMULAREA DISTRIBUTIEI TENSIUNILOR REZIDUALE IN CAZUL PIESELOR REALIZATE DIN TABLE METALICE OMOGENE SI ETEROGENE	69

CÂNDEA, V. , LĂPUȘAN, S., POPA, A., ZLATE, I., CHENDE, R., ASPECTE PRIVIND COMPORTAREA LA PRESARE SI REPRESARE A UNUI SUPERALIAJ CU BAZA Ni	75
CIUCESCU, E.P., CIUCESCU, D., O METODĂ PENTRU DETERMINAREA DISTRIBUȚIEI TEMPERATURII ÎN SCULELE AȘCHIETOARE DE CONFIGURAȚIE DATĂ	81
ANTON, A.D., SLĂTINEANU, L., ONOFREI, R., MODEL DE CALCUL AL BILANȚULUI ENERGETIC ÎN CAZUL PRELUCRĂRII PRIN EROZIUNE ELECTRICĂ	87
DIMA, A., MINEA, AA., DEZVOLTAREA INDUSTRIALA DURABILA, SINGURA SANSA A ROMANIEI IN CONTEXTUL INTEGRARII EUROPENE	91
BURCEA, C.O., MINEA, A.A., DIMA, M I, IBN OMER MOHAMED ABDALLA MOHAMED ABUGUSSAISSA, ASPECTE PRIVIND COMPORTAREA LA DEFORMARE PLASTICA LA CALD A UNOR OTELURI MICROALIAATE CU VANADIU	95
DIMA, A., MINEA, A.A., DIMA, MI., IBN OMER MOHAMED ABDALLA MOHAMED ABUGUSSAISSA, STIINTA SI INGINERIA MATERIALELOR, DOMENIU DEFINITORIU AL UNEI DEZVOLTARI DURABILE	99
PITICESCU , RR., TRANSFERUL TECHNOLOGIC IN DOMENIUL MATERIALELOR ADVANSATE IN ROMANIA: UN DOMENIU KEY CHEIE PENTRU DEZVOLTAREA DURABILA	103
TIMOFTE, N., NICOLAU, B., STUDIUL NISIPULUI DIN ZONA VĂLENI VALEA FÂNTÂNELE (HUȘI)	109
PITICESCU, R. M., PITICESCU, R.R., VASILE, E., PROCEDEELE HIDROTHERMALE: METODE NOI ECOLOGICE IN DEZVOLTAREA NANOMATERIALELOR	117
SPOREA,I., MANDEK,FR., BORDEASU,I., STOICAN, I., SPOREA,M., STUDII REFERITOARE LA EFECTUL TRATAMENTULUI TERMIC AL CLASIFICARII PRECIPITARII COMPLETE A ALIAJELOR DE AL TURNATE IN PISTOANELE MOTOARELOR TERMICE	125
SUSAN, M., ILIESCU, V., DUMITRAȘ, P., MODIFICARI ALE CARACTERISTICILOR MECANICE PENTRU SARME DE INALTA REZISTENTA TREFILATE IN CAMP ULTRASONOR	131
OMER MOHAMED ABBALLA MOHAMED, DIMA, A., CONSIDERATII PRIVIND FRECARA DE CONTACT METAL-DOP LA TRAGEREA TEVILOR CU VIBRATII ULTRASONICE	137
ONOFREI, RI., NEGURA, C., CERCETĂRI PRIVIND EVALUAREA UNOR PARAMETRI DE IEȘIRE AI LASERULUI CU CO₂	143
ALEXANDRU, M., BADARAU, G., RUSU, L., MIRON, V., MANEA, R., TENDINTE DE MODERNIZARE IN LAMINAREA LA RECE SI CONSIDERATII PRIVIND DETERMINAREA OPTIMA A FORTEI DE LAMINARE	151
DIA, V., ALEXANDRU, M., COJOCARA, M., HINCUI, D., BADARAU, G., IDENTIFICAREA SI MĂSURAREA PARAMETRILOR DE CALITATE DIN APELE UZATE, SPECIFICE PROCESULUI TEHNOLOGIC DE ZINCARE TERMICĂ A ȚEVILOR, ÎN VEDEREA SOLUȚIONĂRII EFICIENȚEI PROCESULUI DE EPURARE A APELOR UZATE, CU IMPLICAȚII DIRECTE ASUPRA PROTECȚIEI MEDIULUI INCONJURĂTOR	155
MIRON, V., HINCUI, D., ALEXANDRU, C., DIA, V., COJOCARU, M., CERCETARI DESPRE DEZVOLTAREA DURABILA SI DESPRE GALVANIZAREA PATRUNSA	163

MNERIE, D., ANGHEL, GV., CATEVA MATERIALE SI TEHNOLOGII AVANSATE DESTINATE ELECTRONICII	171
ALEXANDRU, I., ALEXANDRU, A., IACOB STRUGARIU, S., BACIU, M., STUDIUL DEGRADARII PRIN IMBATRANIRE A OTELULUI TERMOREZISTENT 13CRMO4-5 FOLOSIT IN TUBULATURA DE ABUR VIU A TERMOCENTRALELOR ELECTRICE	179
ALEXANDRU, A., IACOB STRUGARU, S., ALEXANDRU, I., GHEORGHIAN, M., EFECTUL RACIRII LA TEMPERATURI SUB 0°C ASUPRA STRUCTURII SI DURITATII OTELURILOR PENTRU RULMENTI	185
BACIU, C., ALEXANDRU, I., GEORGESCU, S., DEZVOLTAREA DURABILĂ A SISTEMELOR DE PRODUCȚIE. INTEGRAREA ERGONOMIEI ȘI PREVENȚIEI ÎN CADRUL UNUI PROIECT DE CONCEPȚIE A UNEI TURNĂTORII DE ALUMINIU	191
BRABIE, G., CHIRITA, B., CHIRILA, C., APLICATII ALE METODELOR DE ANALIZA A IMAGINILOR, MIXTURII SI TENSIUNILOR PARALELE IN DETERMINAREA PROPRIETATILOR METALELOR SUDATE, IN CAZUL ARBORILOR	197
CORĂBIERU, A., ALEXANDRU, I., VELICU, S., CORĂBIERU, P., VRABIE, I., BUTNARU, S., SUPERFICIAL HARDENING OF TOOLS THROUGH SUCCESSIVE ALLOYING	203
CORĂBIERU, P., PREDESCU, C., CORĂBIERU, A., BUTNARU, S., EXPERIMENTS REGARDING THE CASTING OF BIMETALLIC CYLINDERS WITH SMOOTH BARREL ROLL	211
DRUGESCU, E., BALINT, L., BALINT, S., COMPOZIT DE CO-FETI CU PROPRIETĂȚI MAGNETICE MOI	217
MIHAI, D., STEFAN, M., BADARAU, G., COMPORTAREA LA FLUAJ LA 500 °C A OTELULUI 41MOCR11	225
VIZUREANU, P., PROGRAMAREA EXPERIMENTULUI ÎN ȘTIINȚA MATERIALELOR	239
PAPADATU, CP., ASPECTE PRIVIND INFLUENTA TRATAMENTELOR TERMOMAGNETICE ASUPRA DURITATII OTELURILOR SI EVOLUTIA STRATURILOR SUPERFICIALE NITRURATE, IN TIMPUL FUNCTIONARII	243

THE STUDY OF FLOW AND THE EVALUATION OF STRAIN BY EQUAL CHANNEL ANGULAR PRESSING

BY

LUCHIAN ZAHARIA*, RADU COMĂNECI*, ROMEO CHELARU*, MIHAI CHICHIRĂU**

ABSTRACT: Severe Plastic Deformation (SPD) has been recently used in order to produce nanometric granulations, required for superplastic deformation. Nanostructural materials by severe plastic deformation can be produced by several processes, such as: Equal Channel Angular Pressing (ECAP), Cycling Upsetting in Channel Die (CUCD), Accumulative Roll-Bonding (ARB), High Pressure Torsion (HPT) etc. This paper presents the analysis of flow and evaluation of deformation in the case of ECAP. For the study of flow the rectangular grid method was used and for evaluation of deformation the engineering and true strain method was applied. A geometrical relation for evaluation of deformation was determined and the theoretical results were compared with the experimental ones.

KEYWORDS: severe plastic deformation, ECAP device, rectangular grid method, engineering strain, true strain

1. Considerations regarding severe plastic deformation

Equal Channel Angular Pressing (ECAP) is a method of Severe Plastic Deformation (SPD) of metallic materials. The notion of SPD is used to define the type of plastic deformation in which severe sliding of atomic planes occurs, that leads to strains over the limit attained with classical processes.

Usually, SPD is obtained by cyclical processes, after which high accumulative strains result, in order to produce very fine granulations, within the nanometric range, required for the superplastic state [1]. The idea of SPD appeared as an alternative to industrial plastic deformation processes (rolling, extrusion, drawing) and to classical methods of achieving microstructural superplasticity (thermomechanical treatments combined with dynamic recrystallisation, controlled diffusion and precipitation of secondary phases, sudden cooling followed by ageing at low temperatures, etc.). Through these methods microgranular structures can be obtained, with grain sizes up to 1-2 μm [2]. It has been observed that by decreasing the grain size in the nanometric range, normal metallic materials can be superplastically deformed [3], and the strain can be increased to acceptable values for competitive industrial production. That is why the interest in these techniques that lead to decreasing the grain size beyond the micrometric range has recently been raising. Innovative concepts have been used to

obtain nanometric grain sizes, materialised in new deformation methods and devices. According to these concepts, several methods of SPD through which the grain size can be brought in the $1\mu\text{m} - 100\text{ nm}$ range imposed themselves. Thus, the so called nanostructural materials have been realised. Among the SPD methods, the most common are [4, 5]:

- **Equal Channel Angular Pressing (ECAP)**. This method resembles the working scheme of lateral extrusion, the only difference being that the dimension of the exit (lateral) section is equal to the dimension of the main channel section (where the punch works). The shape of the cross section of the channels can be square or circle. When the sample is passed from one channel to the other a shearing in the entire cross section takes place. The area of the cross section after deformation remains the same, which allows the sample to be reintroduced in the main channel for a new deformation. The effect on deformation of the repeated passes is cumulative, which leads to very high strains (severe plastic deformation).
- **Accumulative Roll-Bonding (ARB)** implies the simultaneous deformation of several layers of sheet, using 50% reduction. Initially there are two sheets of the same dimension, which are overlapped and then rolled with 50% reduction. The resulted sheet is cut in two halves (in length), which are overlapped again to form the initial thickness and then re-rolled with 50% reduction etc. Due to the repetitive cycle the number of layers increases exponentially while the thickness of each layer decreases exponentially. After 10 passes the number of layers reaches 1024. If the initial thickness of the sheet before rolling was several mm (1-2 mm), nanometric thicknesses of the sheet layers can be obtained after rolling.
- **Cycling Upsetting in Channel Die (CUCD)**. Using this method the rectangle-shaped sample (usually squared) is upset in a channel made in a die, having the length equal to the height of the sample. As the lateral walls of the channel prevent the flow of the material, the conditions of a plane state of strain are obtained, while the state of stress is of triaxial compression and, as a consequence, the possibility of cracking is reduced. After upsetting, the resulted sample has the length dimensions of the channel so that, after rotating with 90° the length becomes height for a new upsetting. The described procedure is repeated several times, so that very high strains are reached, which reduces the grain size to nanometric dimensions.
- **High Pressure Torsion (HPT)** is a continuous process of SPD that consists of shearing by torsion of the material situated in between two tools – a fixed one and a rotating one. The torque, which produces the torsion in the material, is created by the friction forces in the contact area between sample and tools. A force is applied on one of the tools, so that a hydrostatic pressure is induced in the material. Thus an excessive reorientation of the grains is produced, which leads to their crushing.

2. Experimental procedure

The schematic layout of the device used for the study of flow of the material, in the case of equal channel angular pressing, is shown in Figure 1. The channel from the die had a squared cross section with a length of 10 mm and the inclination angle between the two channels was 120° .

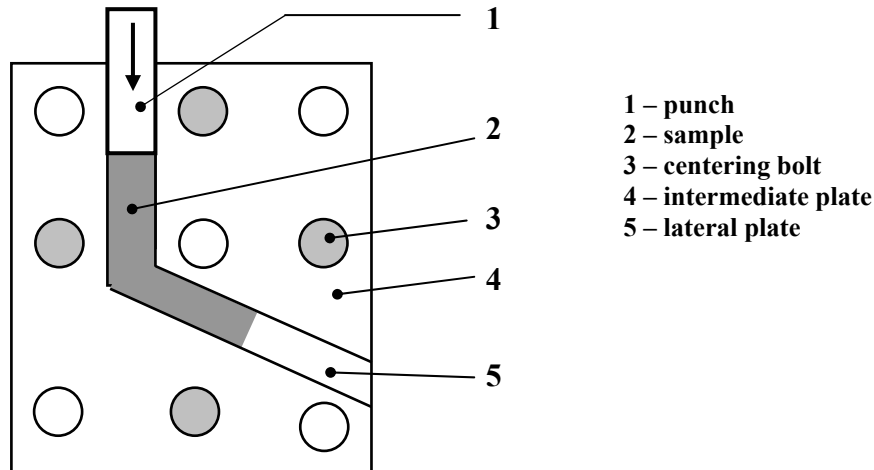


Fig.1: Schematic layout of the device for equal channel angular pressing

Two lead samples were used for the experiments, with initial dimensions of $5 \times 10 \times 50$ mm. One of the samples was marked with 5 mm apart perpendicular lines on the longitudinal axis. This sample was scanned and its image is shown in Figure 2. The two samples were overlapped in order to obtain a sample with the dimensions $10 \times 10 \times 50$ mm and then introduced in the channel of the die where they were pressed and deformed by shearing. The deformation was realised by multiple passes, without the rotation of the sample, repositioning the sample in the channel as at the first pass.

The evaluation of deformation can be made using the engineering (relative) and true(logarithmic) strain.

One of the easiest ways of representing the severity of deformation during ECAP is using the relative area ratio:

$$\varepsilon_A = \frac{A_0 - A_f}{A_0}$$

$$\varepsilon_A \% = \frac{A_0 - A_f}{A_0} \times 100 = \left(1 - \frac{A_f}{A_0}\right) \times 100 \quad (1)$$

where: A_0 - area of the initial cross section (equal to the squared value of the side of the square)

A_f - area of the deformed cross section (on the rectangular grid)

ECAP was made by multiple passes to decrease the grain size. It is known that when the final deformation is obtained by multiple passes, the ratio of the final and initial area is determined by multiplying the partial relative area ratios after each pass [6]:

$$\left(\frac{A_f}{A_0}\right)_{total} = \left(\frac{A_f}{A_0}\right)_1 \left(\frac{A_f}{A_0}\right)_2 \dots \left(\frac{A_f}{A_0}\right)_n \quad (2)$$

During the ECAP deformation only one side of the final cross section is modified; the other side remains constant. It can be written:

$$\frac{A_f}{A_0} = \frac{a_f * a_0}{a_0 * a_0} = \frac{a_f}{a_0} \quad (3)$$

where: a_f - the deformed side of the cross section after each pass

a_0 – the initial side of the cross section (corresponds to the side of the channel)

The dimensions of a_f and a_0 can be easily seen in Figure 2.

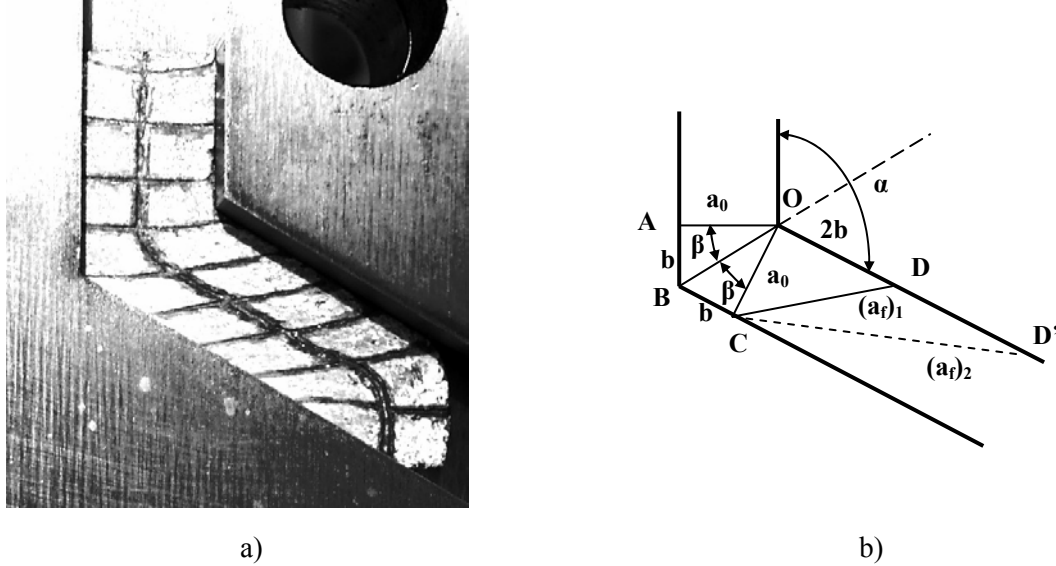


Fig.2: Geometrical scheme for evaluation of deformation: a) experimental; b) theoretical

The dimension of a_f can be determined both experimentally (by direct measurement) and theoretically. For the theoretical calculation the notations from Figure 3.b are used, plus the fact that $OD=2b$.

From the right-angled triangle OCD one can obtain:

$$(a_f)_1 = CD = \sqrt{OC^2 + OD^2} = \sqrt{a_0^2 + 4b^2} \quad (4)$$

From the right-angled triangle OAB:

$$b = AB = a_0 \operatorname{tg} \beta \quad (5)$$

$$\text{where: } \beta = \pi - \left(\frac{\pi}{2} + \frac{\alpha}{2} \right) = \frac{\pi}{2} - \frac{\alpha}{2} \quad (6)$$

$$\text{and thus: } b = a_0 \operatorname{ctg} \frac{\alpha}{2} \quad (7)$$

Using equation (3) one can obtain:

$$(a_f)_1 = a_0 \sqrt{1 + 4 \operatorname{ctg}^2 \frac{\alpha}{2}} \quad (8)$$

Equation (8) shows that a_f depends on the angle between the two channels.

At the second pass OD becomes $OD' = 4b$ and thus:

$$(a_f)_2 = a_0 \sqrt{1 + 16 \operatorname{ctg}^2 \frac{\alpha}{2}} \quad (8')$$

At the third pass OD becomes $OD'' = 6b$ and thus:

$$(a_f)_3 = a_0 \sqrt{1 + 36 \operatorname{ctg}^2 \frac{\alpha}{2}} \quad (8'')$$

It can be observed that at pass n , a_f can be written in the following manner:

$$(a_f)_n = a_0 \sqrt{1 + (2n)^2 \operatorname{ctg}^2 \frac{\alpha}{2}} \quad (9)$$

where n represents the number of the pass.

Another attractive way of representing the severity of deformation is through the natural logarithm of the ratio between the final and initial area of the cross section:

$$\varphi = \ln \frac{A_f}{A_0} = \frac{a_f}{a_0} \quad (10)$$

When the deformation takes place by multiple passes the total strain is calculated as a sum of the partial strain at each pass:

$$\varphi_{total} = \varphi_1 + \varphi_2 + \dots + \varphi_n = \left(\ln \frac{A_f}{A_0} \right)_1 + \left(\ln \frac{A_f}{A_0} \right)_2 + \dots + \left(\ln \frac{A_f}{A_0} \right)_n \quad (11)$$

3. Experimental results

The sample was deformed in 3 passes with the above described procedure. The number of passes was limited to 3 because the length of the sample after the third pass is higher than the height of the entering channel. The images after each pass are presented in Fig. 3:

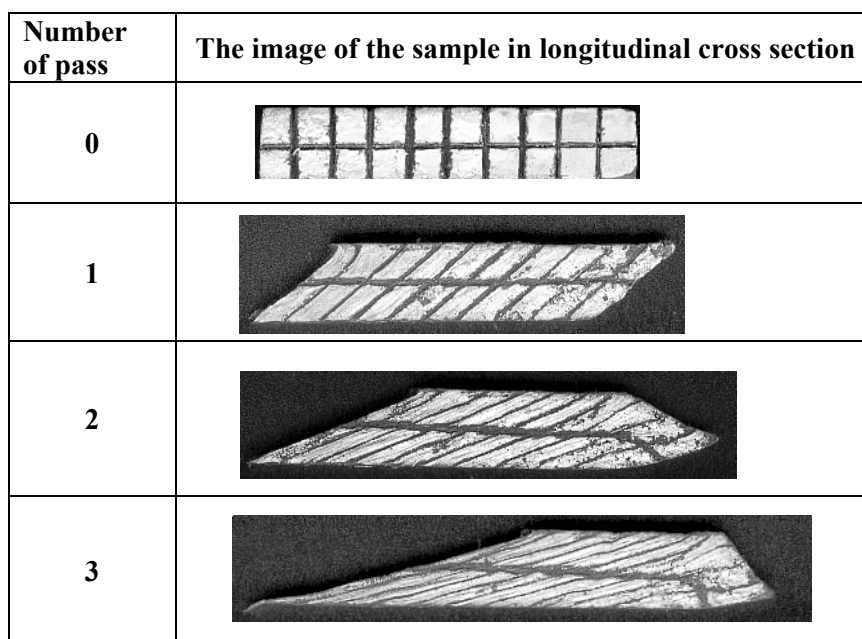


Fig.3: Images of the sample before (pass 0) and after deformation (pass 1,2,3)

The dimension of a_f was measured after each pass, in order to determine the strain experimentally. The results were then compared with theoretical values. The synthesis of the results is presented in Table 1.

Table 1: Theoretical and experimental strains at ECAP

Number of pass		0	1	2	3
Dimension of a_f , mm	Theoretical	10	15,1	24,8	35,3
	Experimental	10	15,2	25	35
Engineering strain ε , %	Theoretical	-	51	64	42
	Experimental	-	52	66	40
True strain φ	Theoretical	-	0,41	0,49	0,35
	Experimental	-	0,42	0,49	0,33

4. Conclusions

The images from Figure 3 show the flow of material due to shearing when passing from one channel to the other. It can be observed that during the shearing process the transversal planes, initially perpendicular on the longitudinal axis, are rotating and inclining more and more as the number of passes increases.

ECAP is a severe deformation process, capable of producing very high strains. In our experiments, after the 3 passes a cumulative total strain rate of 235% was obtained, to which it corresponds a real (logarithmic) strain of 1.25. The experimental results are very close to the theoretical values, which make equation (9) very useful when calculating the deformed side of the sample for practical applications. Thus the size of strain can be anticipated after a certain number of passes.

REFERENCES

1. Sitdikov O.S., Kaybyshev R.O., Safarov I.M., Mazurina I.A., Evolution of the microstructure and mechanisms of formation of new grains upon severe plastic deformation of the 2219 aluminum alloy, *Physics Of Metals and Metallography*, 92 (3), 2001, 270-280
2. T.Y.M. Al Naib, L. Duncan – Superplastic Metal Forming, *Int. Journal of Mech. Sciences* nr.7/1970
3. Umemoto, M, Nanocrystallization of steels by severe plastic deformation, *Materials Transactions*, vol. 44, 10, 2003, 1900-1911.
4. Furukawa, M., Nemoto, M., Horita, Z., Processing of metals by equal-channel angular pressing, *Journal of Materials Science*, 36, 2001, 2835-2843
5. Furukawa, M., Horita, Z., Langdon, T., Processing by equal-channel angular pressing: applications to grain boundary engineering, *Journal of Materials Science*, 40, 2005, 2835-2843
6. B. Avitzur – *Handbook of Metal Forming Processes*. John Wiley & Sons, 1983

Received 12.12.2005

**Technical University "Gh. Asachi" Iași
**S.C. Tehnoton S.A. Iași*

STUDIUL CURGERII ȘI EVALUAREA DEFORMĂRII LA PRESAREA UNGHIULARĂ ÎN CANALE EGALE

REZUMAT: În ultimii ani se folosește deformarea plastică severă (DPS) pentru a produce în materialele metalice granulații nanometrice, necesare în deformarea superplastică. Sunt cunoscute câteva procese de deformare plastică pentru a obține materiale nanostructurale: presarea unghiulară în canale egale (PUCE), refularea ciclică în canalul unei matrițe (RCCM), laminarea cumulativă multistrat (LCM), torsiunea la presiune înaltă (TPI).

În lucrare se prezintă un studiu asupra curgerii și evaluarea mărimii deformării la DPS pe un dispozitiv de PUCE. Pentru studiul curgerii s-a folosit metoda rețelei rectangulare iar pentru evaluarea deformării s-au utilizat gradele relative și reale de deformare. S-a determinat o relație geometrică care dă lungimea secțiunii transversale deformate, necesară pentru calculul gradelor de deformare. Rezultatele teoretice au fost comparate cu cele experimentale, rezultând o bună concordanță.

HARD LAYERS OBTAINED BY COATING WITH NICKEL BASE SUPERALLOYS

BY

I.VIDA-SIMITI¹, N. JUMATE¹

***ABSTRACT:** The parts sintered from iron powder have a low hardness and resistance to wear and corrosion. This study presents the studies made on the high-resistance and high-hardness layers obtained by the diffusion of the Ni-base superalloy in parts sintered from iron powder. Diffusion-coated layers have been obtained, by the application of powder metallurgy processes. The study presents the processes used to obtain the layers and the microstructure investigations of the obtained layers.*

***KEYWORDS :** diffusion, coating, hardness, powder*

1. Introduction

The phenomena of wear, fatigue and corrosion which are taking place mostly in the surface layer, are the most important factors leading to the damage of parts, including their deterioration.[1].

The goal of the change in structure and chemical composition of the surface layers using the coated process by diffusion is the improvement of the physical-chemical and mechanical properties of these layers compared to the core [2,3]. The most important goal is to obtain a wear-proof, corrosion-proof, heat-resistant and fatigue-proof structure over a strong core [4].

2. Experimental Method

D.W.P. 200 powder type, low-alloy iron powder was used, with a total alloying elements of approx. 0.25%. We selected this material with a very low content of alloying elements on purpose, because it allows us to accurately analyze the reciprocal layer-sublayer diffusion.

The coating material used is a nickel and chromium-base powder with content boron, carbon and silicon.

The study of the interface phenomena during coating of the sintered carbon steel parts with Nickel-base superalloys has been carried out by the application of 4 technological coating methods on carbon steel samples [5]:

- diffusion in vacuum (CAP method (**C**ompaction by **A**ir **P**ressure));

- diffusion in reagent atmosphere (dissociated ammonia);
- diffusion in inert atmosphere (argon);
- thermal spraying with flame.

For the obtaining of the samples and the study of coating we used: casts, hydraulic press, tubular furnace, vacuum apparatus, active and protective gas apparatus, optical and electronic microscopes, hardness testers, micro-hardness testers, etc.

The analysis of the structure of the samples by X-ray diffraction has been carried out using a Dron 3 type X-ray diffractometer.

The micro-hardness was determined for the structural components of the layer and the sublayer, as well as for the base matrix. For determinations we used a Hannemann type microhardness tester attached to a Neophot type metallographical microscope.

3. Results and Discussions

In figures 1 a selection of the representative diffractograms of the samples are shown. After the calculation of the d interplanar distances for a sample, the phases existing in the material of the sample are identified using the ASTM (American Standard Testing Materials) material specifications.

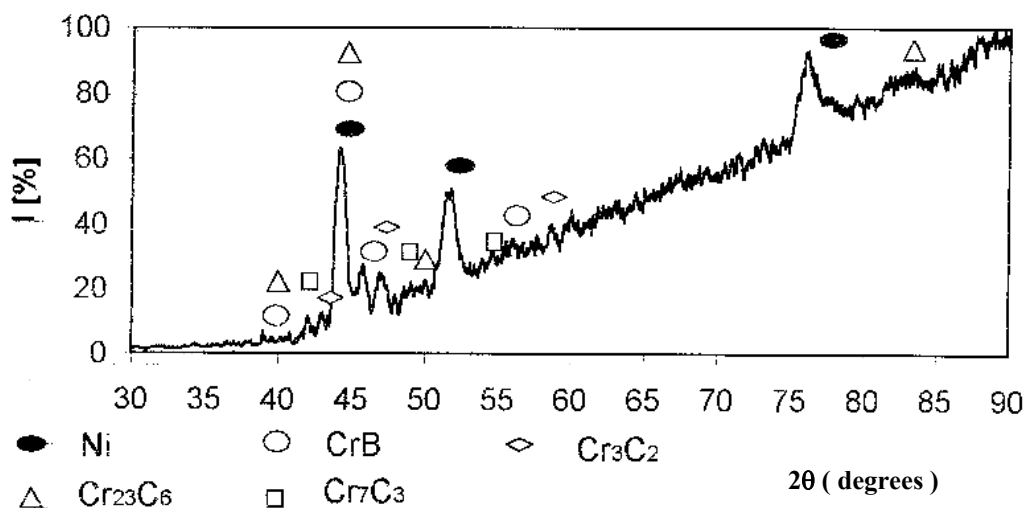


Fig.1. The X-ray diffractogram of the NiCrBSiC superalloy layer coated in vacuum

On the NiCrSiBC alloy coating layer the following phases have been identified:

- FCC crystallized Ni_γ solid solution;
- Chromium borides CrB (orthorombic crystals);
- Chromium carbides: $Cr_{23}C_6$ (complex cubic crystals); Cr_7C_3 (hexagonal structure); Cr_3C_2 (orthorombic structure)

Comparing the data obtained using the optical microscopes (Fig. 2) and X-ray diffraction, the phases obtained in the layer and the interface are the following:

- Ni_γ solid solution with boron and silicon;
- binary eutectic (Ni_γ solid solution + CrB);
- polinary eutectic (Ni_γ solid solution + chromium carbides + silicon borides);
- $Fe\alpha$ (Ni,Cr,C) solution, CVC crystallized (at the interface).

Figures 2 a, b, c and d show diffusion areas of samples coated in vacuum, in inert and reagent environment, and sprayed with flame. Note that the microstructure and width of the diffusion zone are depending on the coating method.

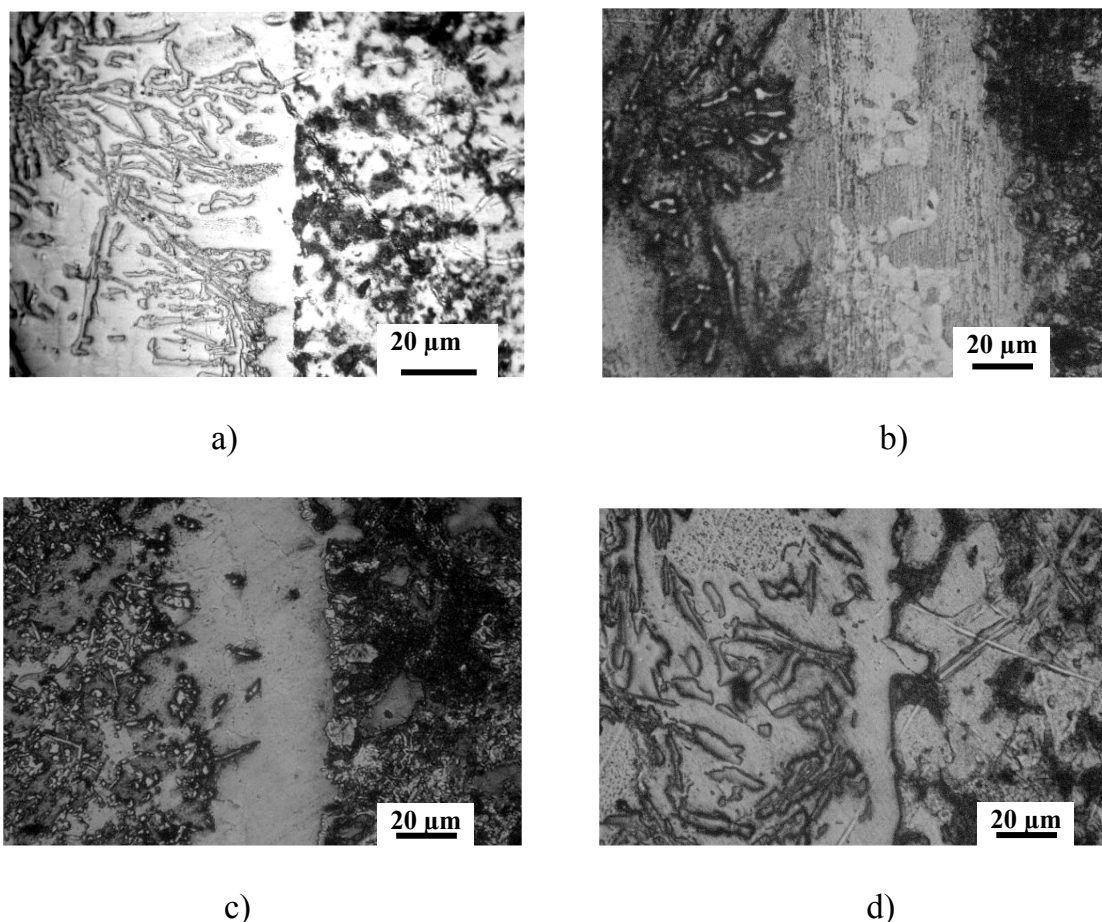


Fig. 2. The diffusion zone for the layer coated
 a – in vacuum, b – in reagent environment, c – in inert environment,
 d – by spraying with flame

The variation of the microhardness of the coating layer in the diffusion zone (coating in vacuum) is show in figure 3. These microhardnesses have been determined, as much as possible, at equal distances (steps of $50\ \mu\text{m}$) in the base matrix, interface or substrate. Note that the highest microhardnesses for the $\text{Ni}\gamma$ solid solution appear at the samples coated in vacuum and neutral environment.

In the case of spraying with flame , the microhardnesses are lower than for the other methods, probably due to the fact that the alloy elements are burnt by the flame (especially boron and carbon in the NiCrBSiC powder used for spraying).

Moreover, a higher level of microhardness is found compared to the ferrite in the sublayer, due to the diffusion of the chemical elements within the layer.

As a result of the iron diffusion in the layer, in the transition zone a $\text{Ni}\gamma(\text{Fe})$ solution is formed that reduces the microhardness

In addition to the microhardnesses determined in the layer-sublayer matrix, the microhardnesses of other components have been determined :

- note the presence in the layer (fig 2, in the eutectic) of dispersed white colored particles of chromium boride and carbide with dimensions of 1 to $4\ \mu\text{m}$ (stable phase)

CrB with a microhardness of $4000\text{HV}_{0,02}$ and acicular Cr_7C_3 carbides with a microhardness of $2500\text{HV}_{0,02}$

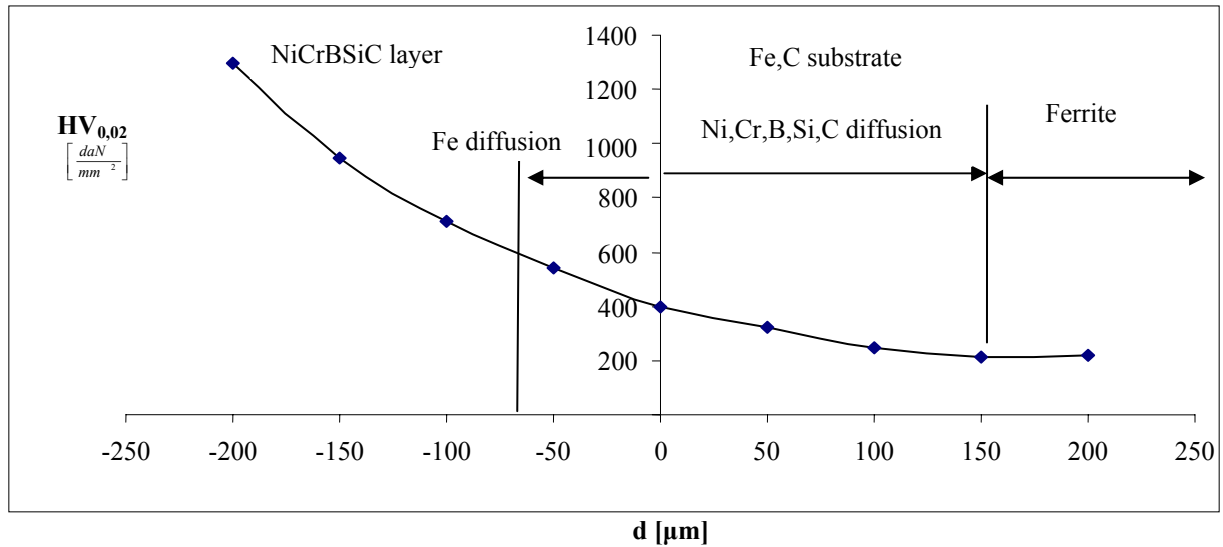


Fig.3. The variation of the microhardness of the coating layer in the diffusion zone (coating in vacuum)

- white colored Ni_y solid solution grid with a microhardness of $480\text{HV}_{0,02}$
- dark colored intergranular grid with a microhardness of $1480\text{HV}_{0,02}$ (ternary or polinary eutectic).

Figures 4-6 show the Vickers hardness variance for the coated samples depending on the distance from the coated surface.

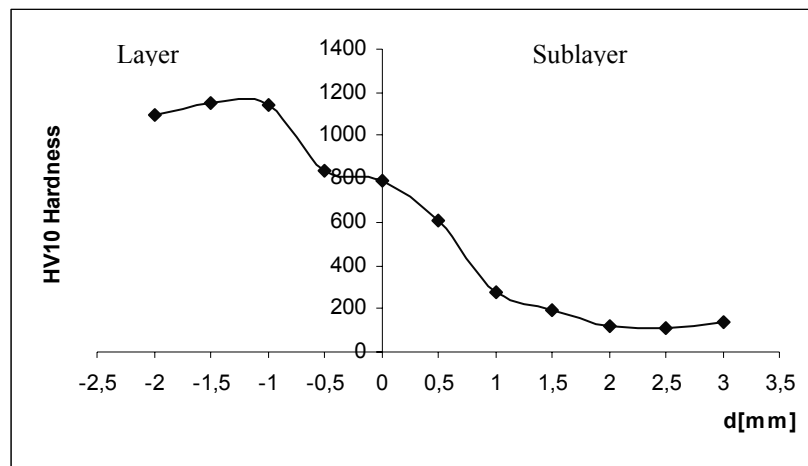


Figure 4. Variance of the hardness of the samples coated in vacuum, depending on the distance from the surface of the samples (coating at 900°C)

These graphics show that on the surface of the layer the hardness is lower. This reduction of hardness is due to the interaction of the layer with the coating atmosphere. The percentage of the elements such as boron and carbon decreases in this part of the layer. The ferrite layer near the interface has a higher hardness due to the diffusion of

the sublayer elements to a distance of 0.5-1.5 mm. The samples with the highest degree of hardness in the interface area are those coated thermally or in vacuum.

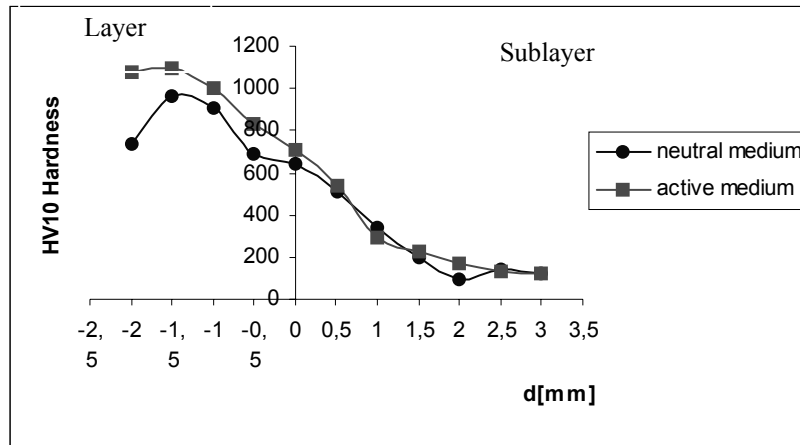


Figure 5. Variance of the hardness of the samples coated in active or neutral medium, depending on the distance from the surface of the samples (coating at 900°C)

In case of coating at temperatures exceeding approx. 950°C (sintering in liquid phase), the hardness values obtained are lower due to the diffusion of iron within the layer, stronger at higher temperatures (Figure 6).

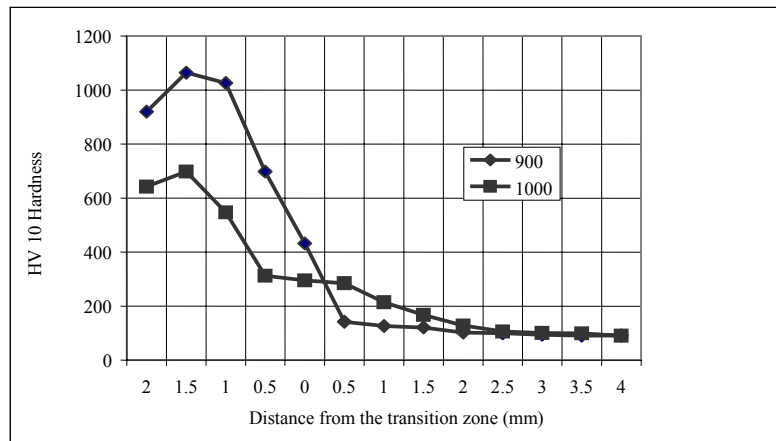


Figure 6. Variance of hardness for the samples sintered at 900 °C and 1000 °C and the distance from the metal-coated surface of the samples.

It can be observed that in case of an active medium (25% H_2 +75% N_2), the hardness values in the layer are higher as in case of a neutral medium, and this is probably caused by the formation of nitrides when interacting with the coating atmosphere.

4. Conclusions

-The pressed DWP 200 iron powder sample has been coated with a nickel-base superalloy layer.

-For all the methods used it has been observed that the hardness of the deposited layers decreases from the superalloy towards the pressed sublayer of iron powder, due to the following:

- the diffusion of the hard nickel-base and chromium-base elements (borides, silicides etc.) towards the iron powder sublayer
- the inverse diffusion of iron in the sublayer towards the superalloy layer.

-Since the superalloy powder based on nickel melts at temperatures exceeding 950°C, the phenomenon of diffusion takes place in liquid state and becomes increasingly intense as temperature rises.

-It has been observed that usually the same phases and components of the interface structure are produced during each coating method. Their quantity and distribution determines the physical-chemical properties of the layer-sublayer pair.

-It has been identified the following phases at the layer-substrate interface : CFC crystallized $Ni\gamma$ solid solution, chromium borides CrB (orthorombic crystal), chromium carbides: $Cr_{23}C_6$ (complex cubic crystal), Cr_7C_3 (hexagonal structure), Cr_3C_2 (orthorombic structure), binary and polinary eutectic, $Fe\alpha$ (Ni,Cr,C) solution, CVC crystallized.

-The samples coated in vacuum at the temperature of 1100°C (coating-sintering with liquid phase) have the lowest interface porosity. The porosity of samples coated by thermal spraying is lower than the porosity of samples coated in active or neutral environment.

-The highest microdurity is obtained by samples coated in vacuum, active and neutral environment. The microdurity of samples coated by thermal spraying is lower.

REFERENCES

1. O.Knotek, E. Lugscheider, H.Eschnauer: Hartlegierungen zum Verschleisschutz, Düsseldorf, Verlag Stahleisen, 1975;
2. G.Matei, E.Bicsak, G.Lindeman: Practical Metallography, Düsseldorf, 22 (1985), p. 124-134;
3. N.A.Rhodes, J.V.Wood, and J.R.Moon: Powder Metallurgy, 2000, vol.43, No.2, 157-162
4. C.E.Campbell, s.a., Development of a diffusion mobility database for Ni-base superalloys, Acta Materialia 50 (2002), pag. 775-792;
5. R.D.Knobloch, N. Jumate, I. Vida-Simiti, Study of the Hardness of Layers Created By Coating with NiCrBSi Powders, Acta Technica Napocensis, Serie Materials, Cluj-Napoca, 2005, p. 109-113.

Received 12.12.2005

¹Technical University of Cluj-Napoca, Romania

STRATURI DURE OBȚINUTE PRIN ACOPERIRE CU SUPEALIAJE PE BAZĂ DE NICHEL

REZUMAT: Această lucrare prezintă studiile efectuate pe straturi de înaltă rezistență și duritate obținute prin difuzia elementelor din superaliaje pe baza de nichel în piese sinterizate din pulbere de fier. Au fost obținute straturi placate prin difuzie aplicând procedee ale metalurgiei pulberilor. Sunt prezentate și comentate rezultatele asupra investigațiilor microstructurii, durității și microduritățile straturilor obținute.

CHARACTERIZATION OF SOME POLYURETHANE ELASTOMERS WITH 1,4-BUTANEDIOL CHAIN EXTENDER AND DIBENZYL DERIVATIVES

BY

CRISTINA PRISACARIU¹, ELENA SCORTANU¹, VICTOR ADRIAN PRISACARIU²

ABSTRACT. *Segmented polyurethane elastomers (PUs) of different structures have been synthesized based on two hard segments derived from 1,4-butanediol (BD) and two isocyanates of different geometries: (MBI) 4,4'-methylenebis-(phenylisocyanate) with a rigid geometry, and flexible DBDI (bibenzyl 4,4'-dyil diisocyanate) with internal –C-C- rotation axis. PUs structural properties and the effects of varying hard segment have been investigated by means of wide angle X-Ray scattering (WAXS), dynamic mechanical analysis (DMA) and scanning electron microscopy (SEM). Results were discussed in terms of the effect of PUs crystallinity. The couple consisting of the flexible bibenzyl 4,4'-dyil diisocyanate (DBDI) - BD giving rise to a special hard segment conformational mobility induces a specific physical-mechanical behaviour in PU and leads to a high tendency of crystallization and hard segment block phase separations.*

KEYWORDS: *macromolecular chain flexible bibenzyl 4,4'-dyil diisocyanate, 1,4-butanediol, crystallinity*

1. Introduction.

Segmented polyurethane elastomers (PUs), which are composed of alternating soft and hard segments along with a high molecular weight polymeric backbone, are very versatile polymers with a wide range of applications. This is a direct result of the availability of three main starting materials for their synthesis, e.g. diisocyanates (DI), polymeric glycols (MD) and diol or diamine chain extenders (CE), [1-7]. The mechanical properties of PUs are mainly determined by their microphase structure. The morphology of PU elastomers consists of a continuous soft segment phase, linked to each other with strongly hydrogen bonded hard segment domains, (Figure 1). An essential factor that influences the microphase morphology of PUs is the conformational structure of the adopted isocyanate of a rigid geometry [1,2] or based on a variable conformational mobility as shown in Figure 2. As shown in our previous works [1-7], the investigation of a new diisocyanate (DI) with a variable geometry, as in the case of bibenzyl 4,4'-dyil diisocyanate (DBDI) in the PU synthesis, brings dramatic changes in the properties of the so-obtained elastomers if compared to other similar usual polyurethane elastomers obtained with classical diisocyanates as 4,4'-methylenebis-(phenylisocyanate) (MBI) or 1,5 – naphthalene diisocyanate (NDI) with rigid geometries.

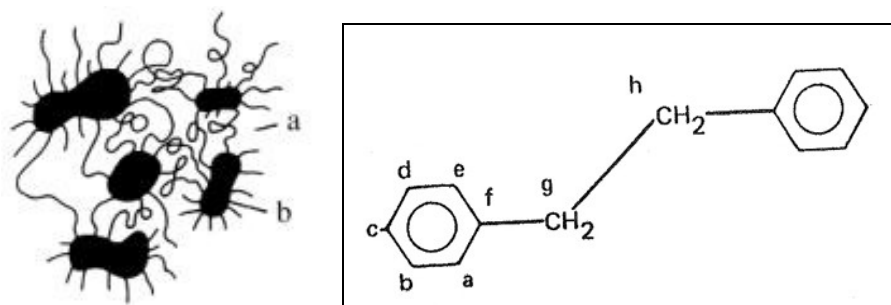


Figure 1. PU Structures; (a) soft block domain; (b) hard block domain (adopted from Ferguson, 1991)
Figure 2. Schematic of DBDI (bibenzyl 4,4'-diyl diisocyanate)

In the present study, the PU synthesis was made on employing 1,4-butanediol (BD) as a chain extender (CE), thus generating hard segments of the DBDI – BG couple types. The aim of this work was to assess the capacity of the so-obtained polymers to segregate into hard crystalline phases.

2, Experimental Procedure.

The soft segment macrodiol (MD) was poly(ethylene adipate) (PEA) of molar mass 2000 ± 50 . The CE used in the synthesis was 1,4-butanediol (BG) according to Table 1. To obtain better elastomeric properties, reactive PU with a small excess of NCO groups was prepared, by using a deficit of CE with molar concentrations such as DBDI:PEA:BD = 3:1:1.727, giving isocyanic index $I = 110$ as shown in our previous publications [3,4]. The synthesis was complete only after performing the total consumption of the isocyanate group excess by postcuring with water present in ambient atmospheric humidity. The description of the PU synthesis envisaged in this paper has been described elsewhere [1,2].

Table 1. Casted PU adopted structure

PU #	DI	MD	CE	DI:MD:CE
1	DBDI	PEA	BD	3:1:1.727
2	MBI	PEA	BD	3:1:1.727

Isocyanic index was $I=110$ where I (isocyanic index %) = $100 \times [\text{NCO}] / ([\text{OH}]_{\text{MD}} + [\text{OH}]_{\text{CE}})$.

3. Results and Discussion

3.1. Structural studies. Crystallinity

The remarkable PU properties are mainly due to their special tendency to form discrete regions in which the hard segments made up by diisocyanate and chain extender tend to self associate in separate microdomains. As shown, PU obtained by the reaction between DBDI and BD are polymers with a high tendency of crystallization as in the case when using DBDI and ethylene glycol (EG) as a CE [1,3]. Figure 3.a displays typical Wide Angle X-ray scattering curves of PUs with MDI and DBDI and corresponding homopolyurethane [1,2] based on DBDI made up only by hard segments of the MBI-BD or DBDI-BD type[1,4]. WAXS experiments were made using copper $K\alpha$ radiation. Phase separation, crystallization and orientation phenomena in the present materials were also studied by means of DSC and IR dichroism from which results are reported elsewhere [1]. As ascertained from Figure.3.a and b., characteristic to PUs based on DBDI, in comparison to the WAXS

curve 3.c of the MBI-based PU, the X-ray diffraction patterns of the $[\text{DBDI-BD}]_n$ homopolyurethane and the corresponding DBDI-based copolyurethane show that crystallization did not disappear with the inclusion of the hard segments in a block copolyurethane elastomeric matrix, indicating the appearance of more or less phase separations associated with the formation of crystalline hard domains.

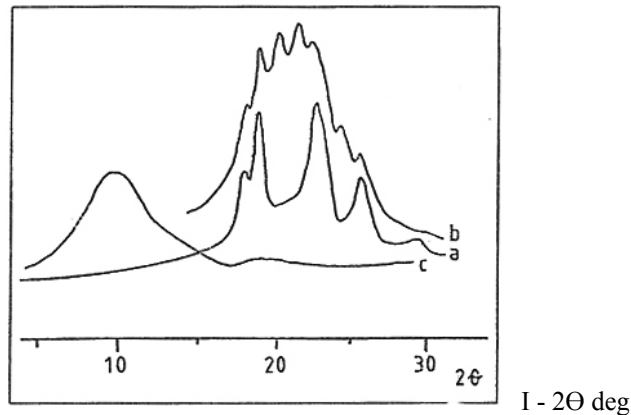


Figure 3. WAXD of PU with MBI-BD and DBDI-BD hard segments: (a-) homopolyurethane - $[\text{DBDI-BD}]_n$ - model; (b) – a DBDI based PU with structure DBDI:PEA:BD = 3:1:1.727; (c) – a MBI based PU with structure DBDI:PEA:BD = 3:1:1.727. where $I=110$ in both cases.

The presence of these structures induces a special mechanical behaviour in the obtained elastomers. The disordered orientation of these domains in the soft polymer matrix appears initially isotropic on the macroscale but when subjecting the polymer to stretching, the crystalline microdomains tend to orient in parallel directions, maintaining in some extent their anisotropy even after removing the stress. As a result some enhanced residual elongation was evident. This stress induces orientation was substantially confirmed by SEM or even by using a simple polarizing optical microscope [1]. It should be noted that after annealing the elastomer at 110°C for 60 minutes, the crystallinity of PU with DBDI decreases significantly [2].

3.2. DMA measurements

The DMA measurements were carried out with a Gabo Qualimeter Eplexor 150 N. The samples were tested in tensile mode with a starting distance between the clamps of 45 mm. The cross section area of the specimen was 5 mm x 1-2 mm. The samples were placed in the temperature chamber and cooled down to the starting temperature of -140°C . The cooling conditions were: room temperature till -60°C cooling rate of 10 Kelvin/minute, -60°C to -120°C 3,5 K/min and -120°C to -140°C 2 K/min.

The tests started at -140°C and the complex modulus (E^*), storage modulus (E'), loss modulus (E'') and the loss factor ($\tan \delta$) were measured as a function of temperature at a heating rate of 1 K/min. The instrument was operated with controlled sinusoidal force with a frequency of 1 s^{-1} . As shown in Figure 4, for the DBDI-based PU 1 the DMA measurements have shown that the storage modulus (E') in the temperature range above the glass transition region is the highest for the DBDI-based PU1 which is controlled by the crystalline content of hard segments given by the stronger tendency of the DBDI-BG hard segments to self-associate in a coplanar packing [1-3].

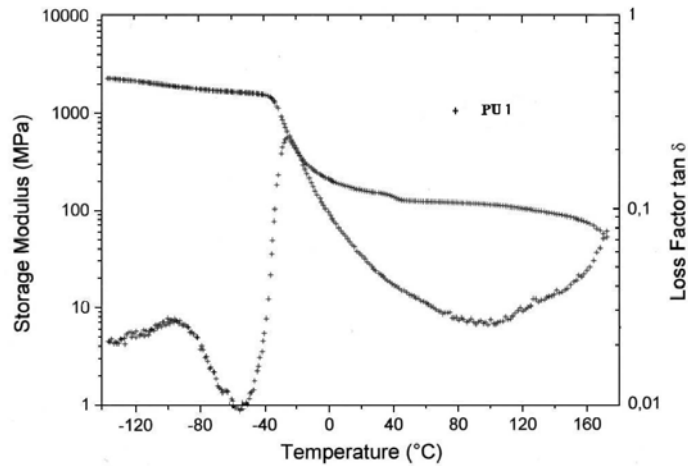


Figure 4. Storage modulus and Loss Factor as a function of temperature for PU₁ based on DBDI with the structure BD:PEA:DBDI(3:1:1.727), I=110).

The decrease of the modulus at about 150°C is connected with the softening/melting of the samples. The glass transition temperature in the maximum of the loss factor at $f=1 \text{ s}^{-1}$ has ranged among -10°C to 21°C , and the lowest T_G value corresponds to PU₁, BG:PEA:DBDI(3:1:1.727), I=110), based on hard segments of conformational mobility. The glass transition temperatures in the maximum of the loss factor at $f=1 \text{ s}^{-1}$ are: for PU 1, $T_G = -24^{\circ} \text{C}$. $\text{Tan } \delta = 0.198$ and for PU 2, $T_G = -16^{\circ} \text{C}$, with $\text{Tan } \delta = 0.418$.

3.3. Morphology

Previous SEM examination of stretched PUs when recovered after uniaxial tension at a 300% extension was made and it was shown that after the materials are stretched under the above mentioned conditions and allowed to recover, they respond differently. Their response varies between different types of PUs derived from the two isocyanates with either rigid or variable geometries [2]. In the present paper the polymer surface structure was examined initially after synthesis, on original PU sheets. Both of the PU 1 and PU 2 materials display a relatively coarse structure on 10 μm scale but which varies from a polymer to another. This is shown in Figure 5.

Scanning electron microscopy (SEM) was performed on the outer surface of the original cast sheets. Specimens were coated with a sputtered film of gold to prevent charging, and were tilted at 45° in the specimen chamber to improve contrast. For the materials subjected to stretching/rupture and then relaxed, the specimens were rotated so that the draw direction lies approximately from bottom left to top right of the rectangular pictures displayed.

Figure 5.a displays the features of PU 1 original sheet. At 0.1 mm magnification the arrow points to a particularly prominent area of the banding which is typical of this specimen. The most prominent feature is what is referred to as the *coarse structure* of about 10 μm in scale (Fig.5.a): this is due to large extent of PU phases separation in the PU1 dibenzyl-based material. There are only the faintest hints of a texture on this scale in the equivalent in PU 2.

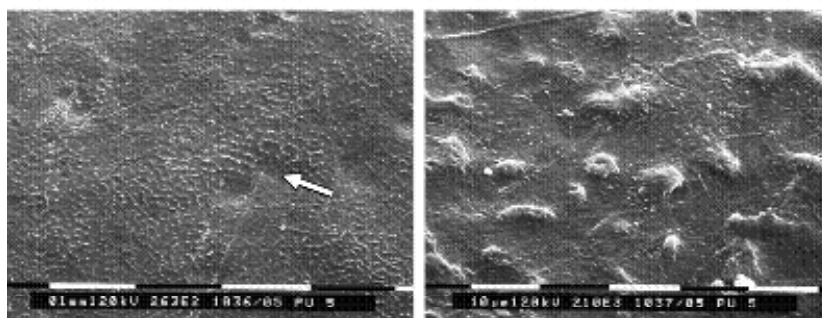


Figure 5.a. SEM of PU 1 original sheet at two magnifications.

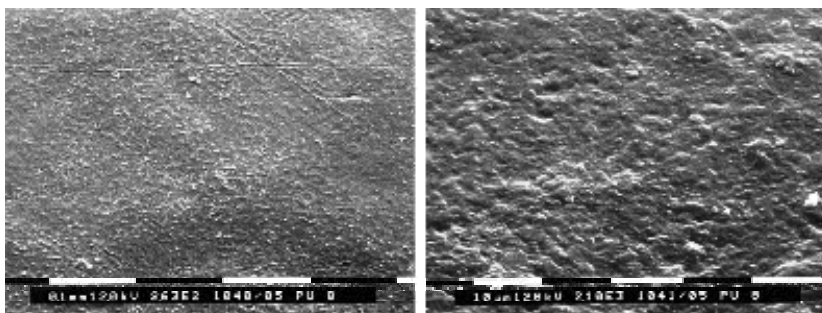


Figure 5.b. SEM of PU 2 original sheet at two magnifications.

This banding is made up of phase-segregated lumpy regions, which are either finer or not present at all in PU 2.

Figure 5.b displays the features of PU 2 original sheet. The banding also appears, but much less pronounced. PU 1 which displays X-ray crystallinity tends to give a rougher surface morphology than PU 2.

4. Conclusions

The role of the hard segment nature and geometry on the polyurethane elastomers structure/morphology and properties of polyurethane elastomers has been followed. Segmented PUs of two different structures have been designed and synthesized based on the couple made up by BD as a chain extender and on two isocyanates of different geometries: (MBI) 4,4'-methylenebis-(phenylisocyanate) with a rigid geometry, and flexible DBDI (bibenzyl 4,4'-diyl diisocyanate) with internal -C-C- rotation axis. Two types of hard segments were differentiated based on MBI-BD and DBDI-BD. As in the case of the MBI-EG and DBDI-EG hard segments containing PU systematic differences were observed between PU made up of the classical isocyanate MBI as compared to the polyurethane derived from the isocyanate of conformational mobility DBDI. Polymer with DBDI has a higher flow stress than polymer derived from MBI, but shows less pronounced strain stiffening. As in other previous studies PU phase separation tendency is significantly more pronounced in the case of polyester polyurethanic material based on PEA as soft segment, BD as a chain extender and dibenzyl structures then in the case of similar hard segments based on classical MDI. The DMA measurements have shown that due to the higher content of hard segments derived from DBDI, the storage modulus (E') in the temperature range above the glass transition region is the highest for the DBDI based PU of the type PEA-DBDI for which 1,4-butanediol (BG) was used as a chain extender. In all cases the more mobile DBDI structure leads to hard segments with a higher tendency to self associate

evidenced by higher melting points and crystallization tendency which is visible even when such structures are included in the polyurethane soft segment matrix.

5. References

1. Prisacariu Cr., *Interaction between physical-mechanical properties and chemical Istructure of polyurethane elastomers with dibenzyl structures, Doctorate Thesis, "Gh.Asachi" University, Iasi, Romania, June, 1998.*
2. Prisacariu C, Olley RH, Caraculacu A, Bassett DC and Martin C., *Polymer*, (2003); 44: 5407.
3. Prisacariu C, Buckley C.P, Caraculacu A., *Polymer*, (2005); 46(11): 3884-3894
4. Prisăcariu C, Agherghinei I, *J.M.S.-Pure Appl. Chem.*, A37 (7), 785-806 (2000)
5. Buckley C.P., Prisacariu C. and Caraculacu A.A, *Constitutive response of model segmented copolyurethane elastomers*, Euromech Colloquium and Workshop, Vienna, July 2002, 96-99 (2002),.
6. Buckley C.P., Prisacariu C. and Caraculacu A.A., *Effects of hard segment crystallinity on constitutive response of copolyurethane elastomers*, 12th International Conference on Deformation, Yield and Fracture of Polymers, Cambridge, UK, 7-10 April 2003, 349-352 (2003).
7. Prisacariu C, Caraculacu A.A. and Olley R.H, *Approaches for novel polyurethanic materials of variable crystallinity*, Biennial Polymer Conference, Polymer Physics Group, UK, 10-12 September 2003.

Received December 12, 2005

¹The Romanian Academy's Institute of Macromolecular Chemistry "Petru Poni", Iasi, Romania

²"Gh. Asachi" Technical University, Faculty of Automatics and Computers, Iasi, Romania

CARACTERIZAREA UNOR ELASTOMERI POLIURETANICI PE BAZĂ DE ALUNGITORUL DE LANȚ 1,4 - BUTANDIOL ȘI DERIVAȚI DIBENZILICI

REZUMAT: A fost sintetizată o serie de elastomeri poliuretanic (PUs) cu diferite structuri având la bază 1,4-butandiol (BD) și doi izocianați cu geometrie diferită: (MBI) 4,4'-metilenebis-fenilizocianat care prezintă o geometrie rigidă și izocianatul DBDI (bibenzil 4,4'-diil diizocianat) cu geometrie variabilă datorită posibilității de rotație internă a axei -C-C-. Proprietățile structurale ale PUs și efectele varierii tipului de segment dur au fost investigate prin intermediul studiilor de raze X la unghi mare (WAXS), prin analize mecano-dinamice (DMA) și prin experimente de microscopie electronică de baleiaj (SEM). Rezultatele obținute au fost discutate în raport cu efectul produs asupra cristalinității PUs. Cuplul flexibil DBDI - BD capabil să genereze o mobilitate conformațională specială a segmentelor dure induce un comportament fizico-mecanic specific în aceste tipuri de polimeri și determină o tendință mai pronunțată de cristalizare și fenomene de separare fazică.

SOCIAL ENGINEERING - A NEW INSTRUMENT FOR ENGINEERS TO MAKE OPERATIONAL THE CONCEPT OF SUSTAINABLE DEVELOPMENT

BY

CRISTIAN PREDESCU¹, G.G. CALEA¹, AVRAM NICOLAE¹

ABSTRACT. *The penetration of zones outside the technical sciences becomes a special task for engineers. An example in this sense is making operational the concept of sustainable development by help of social engineering. It is demonstrated that this is a new scientific branch studying the optimization of the impact of industrial policies, technologies and equipments on life quality.*

KEYWORDS: *social engineering, sustainable development, life quality, industrial policies, political technology.*

1. INTRODUCTION

In our opinion, *the social engineering represents the scientific branch and education field the object of which is the optimisation of the impact of industrial policies, technologies and equipments on life and environment quality.*

The launch of social engineering on the scientific market is sustained also by the fact that the man acts within the social-ecological system for fulfilling his own wishes, which concern the social aspect too, his highest acception, i.e. that including also the cultural aspect. The social engineering can be a support for both the life level and life standard, between them being the following distinction: the first represents the real living conditions and the second - the aimed life conditions.

Taking into account other literature data, we are tempted to assume that there are obvious similitudes between the social engineering and what in other works is known as *political technology*.

The political technology stands out as a field studying the social consequences of the new technologies and examines possible or realisable technologies in order to help the actual society to evaluate to a superior stage. In the same time, the political technology has the responsibility to study the consequences of the new technologies on the human psychology and hence, on the society, mutations which are and will be produced in the manpower structure, the use by the people of production and extraproduction time, as well as a whole serie of other aspects. The political technology can recommend the society adaptation in advance to the new processes.

2. DISCUSSIONS

The political technology can formulate requirements to the technology and even to the science for satisfying, in perspective, the society needs, thus establishing a number of social functions, which the technical systems are to fulfill and searching the way in which these functions can be realised. For this reason it is suitable for the scientists and researchers of technology and technical systems too. Thus, the political technology has two major aspects, one addressed to the way of governing the society and the other - to the innovation way. It put together the social and the technological - in which way the social can favorize those technologies contributing in the highest measure to the economical and social process, but also the way in which the science and technology must turn their efforts to satisfy the large needs of the society in the making.

Regardless of name, the social engineering or political technology means for an engineer a way of making operational the new concept defined in EU as CSR (corporate social responsibility). As it is shown in the paper "Green Paper - Promoting a European Framework for Social Corporate Responsibility", Brussels, COM, 2001, 366, one works so that by using CSR the European economy "become the most competitive and dynamic economy based on worldwide knowledge and be able to ensure the permanent economical development, offering better jobs and social cohesion".

The Company Social Responsibility is a concept which includes the social and environmental concerns in the business strategies and at the level of relationships with the other interested parts, voluntarily, in the continuous trying to improve the performances, increase the profit and of development.

A more succinct definition shows that CSR is a concept by which the companies integrate social and ecological concerns into their commercial activities and interactions with the involved factors on a voluntary basis.

The social responsibility is a SD subject, at least because it makes us to think of:

- the concern for that the future reserves us is the best way of progress for all of us;
- it is right to look for solutions regarding the energy demand and improve the social and environmental performances on medium and long terms;
- satisfied customers: 70% of customers of the European firms say that the firm adhesion to the principles of social responsibility is an important criterion, when the decision to buy a product or a service is taken;
- satisfied employees: the companies which introduce benefits programmes, competitive for the employees, record a costs decrease by reducing the absenteeism, personal fluctuation, seak leaves etc.;
- better access to the capital: the experts assert that the investments are obtained easierly when the principles of social responsibility are respected;
- better relationships with the local community.

The above mentioned general considerations must be taken into account if a new scientific sub-branch known as “**metallurgical social engineering**” is projected. In its framework the metallurgical engineer should define and make operational the specific ways by help of which life and environment quality will be risen, as one try to predict below.

- An important mutation concerning people cares is recorded: the transition from the preponderently technological concerns to those with social feature. They must yield in such a technological frame, in that the technologies of the primary sector must gain new qualities and, especially, functions, so that the goods and needs made at disposal by the primary industries be evaluated and appreciated as key factors, which contribute to the liquidation of physical discrepancies, but human and social too bewteen persons, regions or countries.
- *Life conditions* (directly related in the human environment, respectively with the society conditions and their physical medium,) and *human needs* (material goods) produced as well by the metallurgical industry are blended objectively within the contour of life quality.
- Today, the socio-eco-systems improve themselves on the basis of the transition from the *interaction duo* (natural-social) to the *interaction trio* (natural-artificial-social), the artificial being represented in fact by the industry of metallic materials too.
- Life quality rising is based more and more upon the utilization of *eco-standards, eco-materials and eco-products* resulted obviously from the engineering activity.
- The increase of consumption per capita (inclusively of the social-cultural one) was and is possible due to the industrial rising. The richness is realised there where the new industrial technologies act.
- The support of the cultural needs could be materialised, e.g., as an answer to questions as follows: what is the relationship between the technological performances at the Integrated steel plant - Galatzi and the audience of the local theatre?

REFERENCES:

1. “Dezvoltare durabilă în siderurgie prin valorificarea materialelor secundare”, Ed. Printech, Bucureşti, 2004, Nicolae, Maria, Tudor, P., Predescu, C., Licurici, M., Serban, V., Mândru, C., Calea, G., G., Ioana, A., Sohaciu, Mirela, Semenescu, Mihaela, Parpala, Diana, Nicolae, A.
2. “Convergențe juridico-inginerești în dreptul mediului”, Ed. Printech, Bucureşti, 2005, Nicoale, A., Predescu, C., Calea, Gh., Gh.,ș.a.
3. Volumul “Societatea informațională- Societatea cunoașterii “, Academia României, Ed. Expert, Bucureşti, 2001.

Received December 12, 2005

¹POLITEHNICA UNIVERSITY - BUCHAREST

**“INGINERIA SOCIALĂ-NOU INSTRUMENT DE OPERAȚIONALIZARE DE CĂTRE
INGINERIA CONCEPTULUI DE DEZVOLTARE DURABILĂ”**

REZUMAT. Penetrarea zonelor din afara științelor tehnice devine o sarcină deosebită pentru ingineri. Un exemplu în acest sens este operaționalizarea conceptului de dezvoltare durabilă cu ajutorul ingineriei sociale. Se demonstrează că aceasta este o nouă ramură științifică care studiază optimizarea impactului politicilor, tehnologiilor și echipamentelor industriale asupra calității vieții.

MODIFICATIONS INDUCED BY STATIC TENSILE TESTINGS IN THERMOPLASTIC POLYURETHANIC FILMS

BY

CRISTINA PRISACARIU¹, ELENA SCORTANU¹

ABSTRACT. *The present paper deals with the study the modifications induced by static tensile testing experiments on a series of novel thermoplastic polyurethanic films prepared by using one or mixtures of isocyanates Thermoplastic polyurethane elastomeric films (PUs) of different structures have been synthesized based on two hard segments derived two isocyanates of different geometries: (MDI) 4,4'-methylenebis-(phenylisocyanate) with a rigid geometry, and a flexible diisocyanate, DBDI (4,4'-dibenzyl diisocyanate). The aim of this work was to determine how the PU tensile testing properties change when the linearity of macromolecules is not anymore perturbed by the used isocyanate excess, thus allowing a higher mobility of individual macromolecules. PU materials with hard segments based on a single diisocyanate (DBDI) display a higher resistance in the first deformation phases, followed then by values of strain which necessitate smaller stress increments. By contrast, in the case of PU based on one diisocyanate MDI, which contains hard segments of a rigid geometry, the crystallinity is practically absent, and the corresponding polymer exhibit a more constant proportionality between the enhance of the stress and the resulted degree of deformation.*

KEY WORDS: polyurethane elastomers, flexible hard segments, isocyanic index, tensile testing

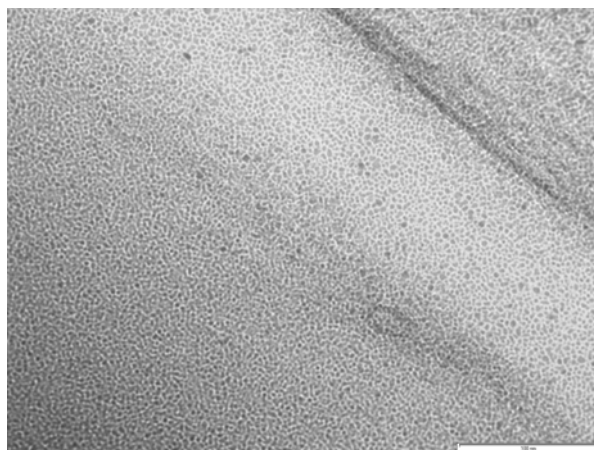
1. Introduction.

Polyurethane (PUs) polymers form a class of materials with unique versatility. They consist of alternating flexible (soft) and relatively rigid (hard) segments. In a previous work we studied a series of PUs in the synthesis of which we used a technique which leads to the appearance of valorous resistant polymer networks obtained in the final stage of the process by the interaction of some residual isocyanic (NCO) groups, generated when using a 2-10% diisocyanate excess, with the atmospheric humidity [1-6].

The aim of this work is to determine how the PUs tensile testing properties change when the linearity of macromolecules is not anymore perturbed by the used isocyanate excess, thus allowing a higher mobility of individual macromolecules.

Under the conditions, the segregation is expected to perform to a greater extent and thus it can be the better evidenced. As already known, the PUs phase segregation occurs during and after polymerization, to produce an elastomeric matrix of the soft segments, containing rigid inclusions (of size scale 10-100 nm) formed by association of the hard segments as shown in Figure 1. Therefore the PUs structure can be regarded as a polymer matrix microcomposite.

The aim of the specific work reported here was to investigate the role of hard segment structure on the PUs properties, when the phase segregation is no more perturbed by any potential crosslinking.



↔ 100 nm

By courtesy of Dr Kayleen Campbell, University of Queensland

Figure 1 TEM photo of the two – phase microstructure of a thermoplastic polyurethane elastomer derived from DBDI

Two hard segment types were compared, based on the two diisocyanates (DI): 4,4'-methylene bis(phenyl isocyanate) (MDI) [2] and 4,4'-dibenzyl diisocyanate (DBDI) [3,4]. The former is widely used in commercial PU materials. The latter is a novel diisocyanate, also available commercially, first synthesized in our Romanian laboratory. The two DI differ only in that DBDI contains two methylene groups between the aromatic rings, while the conventional MDI has only one [1-4]. This apparently small difference nevertheless produces substantial changes in properties of the resulting polymer, due to the possibility of rotation around the central -C-C- bond, allowing a more compact interchain packing and even the appearance of crystallization involving the hard segments blocks. Rotation around the central -CH₂-CH₂- bond in DBDI allows alignment of successive aromatic rings thus favoring the tendency of crystallization which involves the DBDI hard phase. MDI hard segments do not exhibit crystallization in the polymers studied here.

2. Experimental

In the present study two hard segments were used based on DI, MDI and DBDI. MDI is from Aldrich and DBDI is an experimental product from the pilot plant (CIFC Savinesti, Romania) and it was recrystallized twice from anhydrous cyclohexane mp 88-89^o C. Three sets of PUs have been achieved: (a) thermoplastic polyurethane elastomers derived from a single diisocyanate: (PU₁) PU 94 and (PU₂) PU 95 in Table 1; (b) thermoplastic polyurethane elastomers derived from two isocyanates randomly distributed, (PU_{c1}) PU 91 in Table 1; (c) PUs from two isocyanates with selective diisocyanate distribution, (PU_{c2}) PU 92 based on MDI and (PU_{c3}) PU 93 based on DBDI respectively. The macrodiol was a hydroxyl-terminated polyethylene adipate PEA $M_w = 2000 \pm 50$ (PEA₂₀₀₀), a commercial product from CIFC Savinesti, Romania while the extender was anhydrous ethylene glycol (EG). In all cases the adopted value of the isocyanic index was $I = 100$. Molar proportions were diisocyanate DI:PTHF:EG = 4:1:3. The general procedure in the case of PUs derived from a single isocyanate and from mixtures of diisocyanates was previously reported elsewhere [1].

Results and discussion. Results of the tests have shown significant differences between PU, revealing differences in the mechanical contribution of the hard phase, since the matrix was formed from the same macrodiol (PEA) and same chain extender (CE), in each case ethylene glycol (EG).

Table 1. Thermoplastic PU adopted structure

Recipe	PU structure
PU _{C1} (PU 91)	EG-PEA-(DBDI-MDI)
PU _{C2} (PU 92)	EG-(PEA-DBDI)-MDI
PU _{C3} (PU 93)	EG-(PEA-MDI)-DBDI
PU ₁ (PU 94)	EG-PEA-DBDI
PU ₂ (PU 95)	EG-PEA-MDI

As a rule the higher the disorder in the PUs matrix, the better the elastic properties of the PU elastomeric film. This fact is characterized by a lower variation of the Young's Modulus (E) during the augmentation of deformation, and also by a lower residual elongation. Similar conclusions can be obtained with regard to the general strain energy (mechanical yield) of polymer (intermolecular cohesion) measured when stretching the polymer to 0–300% elongation [1,2,6]. Due to the variable geometry of DBDI, the PUs derived from dibenzyl structure were found to display a stronger capacity of crystallization.

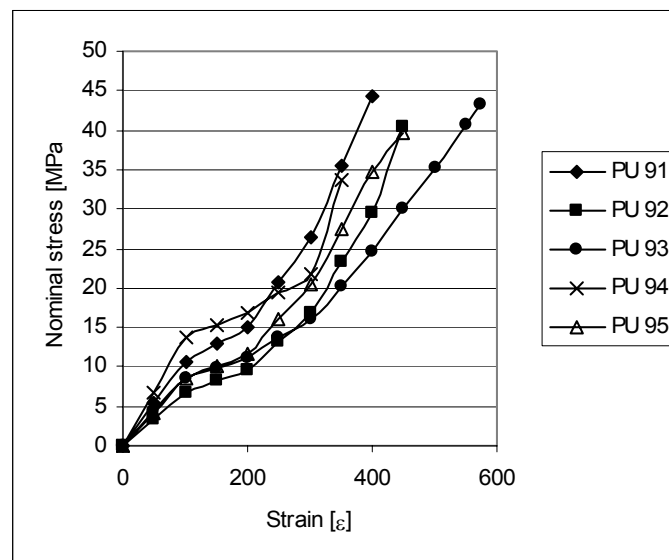


Figure 2. Nominal stress vs. Strain for the series of PUs of Table 1

As seen in Figure 2, the studied PUs exhibit a different stress-strain behaviour regarding the proportionality between the increase of stress and the resulted degree of deformation. Thus, in general it ascertains that the materials with hard segments based on DBDI (PU 1) display a higher resistance in the first deformation phases, followed then by values of strain which necessitate smaller stress increments. This phenomenon seems to be correlated to the appearance of better structured hard segment domains, in the case of the DBDI-EG couple, determined by their more advanced tendency to associate in hard crystalline zones which are preferentially affected in the first steps of the PU deformation. By contrast, PU 2 based on MDI, which contains hard segments of the MDI-EG structure type, in which the crystallinity is practically absent, exhibit a more constant proportionality between the enhance of the stress and the resulted degree of deformation. With regard to the copolymers which contain mixtures of

DBDI and MDI, they generally exhibit a intermediary behaviour. The best advantageous network organization is retained in the case of PU_{C1}, when MDI and DBDI were mixed together prior to the synthesis. It also observes that the most easy deformable networks were obtained when DBDI was added after the formation of the prepolymer with the structure MDI-PEA-MDI.

3. Conclusions

New contributions have been brought to the study of the thermoplastic polyurethanic elastomeric films prepared by using mixtures of isocyanates. In general, the properties of these polymers were similar to that obtained when in the synthesis it was used an isocyanate excess (index I was greater than 100) [1]. Mechanical and thermal improvement in PU properties with DBDI was retained when both diisocyanates are included, especially when reacted together in a random fashion, rather than sequentially by means of a prepolymer stage, whereas the values of PU residual elongation returned to that of a more conventional polyurethane, eliminating the major inconvenience derived from the high permanent deformability and high crystallinity which is undesirable for an elastomer measurements.

Acknowledgements: With many thanks to Professor Adrian A. Caraculacu, Institute of Macromolecular Chemistry "Petru Poni", Iasi, Dr Kayleen Campbell, University of Queensland and Dr. Paul C. Buckley, University of Oxford, for helpful assistance in the synthesis of polymers and TEM experiments.

REFERENCES

- [1] Prisacariu C., Olley R.H., Caraculacu A.A., Bassett D.C, Martin C., *Polymer* 44, 2003, 5407-5421.
- [2] Hepburn C., *Iranian Journal of Polymer Science & Technology*, vol. I, No.2, 1992, 84-108.
- [3] Oertel G., *Polyurethane Book*, Munich: Hanser Publishers, 1985.
- [4] Caraculacu A. et al., *Romanian Patent* 6578/27.07.1977.
- [5] Geanau L., Caraculacu et al. "*Proces tehnologic de fabricare a Moldotanului D*" - Institute of Macromolecular Chemistry 'Petru Poni' Iasi, 1978.
- [6] Prisacariu C, Buckley C.P, Caraculacu A., *Polymer*, (2005); 46(11): 3884-3894

Received December 12, 2005

¹The Romanian Academy's Institute of Macromolecular Chemistry "Petru Poni", Iasi, Romania

MODIFICĂRI INDUSE DE SOLICITĂRI DE ÎNTINDERE STATICĂ ÎN FILME POLIURETANICE TERMOPLASTE

REZUMAT Scopul acestei lucrări a fost acela de a studia modificările induse prin solicitări de întindere statică asupra unor noi tipuri de filme poliuretanic termoplaste (PUs) având la bază un izocianat și/sau combinații ale acestora. PUs cu diferite structuri au fost sintetizați prin utilizarea a doi izocianați cu geometrie diferită: (MDI)- 4,4'-metilenebis-fenilizocianat) ce prezintă o geometrie rigidă și respectiv izocianatul flexibil DBDI (4,4'-dibezil diizocianat). Scopul acestei lucrări a fost acela de a determina modul în care proprietățile mecanice la întinderea PUs se modifică în cazul în care linearitatea macromoleculii nu mai este perturbată de utilizarea unui exces de grupe izocianice, permițând astfel o mobilitate crescută a macromoleculilor individuale. PUs având la bază segmente dure pe bază de un singur izocianat (DBDI) prezintă o rezistență mecanică mai mare în primele etape ale deformării, urmată ulterior de valori ale deformației care necesită creșteri mai mici ale tensiunilor de întindere. Prin contrast, în cazul PUs pe bază de MDI, care conțin segmente dure cu o geometrie rigidă, cristalinitatea este practic absentă și polimerii de acest tip prezintă proporționalitate între creșterea tensiunii și gradul de deformație produs.

FOREVER YOUNG AND GREEN, STEEL WILL BE IN THE FUTURE A SUSTAINABLE MATERIAL

BY

MARIA NICOLAE¹, MIRELA SOHACIU¹, DIANA PARPALA¹,
AVRAM NICOLAE¹

ABSTRACT. *The steel is one of the few materials that satisfy largely the claiming of sustainable development concept.*

Firstly, because it is a performant material due to high values of technological properties it is practically indispensable for all building industries.

Secondly, because is young: the steel making technologies are in a continuous perfecting.

At the third place, because is green: steel in the form of scrap, it is almost entirely recyclable.

KEYWORDS: *eco-material, (green material), advanced material, performant material, steel, metallurgical technologies.*

1. INTRODUCTION

Because, has some of the highest values for the utilization (technological) properties and characteristics and is used practically in all domains, steel is considered the first “**sustainable material**”. This new conception about what would mean the notion of material for the next generations determines us to assume that the sustainable (development) material is a larger category than “advanced material” or “ecological material (eco-material)”.

In our opinion the sustainable material is a complex idea emerging the strains imposed by the three materials’ categories: *performant material*, *eco – material* (green material) and *young material* (perfectible material).

The performant material quality is given by the fact that the steel is and will be for the next generation the *metallic vector developing the principal* direction of a modern economy. Achieving such a quality is explained primarily by designing and elaborating new steel brand with *tremendous properties*.

The wide variety of mechanical and technological properties of the new steel brand allow to the designing companies to obtain elevated final properties for the most demanding beneficiary.

2. DISCUSSIONS

Some of these new brands has been taken into consideration for different European projection demonstrating the steel potential to any type of construction in high industry mentioned above.

- In the *automobile industry* the steel provides:
 - the comfort, in all respects;
 - long working life by high values of fatigue and corrosion resistances;
 - the decrease of the gasoline and oils consumption as a logical result of the whole assembly lightening;
 - the decrease of the wastes amount at the end of their economic life and the increase of the recycling level;
 - the increase of the construction reliability;
- In the *branch of metallic constructions* it was demonstrated that steel selling prices rise much slower than the resistance of the material for mechanical (sub) assemblies.
- *The household utensils* for induction or microwaves heating are manufactured today generally from special steels with Joule effect remarkable values;
- The stainless steel is used on a large scale in the agricultural-food industries because it meets all requirements of this sector;
- The European norms concerning the unpollution of the exhaust gas(es) from the vehicles and industrial furnaces determine the use of high amounts of special steels resistant to high temperatures and corrosion;
- The exceptional corrosion resistance, the increased mechanical characteristics and the good moulding capacity make steels the most suitable materials for the *transport assemblies*;
- Steel became an indispensable material for *electrical motors* because of its magnetic and electric properties;
- The *antiphonic protection* (“the world of silence and anti-vibrations”) requires special steels for sandwich plates used in the constructions coating to protect them against sounds, noise and vibrations;
- The *constructions coating* with steel prevarnished with esthetic and resistant foils is also a new orientation of steels utilization in the building industry;
- The branch of *metallic packages* profits by some special steel properties.

The eco – material quality (green material) is underlined by large number of aspects as:

- the fabrication technologies which are the object of a wide strategy, policy and ecologising measures;
- by its product, steel, the steel industry creating the necessary condition for application *the environmental quality and quality of life standards*.
- the objective that has to reach by the *social engineering* is realized today using the steel on large scale.

- as scrap iron the steel is recyclable; most specialists do not consider scrap iron as scrap but as raw material.
- the globalization of steel industry creating condition for diminishing the poisoning.
- by its recycling the steel ensures the next generation reserves of natural metals.
- the steel industry is a field providing a lot of working places at a high level of personnel qualification.

The *eco-material quality* is certified by the fact that in metallurgy the researches of reducing pollutant energetical consumption consequently to economize primary energy supply.

In metallurgy are used different sources of energy. The *primary energy sources* are those expandable and non-recoverable constituents of the natural capital, generating energy. The *primary fuels (fossil)* represent the main source of primary energy used in metallurgy. The *primary energy*, E_p is the energy contained in the *deposit*, the primary source of energy. For making the difference between sources, it is measured in $[J]_p$ or $[Wh]_p$. Its value is:

$$E_p = M_z \times P_c$$

in $[J]_p$ or $[Wh]_p$ /deposit.

The young material quality can be proved by consideration as:

- The steel industry is a branch that is self perfecting permanently improving its scientific- technological possessions.
- *Steel and siderurgy base their evolution on industrial fitness.*

As an element of the sustainable development, the industrial fitness represents the model by which an industrial segment remains permanently present and necessary. The industrial fitness is, shortly, the method by which an industrial branch keeps its youth, for the metallurgists this being not an age problem but a question of inner attitude. To be forever young from the industrial point of view by using fitness means to be never finished, to learn permanently, to try all the time something new even some times the things go wrong.

Steel and industry will remain young long time, because the fitness used for their evolution is already projected on modern goals, as:

- practically, the complete recycling of steel, which is a classical example eco-material;
- the most advanced branches cannot plan the added value without steel utilization, a material with remarkable application characteristics; in this context, one can that the fitness-base "training" is owned in siderurgy firstly to the pressure exerted by the top industrial branches;
- the siderurgy develops its partnership both upstream and downstream on modern and efficient principles of management and marketing; the new generations of steels are designed function of the customers;
- the remarkable technological innovations and engineering services concerning both the development of the new steel products and construction of new aggregates and installations are the base of the economical success in siderurgy; the research activity demonstrates that innovation potential is not in the least exhausted;

- in the context of a health global economy, the siderurgy does not necessitate state support, its aim being only a correct and ordered legal framework;
- the development based on modern fitness means robustness and perseverance (some times even stubbornness); face to face with a challenge provoked by the disadvantages of the supplying market, restrictions of ecological nature and existant political-economical instability, the siderurgy was “stubborn”, we can say it was even “refractory” and always has returned spectacularly.
- A qualitative leap is registered also in the field of the *new siderurgical deontology*.
- *The siderurgy turns from an exclusive materials provider into a systems provider.*

Changes take place inside the branch too. In the future, the associated members will deliver not only steel of different sizes with various alloying degrees but, often and often, steel structures too. The steel industry will go beyond the tradition to a certain extent. The separated until now levels of values making merge and form higher units.

- *The attitude towards the mass-media is permanently improved.*

Our industry has problems related to its impact with the fourth power of the contemporary world-the mass-media-and its utilization.

The steel publicity had a technical, dry character until now. The people have also an emotional level and for this reason they must be addressed properly, in order to obtain an as high as possible horizontal effect, thus making deeper the product between a positive action and its emphasising in different ways.

REFERENCES

1. “Dezvoltare durabilă în siderurgie prin valorificarea materialelor secundare”, Ed. Printech, București, 2004, Nicolae, Maria, Tudor, P., Predescu, C., Licurici, M., Serban, V., Mândru, C., Calea, G., G., Ioana, A., Sohaciu, Mirela, Semenescu, Mihaela, Parpala, Diana, Nicolae, A.
2. Ciocănea, A. – “Dezvoltarea socio-economică durabilă și metabolismul sistemelor industriale”, În vol. “CNDD”, București, 2003, p. 41-46.
3. Ameling, D.- “Oțelul – material inovator”, În “Stahl & Eisen”, 1999, nr. 6, p. 83.

Received December 12, 2005

“POLITEHNICA” UNIVERSITY OF BUCHAREST.

“ÎNTOTDEAUNA TÂNĂR ȘI VERDE, OȚELUL VA FI ÎN VIITOR UN MATERIAL DURABIL.”

REZUMAT. Oțelul, este unul dintre puținele materiale care satisfac pe deplin pretențiile conceptului de dezvoltare durabilă.

În primul rând deoarece este un material performant, datorită valorilor ridicate ale proprietăților tehnologice și este practic indispensabil pentru industriile constructoare.

În al doilea rând deoarece este tânăr tehnologiile de fabricare ale oțelului sunt într-o continuă îmbunătățire.

În al treilea rând deoarece este tânăr oțelul în forma de fier vechi este reciclabil aproape complet.

STUDIES ABOUT THE COOLING CHARACTERISTICS OF THE POWDER BACKING IN FLUIDIZED BED TIP SALT, FERRO-MANGANESE PARTICLES, CAST-IRON SPLINTERS BARBOTAGED WITH AIR

BY

NEJNERU CARMEN¹, BERNEVIG MIHAI¹, CARABET ROXANA¹, HOPULELE ION¹

ABSTRACT. *The paper presents the researches on the cooling thermal transfer in fluidized beds. There were used for the experiments three types of particles: 1) salt with size of particles $1400 < d_p < 3000$ [μm]; 2) ferro-manganese particles with size $1200 < d_p < 1400$ [μm]; 3) cast-iron splinters. The cooling curves were drawn with a silver control cylinder within a chromel-alumel thermocouple connected to an y-t recording apparatus.*

KEYWORDS: *fluidized bed, cooling velocity, cooling curve, heat transfer, salt, ferro-manganese particles, cast-iron splinters particles.*

1. Introduction

Fluidization is a technique in which a particle bed is brought into a condition where it behaves like a liquid, each particle being separated by the others through a gas stream. The fluidized bed is a heterogeneous, non-adiabatic system where the solid particles are executing a continuous motion on the enclosure, under the influence of a turbulent beat of pulses of a fluid stream.

The nature, size and form of the solid particles belonging to the fluidized bed influence directly the structure and the characteristics of yield of fluidized bed.

The size of the particles is one of the most important parameters of the fluidization, both hydrodynamic and heat and mass change. For the achievement of an optimum fluidization it is necessary that the field scattering of the particles size must be as limited as it can.

The size of the particles influences directly the velocity of the fluidization (specially the minimum fluidization speed) which grows proportionally with d_p^2 , and also influences the pressure loss and specific weight of the layer.

In fluidization are used materials such as: sand, salt, cast-iron splinters, corundum, graphite, aluminum oxide and other particles which are physical and chemical stable at the work temperature. The volume weight of the particles determines the specific weight of the fluidized bed and influences the minimum fluidization velocity and also the loss pressure in the layer.

2. Objectives

The fluidized beds can be used in heat and thermo-chemical treatments as active mediums, as heating mediums, soaking steps, and also as cooling mediums.

The cooling velocity is an important parameter of the heat and thermo-chemical treatments.

The paperwork is presenting an experimental study concerning the cooling capacity of the fluidized bed using different solid backing and as fluidization agent: air.

Advantages comparing to salt baths:

- it is favorable for an uniform cooling but slow, being used lesser in hardening and more in annealing.

- it is non-toxic comparing to salt baths.

- it is easy to handle and to get, and there are needed simple installations easy to be upkeep.

- it do not consume and damage like salt baths (it must always be added substances in order to be built-up the percentage).

- it is cheaper than the salt baths, and easier to be maintained constant as properties.

As a disadvantage is the fact that they cannot be used for pieces bigger than 100 mm, the fluidization could be badly bred, the specific convection of the fluidized bed being clogged.

Conclusion:

- the most important advantage is that in certain circumstances they can replace the salt baths.

It was experimentally analyzed the factors which influence thermic transfer in fluidized bed.

3. Experimental results

In order to determine the cooling medium like fluidized bed, it was used a control cylinder from silver within a chromel-alumel thermocouple which permits temperature measurement with a recording apparatus y-t. The control cylinder is heated up to the desired temperature (800°C) and cooled down in the fluidized bed.

The silver test bar has the following sizes and characteristics:

$$\begin{aligned} \text{Ø} &= 13 \text{ [mm]}, h = 28 \text{ [mm]}, S = 1408 \text{ [mm}^2\text{]}, m = 39.9 \text{ [g]}, \rho_{\text{Ag}} = 10.5 \text{ g/cm}^3 \\ \lambda_{\text{Ag}} &= 418.5 \text{ W/m}\cdot\text{K} \end{aligned}$$

The equipment used in experimental determination of the cooling curves is formed from:

- air fluidization system;
- heating system of the silver test bar (circular pipestill with electrical resistance);
- measurement system represented by an y-t recording apparatus(with modification apparatus of the shifting rate of the recording apparatus);
- Transformer of the filling variation of the ventilator for modification the air velocity.



Fig.1 Equipment for the determination of fluidized beds cooling characteristics

At salt, ferro-manganese particles, cast-iron splinters there were used grain sizes $1200 < d_p < 1400$ where : particle diameter (the eye sieve) - in μm

The dusty environments mentioned before were fluidized with air.

The silver test bar was conducted in a circular pipestill until 800°C and then was introduced in the fluidized bed, the cooling curve being recorded by the y-t recording apparatus.

For each cooling environment was calculated:

- the maximum and medium cooling velocity;
- global factor of heat transfer;

$$\alpha_g = \frac{\alpha_1 \cdot \Delta t_1 + \dots + \alpha_s \cdot \Delta t_s}{t_{total}} ; \text{ where: } \alpha_i = \frac{3600 \cdot m \cdot c}{\Delta t_i \cdot S} \ln \frac{T_i - T_o}{T_f - T_o} \text{ [w/m}^2\text{k]}$$

where:

$m=0,0399$ Kg, the test bar weight;

$c=0,056$ Kcal/Kg, specific heat capacity at silver;

$S=0,001408$, the test bar surface;

Δt , sec= time interval;

$T_i, T_f, ^\circ\text{C}$ the initial and final temperature interval;

T_o environment temperature;

- cooling intensity $H = \frac{\alpha_g}{2\lambda} \text{ [m}^{-1}\text{]}$

$$\lambda_{Ag} = 418,5 \text{ w/mk}$$

The results have been written in tables where we can find cooling intensities(H)

All the studied environments are for annealing (they cannot be used for hardening because of the small cooling velocities)

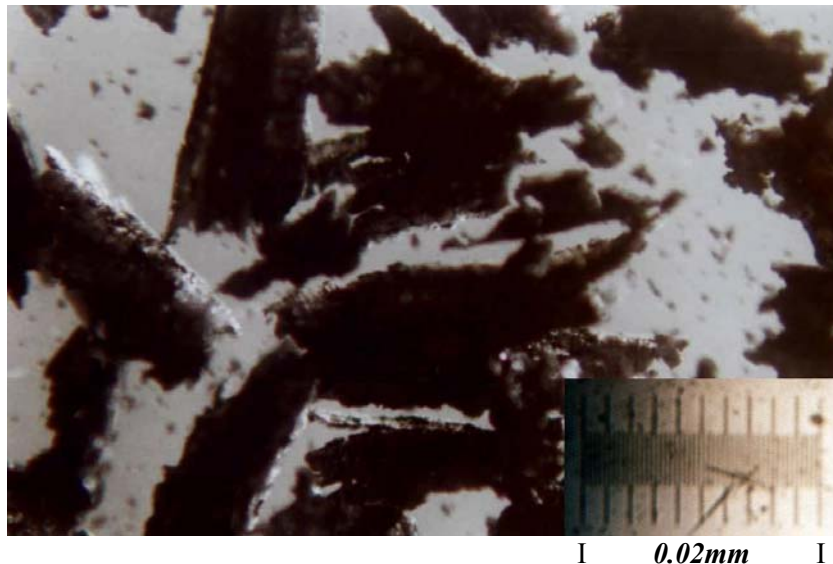


Fig.2 Cast-iron splinters

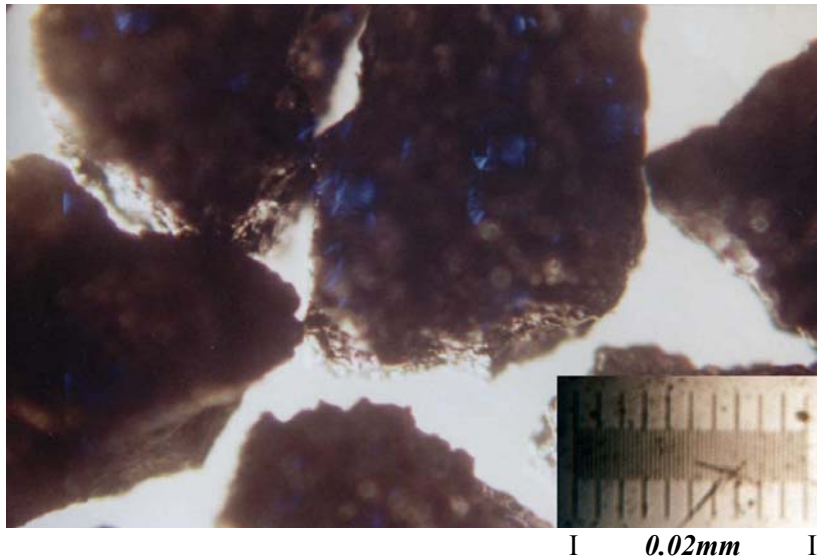


Fig.3 Ferro-manganese particles

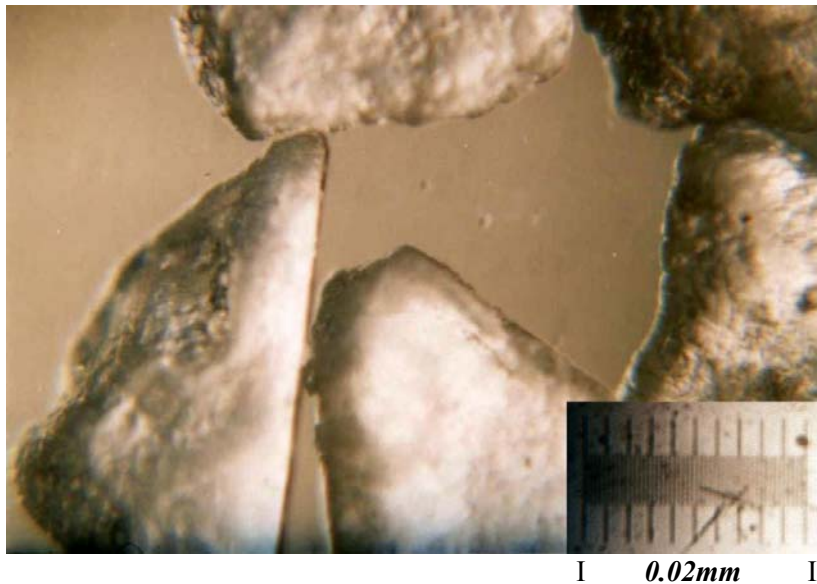


Fig.4 Salt particles

3. Conclusions

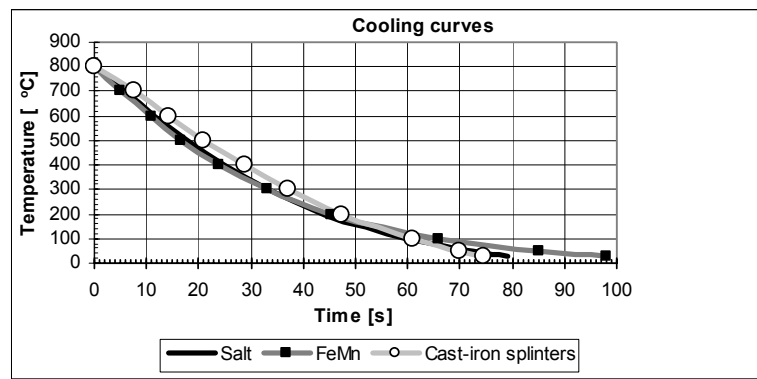
Observing the graphs we can notice the cooling particularities in those three types of powder.

As a first step, the salt, being a good insulator, absorbs the heat from the test bar and yields it when the cooling velocity gets slower.

The form and the irregularity of the salt grains, Fe-Mn particles and cast-iron splinters have an important influence; the form of the salt grains is semi-elongation with amount of crown. Fe-Mn particles have the same form, but cast-iron splinters have a irregular form like needle that make to lose heat more than salt and Fe-Mn particles. The cast-iron splinters have a heat transfer more intense than salt and Fe-Mn particles which means that the velocity is more uniform on intervals by firstly absorbing the heat and then yielding the heat. The process is very intense so that the cooling velocity in cast-iron splinters is the smallest.

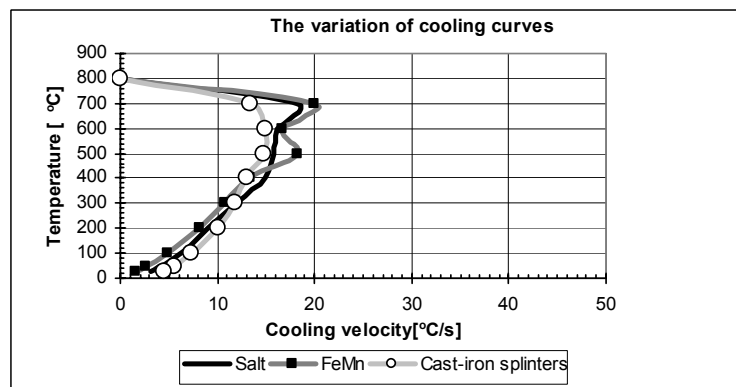
The cooling curves for salt, FeMn and cast-iron splinters

T [°C]	salt, t [s]	FeMn, t[s]	cast-iron	T [°C]
800	0	0	0	800
700	5.5	5	7.5	700
600	11.7	11	14.2	600
500	18	16.5	21	500
400	24.7	24	28.7	400
300	33	33.25	37.2	300
200	44	45.5	47.2	200
100	60	66	61	100
50	72.5	85	70	50
30	79	98	74.5	30



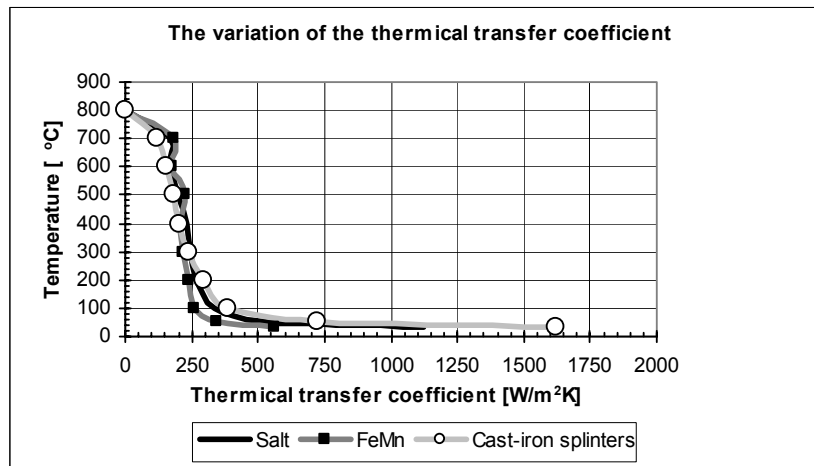
The variation of cooling velocities for salt, FeMn and cast-iron

T [°C]	salt	FeMn	cast-iron	T [°C]
800	0	0	0	800
700	18.18	20	13.33	700
600	16.13	16.67	14.93	600
500	15.87	18.18	14.71	500
400	14.93	13.33	12.99	400
300	12.05	10.81	11.76	300
200	9.09	8.16	10	200
100	6.25	4.88	7.25	100
50	4.00	2.63	5.56	50
30	3.08	1.54	4.44	30



The variation of thermic transfer coefficient

T [°C]	salt	FeMn	cast-iron	T [°C]
800	0	0	0	800
700	165.30	181.8	121.2	700
600	170.00	175.7	157.3	600
500	199.10	228	184.4	500
400	231.10	206.4	201.1	400
300	243.80	218.8	238.1	300
200	266.20	239	292.8	200
100	335.90	262.1	389.4	100
50	520.00	342.1	722.2	50
30	1120.10	560	1617.9	30



References

1. C. Samoila, M.S. Ionescu, C. Druga - Tehnologii si utilaje moderne de incalzire metalurgie, Editura Tehnica, Bucuresti, 1986

Received December 12, 2005

¹TECHNICAL UNIVERSITY "GH. ASACHI" IASI

STUDII PRIVIND CARACTERISTICILE DE RĂCIRE ÎN PAT FLUIDIZAT A MEDIILOR PULVERULENTE TIP SARE, FEROMANGAN, SPAN DE FONTA BARBOTAT CU AER

REZUMAT: Lucrarea prezintă cercetările experimentale asupra transferului termic la răcire în medii pulverulente barbotate cu aer.

Pentru experimente s-a folosit sare, feromangan, span de fonta cu mărimea granulelor (diametrul mediu al particulei) variind în intervalul: $d_p \in (1200 \div 1400) \mu m$.

Curbele de răcire au fost tratate cu ajutorul unei epruvete de argint cu termocuplu înglobat și conectat la un inceptor y-t.

WORKED EXAMPLES IN THE FIELD OF HOT ISOSTATIC PRESSING

BY

VIRGIL GEAMĂN¹, VASILE JIMAN¹

ABSTRACT. Hot isostatic compression involves the simultaneous application of pressure and elevated temperature to materials. The pressure applied, usually by a gas, is isostatic because it's developed in a suitable pressurized vessel by a fluid (even a gas is a fluid). Under these conditions of heat and pressure, internal pores or defects within a solid body or a powder compact collapse and weld up. Encapsulated powder and sintered components densify easily and faster than due to sintering alone. Therefore HIP (hot isostatic pressing) is today used for a lot of applications, like upgrading castings (removing shrinkage pores in interdendritic space), densifying pre-sintered components, consolidation of powders and interfacial bonding. In this paper we try to give two worked examples used in the field of HIPping applications.

KEYWORDS: HIP, compression mechanism, full density.

1. INTRODUCTION

The principle feature of HIP is described below: a component is put into a vessel which can be pressurized by a gas (usually argon, but in special cases also helium or nitrogen). The whole vessel is heated up to approximately 0.8 of the absolute melting point of the material. The very hot gas is then under very high pressure such that it acts like a hot forge isostatically. Typical gas velocities are around 1000 m/s and one can calculate from the kinetic theory of gases, assuming ideal gas laws to hold, that 10^{30} collisions square meter and second occur on the component walls. The density of the gas used usually increases considerably (such that even ideal gas laws may not further be applicable). For instance argon, which has a density at standard conditions of 1.8 kg/m³ will have a density of 370 kg/m³ under HIPping conditions at 1500 K and 1000 atm.

2. BREAKDOWN IN THE IDEAL GAS LAWS UNDER THE TEMPERATURES AND PRESSURES USED IN HIPping.

Question

For the ideal gas laws to apply, the following requirements must be met:

- the attraction between gas atoms or molecules must be negligible;
- the volume of the atoms or molecules must be negligible in comparison with the volume occupied by the gas;
- the atoms or molecules must behave like perfectly elastic spheres;
- the duration of their collisions must be negligible in comparison with the time between collisions.

The intention here is not to prove that the ideal gas laws break down during HIPing but rather that the conditions developed are such that the above conditions are unlikely to apply. Calculate the mean atom spacing in argon gas under STP (STANDARD TEMPERATURE AND PRESSURE - i.e. 298 K and 1 atm.) conditions and compare this with the mean spacing under typical HIPing conditions of 1000 atm. and 1500 K. Calculate the density of argon under these conditions given that the density at STP is 1.8 kgm^{-3} .

Answer

Under STP (i.e. 298 K and 1 atm.) the atom spacing d_1 is given by

$$d_1 = \left(\frac{\text{volume occupied by 1 mol at STP}}{\text{number of atoms in 1 mol}} \right)^{\frac{1}{3}} \quad (1)$$

$$d_1 = \left(\frac{22,4 * 10^{-3}}{6 * 10^{23}} \right)^{\frac{1}{3}}$$

$$d_1 = 3,4 * 10^{-9} \text{ m} \quad (2)$$

$$d_1 = 34 \text{ \AA}$$

This compares with an atom spacing of about 2 \AA in solids. Assuming that the ideal gas laws apply (an assumption which is not in fact justified), then the volume V_2 of 1 mol of gas under HIPing conditions can be obtained from:

$$\frac{p_1 V_1}{T_1} = \frac{p_2 V_2}{T_2} \quad (3)$$

where: $p_1 = 1 \text{ atm}$, $V_1 = 22.4 \times 10^{-3} \text{ m}^3$, $T_1 = 298 \text{ K}$, $p_2 = 1000 \text{ atm}$. and $T_2 = 1500 \text{ K}$.

$$V_2 = \frac{p_1 V_1 T_2}{p_2 T_1}$$

$$V_2 = \frac{1 * 22,4 * 10^{-3} * 1500}{1000 * 298} \quad (4)$$

$$V_2 = 1,1 * 10^{-4} \text{ m}^3$$

The atom spacing d_2 under HIPing conditions is then given by:

$$d_2 = \left(\frac{\text{volume occupied by 1 mole under HIPping conditions}}{\text{number of atoms in 1 mol}} \right)^{\frac{1}{3}}$$

$$d_2 = \left(\frac{1,1 * 10^{-4}}{6 * 10^{23}} \right)^{\frac{1}{3}} \quad (5)$$

$$d_2 = 6 \text{ \AA}$$

Despite the fact that this calculation requires an assumption that the ideal gas laws do in fact apply, when the result shows that strictly they cannot, it does illustrate that the atomic spacing in the HIPing gas is much closer to that of a solid or liquid than to that of a gas at STP. Given the density at STP of 1.8 kgm^{-3} for argon, and the fact that, from the above calculation, the volume is reduced by a factor of $1.1 \times 10^{-4} / 22.4 \times 10^{-3}$ between STP and HIPing conditions the density ρ_2 under HIPing conditions will be:

$$\rho_2 = \frac{\text{mass}}{\text{volume}}$$

$$\rho_2 = \frac{1,8}{1,1 * 10^{-4} / 22,4 * 10^{-3}} \quad (6)$$

$$\rho_2 = 370 \text{kgm}^{-3}$$

This should be compared with the density of water which is 1000 kg m^{-3} . Since increasing the pressure increases the density while increasing the temperature reduces it, there is in fact a temperature at which the argon density is a maximum. This occurs at around 733 K for a pressure of 1000 atm. and the density then is approximately equivalent to that of water.

Where the ideal gas laws break down at high pressure the Van der Waals equation is used:

$$\left(p + \frac{a}{V^2}\right)(V - b) = RT \quad (7)$$

where: a and b are constants and $R = 8.314 \text{ Jmol}^{-1} \text{ K}^{-1}$.

3. CALCULATION TO INVESTIGATE WHETHER MICROWELDING AT MICROSCOPIC POINTS OF CONTACT IS FEASIBLE

Question

Using the Clausius-Clapeyron equation which allows the change ΔT in a melting point due to the application of pressure to be calculated, find the change in melting point for 1 kg of iron if the HIPing pressure is 100 MPa. The Clausius-Clapeyron equation is

$$\frac{\Delta T}{T_m} = \frac{\Delta p \Delta V}{\Delta H_m} \quad (8)$$

where: - T_m is the melting temperature;

- Δp the difference in pressure between STP and HIPing pressure;

- ΔV the change in volume on making the transition from solid to liquid at the melting point;

- ΔH_m the latent heat of fusion. (For iron the density is 7860 kgm^{-3} , $\Delta H_m = 27 \cdot 10^4 \text{ Jkg}^{-1}$, $T_m = 1808 \text{ K}$ and $\Delta V/V = 3\%$ at the melting point).

Comment on whether microwelding would ever take place in HIPing and in what other situations it might occur.

Answer

Since $\Delta V/V = 3\%$ then $\Delta V = 0.03V = 0.03m/\rho$; $m = 1 \text{ kg}$ from above and $\rho = 7860 \text{ kgm}^{-3}$; hence $\Delta V = 0.03/7860$. Then substituting values in the Clausius-Clapeyron equation gives:

$$\Delta T_m = \frac{T_m \Delta p \Delta V}{\Delta H_m}$$

$$\Delta T_m = \frac{1808 * 10^8 * 0,03}{27 * 10^4 * 7860} \quad (9)$$

$$\Delta T_m = 2,5K$$

Typically for iron the HIPing temperature is at least 200 K below the melting point. Therefore the local pressure at the contact points would have to be at least two orders of magnitude higher than the HIPing pressure in order to lower the melting point sufficiently for microwelding to occur. In practice, this would never take place because such a high local concentration of stress would lead to yielding. Microwelding could occur in situations such as DPC – DYNAMIC POWDER COMPACTION where localized frictional heating can lead to surface melting.

4. CONCLUDING REMARKS

There are a lot of phenomena that occur to make a good practice for industrial application in the field of HIPing consolidation for metallic or ceramic materials. But these phenomena are very difficult to be controlled. In the last years a lot of scientist are trying to give more details in this field to help the designers to have more complete data bases.

REFERENCES

1. Atkinson H.V. and Rickinson B.A. – *Hot Isostatic Processing*. Adam Hilger Series, U.K. 1991.
2. Frost H.J. and Ashby M.F. - *Deformation Mechanism Maps*, Pergamon Press, Anglia, 1982.
3. Geamăn V. and Varga B.- *Cold and Hot Isostatic Pressing Diagrams for Aluminum Alloys*, in microCAD'94, Miskolc, Hungary, Vol. C, pag. 17 - 24.
4. James P.J - *Isostatic Pressing Technology*, in *Metals and Materials*, Nr. 10/1992 pag. 541 - 546.
5. Swinkels F.B. s.a. - *Mechanisms of Hot Isostatic Pressing*, in *Acta metallurgica*, Vol.39, Nr. 4/1991, pag. 641 - 649.

Received December 14, 2005

¹Transilvania University of Braşov

APLICAȚII PRACTICE CU EXEMPLIFICĂRI ÎN DOMENIUL COMPACTĂRII IZOSTATICE LA CALD

REZUMAT: Compactarea izostatică la cald impune aplicarea simultană asupra materialelor a presiunii și temperaturii. Presiunea izostatică se aplică uzual unui fluid, de obicei unui gaz într-o incintă de presare. În aceste condiții de încălzire și presare simultană, o serie de defecte interne ale materialelor se elimină sau se remediază (eliminarea porilor, sudarea microretasurilor, etc.). Deoarece compactitatea corpurilor crește rapid comparativ cu sinterizarea, aplicarea compactării izostatice la cald are o serie întreagă de aplicații cum sunt: compactarea pieselor turnate, compactarea pulberilor, a componentelor presinterizate, etc.

Lucrarea tratează două exemple ale aplicațiilor concrete ale consolidării materialelor prin presare izostatică, care vin în sprijinul proiectanților care se ocupă de acest domeniu.

RESEARCHES CONCERNING THE ANALYSIS OF CASTING SOLIDIFICATION USING THE REAL SOLIDIFICATION MODULE

BY

CIOBANU IOAN¹, MUNTEANU SORIN ION¹, CRISAN AUREL¹

ABSTRACT: In the paper there are presented the results of a research about casting solidification analysis using the real solidification modules method. It is analyzed the solidification of a casting from the range of small wheels. Based on the values of real partial solidification modules of the elements that compose the wheel and of the runner it was evidenced the possibility to realize an uniform solidification or a directional solidification, with the but of obtaining castings without defects caused by solidification. It is highlighted that in some situations the elimination of shrinkage in the wheel hub it is only possible by using heat insulated runners.

KEYWORDS: casting, solidification module

1. Introduction

The casting solidification analysis based on real solidification module is applied in casting technology design as result of the following advantages: need simple calculation accessible for medium level designer; can evidence the solidification orientation; do not need investments in hardware and software.

The notion of solidification module (M) for castings defined by N. Chvorinov [4, 5] is expressed throw:

$$M = \frac{V}{S} \quad (1)$$

where: V represent the casting volume; S- casting area in contact with the mould, surface passed by the heat flux from liquid alloy to mould.

In previous papers [1÷3] we evidenced the deficiencies of the equation proposed by N. Chvorinov. The deficiencies come from the fact that the equation (1) is based on an ideal hypothesis that specific heat transfer has the same intensity on the entire surface of the casting. As result we defined the **real solidification module** of casting. This can be calculated throw equation:

$$M = \frac{V}{\sum_{i=1}^{i=n} k_i \cdot S_i} \quad (2)$$

where V represent the casting volume; n – number of casting surfaces; S_i – area of the surface with the index “i”; k_i – the cooling coefficient corresponding to surface S_i.

This relation considers the real conditions of heat transfer inside the mould. The cooling coefficient k_i considers the real contribution of each surface of casting in contact with mould at heat transfer liquid alloy-mould during solidification. For the surfaces where the heat transfer develop normally (large plane surfaces situated far away from walls or other castings) this coefficient has the value $k_i=1$. In the case of part surfaces throw which the heat transfer part-mould during solidification is attenuated (partially or entirely) by local saturation in heat of the mould wall (as example in the case of very thin cores, in the case of other parts vicinity or by reason of local using of heat insulated materials) the coefficient k_i has values less than one ($0 \leq k_i < 1$). In the case of the surfaces throw which the heat transfer part-mould during solidification is intensified (as example in the case of surfaces in contact with external coolers) the coefficient k_i has values more than one ($k_i > 1$).

The value of the cooling coefficient depends on the following factors: casting geometry and dimensions; thermal properties of mould walls; initial temperature of mould walls; number of casting simultaneously cast in a mould and the distance between them; the position of feeders and gating system in rapport with part.

The cooling coefficient values for some practical situations encountered in moulds (plane walls or plane plates parallel situated in the same mould, bars with U section) were determined based on previous researches about solidification simulation on computer [2,3,6]. There were determined too the equations to calculate the cooling coefficients in the case of variation of the mould walls thermo-physic characteristics (using coolers or thermo insulated materials) and in the case of temperature variation of the mould walls [7, 8].

2. Paper target

In this paper there are presented the results of a research about the using of **real solidification module method** to analyze the solidification of casting when it pursue to obtain uniform or directional solidification. The research was realized for the case of small wheels cast in sand moulds.

In the figure 1 there is presented the sketch of the cast wheel studied. This is composed by the three constructive

elements specific to this group of parts: hub, rim and disk that connects these. The geometry of this kind of parts is characterized in function of the walls thickness for the three elements, and the rapport between wall thickness and the radius of the elements (relative walls thickness). The small wheels are characterized by small radius and high thickness of the walls. The wheel presented in figure 1 has uniform thickness of the walls. This construction was conceived in the intention to obtain a uniform solidification and to avoid concentrated shrinkage at solidification. The solidification

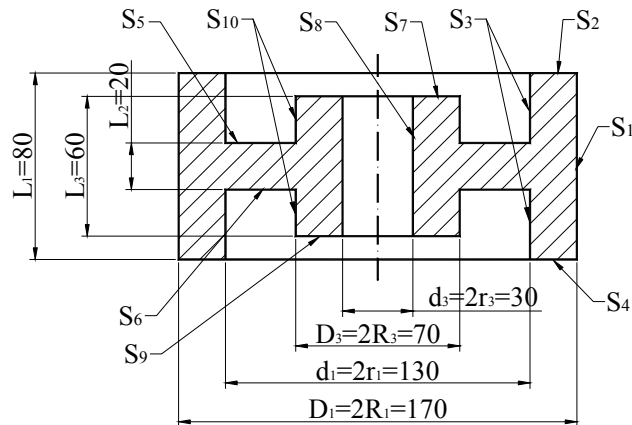


Fig.1. Small dimensions cast wheel. Sketch to compute solidification modules

analysis for this part is done calculating the partial solidification modules of the three zones rim, disk and hub.

In the research were analyzed many variants of casting, constructive and technological. From space limit consideration, in this paper are presented only the variants which assure to obtain casting without defects caused by solidification.

3. The solidification analysis for a wheel with uniform wall thickness

In a first variant were analyzed the real solidification partial modules of the three elements of part having the geometry and dimension from figure 1. In the real solidification modules calculation it was considered that the molding batch inside the hub and that between hub and rim strongly heat because of the small diameter of the core (d_3) and small width of the disk (r_1-R_3). As result the heat transfer from part to mould throw $S_8, S_{10}, S_6, S_5, S_3$ surfaces is diminished, and the cooling coefficients for this surfaces have values less then 1. In the table 1 there are presented the equations to calculate the real solidification modules and their values. There are presented too the cooling coefficients values for each surface of the part. In this variant the real solidification modules were calculated without considering the gating system. The research evidenced that, generally, the presence of the pouring gate has a small influence on the real solidification modules by reason of small section of the runner.

Table 1. Real solidification modules of the wheel zones from figure 1 computed in the hypothesis of no gate system, no feeders and coolers.

No.	Part zone	The equation to calculate the real solidification module	Cooling coefficient value	Real module value [mm]
1	Rim	$M_1 = \frac{V_1}{k_1 S_1 + k_2 S_2 + k_3 S_3 + k_4 S_4}$	$k_1=1, k_2=1$ $k_3=0,75, k_4=1$	9,43
2	Disk	$M_2 = \frac{V_2}{k_5 S_5 + k_6 S_6}$	$k_5=0,5, k_6=0,5$	20
3	Hub	$M_3 = \frac{V_3}{k_7 S_7 + k_8 S_8 + k_9 S_9 + k_{10} S_{10}}$	$k_7=1, k_8=0,5$ $k_9=1, k_{10}=0,5$	13,95

Analyzing the results from table 1 there is highlighted that even the wall thickness is uniform, this geometry is entirely non technological by casting point of view. Because the real solidification module of the disk is much higher than the real solidification modules of others elements (hub and rim), the hub and rim solidifies faster then the disk between them. So the feeding of the disk with liquid alloy during solidification is cut off anywhere will be the pouring gate or feeders, on the hub or rim. As result inside the disk it will appear a concentrated shrinkage. This shrinkage can be eliminated in two kinds by modifying the part solidification: assuring uniform solidification conditions or using feeders and assuring a directional solidification to these.

4. Assuring uniform solidification

To obtain uniform solidification for this casting it is necessary that the real solidification modules to be equal for the three elements of the casing. In this but it is necessary to reduce the disk thickness at half ($L_2=10\text{mm}$) to diminish the real

solidification module at a value nearest of the others elements module, so it is shown in figure 2. Diminish of the disk thickness determine in the same time a small diminish of the real solidification module of the hub because its external surface is increasing (S_{10}). In the table 2 there are presented the equations to calculate the real solidification modules for wheel parts from figure 2 in the conditions of reducing the disk thickness at $L_2=10\text{mm}$ and without gating system.

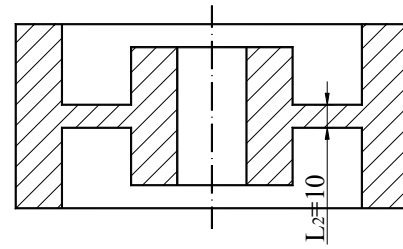


Fig.2 The sketch of the wheel with disk thickness diminished in the view of uniform solidification

Table 2. The real partial solidification modules for the wheel elements from figure 3, computed in the conditions of reducing the disk thickness at $L_2=10\text{mm}$, without gating system and without feeders or coolers

No.	Part zone	The equation to calculate the real solidification module	Cooling coefficient value	Real module value [mm]
1	Rim	$M_1 = \frac{V_1}{k_1 S_1 + k_2 S_2 + k_3 S_3 + k_4 S_4}$	$k_1=1, k_2=1$ $k_3=0,75, k_4=1$	9,08
2	Disk	$M_2 = \frac{V_2}{k_5 S_5 + k_6 S_6}$	$k_5=0,5, k_6=0,5$	10
3	Hub	$M_3 = \frac{V_3}{k_7 S_7 + k_8 S_8 + k_9 S_9 + k_{10} S_{10}}$	$k_7=1, k_8=0,5$ $k_9=1, k_{10}=0,5$	10,62

It is observed that by diminish the disk thickness, the real solidification modules for the three elements of the wheel become quite equals, that assure practically simultaneously solidification. So, the concentrated shrinkage that appear in the disk is eliminated.

In this research was analyzed too the casting solidification when it is considered the presence of gating system (for the disk thickness $L_2=10\text{mm}$). It was analyzed the case when the casting is feed throw a circular pouring gate with feeders symmetrically disposed on the exterior of the rim. The presence of feeder system near the rim modifies a little the cooling conditions throw the external surface of the rim (S_1). This area diminish with feeders section and the cooling coefficient for this surface became $k_1=0,9$ because the molding batch between rim and distribution canal is heated by the heat released by this one. In the presence of the pouring system, the real solidification modules for the elements of the wheel with thin disk ($L_2=10\text{mm}$) became $M_1=9,58\text{mm}$, $M_2=10\text{mm}$ and $M_3=10,62\text{mm}$. It can be observed that, considering the pouring gate, the real solidification module of the rim little augment comparing with the values from table 2, which correspond to a better uniformity in part solidification. In these conditions the part geometry assures the obtaining of casting without concentrated shrinkages and don't need feeder head. These constructive and technological variants represent an economic solution by small consumption of liquid alloy. However in the case of uniform solidification there is the tendency to appear micro shrinkage as axial porosity. The extension of this zone depends on the degree of compensation of the solidification contraction with liquid alloy from the pouring system and of the thickness of the casting walls.

5. Assuring directional solidification

To obtain a directional solidification of the casting it is necessary that the real partial solidification modules to increase continuous from one end to other end or from the middle to extremity. In this case for obtaining casting without defects it imposed that in the neighborhood of zones with the greatest solidification module to use feeders that feed these zones with liquid alloy during solidification. For this purpose the feeders must have solidification modules bigger then the neighbor zones.

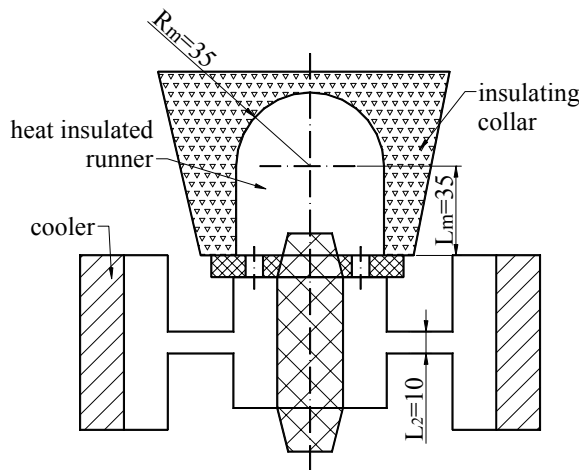


Fig. 3. Sketch to calculate real solidification modules in the conditions of the wheel with modified disk ($L_2 = 10$ mm), heat insulated feeder on the hub and an external cooler on the rim

In the case of the wheel analyzed it can be applied many variants of directional solidification. One of them is presented in figure 3. In this variant the solidification is directed from rim to hub by applying a cooler on the external surface of the rim and a feeder with thermo insulated cover placed on the hub. So the real solidification module of the rim decrease to become smaller then disk module. As result the rim solidifies before the disk.

The direct feeder placed on the hub determine an increasing of solidification module of the hub and as result a slowly solidification of this

one. The superior surface of the hub does not contribute to heat transfer casting-mould. The results and expressions for solidification modules as well as the cooling coefficients values in this case are given in table 3.

Table 3. The real solidification modules for the wheel from figure 4, computed in the conditions of reducing the disk thickness, using a heat insulated feeder on the hub and an external cooler on the rim.

No.	Part zone	The equation to calculate the real solidification module	Cooling coefficient value	Real module value
				[mm]
1	Rim	$M_1 = \frac{V_1}{k_1 S_1 + k_2 S_2 + k_3 S_3 + k_4 S_4}$	$k_1=10; k_2=1$ $k_3=0,75; k_4=1$	1,61
2	Disk	$M_2 = \frac{V_2}{k_5 S_5 + k_6 S_6}$	$k_5=0,5; k_6=0,5$	10
3	Hub	$M_3 = \frac{V_3}{k_8 S_8 + k_9 S_9 + k_{10} S_{10}}$	$k_8=0,5; k_9=1$ $k_{10}=0,5$	16,44
4	Heat insulated feeder	$M_m = \frac{V_m}{k_m S_m}$	$k_m=0,25$	58,33

It is observed that the real solidification modules values for the wheel elements and feeder are in the relationship $M_1 < M_2 < M_3 < M_m$ (M_m represent the solidification module of the feeder). A big gradient between this modules assure a strong directional solidification from rim to hub that represent a guaranty to obtain casting without

shrinkage. The values for the cooling coefficients for the surfaces where is applied the external cooler ($k_1=10$) and for the feeder surface in contact with thermo insulated material ($k_m=0,25$) were determined conform the dates from previous papers [9].

In the research was analised too the case of using a simple feeder on the hub (without thermo insulated cover). In this case the feeder has a real solidification module $M_m=14,58\text{mm}$ (for a coolig coeficient $k_m=1$). This value of the solidification module is smaller then the hub solidification module and so can not assure the shrinkage elimination from the hub.

5. Conclusion

The results of the researches presented in this paper lead to the following conclusions:

- In computing the real solidification modules must consider the saturation in heat of mould walls, as well as the position of gating system and feeders;
- The uniform solidification can be assured by modifying of the wall thickness of castings so to realize equal real solidification modules for all the casting elements;
- In the case of wheels that have the internal radius of the hub small in rapport with the thickness of the hub wall, the heat transfer throw its inner surface is strongly attenuated by reason of the saturation in heat of the core. For this reason the solidification module of the core has a higher value and simple feeders can't assure shrinkage elimination. In this case it is imposed to use heat insulated feeders or exothermal feeders that have a higher solidification module.

References:

1. **Ciobanu I., Munteanu S.I., Crişan A.**- Un nou concept în turnătorie: modulul de solidificare real al pieselor turnate.- Revista de turnătorie, nr. 1-2, 2005, pag 27 – 33, ISSN 1224-21-44
2. **Ciobanu I., Munteanu S.I., Crişan A.**- Modulul de solidificare al barelor cu secţiune U.Partea I: Modulul de solidificare ideal.- Revista de turnătorie, nr. 3-4, 2005, pag3–7, ISSN 1224-21-44.
3. **Ciobanu I., Munteanu S.I., Crişan A.**-Modulul de solidificare al barelor cu secţiune U.Partea II: - Modulul de solidificare real.- Revista de turnătorie, nr. 5-6, 2005, pag 9 –16, ISSN 1224-21-44
4. **Chvorinov N.** – Teoria solidificării pieselor turnate. – Giesserei 17 mai 1940, pag.177-186, Giesserei 31 mai 1940, pag.201-208, Giesserei 17 iunie 1940, pag.222-225.
5. **Defretin G.** - Calcul des modules de solidification apparents des pieces de fonderie. – Fonderie 384, decembrie 1978, pag. 355-361.
6. **Ciobanu I., Munteanu S., Crişan A.**-Influenţa distanţei dintre piese în formă asupra solidificării pieselor turnate_ Metalurgia, nr. 8, 1998, pag. 18 – 27, ISSN 0461/9579
7. **Ciobanu I., Crişan A., Munteanu S.I.**- Influenţa caracteristicilor termofizice ale formelor de turnare asupra modulului de solidificare real. - Metalurgia, nr. 11, 2005, pag. 26 –37, ISSN 0461/9579
8. **Ciobanu I., Munteanu S., Crişan A.**-Influenţa temperaturii pereţilor formei de turnare asupra modulului de solidificare real al pieselor turnate- Metalurgia, nr. 12, 2005, pag. 12 –23, ISSN 0461/9579

Received December 12, 2005

¹TRANSILVANIA UNIVERSITY OF BRASOV

CERCETĂRI PRIVIND ANALIZA SOLIDIFICĂRII PIESELOR TURNATE PRIN METODA MODULULUI DE SOLIDIFICARE REAL

REZUMAT: În lucrare se prezintă rezultatele unei cercetări privind analiza solidificării pieselor turnate prin metoda modulelor de solidificare reale. Se analizează solidificarea unei piese din categoria roţilor de dimensiuni mici. Pe baza valorilor modulelor de solidificare reale parţiale ale elementelor componente ale roţii şi ale maseletoei, s-a pus în evidenţă posibilitatea de obţinere a unei solidificări uniforme sau a unei solidificări dirijate, cu scopul de a obţine piese turnate fără defecte cauzate de solidificare. Se evidenţiază că în anumite situaţii eliminarea retasurilor din butucul roţilor este posibilă numai prin utilizarea maseletoei izolate termic.

STUDIES ABOUT THE SIZE OF PRECIPITATES IN PARTIAL SOLUTION QUENCHING OF SOME ALUMINUM ALLOYS

BY

CARMEN NEJNERU¹, DRAGOȘ ACHIȚEI¹, ROXANA CARABET¹,
NICANOR CIMPOEȘU¹, IOAN HOPULELE¹

ABSTRACT : *Taking into consideration the alloying elements of the alloy used for the experimental tests, the tests were made at three different making temperatures for the partial solution quenching heat treatment (570°C, 580°C, 590°C) and at three soaking times (4h, 6h and 8h) in order to obtain a dissolving of the secondary precipitates as complete as it can be (intermetallic compounds Al – Cu – Ni – Fe) to obtain a better cutting workability.*

Metallographic photos were made on the bar tests which were heat treated in order to show precipitates dissolving and also was using the Surface Scan – program to measure the R_{max} to determine the efficiency of the heat treatment.

KEYWORDS : *partial solution quenching, secondary precipitates.*

1. Introduction

The intermetallic compounds that can exist into alloys are primary or secondary. The primary intermetallic compounds have much bigger dimensions and come directly from the melting comparatively with secondary intermetallic compounds that appear mostly because the solubility variation of chemical elements that compound them and have much smaller dimensions.

Biphasic structures have the disadvantage to be cracky and cannot be processed through cold deformation.

The solution quenching heat treatment is a treatment applied to the alloys that presents a biphasic solid structure composed from a solid solution α + a precipitate (usually an intermetallic compound).

When this treatment is applied takes place a total or partial dissolve of the precipitates which confer the alloys a good workability in cold deformation.

If in the structure of the alloy are only secondary precipitates the quenching is total; if we have in the structure also primary and secondary precipitates the quenching is partial. In the second case the alloy gets after the heat treatment a lower hardness and this is a good thing because it gets cutting workability.

2. Experimental results

The work presents an experimental study on the efficiency of the solution quenching heat treatment applied to an aluminum alloy with the following chemical composition:

Table 1.

Chemical composition [%]												
Cu	Fe	Ni	Zn	Ti	Sn	Pb	Cr	Co	Mn	Si	Cd	Al
2.618	1.21	1.20	0.59	0.077	0.003	< 0.003	0.04	< 0.001	0.03	0.16	< 0.001	rest

Based on the ternary equilibrium diagrams Al-Cu-Ni and Al-Cu-Fe and using the determined chemical composition it is ascertained that the studied alloy has a biphasic structures having in the basic metallic weight intermetallic complex compounds type: Al_2Cu , $\text{Al}_7\text{Cu}_2\text{Fe}$, Al_3Fe , $\text{Al}_9\text{Cu}_3\text{Ni}$, AlFe_2Ni , Al_2FeNi , Al_9FeNi and Al_3Fe . For the studied alloy the solution quenching can be only partial.

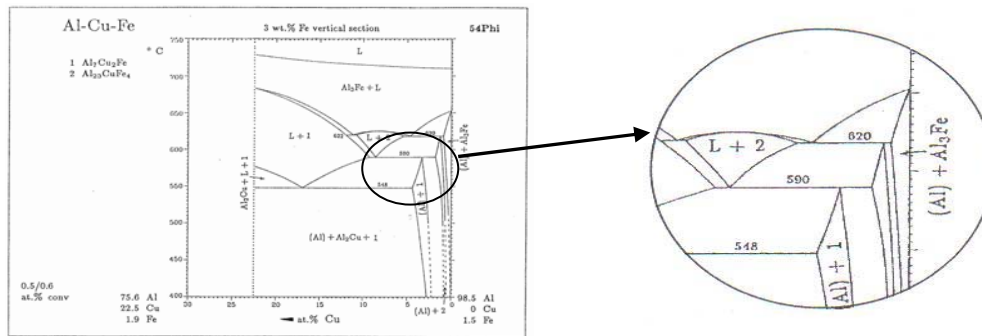


Figure 1. Ternary equilibrium diagram Al-Cu-Fe

It can be noticed from the Al-Cu-Ni ternary equilibrium diagram that the solution quenching temperature can vary in the interval 570...600°C and from technologic point of view in order to obtain a complete dissolving of the precipitates, the soaking time can vary in the interval 4...8 h.

The experiments were made on the following test matrix, in the soaking temperatures of 570, 580 and 590°C and at the soaking times of 4, 6 and 8 hours.

There were made tests also at 620°C but the test bars were partially melted which imposed the superior limit of the experiment at 590°C.

We must say that before the solution quenching heat treatment the test bars have suffered a stabilization annealing which consisted in heating and maintaining for an hour at 500°C followed by slow cooling with the furnace having in view to obtain into the alloy an equilibrium structure.

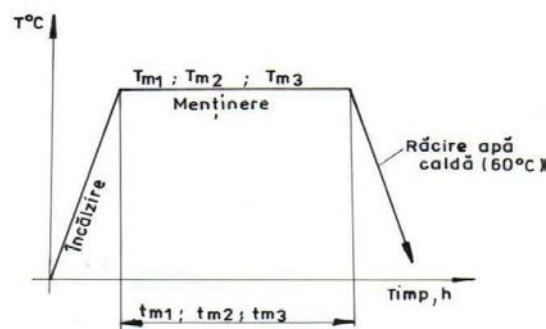


Figure 2. Heat treatment.

The heat treatments were made into an electric conducting-hearth furnace.

The ATNSi9 alloy because of the high thermal conductivity presents a high sensibility to the temperature variations which can reach on the entire length of the furnace until 10°C.

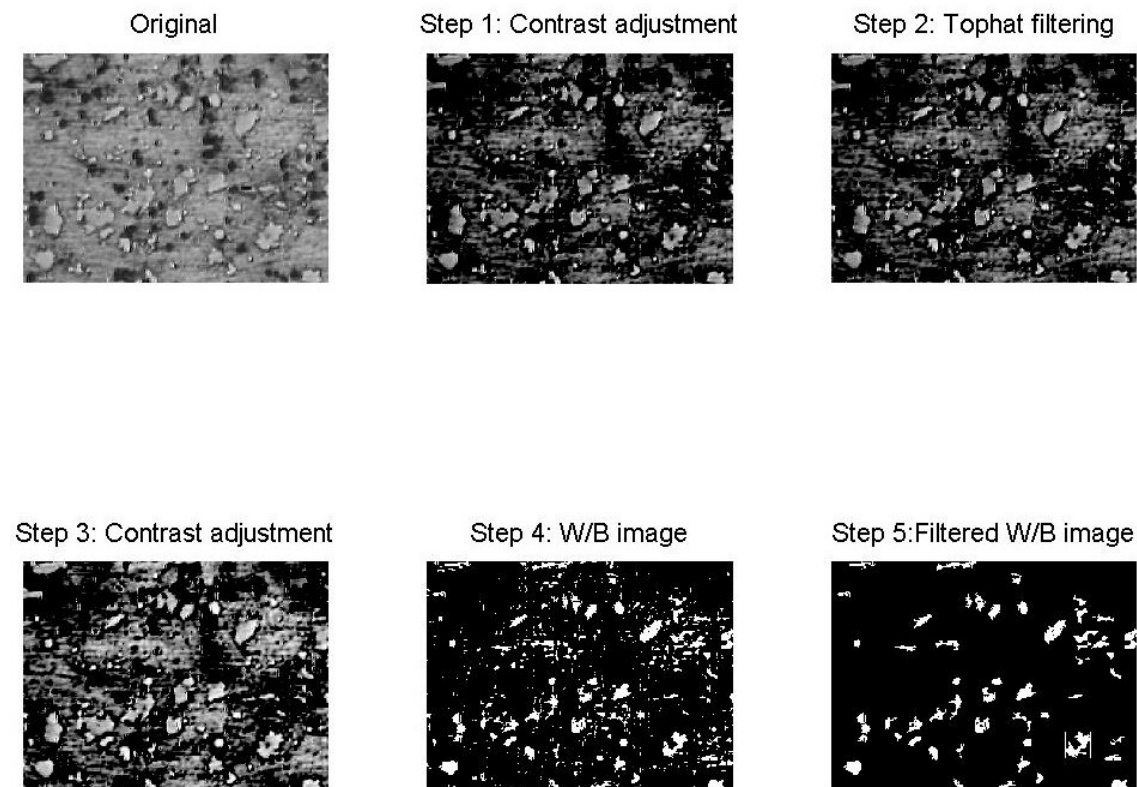
For this reason the heat of the test bars it is realized with the help of a cylinder piece with thick wall made from OLC 45 steel and to handle the test bars it was used a wire device. After heating and maintaining at the desired treatment temperature the test bars are cooled in water with high velocity at 60°C. The water had been before-hand heated into a calorimeter.

There were realized metallographic photos of the test bars before and after the heat treatment. The test bars were before-hand sanded and attacked with 10% NaOH solution.

In the metallographic photo of the untreated test bar it can be noticed easily the primary and secondary precipitates of the alloy.

In the metallographic photos of the heat treated test bars at soaking temperatures of 570, 580 and 590°C and soaking time of 4 h, it can be noticed a slight dissolving of the precipitates at the same time with the increase of the temperature.

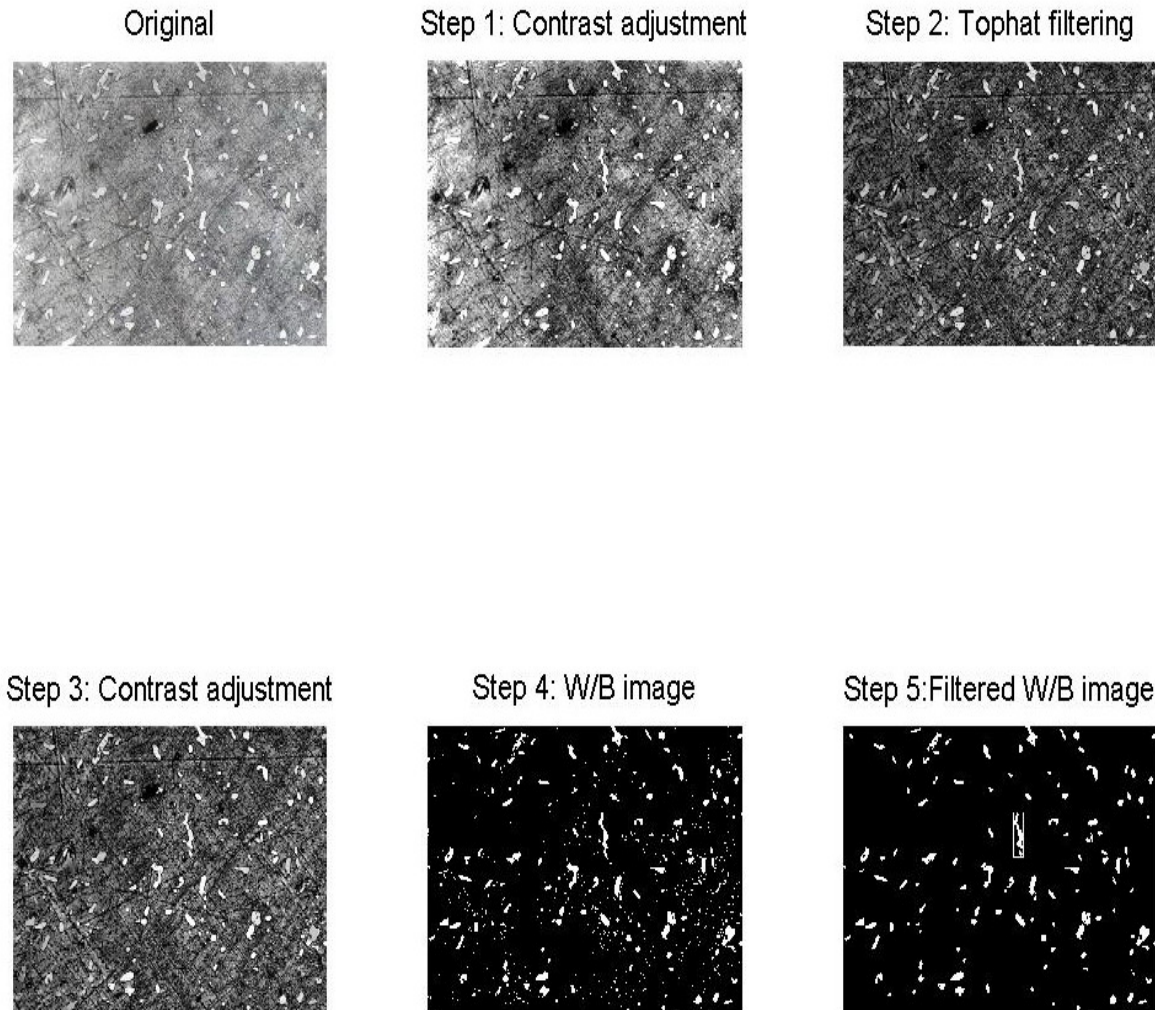
With the help of the metallographic photos and wit the SURFACE SCAN program it was made an image analised to determine the sizes of the primary and secondary precipitates.



Rmax = 0.00029443 Rmed = 0.00011609

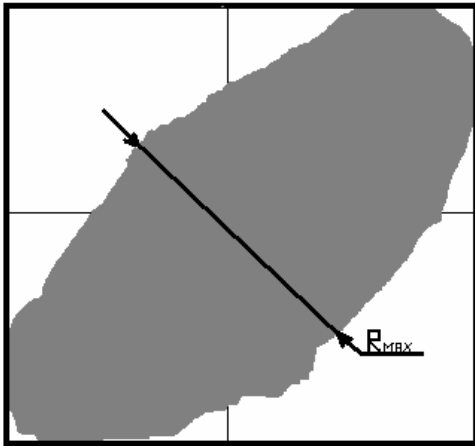
Figure 3. SURFACE SCAN used on test bar untreated.

It was determined the R_{\max} of the precipitated, with a special program, using the placement of the precipitate's form in a rectangle (R_{\max} was the minimal dimension of the oval forms because the precipitate's dissolving is made on the minimal dimension).

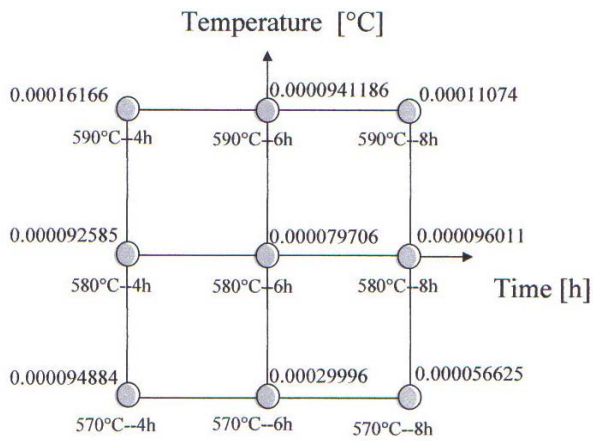


$R_{\max} = 9.4884e-005$ $R_{\text{med}} = 4.897e-005$

Figure 4. SURFACE SCAN used on test bar treated at 570[°C] and 4 [h].

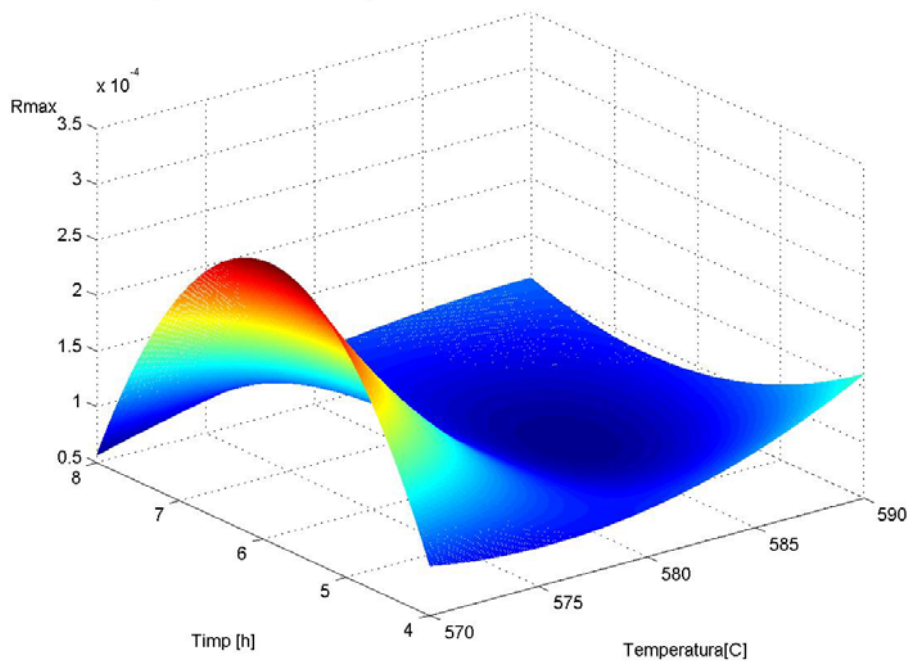


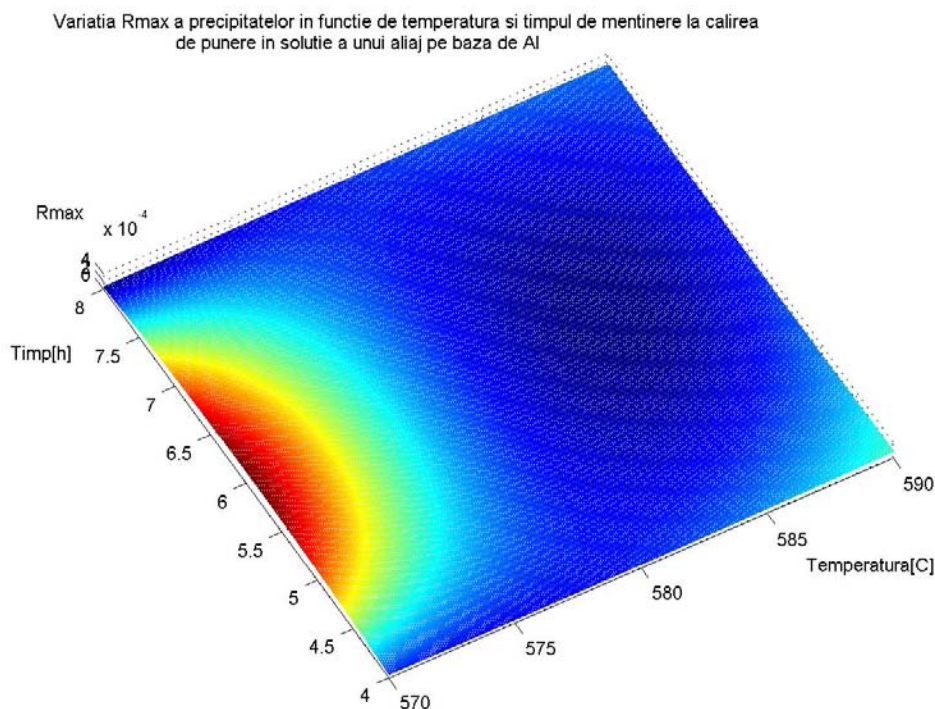
Variation of R_{max} [mm] of precipitates with temperature and time of mentence



Based on these values was traced a spatial graphic in coordinates (T, t, R_{max}).

Variatia R_{max} a precipitatelor in functie de temperatura si timpul de mentinere la calirea de punere in solutie a unui aliaj pe baza de Al





3. Conclusions

It can be noticed by studying the traced spatial graphic based on the measured values of the R_{max} , which a lower value of that though a powerful dissolving of the precipitates was obtained for a soaking temperature of 590°C and a soaking time of 8 and 6 hours.

It also can be noticed from the images analysis of the metallographic photos of the heat treated test bars that R_{MAX} of the precipitate is directly proportional with soaking time.

REFERENCES

- [1.] I. Hopulele, G. D. Gălușcă, I. Alexandru – Tratamente termice și termochimice, vol. I și II, Rotaprint Iași, 1983.
- [2.] S. Gadea , M. Petrescu – Metalurgie fizica si studiul metalelor ,Editura Didactica Pedagogica , Bucuresti ,1983 .
- [3.] T. Dulamita , E .Florian – Tratamente termice si termochimice ,Editura Didactica Pedagogica, Bucuresti ,1982 .
- [4.] N .Geru – Metalurgie fizica ,Editura tehnica , Bucuresti ,1981 .
- [5.] *** - Handbook of Ternary Alloy Phase Diagrams .

Received December 12, 2005

¹TECHNICAL UNIVERSITY IASI

STUDII PRIVIND MARIMEA PRECIPITATELOR LA CALIREA DE PUNERE IN SOLUTIE PARTIALA A UNOR ALIAJE PE BAZA DE ALUMINIU

REZUMAT: Tinand cont de elementele de aliere ale aliajului folosit pentru incercarile experimentale. s-au facut incercari la 3 temperaturi diferite de mentinere pentru tratamentul termic de calire de punere in solutie partiala (570°C, 580°C, 590°C) si 3 timpi de mentinere (4h, 6h si 8h), pentru a obtine o dizolvare cat mai completa a precipitatelor secundare (compusi intermetalici Al – Cu – Ni – Fe) in vederea obtinerii unei bune prelucrabilitati prin aschiere.

S-au realizat fotografiile metalografice, pe probele tratate termic pentru evidentiarea dizolvarii precipitatelor si folosind programul SURFACE SCAN s-a determinat raza maxima a precipitatelor, pentru a determina eficienta tratamentului.

IMPLICATIONS OF THE THERMAL AND THERMO-CHEMICAL TREATMENTS IN ELECTROLYTIC PLASMA IN THE PHYSICAL STRUCTURE OF THE STEELS OLC15 AND 21MoMnCr12

BY

MARIA BACIU¹, IOAN ALEXANDRU¹, CONSTANTIN BACIU¹, ADRIAN ALEXANDRU¹

ABSTRACT. *By the X-ray diffraction we identified the phases in the structure of steels OLC15 and 21MoMnCr12 treated thermally and thermo-chemically in electrolytic plasma as well as the influence of these proceedings on the physical structure of the steels analyzed.*

KEYWORDS: *thermal treatments, electrolytic plasma, carbiding, carbonitriding, diffractogram*

1. Introduction

The analysis of the physical composition of the steels OLC15 and 21MoMnCr12 treated thermally and thermo-chemically in electrolytic plasma permits to establish a correlation between the technological parameters of the processing process and the physical-mechanical properties obtained in the end.

The experimental determinations were made by X-ray diffraction, the analysis of the diffractograms allowing us to calculate the inter-planar distances d_{hkl} and the identification of the phases in the structure of the steels studied.

2. Experimental procedure

The experimental researches were made on cylindrical specimens $\varnothing 15 \times 50$ mm of the steels OLC15 and 21MoMnCr12 processed thermally by anodic warming in watery electrolytes according to the conditions presented in table 1 and figure 1.

Table 1. Technological parameters of thermal and thermo-chemical treatment in electrolytic plasma

No. crt.	Type of steel	Specimen	Thermal and thermo-chemical treatment applied	Technological parameters of thermal processing
1	OLC15	1D	carbiding + chilling	$T_{inc} = 850^{\circ}C; t_{inc} = 9 \text{ min}$
2	21MoMnCr12	2G		$T_{inc} = 700^{\circ}C; t_{inc} = 3 \text{ min}$
3	OLC15	1F	carbonitriding + chilling	$T_{inc} = 850^{\circ}C; t_{inc} = 3 \text{ min}$
4		1O		$T_{inc} = 700^{\circ}C; t_{inc} = 9 \text{ min}$
5	21MoMnCr12	2L		$T_{inc} = 700^{\circ}C; t_{inc} = 3 \text{ min}$

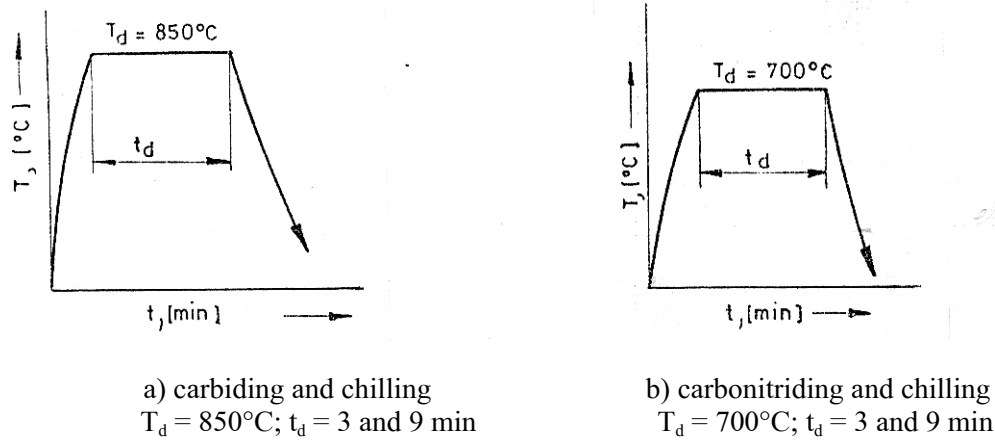


Figure 1. Variants of thermal treatments in electrolytic plasma

The diffractograms were obtained by the device DRON-2, using the radiations M_oK_α and FeK_α . The interval analyzed goes between the values $2\theta = 15^\circ \dots 40^\circ$. The exterior surfaces were radiated of the two steels by carbiding and carbonitriding followed by chilling in electrolyte.

3. Experimental results

In figures 2...6 we illustrate the diffractograms obtained. On them one can identify the peaks of maximum intensity specific to the phases and plans of diffraction:

- austenite (111); (220); (311);
- ferrite and martensite : (200); (002); (211); (112);
- cementite; coals, nitro-carbides and nitrides \square - $F_{2,3}N$; Fe_4N ; Fe_3N

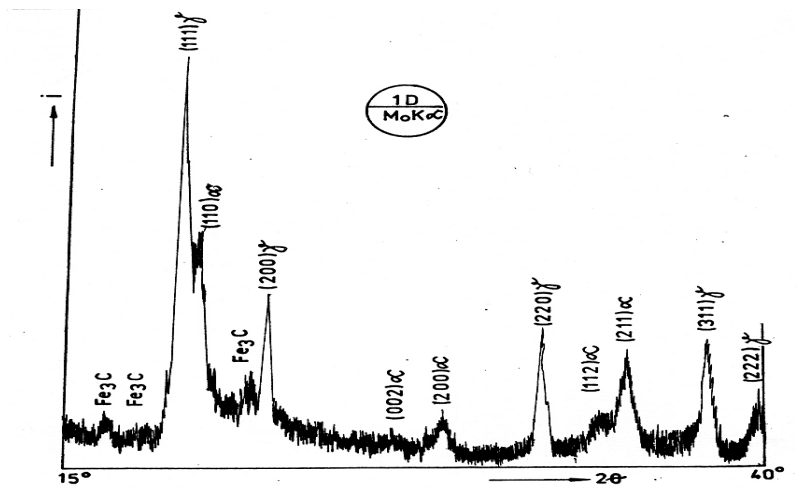


Figure 2. Diffractogram of steel OLC15 carburized and chilled in electrolytic plasma – specimen 1D

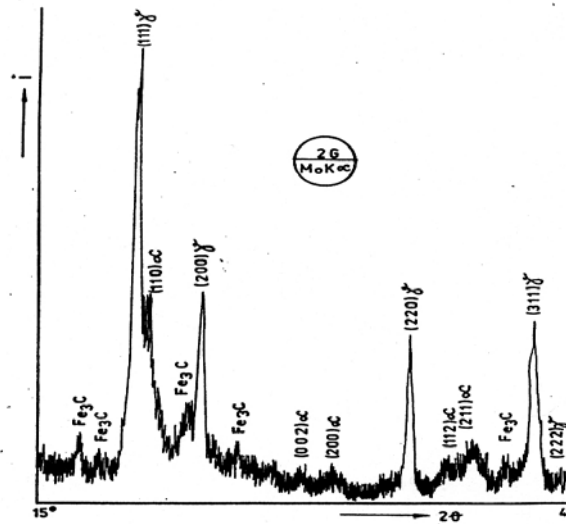


Figure 3. Diffractogram of steel 21MoMnCr12 carburized and chilled in electrolytic plasma – specimen 2G

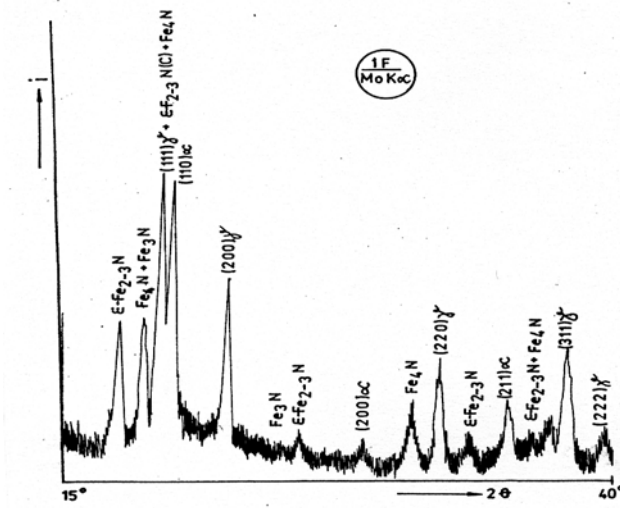


Figure 4. Diffractogram of steel OLC15 carbonitridated and chilled in electrolytic plasma – specimen 1F

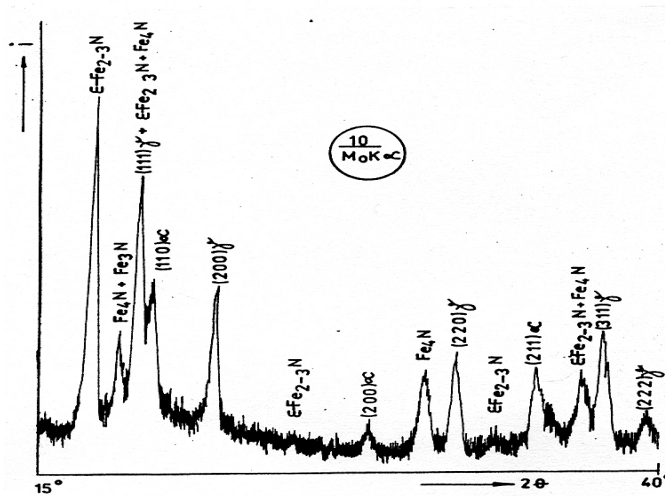


Figure 5. Diffractogram of steel OLC15 carbonitridated and chilled in electrolytic plasma – specimen 10

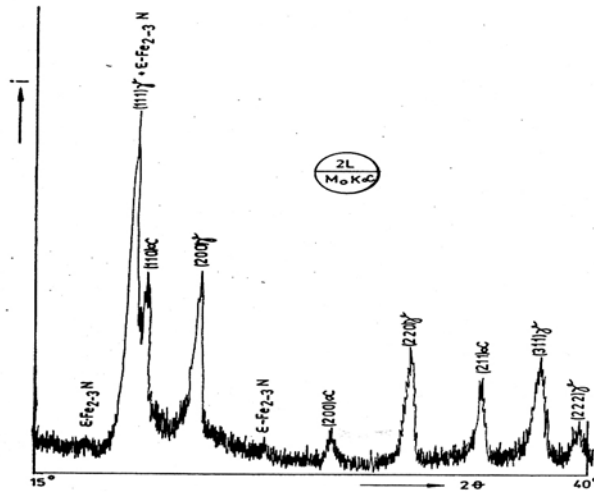


Figure 6. Diffractogram of steel 21MoMnCr12 carbonitrated and chilled in electrolytic plasma – specimen 2L

The analysis of these diffractograms allowed us to calculate the inter-planar distances d_{hkl} and to identify the phases in the structure of each specimen. (tables 3...7)

Table 3. Inter-planar distances and the phases in the structure of the steel OLC15 carbided and chilled in electrolytic plasma (specimen 1D).

d_{hkl}	Phase
2,392	Fe_3C
2,257	Fe_3C
2,213	Fe_3C
2,054	□
2,003	□
1,8543	Fe_3C
1,8023	□
1,5140	Fe_3C
1,4221	□
1,2734	□
1,1976	Fe_3C
1,1682	□
1,0849	□

Table 4. Inter-planar distances and the phases in the structure of the steel 21MoMnCr12 carbided and chilled in electrolytic plasma (specimen 2G).

d_{hkl}	Phase
2,402	Fe ₃ C
2,284	Fe ₃ C
2,235	Fe ₃ C
2,085	□
2,016	□
1,8535	Fe ₃ C
1,6869	Fe ₃ C
1,5819	Fe ₃ C
1,5072	Fe ₃ C
1,4313	□
1,2806	□
1,2172	Fe ₃ C
1,1737	□
1,1272	Fe ₃ C
1,0889	□
1,0434	□

Table 5. Inter-planar distances and the phases in the structure of the steel OLC15 carbonitratred and chilled in electrolytic plasma (specimen 1F).

d_{hkl}	Phase
2,311	□ - Fe _{2,3} N
2,172	Fe ₄ N + Fe ₃ N
2,088	□ + Fe ₄ N + Fe ₃ N + □
2,039	□
1,8139	□
1,6385	Fe ₃ N
1,5717	□
1,4341	□
1,3326	Fe ₄ N
1,2812	□
1,2313	□
1,1728	□
1,1376	Fe ₄ N + □
1,0948	□
1,0504	□

Table 6. Inter-planar distances and the phases in the structure of the steel 21MoMnCr12 carbonitrated and chilled in electrolytic plasma (specimen 1O).

d_{hkl}	Phase
2,319	$\square - \text{Fe}_{2,3}\text{N}$
2,189	$\text{Fe}_4\text{N} + \text{Fe}_3\text{N}$
2,101	$\square + \text{Fe}_4\text{N} + \text{Fe}_3\text{N} + \square$
2,055	\square
1,8323	\square
1,6148	$\square - \text{Fe}_{2,3}\text{N}$
1,4443	\square
1,3343	Fe_4N
1,2898	\square
1,2351	\square
1,1741	\square
1,1187	\square
1,0987	\square
1,0518	\square

Table 7. Inter-planar distances and the phases in the structure of the steel 21MoMnCr12 carbonitrated and chilled in electrolytic plasma (specimen 2L).

d_{hkl}	Phase
2,322	$\square - \text{Fe}_{2,3}\text{N}$
2,079	\square
2,026	\square
1,8200	\square
1,6068	$\square - \text{Fe}_{2,3}\text{N}$
1,4370	\square
1,2889	\square
1,1741	\square
1,0970	\square
1,0492	\square

4. Conclusions

We drew the following conclusions prior the experimental determination by X-ray diffraction over the specimens of the two steels processed thermally in electrolytic plasma:

- \square in the steels OLC15 and 21MoMnCr12 carbided and chilled in electrolytic plasma these phases are present: martensite, carbides and residual austenite;
- \square for the same steels carbonitrated and chilled in electrolytic plasma we identified the presence of the nitrides of the type $\square - \text{Fe}_{2,3}\text{N}$, Fe_3N and Fe_4N besides martensite and residual austenite.

References:

1. Baciu, Maria – *Contributions in the structural and property modifications of the steels treated thermally and thermo-chemically in electrolytic plasma*, doctoral thesis, Technical University, Iasi, 1999
2. Baciu, C.; Baciu, Maria – *Incalzirea anodica a otelurilor in plasma electrolitica*, Buletinul Sesiunii Academice Romane – filiala Iasi, pp. 42-45, Iasi, 1996

Received December 13, 2005

¹TECHNICAL UNIVERSITY IASI

**IMPLICATIILE TRATAMENTELOR TERMICE SI TERMOCHIMICE ÎN PLASMA
ELECTROLITICA ASUPRA COMPOZITIEI FAZICE A OTELURILOR OLC15 ȘI
21 MoMnCr12**

Rezumat. Analiza compozitiei fazice, permite stabilirea unei corelatii între parametrii tehnologici ai proceselor de prelucrare termica si termochimica în plasma electrolitica (T_{inc} si t_{inc}) si proprietatile fizico-mecanice ale straturilor obtinute în final.

Determinarile experimentale au fost efectuate prin difractie de raze X. Analiza difractogramelor a permis calcularea distantelor interplanare d_{hkl} si identificarea fazelor prezente în structura otelurilor OLC15 si 21MoMnCr12, prelucrate termic prin încălzire anodica în electroliti aposi.

Pentru cele doua aliaje studiate, supuse carburarii si calirii în plasma electrolitica au fost puse în evidenta fazele: martensita, carburi si austenita reziduala.

La aceleasi oteluri carbonitrate si calite în plasma electrolitica a fost identificata prezenta nitrurilor de tip $Fe_{2-3}N$, Fe_4N alaturi de martensita si austenita reziduala.

FINISHING OF THE STRUCTURE OF SILUMINS BY MEANS OF RAPID COOLING

BY

BELA VARGA¹

ABSTRACT: In addition to outstanding casting properties, silumins also have a number of remarkable operational features. Improving operational features implies directing/control of the casting structure. Good results are obtained by the application of high cooling rates (rapid cooling). The paper presents the experimental results obtained by applying cooling rates of orders of magnitude of $10^3 - 10^4$ °C/s.

KEYWORDS: silumins, structure, rapid cooling, primary silicon separations

1. INTRODUCTION

Silumins have a number of special properties: small values of the thermal dilatation coefficient, good corrosion strength, small values of the friction coefficient, small densities and good machinability by cutting. The enumerated conditions imply a fine and uniform distribution of both the primary phases and the eutectic. When using silumins for the casting of IC engine pistons, decreasing the value of the thermal dilatation coefficient to one close to that of the cylinder material requires the use of high silicon contents of 20 to 40%, figure 1. For these compositions the issue of finishing primary silicon separations is even more pressing.

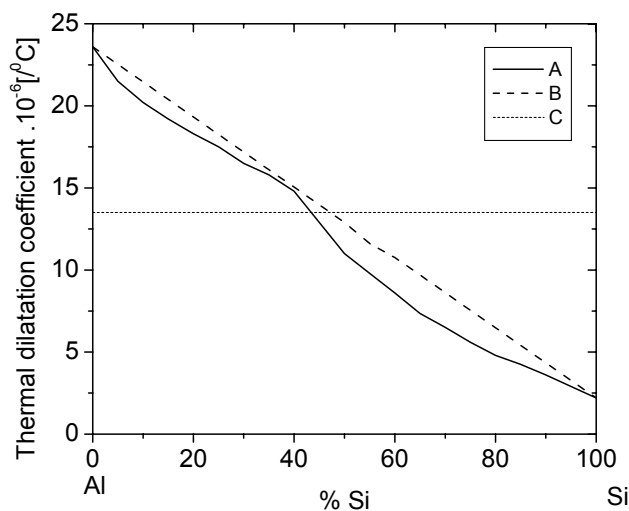


Fig.1 Variation of the thermal dilatation coefficient in the Al-Si system:

A – measured values:

- for chill-cast silumins (0 - 40 % Si);

- processed by atomisation - pressing (50-100 % Si);

B – theoretical values, computed by the law of additivity;

C – for the cylinder material

Hardening at high cooling rates represents the simplest manner of improving the structure, at least from the theoretical viewpoint. Rapid cooling applied to metal workpieces

determines, in addition to finishing of the structure, its deviation from equilibrium. The obtained unbalanced (non-equilibrium) phases cannot be evaluated any longer based on the thermal equilibrium diagrams.

Advanced finishing of structures by increasing the cooling rate requires modifications of both the transformation technology of liquid into solid alloy (table 1), and the technologies applied for the subsequent processing of the solid metallic material.

A number of structural modifications occur by increasing the cooling rate in the alloy subjected to solidification. The modifications are presented further on, in the increasing order of cooling rates:

- decreasing dendrite dimensions and of their internal structure;
- increasing chemical homogeneity by reducing segregations;
- expanding the domain of solid state solubility by generation of supersaturated solid solutions;
- occurrence of new meta-stable crystal phases;
- generation of amorphous materials (metallic glasses).

It is noted that by increasing cooling rate, the quantitative modifications of the structure turn into qualitative ones.

Structure finishing under the influence of rapid cooling is evaluated by the distance between dendrite branches, known as dendrite parameter. This interdependence is described by an equation of form:

$$d = A \cdot v^{-n}, \quad (1)$$

where: d is the dendrite parameter, (μm);

v – cooling rate, ($^{\circ}\text{C/s}$);

A, n – constants.

The mechanical strength of the alloy increases with structure finishing. This correlation is described by the Hall-Petch equation:

$$R = R_0 + k \cdot d^{-1/2} \quad (2)$$

where:

- R is the flow limit
- R_0 and k are constants depending on the quality of the metallic material.

In the case of aluminium the interdependence is represented by the diagram shown in figure 2.

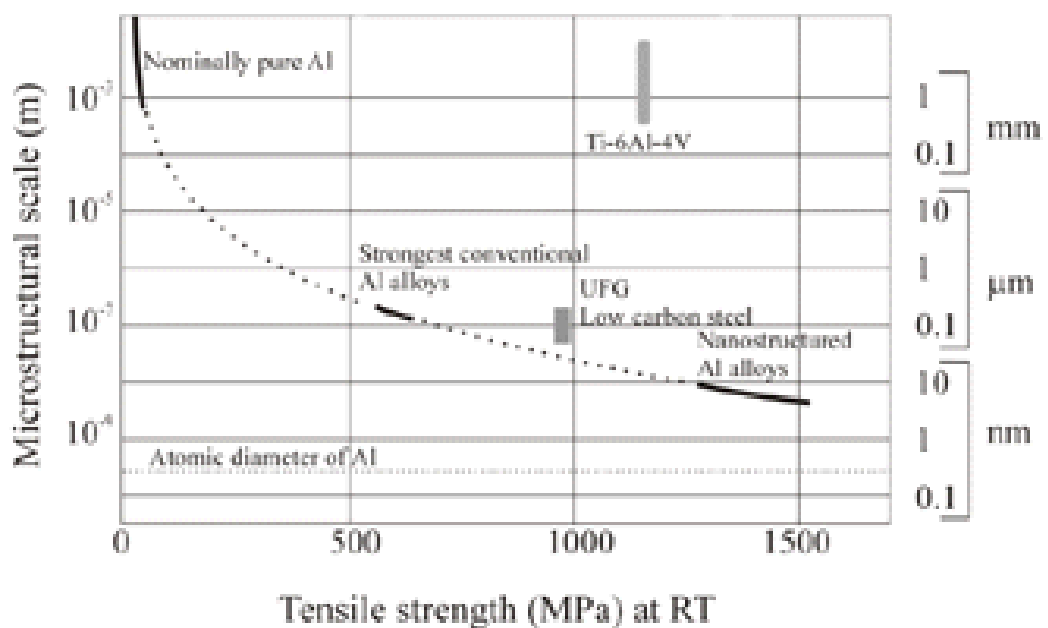


Fig.2 Interdependence: tensile strength – dendrite parameter

The variation of the dendrite parameter in dependence on the cooling rate values typical for various processing technologies are presented in table 2.

Table 1. Cooling rates recorded in the processing of various aluminium based alloy workpieces (1)

Workpiece	Processing conditions	workpiece dimensions (mm)	Cooling rate (°C/s)
Cast parts	sand - cast	medium dimension parts	10^{-2}
	chill - cast		10^0
ingots (pigs)	water-cooled chill-cast	D = 500	10^{-1}
	continuous casting	D = 1000	10^0
		D = 100	$5 \cdot 10^1$
profiled workpieces	flat strip	H=6	10^2
	wire	D = 6	$5 \cdot 10^2$
Grains	water-cast	D = 4	$5 \cdot 10^3$
		D = 0,5	$5 \cdot 10^4$
		D = 0,05	$5 \cdot 10^5$
Powders	Nitrogen atomisation	D = 0,4	$5 \cdot 10^3$
		D = 0,05	$5 \cdot 10^4$
Scales (tape)	on metal support	H=50 □m	$5 \cdot 10^5$
		H=20 □m	10^6
		H<10□m	10^9

Table 2. Cooling rates and dendrite parameter for aluminium based alloys solidified by various processing technologies (1)

Cooling rate (°C/s)	Dendrite parameter (m)	Processing conditions
10^{-3}	1000	sand-casting of parts chill-casting of large diameter ingots (pigs)
10^0	100	chill-casting continuous casting
10^3	10	large grains
10^6	1	small grains and scales
10^9	0,1	superfine scales
10^{12}	0,01	superfine scales with high initial undercooling
10^{15}	0,001	not obtained experimentally

Certain papers (2) consider the variation of the dendrite parameter depending on nature and concentration of the alloying element in the case of deformable aluminium alloys as insignificant. Consequently the diagram of function (1) plotted in double logarithmic coordinates for the linearization of the interdependence, can be used for determining the cooling rate of any aluminium alloy processed under various cooling conditions.

Based on data from literature, table 3 presents for various aluminium based alloys the values of constant n from equation (1).

Table 3. Constant "n" for aluminium based alloys (according to various authors)

alloy	cooling rate (°C/s)	n
duralumin	0,007...2000	0,38
Al + (4,0...5,0) % Cu	<350	0,39
Al + Cu, Mg, Zn, Si	-	0,337
Al + (5,05...3) % Cu	<3	0,276
Al + (1,0...10,6) % Cu	0,67...5,0	0,25
Al + (5,5 ...26,6) % Cu	0,16...1,6	0,25
Al + (1,4...4,3) % Si	0,67...5,000	0,25
Al + (2,0...5,0) % Mn	10^{-10} ... $6 \cdot 10^{-3}$	0,32
Al + Cu, Si, Pd, Fe	10^8 ... 10^9	0,33
Al + Mg	$0,01$... $5 \cdot 10^3$	0,32
Al + Cu	$0,01$... $5 \cdot 10^3$	0,37
Al + Fe	$0,01$... $5 \cdot 10^3$	0,33

Al + Mn	0,01...5.10 ³	0,377
---------	--------------------------	-------

The paper addresses the determination of constants A and n from equation (1), for the primary phases of hypo- and hypereutectic silumins.

It should be mentioned, that in the case of binary Al-Si alloys in addition to the quantitative structural modifications, also a number of qualitative changes occur under the influence of rapid cooling:

- Displacement of the eutectic point to the right;
- Modification of the form of eutectic silicon (modified alloy);
- Modification of the proportion of phases and constituents;
- Generation of silicon supersaturated α solid solution.

In the case of chill-casting of small test-pieces the cooling rate is of 10^2 °C/s, the corresponding modification of proportions of phases and constituents being presented in the diagrams of figure 3.

The diagram of figure 4 presents the influence of the cooling rate on the variation of silicon concentration in α solid solution for alloys with different contents of silicon.

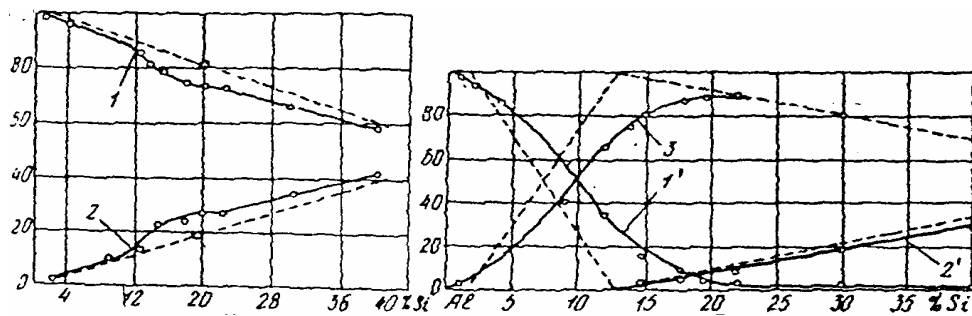


Fig.3 Proportion of phases (a) and constituents (b) in Al-Si alloys, for chill-casting at 100 °C/s cooling rate: 1 – phase; 2 – phase; 1' – primary solid solution; 2' – primary (Si) solid solution; 3 – eutectic; experimental values (continuous line); theoretical values (dotted line) (5)

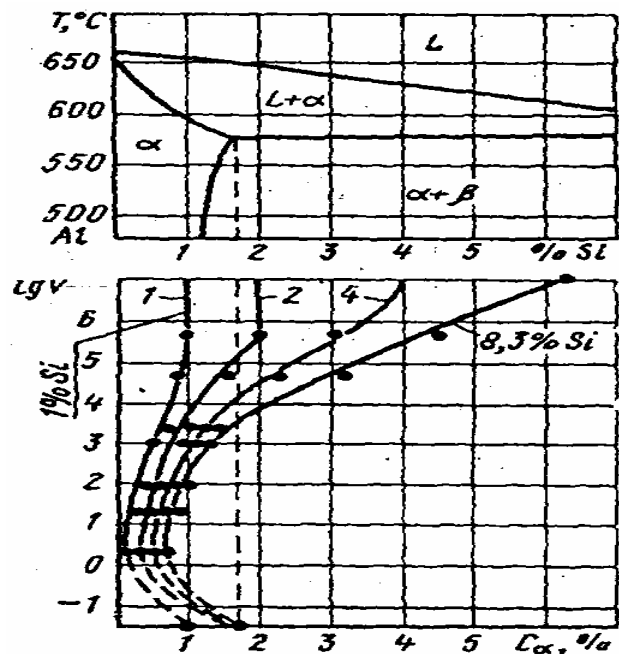


Fig. 4 Variation of silicon concentration versus cooling rate in α solid solution for alloys with various contents of silicon (3)

2. EXPERIMENTAL DETERMINATIONS

Samples were cast under various cooling conditions (in refractory brick and metal moulds of various dimensions and shapes) in order to establish the interdependence of the value of the cooling rate and the dendrite parameter. The conditions of experimenting are those presented in (7).

Test-pieces were taken from the cast samples for determination of the dendrite parameter by microscopic examination.

Table 4 features the values of constants A and n obtained by mathematical processing of the experimental results for ATSi5Cu1 hypoeutectic alloy and Al-Si 18 % hypereutectic composition, together with data from literature concerning foundry alloys.

Table 4. Values of coefficients A and n for different aluminium based alloys

Composition	Analysed phase	n	A	Source
Al – Si 18 %	primary silicon	0,402	2,548	(6)
		0,354	2,013	own determinations
Al- Si 7 %	□ solid solution, silicon dissolved in aluminium	0,4	2,37	(4)
Al- Si 5 %		0,37	2,3	own determinations

The diagram of figure 5 shows the graph of function (1) for the 18% silicon hypereutectic composition. The line plotted for the same composition based on data from literature is presented in parallel.

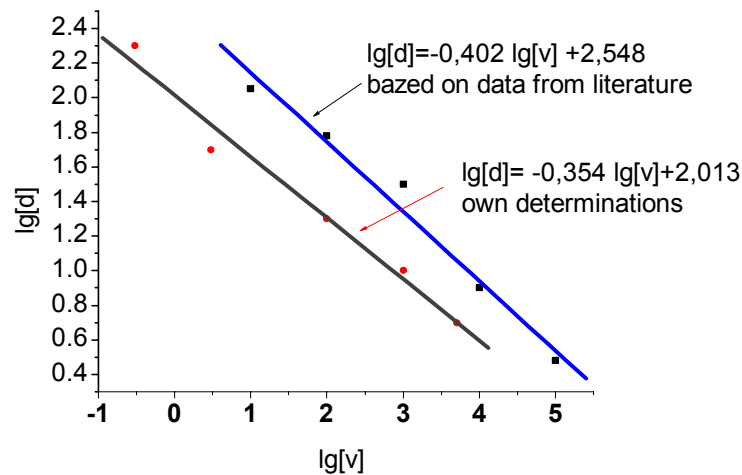


Fig.5 Variation of primary silicon separation dimensions versus cooling rate value

3. CONCLUSIONS

The data presented in table 3 concerning the value of constant “n” from equation (1) highlight the wide variation interval (0.25 ... 0.39) of this constant for aluminium based alloys cooled at rates of 0.007 ... 10⁹ °C/s.

Based on the data of table 4 the closeness of the values of constants A and n for the two categories of silumins is worth noticing, despite the fact that germination and growth of the two pro-eutectic phases is achieved by significantly different mechanisms.

The advanced finishing of the structure by rapid cooling requires the modification of both the transformation technology of liquid into solid alloy (atomisation or casting of tapes or thin wire) and the subsequent processing technologies.

In the case of hypereutectic silumins a high rate of solidification is recommended, also preferred because it allows avoiding silicon segregation.

It should be mentioned that rapid cooling also contributes to decreasing the negative influence of metal impurities, thus allowing the increased use of recyclable materials for generation of the solid charge.

REFERENCES

- (1) Dobatkin V. I., Elagin V. I., Federov V. M.: *Bâstrozakristalizovannie aliuminievie splavâ*, Moskva, VILS, 1995, p. 341
- (2) Gâdea S., Petrescu M., Vavernea M., Minciunescu C.: *Cercetari asupra calirii din stare lichida pentru obtinerea de noi aliaje*, în *Metalurgia* nr.11, 1984, p. 572...580
- (3) Badaev V. G.: *O raspredelenii legiruiutcih elementov mejdu fazovîmi sostavliaiucimi v litîh dvukomponentnîh aliuminievih splavah*, în *Metallovedenie i termiceskaia obrabotka metallov*, nr. 10, 1983, p. 8...11
- (4) Shivkumar S., Wang L., Apelian D.: *Molten Metal Processing of Advanced Cast Aluminium Alloys*, JOM, 1991, nr.1. p. 26-33
- (5) Badaev V. G., Lermontova L. M., Zaharov A. P.: *Vliianie skorosti ohlajdenia rasplava pri kristallizacii na sostav i kolicestvo faz v splavah sistemi Al-Si*, Tehnologia Liogkih splavov, 1992, nr. 3. p. 21...24
- (6) Tmakov Iu. V., Zenina M. V., Riabov I. V.: *Sovremennoje sostojanie i dalnejtee razvitie portnevâh splavov na Al-osnove*, Liteinoe Proizvodstvo 2000, nr. 11. p. 3...4
- (7) Varga B.: *Structura siluminurilor racite rapid si metoda de realizare a acesteia*, Revista de Turnatorie 2003, nr. 1-2. p. 13...16

Received December 15, 2005

¹University Transilvania of Brasov

FINISAREA STRUCTURII SILUMINURILOR PRIN APLICAREA UNOR VITEZE MARI DE RACIRE

REZUMAT: Siluminurile pe langa proprietatile excelente de turnare poseda o serie de proprietati de exploatare remarcabile. Îmbunatatirea proprietatilor de exploatare presupune dirijarea structurii de turnare. Rezultate bune se obtin prin aplicarea unor viteze de racire marite. În lucrare sunt prezentate rezultatele experimentale obtinute prin aplicarea unor viteze de racire de ordinal $10^3 - 10^4$ °C/s.

SIMULATION OF THE RESIDUAL STRESS DISTRIBUTION IN THE CASE OF DRAW PARTS MADE FROM HOMOGENEOUS AND HETEROGENEOUS METAL SHEETS

BY

G. BRABIE¹, A. ALBUT¹

***ABSTRACT:** The experimental investigation of the residual stress distribution in the case of draw parts is a difficult problem because of complexity of the forming operations and formed parts geometry. A solution to the problem can be the simulation of the forming process and residual stress distribution. The present paper investigates the distribution of the residual stresses by simulating the drawing process in the case of a rectangular part made in homogeneous and heterogeneous steel sheets.*

***KEYWORDS:** forming simulation, residual stresses distribution, homogeneous and heterogeneous sheets*

1. Introduction

The residual stresses that occur in the machined parts after the removing of the tools are the main cause that determines the springback of the draw parts made in metal sheets. Hence, to investigate this instability phenomenon it must be known the state of residual stresses developed in the part by its machining. But, the experimental investigation of the residual stress distribution in the case of draw parts is a difficult problem because of complexity of the forming operations and formed parts geometry. A solution to the problem can be the simulation of the forming process and residual stress distribution. The present paper investigates the distribution of the residual stresses by simulating the drawing process in the case of a rectangular part made in homogeneous and heterogeneous steel sheets.

2. Conditions of simulation

The analysis concerning the residual stress distribution was performed by simulation using ABAQUS-Explicit software. The model was created in order to ensure the simulation of the quasi-static problem and to obtain the state of equilibrium after the forming operation. The simulation was performed for the parts made from: SPE 220BH steel sheets and in TWB obtained by laser welding of FEPO 5MBH and SPE 220BH steel sheets. The materials elastic properties for simulation were as follows: Young's modulus, Poisson's ratio and material density. A three dimensional model was used for the simulation. The blank was considered as deformable with a planar shell base. The integration method was Gaussian with 5 integration points through the thickness of the shell. The elements used for the blank mesh were of S4R type (4 nodes reduced integration shell). The blank-holder, punch and die were

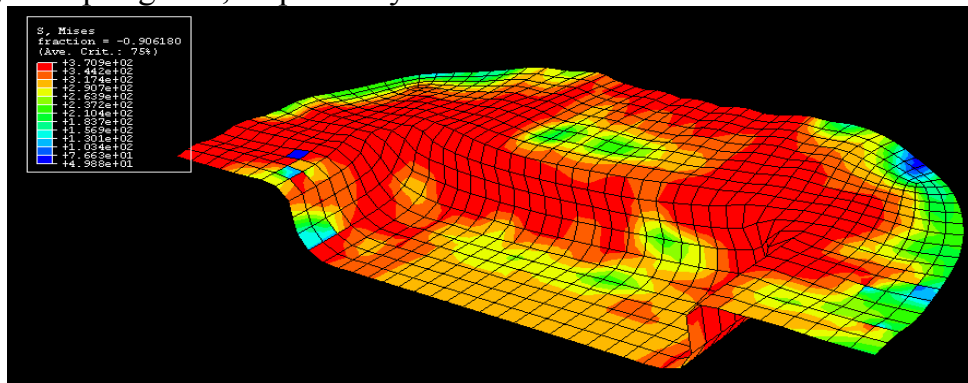
modelled as rigid surfaces. Contact interactions between the blank and the tools were modelled using penalty method. The materials were considered elastic-plastic with an isotropic hardening.

The working parameters were as follows: Drawing depth = 22mm, Drawing speed = 18 mm/min, Blank holding force = 10 kN.

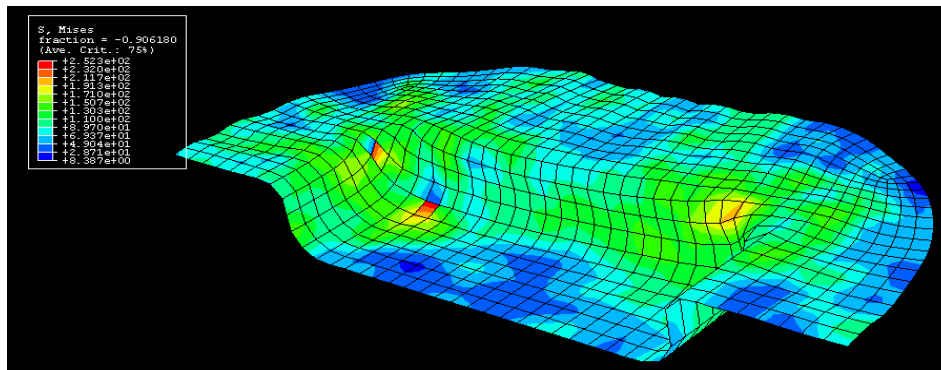
3. Investigation results

The results of simulation for the parts made in SPE 220BH steel sheet have been presented in Figure 1a and b - for the state of stresses resulted after drawing and springback, respectively. The distributions of the von Mises equivalent stress on the sheet thickness and part bottom in the case of part made from SPE220BH steel sheet have been presented in Figure 2.

The results of simulation in the case of parts made from TWBs have been presented in Figure 3 a and b – for the von Mises state of stresses resulted after drawing and springback, respectively.

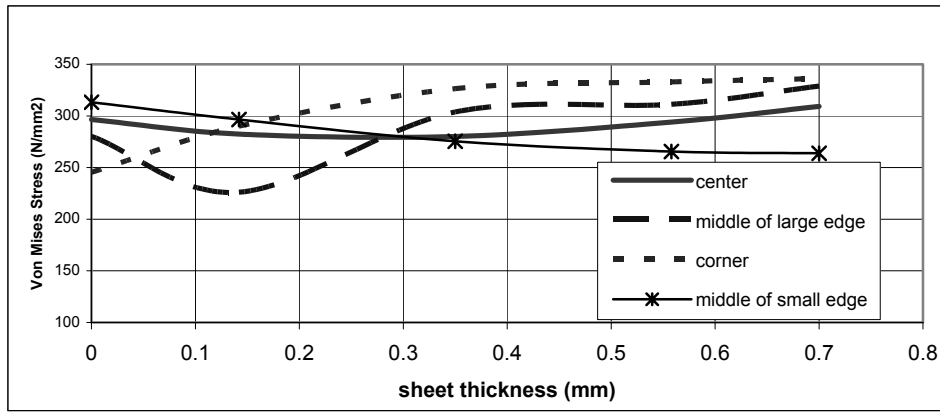


a. after drawing

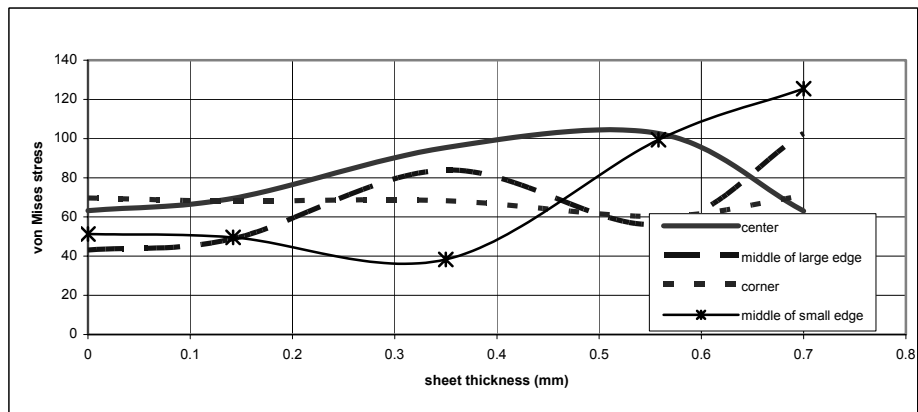


b. after springback

Figure 1 State of stresses in the case of parts made from SPE 220BH steel sheet

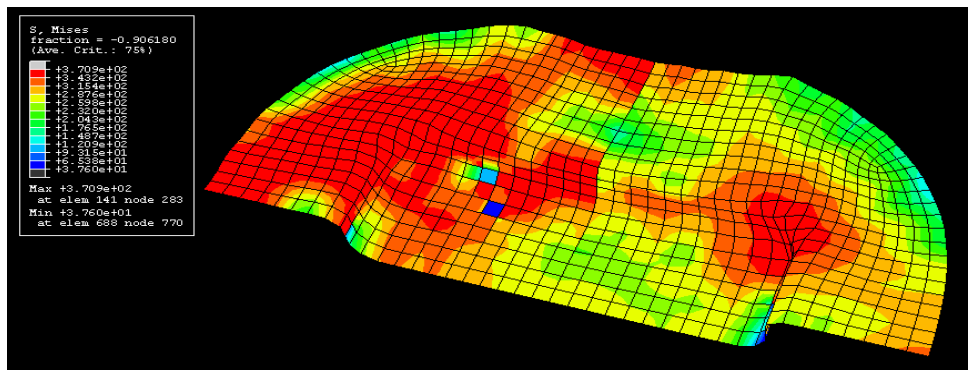


a. after drawing

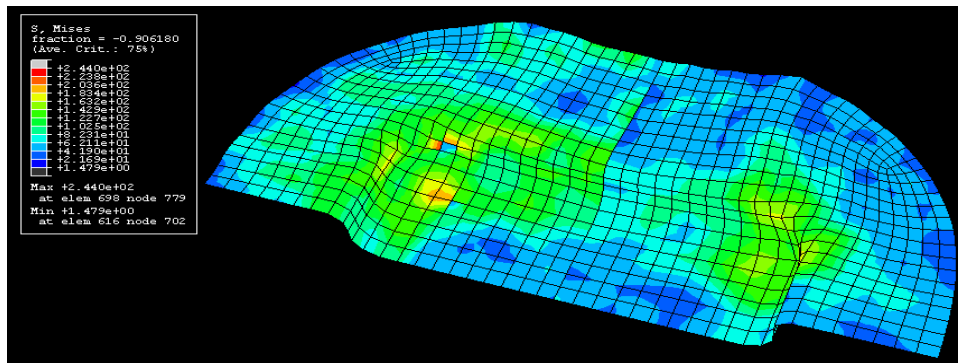


b. after springback

Figure 2 Distribution of the von Mises equivalent stress in the case of parts made from SPE 220BH steel sheet



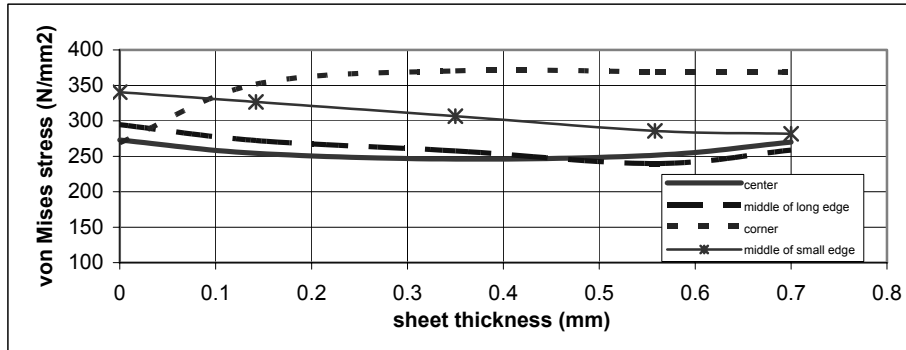
a. after drawing



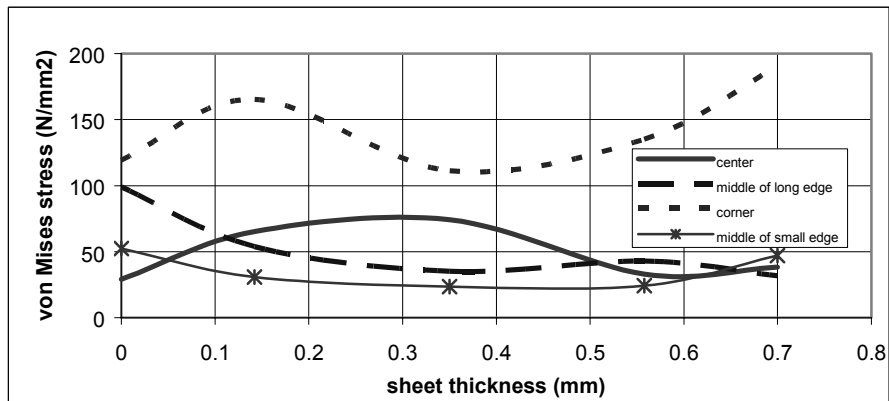
b. after springback

Figure 3 State of stresses in the case of rectangular part made from TWB

The distributions of the von Mises equivalent stresses on the TWB thickness for the half of the bottom in the case of part made from SPE220BH steel sheet are presented in Figures 4.



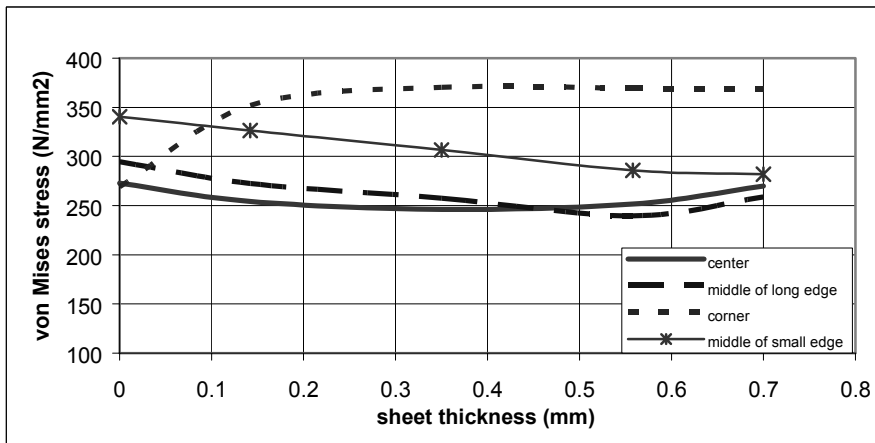
a. after drawing



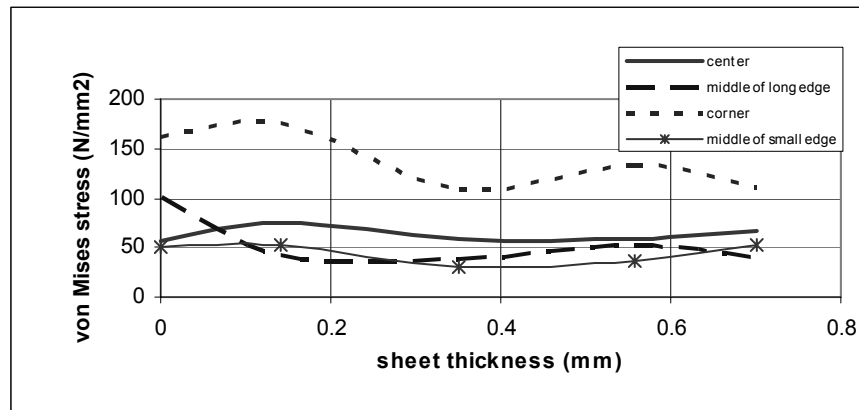
b. after springback

Figure 4 Distribution of the von Mises equivalent stress on the TWB thickness for the half of the bottom in the case of part made from SPE 220BH steel sheet

The distributions of the von Mises equivalent stresses on the TWB thickness for the half of the bottom in the case of part made in FEPO 5MBH are presented in Fig 5.



a. after drawing



b. after springback

Figure 5 Distribution of the von Mises equivalent stress on the TWB thickness for the half of the bottom in the case of part made from FEPO 5MBH steel sheet

4. Conclusions

By analysing the residual stress distribution on the all-draw part, the following aspects can be remarked:

- a concentration of the residual stresses can be observed after drawing in the regions of connection of the part walls with the bottom and flange that are stressed by bending – in the case of both analysed materials (Figures 1a and 3a); a strong concentration of residual stresses can be also observed at the corner of the parts made from both analysed materials.
- a relaxation of the stresses takes place after springback in the case of both analysed materials (Figures 1b and 3b).

By analysing the residual stress distribution on the bottom of the part, the following aspects can be remarked:

- in both cases of analysed materials the stress values vary on the sheet thickness.
- in the case of parts made from homogeneous sheets the lowest values of the residual stresses will result at the middle of the smaller edge; the greatest ones will result with the increase of the sheet thickness in the following regions of the bottom: corner, middle of the longer edge and the bottom centre.
- in the case of parts made from heterogeneous sheets the variation of the residual stresses takes place on a narrow field in the following regions of the bottom: middle of the smaller edge, middle of the longer edge and the bottom centre. By comparing the residual stress values on both halves of the part made from TWB it can be remarked that the greatest values have resulted on the half made from SPE 220BH steel sheet having higher yielding strength.
- by comparing the values of the residual stresses in the case of parts made from homogeneous and heterogeneous sheets we can observe that in the case of parts made from TWB these values are higher than in the case of parts made in homogeneous steel sheets.

References:

1. Brabie G., s.a, Tensiuni reziduale generate de procesele de transformare mecanica a materialelor metalice, Ed. Junimea, Iasi, 2005
2. Brabie G., Chirita B., Chirila C., 2003, Residual stresses control by experiment and simulation in formed tailor welded sheets, MOCM-9, Academia de Stiinte Tehnice, p. 18-22

Received December 14, 2005

¹University of Bacau

**SIMULAREA DISTRIBUTIEI TENSIUNILOR REZIDUALE IN CAZUL
PIESELOR REALIZATE DIN TABLE METALICE OMOGENE SI
ETEROGENE**

REZUMAT: Cercetarile experimentale privind distributia tensiunilor reziduale in cazul pieselor metalice este o problema extreme de dificila datorita complexitatii operatiilor de formare si realizarii configuratiei geometrice. O solutie ar fi simularea procesului de fabricatie al reperului si a starii de tensiuni reziduale.

ASPECTS CONCERNING THE PRESSING AND REPRESSING BEHAVIOUR OF A Ni-BASE SUPERALLOY

BY

V. CÂNDEA¹, S. LĂPUȘAN¹, A. POPA², I. ZLATE,¹ R. CHENDE¹

ABSTRACT: *After elaboration through atomizing from liquid phase of the Nimonic 80 alloy, the coarse fraction (>125 μm) representing useless material was milled in a planetary mill for the improvement of the pressability characteristics. The pressing parameters were determined. After sintering, for the porosity diminishing, a repressing was applied. In order to obtain the specific structure of this superalloys class - γ solid solution with hard phases precipitates - heat treatments were applied.*

KEYWORDS: *superalloy, pressing, repressing, heat treatment, structure*

1. Introduction

The continuous competition between a cost price as reduce as possible and mechanical properties, refractoriness, creep, corrosion and thermal shock resistance as good as possible, required to the superalloys meant for parts which equip the turbo reactors engines, has lead to the development of some researches in this direction, via-PM.

There were greeted difficulties in connection with:

- the powder oxidation during atomizing,
- the weak powder pressability thanks to the improper shape of the particles,
- the obtaining of a high porosity,
- the structural changes induced by the mechanical milling,
- the weak sinterisability thanks to the surface oxides.

The present research tries to solve these problems.

2. Experimental procedure

There were elaborated several charges through vertical atomizing from liquid phase with argon at the 24 bar pressure. The chemical composition of the charge analyzed in the paper contains: 0,10% carbon, 20,08% chromium, 0,46% silicon, 1,64% cobalt, 1,80% titanium, 1,43% aluminum, 1,46% iron, 0,399% oxygen, nickel balance.

The gaseous atomizing agent and the small pressure leaded to the getting of a powder containing about 40% spherical powder and useful fraction below 125 μm, 56% [1]. It was choose nevertheless for argon atomizing and not with water, to avoid

the powder oxidation, and the pressure was of small value for reducing the spherical powder percentage (usually, the nickel alloys have big nodulizing tendency of the particles thanks to the great surface tensions).

After elaboration, the powder was reduced in hydrogen 4 hours at 1150 °C, the oxygen content diminishing to 0,162%.

All the elaborated powder with below 400 µm sizes was milled in a planetary mill, time of 3, 5, respectively 8 hours, using ø15 and ø22 mm balls. After milling for 8 hours, the granules of spherical shape disappear entirely, the powder being able for the pressing operation.

From the three sorts of powder, integral and granulometric fractions sorted from this - table 1, were bilaterally pressed pills with 8 mm in diameter, at 700 and 800 MPa pressures.

Table 1. The particle size distribution of Nimonic 80 powder

Sort	Powder	Granulometric fraction proportion [%]					
		<40 [µm]	40-63 [µm]	63-80 [µm]	80-100 [µm]	100-125 [µm]	125-400 [µm]
1	After atomizing	4.60	7.10	10.20	13.05	21.05	44
2	8 hours milled-ø15mm	32.80	24.60	22.80	16.28	3.52	0
3	8 hours milled-ø22mm	39.50	26.25	15.20	17.00	2.05	0

The sort 1 powder presented very weak pressability characteristics, for this reason further will mention only the experiments effectuated with the powder milled 8 hours, using ø15 and ø22 mm balls.

After pressing, the samples from sorts 2 and 3 were sintered in vacuum at 1400°C temperature for 2 hours. In order to increase compactness, the pills realized both from integral powder and from granulometric fractions until 100 µm were repressed at 700 and 800 MPa pressures.

3. Results and discussion

In figures 1 - 6 it is presented the calculated values of the compactnesses after pressing, sintering and repressing. From the comparative analysis of the data written in the first 4 diagrams it can observe the followings:

- the greatest compactnesses, regardless of compacting pressure, it is obtained to the powder with the granulation under 40 µm: the 71,21% value, respectively 71,61%;
- after pressing, the compactnesses can reach until 65,67%;
- after sintering, the compactness increases percentually from 0,63 to 10,53%;
- after repressing, the compactness can increase with 1,90 until 5,01%;
- the shrinkage after sintering and repressing registers the decreased values comparing to the increasing of the granulometric fraction size.

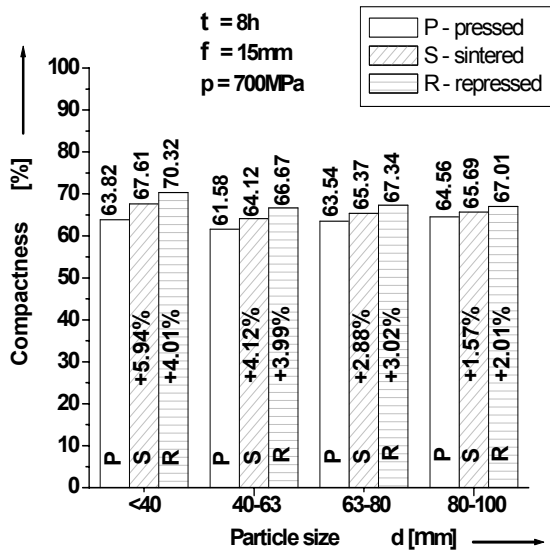


Fig. 1 The graphic representation of the compactness - sort 2 powder

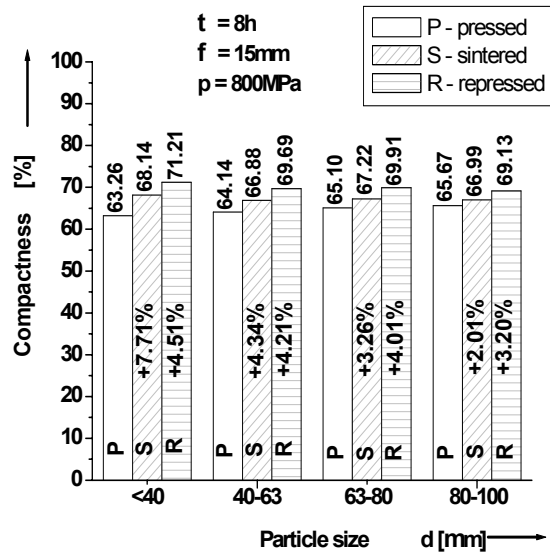


Fig. 2 The graphic representation of the compactness - sort 2 powder

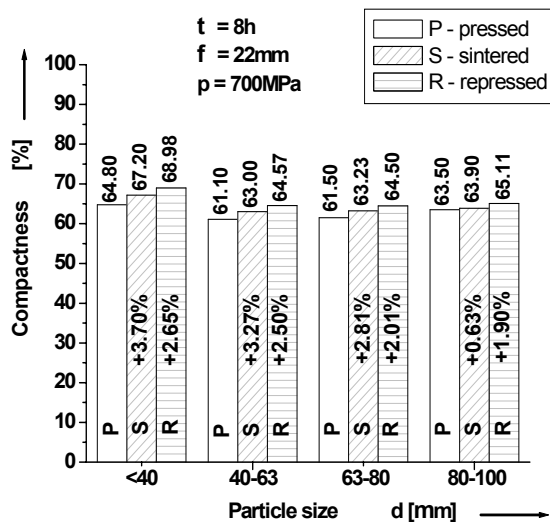


Fig. 3 The graphic representation of the compactness - sort 3 powder

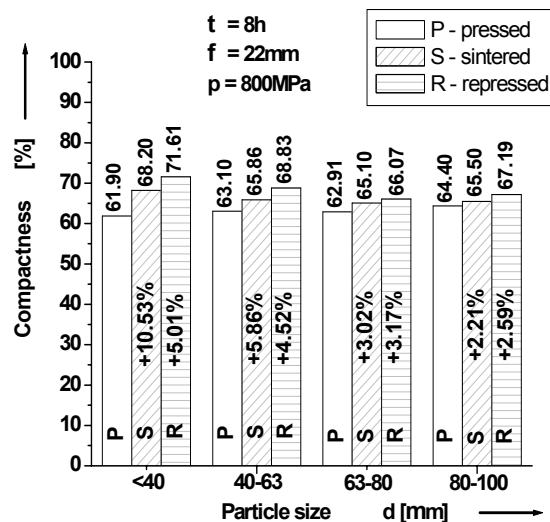


Fig. 4 The graphic representation of the compactness - sort 3 powder

To the integral powder, figures 5 and 6, the analysis of the compactness variation in state pressed, sintered and repressed at 700 respectively 800 MPa pressures shows the followings:

- the pressing capacity of this powder is better than of anyone component granulometric fraction;
- the compactness after pressing at 800 MPa pressures reaches to 69,65%;
- the compactness after sintering varies between 70,82% and 75,86%;
- the repressing improves the compactness with 4,27% until 5,37%, the determined maximum value being of 79,10%.

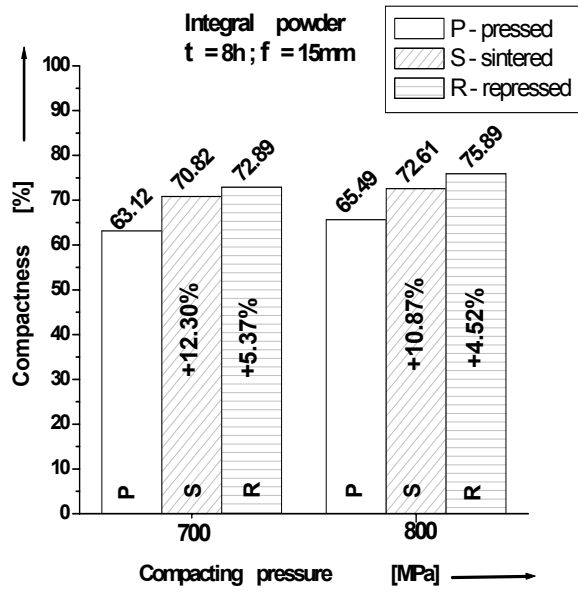


Fig. 5 The compactness variation in accordance with the compacting pressure - sort 2 integral powder

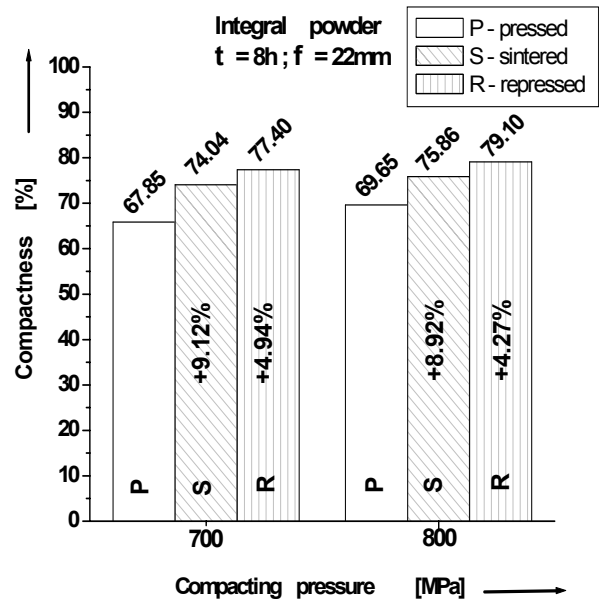


Fig. 6 The compactness variation in accordance with the compacting pressure - sort 3 integral powder

All of these phenomena are accountably through the shape and pores distribution change, figures 7 and 8.

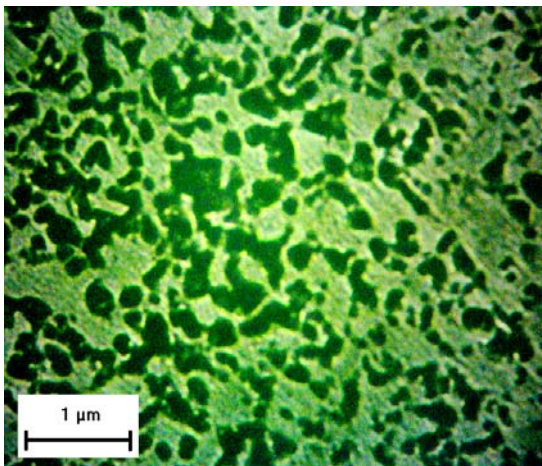


Fig. 7 The pores distribution after sintering - general aspect

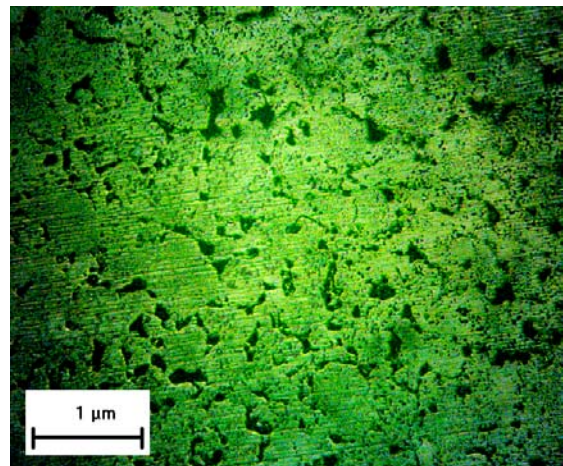


Fig. 8 The pores distribution after 800 MPa repressing - general aspect

The SEM analysis after sintering, figure 9, contrary to those expected, has distinguished a structure formed from a homogeneous solid solution with Ni - base, without hard phases separations, phenomenon due to the mechanical milling process [1], [3].

The samples were quenched in water from 1050 °C, then heated to 850 °C for 24 hour, and colded together with the furnace (in tight containers filled to begin with argon).

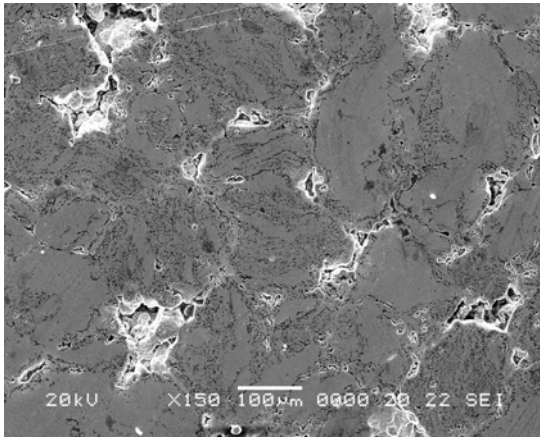


Fig. 9 The alloy structure after sintering - integral powder, 8 hours milled, $\phi 22\text{mm}$, $p_c = 800\text{ MPa}$

The heat treatment has re-established the classic structure (figure 10). It is observe the separation of the chromium carbides in the likeness of some networks and of the γ' compound, $\text{Ni}_3(\text{TiAl})$, in the likeness of some dark color precipitates.

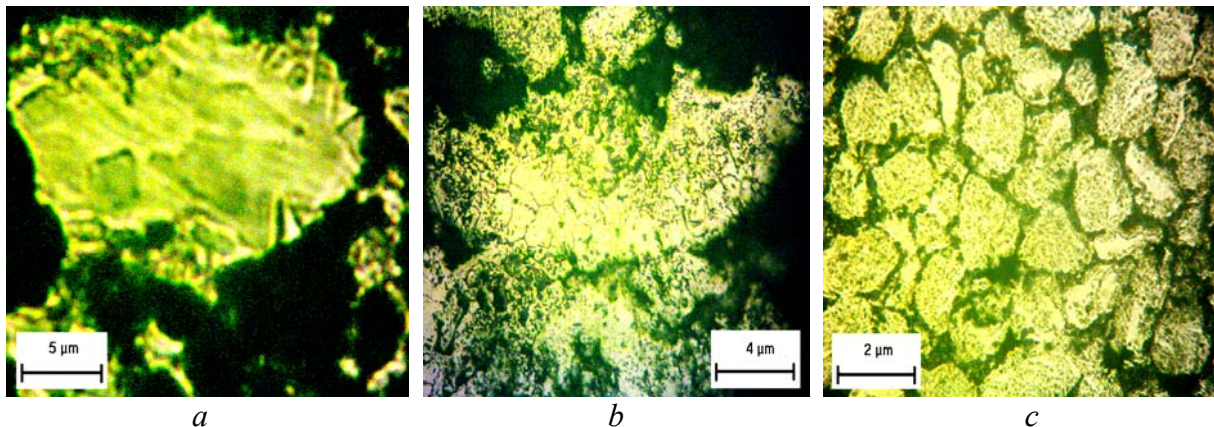


Fig. 10 The alloy structure after heat treatment of quenching and annealing - sort 3 integral powder

3. Conclusions

The powder elaborated through atomizing cannot be compacted because of the spherical shaped granules presence. The mechanical milling resolves this trouble, being possible the reaching some maximum compactnesses as pressed of 65,67% for the powder with (80-100) μm granulation, the sort 2, and of 69,65% for the integral powder, the sort 3, at the 800 MPa pressing.

The sintering and repressing can increase the compactness with maximum 15,54% in the case of the granulometric fractions and with 17,67% for integral powder.

The mechanical milling operation for 8 hours produces the structure change in sense the acceptation in the solution setting of the precipitate phases, resulting a homogeneous solid solution. The heat treatments applied, bring back the hard phases in the basic structure.

REFERENCES

1. V. Candea, S. Lapusan, C. Popa, A. Popa, M. Rosso, Study concerning the increase of the utilization ratio of a Nickel based powder obtained through gas atomization, PM2004 World Congress Vienna, vol PM non ferrous, p. 763-768.
2. *** Metals Handbook, ASM, 8th edition, 1998, vol.7.
3. *** Metals Handbook, ASM, 9th edition, 1998, vol.4.
4. D. Furrer, H. Tech, The performance demands on new superalloys, Advanced materials and processes, January 1999, p. 81-83.

Received December 12, 2005

¹ *Technical University of Cluj-Napoca, Romania*

² *Metallurgical Research Institute of Bucharest, Romania*

**ASPECTE PRIVIND COMPORTAREA LA PRESARE SI REPRESARE A UNUI
SUPERALIAJ CU BAZA Ni**

REZUMAT: După elaborarea prin pulverizare din fază lichidă a aliajului Nimonic 80, fracția grosolană (>125 μm) reprezentând material nefolosit în mod practic, a fost măcinată într-o moară planetară pentru îmbunătățirea caracteristicilor de presabilitate. Au fost determinați parametrii de presare. După sinterizare, pentru reducerea porozității, s-a aplicat o represare. În vederea obținerii structurii specifice acestei clase de superaliaje, soluție solidă γ cu precipitate din faze dure, s-au aplicat tratamente termice.

A METHOD TO DETERMINE THE DISTRIBUTION OF TEMPERATURE IN CUTTING TOOLS OF GIVEN CONFIGURATION

BY

CIUCESCU EDUARD PETRE¹, CIUCESCU DORU²

***ABSTRACT:** In order to predict the behavior of tools is is very important to determine the distribution of temperature during cutting.. The difficulty of this problem is the impossibility to lay out the thermocouples at the surfaces placed between the cutting tool and the part to be cut. It is known that the risung of the tempering temperature leads to a gradual decrease of the fineness of the phase mixture and consequently to a decrease in hardness. In this paper is presented a method to determine distribution of temperature during cutting based on the hardness obtained after tempering.*

***KEY WORDS:** quenching, tempering, hardness, temperature, cutting tools.*

1. INTRODUCTION

The behaviour of tools during running is influenced by the temperature obtained due to the friction with the part to be cut. In order to predict the behaviour of tools during running is very important to know the distribution of temperature in the volume during cutting. The main problem in determining the distribution of temperature during cutting is the impossibility to lay out the thermocouples at the surfaces placed between the cutting tool and the part to be cut.

In the same time it is known that the risung of the tempering temperature leads to a gradual decrease of the fineness of the phase mixture and consequently to a decrease in hardness.

Also, there are many references concerning mathematical modells from which some are developped in the form of softs sold in the markets.

In this paper is presented is presented a method to determine distribution of temperature in the volume during cutting based on a new approach of this problem, which is the hardness obtained after tempering.

2. SOME ASPECTS OF TEMPERING THE STEELS

As it is known, the quenched steel is hard and brittle due to the martensitic transformation wich is made by rising of the volume. The tempering is a subsequent heat treatment made in the attempt to realize a convenient combination of strength and

toughness. This goal is realized by a heating to a temperature less than Ac_1 and a slow cooling.

During tempering, the two solutions –martensite and retained austenite- are suffering a gradual decomposition by diffusion, which arrive in a mixture of ferritic matrix with finely disseminated carbides particles. When the tempering temperature is risen, the fineness of the phase mixture is decreased and, consequently, the hardness is also decreased.

In the case of a plain carbon hypoeutectoid steel with 0,45 %C, the microconstituents obtained during tempering are in the following order: temper martensite, temper toostite, temper sorbite and globular pearlite in which the carbides particles are more and more globular.

The tempering of this steel proceeds in several stages (Fig.1): I. heating up to 200 °C, when the excess carbon is eliminated as submicroscopic carbides; II. heating from 200 °C up to 300 °C, when the retained austenite is decomposed; III. heating from 300 °C to 400 °C, when are eliminated the internal stresses by recovery and recrystallization of ferrite; IV. heating from 400 °C to 700 °C, when is occurring the coalescence and spheroidizing of cementite.

Consequently, the hardness is decreasing gradually (Fig.1).

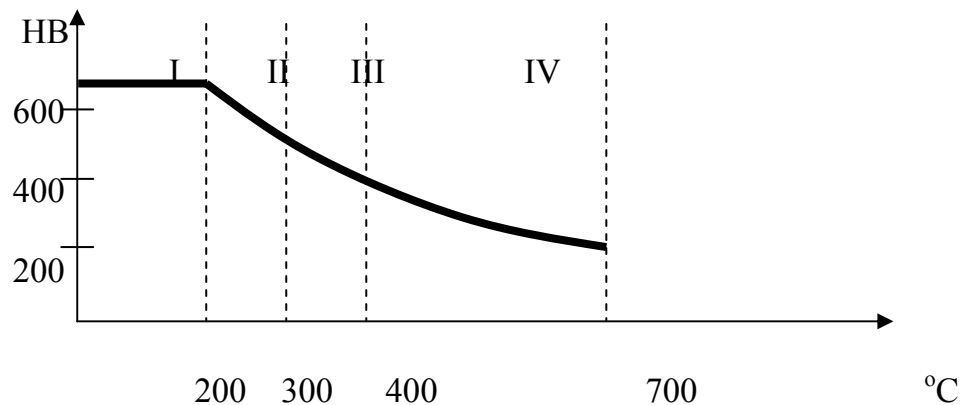


Fig.1. The evolution of hardness during tempering of the steel OLC45.

I. heating up to 200 °C, when the excess carbon is eliminated as submicroscopic carbides; II. heating from 200 °C up to 300 °C, when the retained austenite is decomposed; III. heating from 300 °C to 400 °C, when are eliminated the internal stresses by recovery and recrystallization of ferrite; IV. heating from 400 °C to 700 °C, when is occurring the coalescence and spheroidizing of cementite.

3. DESCRIPTION OF THE METHOD

Firstly, are prepared a number as great as necessary of OLC 45 steel specimens (at least 30 specimens) which have the configuration of the cutting tool to be studied. Also, the part to be cut is a soft steel, as OLC 15.

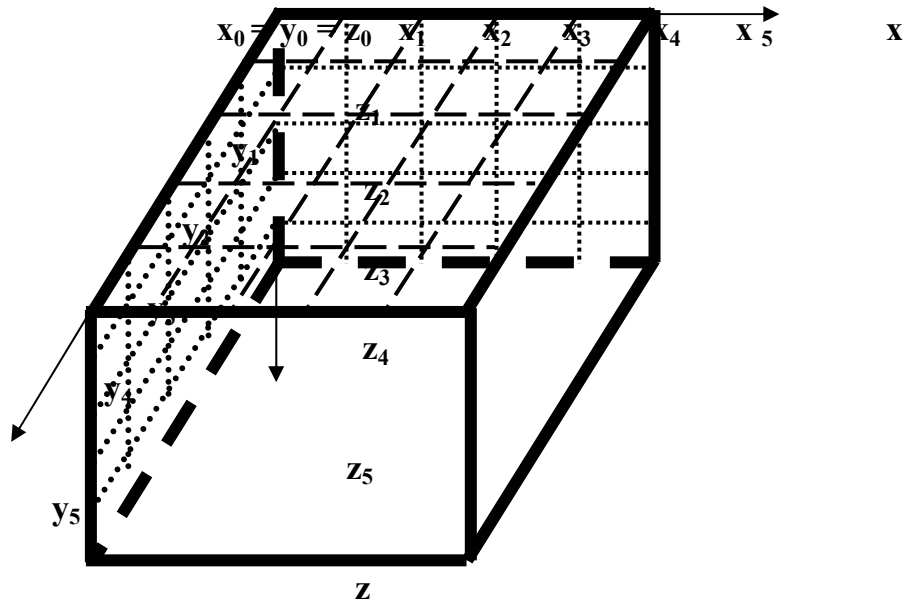
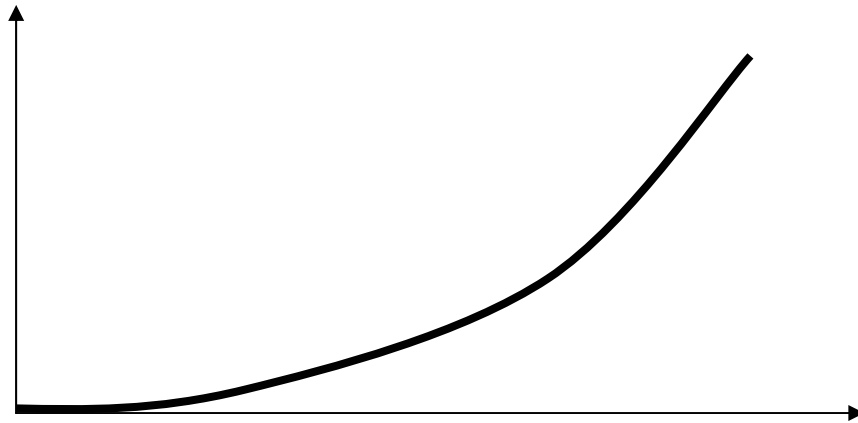


Fig.1. The web of points to determine the hardness and temperature



1 3 5 7 9 11 13 15 17 19 21 23 25 27 29 31 33 35 37 39 41 43 45 49 51 53 55 57 59 s

Fig.2. The evolution of temperature in time

Table 1. The values of hardness and temperature obtained at $t = 1$ s.

x_1y_1		x_1y_2		x_1y_3		x_1y_4	
HRC=	t =						
x_2y_1		x_2y_2		x_2y_3		x_2y_4	
HRC=	t =						
x_3y_1		x_3y_2		x_3y_3		x_3y_4	
HRC=	t =						
x_4y_1		x_4y_2		x_4y_3		x_4y_4	
HRC=	t =						
x_1z_1		x_1z_2		x_1z_3		x_1z_4	
HRC=	t =						
x_2z_1		x_2z_2		x_2z_3		x_2z_4	
HRC=	t =						
x_3z_1		x_3z_2		x_3z_3		x_3z_4	
HRC=	t =						

x_4z_1		x_2z_2		x_3z_3		x_4z_4	
HRC=	t =						
z_1y_1		z_1y_2		z_1y_3		z_1y_4	
HRC=	t =						
z_2y_1		z_2y_2		z_2y_3		z_2y_4	
HRC=	t =						
z_3y_1		z_3y_2		z_3y_3		z_3y_4	
HRC=	t =						
z_4y_1		z_4y_2		z_4y_3		z_4y_4	
HRC=	t =						

The method proceeds in several stages:

- 1) the hardening by bulk quenching of all 30 specimens in the same conditions:
 - heating temperature: 850 °C;
 - maintaining time: at least 30 minutes;
 - water bath;
- 2) the determining the distribution of hardness at a single specimen at the cross points of the web made from lines placed at 3 mm distance for 3 faces, as a verifying of the uniformity of bulk quenching;
- 3) the use, for the same type of cutting, of each specimen, taken separately for different times, for example: 1 s, 3 s, 5 s, 7 s, 9 s, 11 s, 13 s, 15 s, 17 s, 19 s, 21 s, 23 s, 25 s, 27 s, 29 s, 31 s, 33 s, 35 s, 37 s, 39 s, 41 s, 43 s, 45 s, 47 s, 49 s, 51 s, 53s, 55 s, 57 s, 59 s, after which proceeds to a cooling in water to reduce the self-tempering;
- 4) at the last specimen is determined the evolution of the temperature in time in an accessible point, for example, x_2y_2 with a thermocouple (Fig.2);
- 5) the determination of the hardness for all specimens at points x_1y_1 ; x_1y_2 ; x_1y_3 ,..., which are mentioned in corresponding tables, for example: table 1; table 2...;
- 6) on the bases of stages 4) and 5) are converted the values of hardness in values of temperature.

4. CONCLUSIONS

The advantages of this method are the following:

- permits to determine the temperature in the points of the surface where can not be placed thermocouples;
- may be used for all kinds of cutting tools;
- permits the determination of a „cloud” of values of temperature, which is in 3D and variable in time;
- the „cloud” may be used as a verification of an elaborated mathematical model or as data for a new one.

REFERENCES

1. Ciucescu, D. (2001). *Materials Study * Metallic Materials*, Plumb Printing Company, Bacău.
2. Petrescu, M. ș.a. (2000). *Metals, ceramics and polymers*, Tipografia Printing Company, București.

Received December 14, 2005

¹UNIVERSITY “DUNĂREA DE JOS” FROM GALAȚI
²UNIVERSITY FROM BACĂU

O METODĂ PENTRU DETERMINAREA DISTRIBUȚIEI TEMPERATURII ÎN SCULELE AȘCHIETOARE DE CONFIGURAȚIE DATĂ

REZUMAT: Pentru a prevedea comportarea sculelor este foarte important să se determine distribuția temperaturii în timpul așchierii. Dificultatea problemei constă în imposibilitatea plasării termocuplelor pe suprafețele situate între scula așchietoare și piesa de așchiat. Se știe că ridicarea temperaturii de revenire duce la o scădere graduală a fineții amestecului de faze și, în consecință, la o scădere a durității. În această lucrare este prezentată o metodă de determinare a distribuției temperaturii în timpul așchierii bazată pe duritatea obținută după revenire.

Metoda presupune parcurgerea următoarelor etape: 1) durificarea prin călire a tuturor probelor în aceleași condiții; 2) se determină distribuția durității HRC la o singură probă pe direcții paralele între ele, situate la o distanță de 3 mm pe trei fețe sau mai multe fețe; 3) separat, fiecare probă este utilizată la aceeași operație de așchiere pentru durate diferite de timp (după care este răcită prin imersie în apă (răcirea cu apă nu afectează duritatea constituienților de revenire deja formați, dar oprește continuarea procesului de revenire datorată inerției termice); 4) la ultima probă, într-un punct dat se determină continuu temperatura cu ajutorul unui termocuplu și a unui aparat corespunzător; 5) se determină distribuția durității HRC la toate probele și se trec în tabele; 6) pe baza datelor obținute în etapele 4) și 5) se convertește în grade Celsius fiecare duritate obținută și se trece în aceleași tabele.

Avantajele metodei constă, în principal, în posibilitatea determinării temperaturii în orice punct al suprafețelor sculelor așchietoare.

CALCULATIONAL MODEL OF ENERGETIC BALANCE-SHEETS IN THE CASE OF PROCESSING THROUGH ELECTRIC EROSION

BY

ANTON ADRIAN DAN¹, SLĂTINEANU LAURENȚIU¹, ONOFREI ROXANA¹

ABSTRACT: *In general, to calculate useful energies of thing by processing through electric erosion it takes (into consideration) into account for the calculation, just the phenomenon of the melts and evaporation who are in progress in the zone of thing. Taking into account of the other phases which appear on lengthways process, the actual study determines the energetic balance-sheet, totalizing specific energy of each phase.*

KEYWORDS: *balance-sheets, melting temperature, temperature of vaporization*

1. Introduction

The processing through erosion takes part of the series of technological methods from dimensional processing that are fundamental in the technology of manufacturing machines [2].

The processing through erosion is a technological method of finale processing, based on the erosive effect of an electric non-steady discharges, that leads to the destruction integrity and to the overweight material take-off from the surface blank under the form of fluxes of particles solids, liquids, gaseous, of plasma or radiance electro-magnetic [2].

To determine the energetic balance-sheet in zone of thing, it is taken into account the fact that at a discharge, beside temperature of melt and evaporation, there are losses of energy as a result of heating and decomposing the environment of thing [1].

The present study aims to calculate the useful necessary energy processing through electric erosion using four phase of process:

- bring material until temperature of melts;
- effective melting of material;
- bringing of an amounts of material from temperature of melts until temperature of vaporization;
- vaporization of an amounts of material.

Using an equipment of processing through electric erosion that already is in the laboratory (fig.1) we will realize some experimental attempts, and then we will

elaborate a graphic representation of the craters size depending on the capacity condenser.

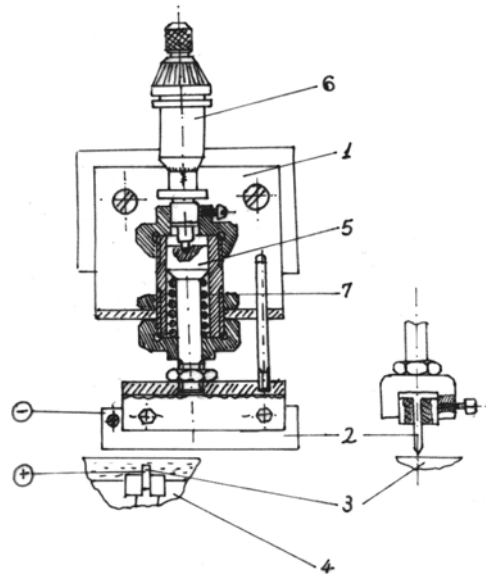


Fig.1

The equipment of processing through electro-erosion using an alone impulse of discharge

Board 1 could be mounted on the vertical slatted of machines tools; the electrode-tool 2 in form of sleazy plate displaced toward the blank 3, immobilized in the box clamp 4, with the help of a system with piston 5, act of micrometer screw 6. At turning in sense reversely of micrometer screw, under action bow 7 will be in progress the withdrawal electrode.

2. The energetic balance-sheet concerning the processing through electric erosion.

Useful necessary energy processing can be written as:

$$W_u = K_1 W_d \quad (1)$$

in which: W_d is the energy discharge;

K_1 - coefficient concerning used energy for the take-off material from blank (not all the discharge energy is used for take-off).

Energy of discharge W_d may be evaluated using these relations [1]:

$$W_d = \frac{C}{2} (U_i^2 + U_f^2) \quad (2)$$

in which: C is the capacity condenser

U_i - feeding tension initial;

U_f - feeding tension final.

To realize the energetic balance-sheets will cause necessary energy for each phase of processing:

1. Necessary energy to bring the material to a melting temperature:

$$W_{t1} = mC \Delta\theta = mC(\theta_t - \theta_i) \quad (3)$$

where: m is the amount of material;

C – specific heat;

$\Delta\theta$ – variation of temperature;

θ_i - initial temperature;

θ_t - melting temperature.

2. Necessary energy for the melting material:

$$W_{t2} = m\lambda_t \quad (4)$$

where: λ_t is the latent heat of melts;

3. Necessary energy to bring the material to a temperature of vaporization:

$$W_{v1} = K_2 m C (\theta_v - \theta_t) \quad (5)$$

where: K_2 is the coefficient concerning the loss of energy which appears before vaporization (not all molten material are transformed in vapors)

θ_v - temperature of vaporization;

θ_t - temperature of melts.

4. Necessary energy for the temperature of vaporization:

$$W_{v2} = K_2 m \lambda_v \quad (6)$$

where: λ_v - latent heat of vaporization.

To realize energetic balance-sheet we will totalize the four energies concordant with each phase:

$$W_u = W_{t1} + W_{t2} + W_{v1} + W_{v2} \quad (7)$$

$$K_1 \frac{C(U_i^2 - U_f^2)}{2} = mC(\theta_t - \theta_i) + m\lambda_t + K_2 mC(\theta_v - \theta_t) + K_2 m\lambda_v \quad (8)$$

From the expression of density $\rho = \frac{m}{V}$ we have the mass of material $m = \rho \cdot V$.

We will consider that volume craters realize for initiation electric discharges is $V = \frac{\pi R^2 h}{2}$ so we can write: $m = \rho \frac{\pi R^2 h}{2}$.

As a result the energetic balance-sheets expression can be written such as:

$$K_1 \frac{C(U_i^2 - U_f^2)}{2} = \rho \frac{\pi R^2}{2} h [C(\theta_t - \theta_i) + \lambda_t + K_2 C(\theta_v - \theta_t) + K_2 \lambda_v] \quad (9)$$

$$R = \sqrt{\frac{K_1 C(U_i^2 - U_f^2)}{\rho \pi h [C(\theta_t - \theta_i) + \lambda_t + K_2 C(\theta_v - \theta_t) + K_2 \lambda_v]}} \quad (10)$$

3. Experimental dates

For the graphic representation specified in the introduction I have achieved experimentally some discharges on a blank from steel, to different discharged capacities and I obtained the set of values for R presented in the table 1.

Table 1. Experimental results

C=330 μ F	U=57 V	R=0,90 mm
C=660 μ F	U=54 V	R=1,14 mm
C=1000 μ F	U=53 V	R=1,16 mm
C=2000 μ F	U=51 V	R=1,32 mm
C=3000 μ F	U=49,5 V	R=1,97 mm

Analyzing the form of the crater section surface it can be noticed that it is approximate circular just as it is presented in (fig.2).

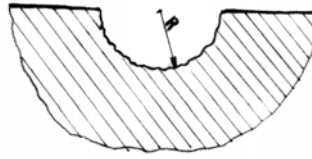
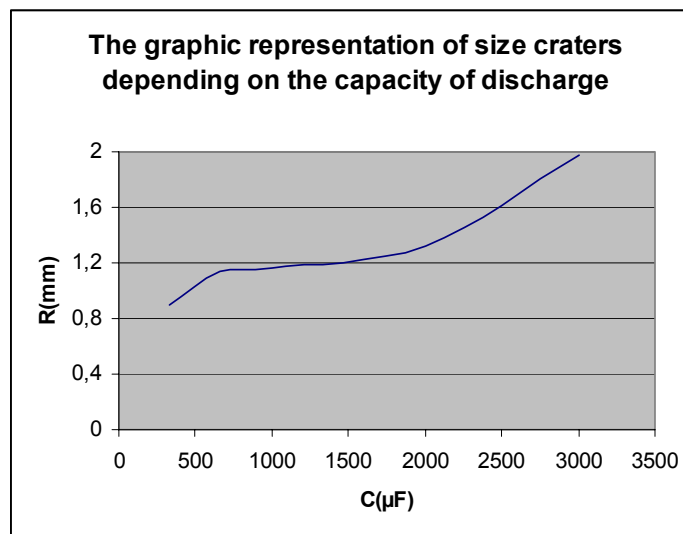


Fig.2
Form of the crater section surface



4. Conclusions:

It has been from the graphic representation and from the experimental dates that if the capacity grows the dimension of the crater grows too.

In the case of processing by erosion electric to establish the balance energetic it is required besides the energy necessary for melting, and vaporization of the material, to be aware of the other losses of energy that appear in the processing time.

REFERENCES

1. Gavrilaş, I., Marinescu, N. Processing ne-conventional in construction of machines. vol 1, Printing House Technique, Bucharest, 1991;
2. Nichici, A., Popa, N., Popovici, V. and. al. Processing through erosion in construction of machines. Romania, Printing House Facla, 1983.

Received December, 15 2005

¹Technical University Gh. Asachi Iasi

MODEL DE CALCUL AL BILANȚULUI ENERGETIC ÎN CAZUL PRELUCRĂRII PRIN EROZIUNE ELECTRICĂ

REZUMAT: În general, pentru calculul energiei utile de lucru la prelucrare prin eroziune electrica se iau în calcul doar fenomenele de topire și evaporare ce au loc în zona de lucru. Ținând cont și de celelalte faze care apar pe parcursul procesului, lucrarea de față determină bilanțul energetic, însumând energia specifică fiecărei faze.

SUSTAINABLE INDUSTRIAL DEVELOPMENT, THE ONLY WAY FOR EUROPEAN INTEGRATION OF ROMANIA

BY

A. DIMA¹, A.A. MINEA¹

***ABSTRACT:** Protecting the environment became, at this time, a major problem of all the humanity. In this context, regarding Romania integration in European community, we must show that one of the principals chapters that were negotiated for time extension is Environment. In the present article, on the basis of the new scientifically ways to board the "TO KNOW HOW" area, we are proposing for analysis an other way to board the sustainable development concept.*

***KEYWORDS:** industrial development, European integration, new concept*

1. Introduction

Protecting the environment became, at this time, a major problem of all the humanity. The irrational industrial developments, the excessive chemicalization of agriculture, town extension are the factors of polluting, with high negative impact on environment. This chaotic development can not contribute to a sustainable development; it goes to a present development with negative effects in future times.

2. Discussions

We must remark that, in the present, are a lot of studies which shows that a brutal action under environment will damage the ecological equilibrium that goes, finally, to disasters. These ecological disasters will negatively influence not only the further development, but the life possibilities in safe conditions, too.

As follows, near United Nations Organizations take place an International Commission of Development and Environment. This commission is supervising the evolution of environment quality and monitor economical activities that could damage the earth ecological equilibrium.

In this context, regarding Romania integration in European community, we must show that one of the principal chapters that were negotiated for time extension is Environment. This chapter can not be closed until full integration, that we all want it in 2007, 1 January.

Making a step back to International Commission of Development and Environment we can show that its activity till now is concretized in creation and consolidation of a new concept called Sustainable Development Concept.

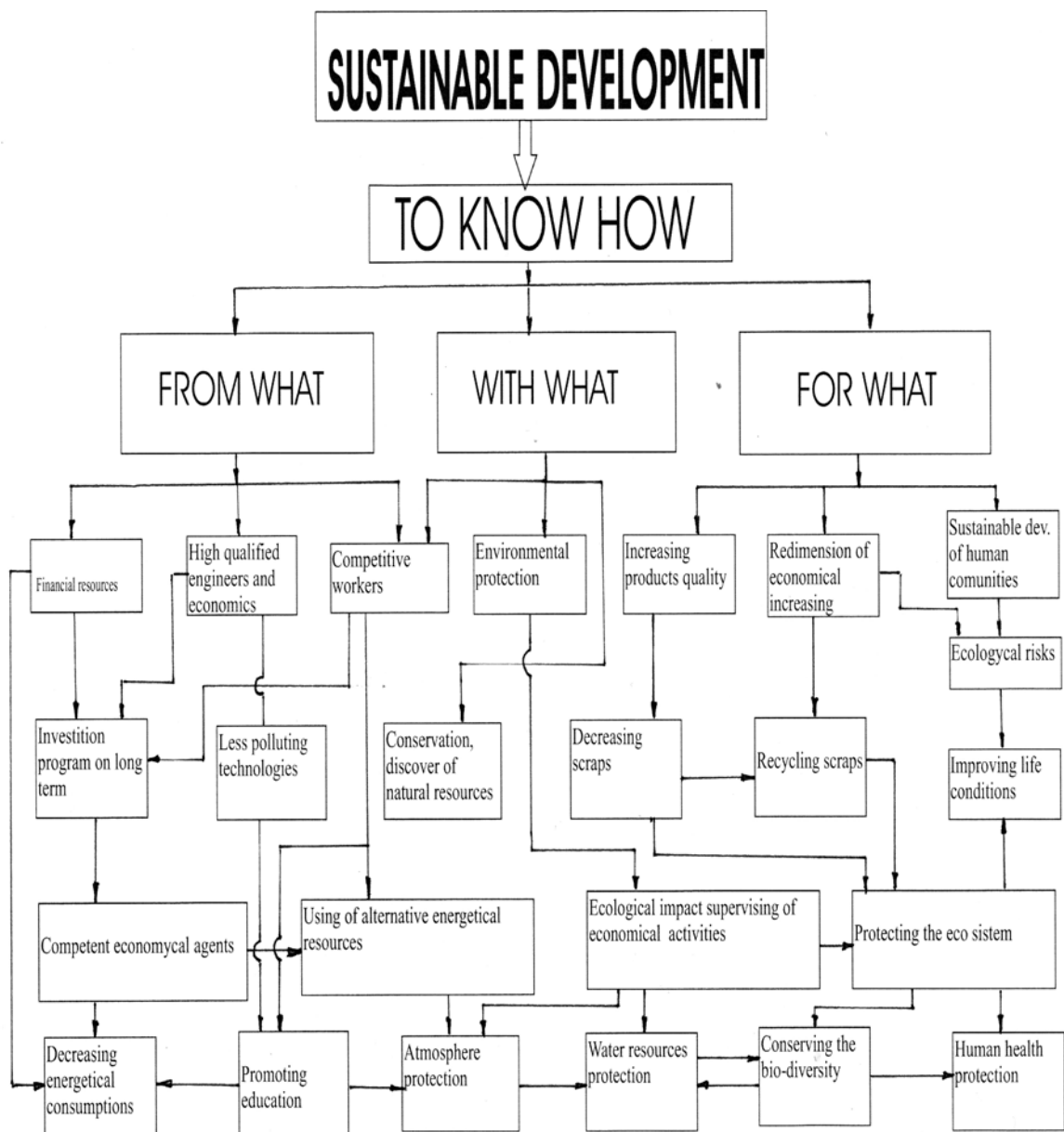


Figure 1. Scheme for illustrating the influence sustainable development concept

The concept is promoting that way of economical development that assure the rational use of conventional energetical resources, resources that assure the use of non conventional energetical resources and the regenerative ones, along with protection and conservation the environment.

This concept shows that, for assuring the welfare of the present and future generations it is highly recommended to preserve and conserve the existing patrimonies.

So, by practically applying this concept, we must find the optimum solutions regarding economical dimensioning in all areas in order to discover and to apply the non polluting technologies and to develop an ecological agriculture.

The concept of sustainable development can be defined like: the developments that accomplish the present necessities without compromising the needs of the future generations.

In conclusion, by applying this concept in the concrete case of our country, it can be said that sustainable development consist in the capacity of the national system and the authorities to realise a perfect equilibrium between social, technical and economical conditions and environment quality that are contributing to the welfare of our country.

The sustainable development concept is creating lot of disagreement in opinions moving to dangerous ideas regarding stopping the economical development and absolutization of environment role.

In this idea, in the rapport of Rome Club regarding human economical development is pointed that it is not normal to absolute the environment role in the disfavour of economical development. Also, in this rapport is shown that sustainable development must sustain human progress on the entire planet for as longer as it can. In this context, there are a lot of comments regarding principal objectives, priorities and concrete actions.

In this article, on the bases of the new scientifically ways to board the “TO KNOW HOW” area, we are proposing for analysis an other way to board the sustainable development concept, as shown in figure 1.

3. Conclusions

In conclusion, by applying this concept in the concrete case of our country, it can be said that sustainable development consist in the capacity of the national system and the authorities to realise a perfect equilibrium between social, technical and economical conditions and environment quality that are contributing to the welfare of our country.

In order to apply the ways and programmes that is going to a sustainable development are necessary important financial and human resources and to understand that, at the moment, it is necessary to minimize our profits to accomplish large benefits later. The difficulties are amplified by the necessity of immediate financial resources, while the positive effect is very hard to quantify it now.

It is obvious the fact that, without European community immediate support, our country can not accomplish a sustainable development at a competitive level. This support will be given to us because the sustainable development issue, that implies environment protection, is a global problem.

REFERENCES

- 1 T.Rusu, L.Moldovan, SE Avram (2003) Managementul activitatilor pentru protectia mediului, Ed. Mediamira, Cluj Napoca
- 2 A. Nicolae (2004) Dezvoltare durabila in siderurgie prin valorificarea materialelor secundare, Ed. Printech, Bucuresti.
- 3 V. Nisteanu (1999). Elemente de ecologie, Ed. Bren, Bucuresti.

Received December 12, 2005

¹“Gh. Asachi” Technical University of Iasi, Romania

DEZVOLTAREA INDUSTRIALA DURABILA, SINGURA SANSA A ROMANIEI IN CONTEXTUL INTEGRARII EUROPENE

REZUMAT: Protectia mediului a devenit, la ora actuala, o problema majora, de o deosebita importanta, cu care se confrunta omenirea.

In acest context, privind integrarea romaniei in comunitatea europeana, trebuie sa aratam ca unul din principalele capite la care s-a negociat prelungirea timpului de rezolvare si dupa integrarea propriu-zisa este Mediul.

In prezenta lucrare, pe baza perceptelor noii modalitati stiintifice de abordare a domeniului „TO KNOW HOW”, va propunem spre analiza o alta modalitate de abordare a conceptului dezvoltarii durabile.

ASPECTS REGARDING MICRO ALIED STEELS BEHAVIOR AT HOT FORGING

BY

C.O. BURCEA¹, A.A. MINEA², M I DIMA³, IBN OMER MOHAMED ABDALLA
MOHAMED ABUGUSSA²

ABSTRACT: *The paper is a presentation of micro allied steels advantages. The experiments were done in accurate conditions and it results clearly the contributions brought by this paper.*

In the case of metallic materials hot forging, in order to examine their deformability, we can twist a pipe with different twisting degrees and the plasticity is given by the number of twisting until test part breaks.

This method have the advantage of a great flexibility and an increased number of tests on a single test part, by applying different temperatures and deformations on different parts of the same test part. Torsion test is the most complete test that can be applied. As a disadvantage is the appearance of a full range of torsion rates in the part section. The hot torsion test was made at 800, 900 and 1000°C. At the first moment, the parts were heated at 1100°C for 300 sec. and cooled at testing temperatures.

We can conclude that the crack deformation and the maximum stress are increased for the micro allied steel.

KEYWORDS: *micro allied steel, hot forging, crack deformation*

1. Introduction

Hot forging is an industrial widely used technological process for steels. It is well known that pure metals are more plastically than their alloys and the fact that monophasic alloys are more deformable than polyphasic alloys. These certain is given by the presence of foreign atoms in metallic network that are producing a phenomenon of distortion, also making harder the cleaving process on high density planes of atoms. So, in these conditions, metal plasticity is decreasing with the increasing of deformability resistance.

In steels case, if carbon percentage is increasing also the plasticity get lower and deformability resistance get higher.

The plasticity of steel with maximum 1% carbon, in the temperature area for austenitic stadium, is high enough getting closer to ferrous plasticity. Increasing the carbon percentage, steels plasticity is decreasing especially because of the higher number of foreign atoms in the base network of α ferric.

2. Experimental

The alloying constituents from base metal can condition the plasticity and also the deformation resistance in many conditions:

- foreign atoms, coming into crystal lattice of base metal, can provoke lattice distortion increasing the deformation resistance – this aspect become more obvious if the foreign atom is from a chemical element that is far from iron in the Mendeleev Periodical Table of elements;
- if the number of alloying elements is very high, also the deformability resistance will be higher, because of the cold-hardening;
- the alloying elements that are contributing to phase transformation from mono to biphasic are a source of plasticity decreasing.

The influence of alloying elements on steels deformability is shown in table 1.

Table 1. Influence of alloying elements on steels deformability

Influence of alloying elements	Plasticity	Deformability resistance
Increasing influence	Cr > 15%, Ti < 0,15%, Mn, V < 1,5%, Co, Ca, Rare earth	Cr < 9%, Ni > 0,03%, W, Ni
No influence	C < 1%, Cr < 0,6%, Ni > 5%, N < 0,03%	Ni < 5%, Al, C, P, Ti, B, As, Cu, S, Pb, Ca, Nb
Decreasing influence	C > 1%, Al, S, Mo, W, Nb, Cr < 9%, As, Cu, P, B, Si, N > 0,03%, Pb, Ti > 0,2%	Cr > 13% Mn > 10%

Vanadium micro – allied steels, that are used for petroleum pipes, have some particularities regarding hot forging.

The recrystallisation and dynamic precipitation that appear during hot forging have a great influence on final austenitic germ size that is conditioning the steel properties. These phenomena can be shown, for many steels, using hot forging stretching methods for different deformation rates. Micro alloying elements are determined for steels characteristics because of their solution in austenitic matrix and of the precipitation (figure 1).

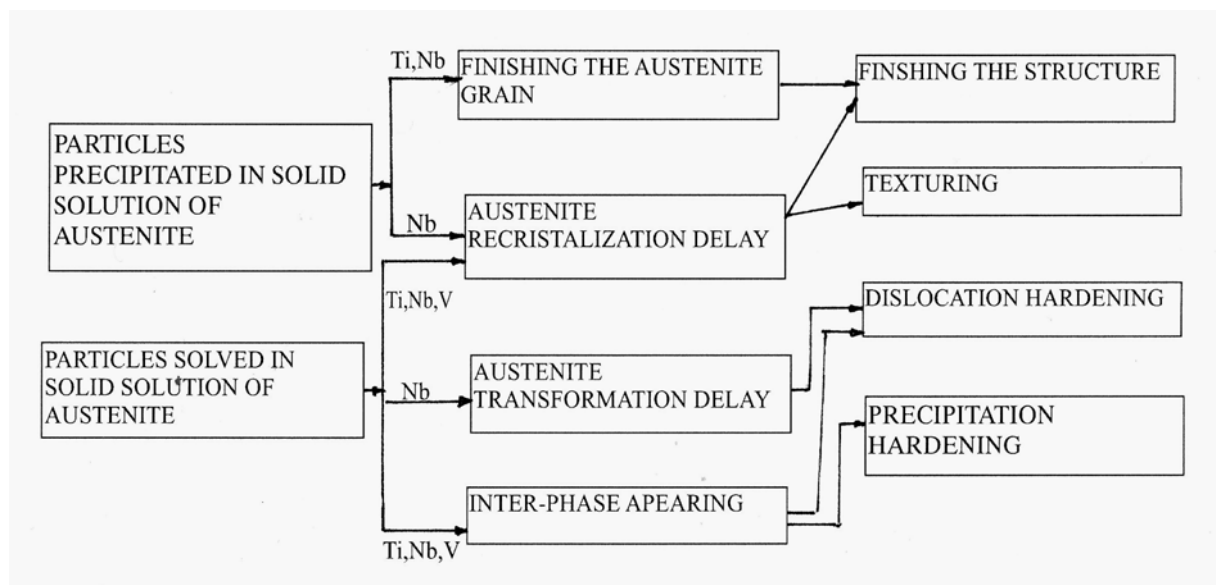


Figure 1. Scheme for illustrating the influence of micro alloying elements

The experimental study was made on two steels, as in table 2, that are used at hot forging petroleum pipes.

Table 2. Chemical composition of studied alloys

steel	Chemical composition									Observations
	C	Mn	Si	P	S	Cr	V	Mo	Al	
OLT 65	0,4 – 0,5	0,7 – 1,0	0,17 – 0,35	Max. 0,04	Max. 0,04	0,09	-	0,001	0,019	Reference steel
31VMn12	0,28 – 0,34	1,1 – 1,4	0,17 – 0,37	Max. 0,035	Max. 0,035	0,11	0,1 – 0,2	0,001	0,018	Study steel

These steels were elaborated in charges of 50 Kg and forged in 20 mm pipes, from which were sampling the test parts for hot forging stretching test. (figure 2) These tests were made on an SETARAM equipment from ICEM Bucuresti.

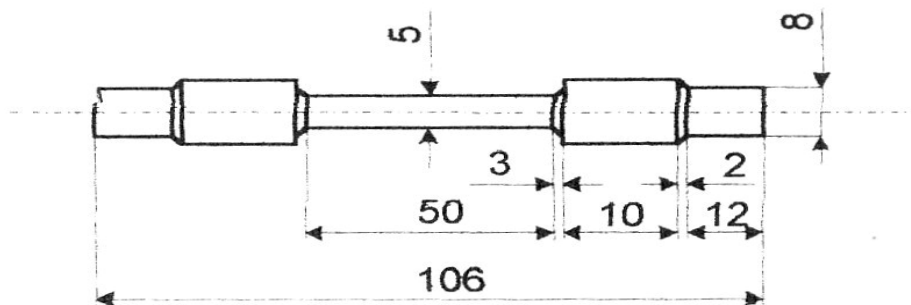


Figure 2. Stretching test part

In the case of metallic materials hot forging, in order to examine their deformability, we can twist a pipe with different twisting degrees and the plasticity is given by the number of twistings until test part breaks.

This method have the advantage of a great flexibility and an increased number of tests on a single test part, by applying different temperatures and deformations on different parts of the same test part. Torsion test is the most complete test that can be applied. As a disadvantage is the appearance of a full range of torsion rates in the part section. The hot torsion test was made at 800, 900 and 1000°C, and is illustrated in figure 3. At the first moment, the parts were heated at 1100°C for 300 sec. and cooled at testing temperatures.

Analyzing the experimental dates that were obtained, we can write, mathematical:

$$\varepsilon = \frac{\gamma}{\sqrt{3}} = \frac{R\theta}{L\sqrt{3}} = \frac{R2\pi n_r}{L\sqrt{3}} = 0,218n_r$$

In this equation, terms are:

R – test part radius, 3 mm

L - test part length, 50 mm

θ – torsion angle

n_r – number of rotations.

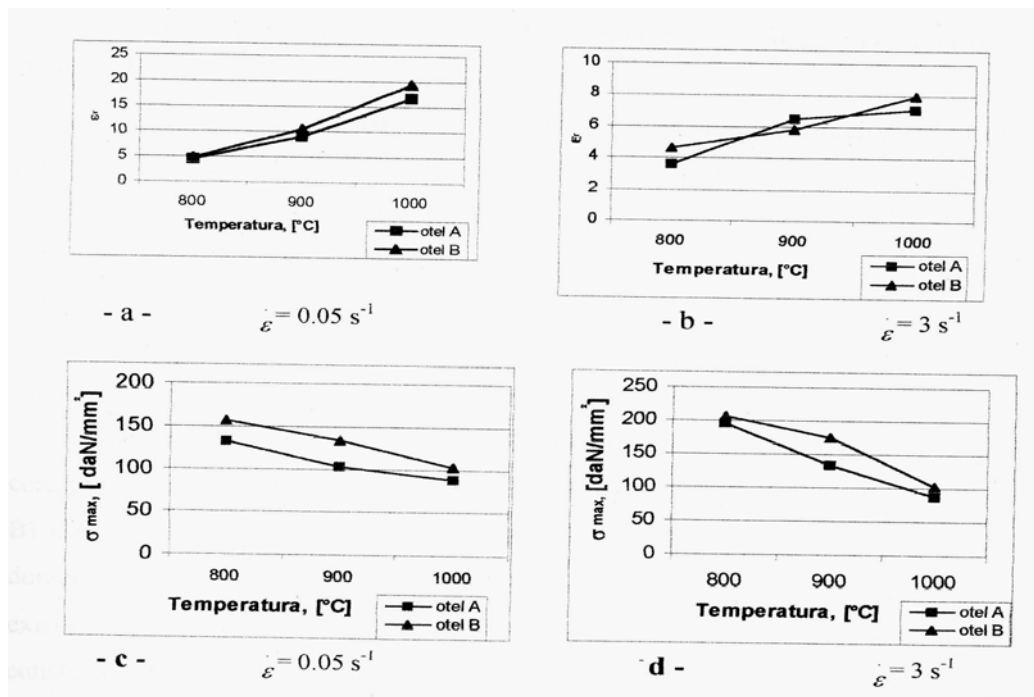


Figure 3. Variation of deformation and tension on forging temperature

3. Conclusions

The experiments were done in accurate conditions and it results clearly the contributions brought by this paper.

Also, we can conclude that the crack deformation and the maximum stress are increased for the micro allied steel, in comparison with the allied steels.

This fact is recommending the micro allied steels for fabrication of petroleum pipes.

REFERENCES

- 1 C.O.Burcea (2002) Cercetari privind influenta microalierii asupra comportarii la procesarea otelurilor destinate tevelor pentru transportul produselor petroliere, Bucuresti
- 2 E. Cazimirovici (1999) Bazele teoriei deformarii plastice, Ed. Bren. Bucuresti.
- 3 Cuida Oleg (2000). Influenta elementelor de aliere reziduale si de microaliere asupra plasticitatii otelurilor, Ed. Image, Bucuresti

Received 12 december 2005

²Gh. Asachi" Technical University of Iasi, Romania

³Tutora School, Tutora, Iasi

ASPECTE PRIVIND COMPORTAREA LA DEFORMARE PLASTICA LA CALD A UNOR OTELURI MICROALIAATE CU VANADIU

REZUMAT: Aceasta lucrare prezinta importanta folosirii microalierii cu vanadiu, in cazul fabricarii prin deformare plastica la cald a tevelor utilizate in industria petroliera.

Rezulta clar, din experimetele efectuate, ca atat deformatia la rupere cat si tensiunea maxima pana la rupere sunt mai mari pentru otelul microaliat, decat cel utilizat clasic.

MATERIALS SCIENCE AND ENGINEERING, AN IMPORTANT AREA OF A SUSTAINABLE DEVELOPMENT

BY

A. DIMA¹, A.A. MINEA¹, MI DIMA², IBN OMER MOHAMED ABDALLA
MOHAMED ABUGUSSAÏSSA¹

ABSTRACT: *The paper is a presentation of materials science and engineering field and its importance in a sustainable development. Materials engineering represent the applicative side of materials science and puts the basis of materials obtaining technologies, which are very important in the actual stadium of the industrial society development.*

In conclusion, Materials Science and engineering represents a science in full evolution in concordance with the necessities of a modern society. Without modern materials and without European integration we can not conceive a society development at the needed level

KEYWORDS: *materials science, engineering, sustainable development*

1. Introduction

In the actual economical situation of our society, economical increasing must remain the principal objective for our integration in European community.

Economical increasing can not be concrete without protecting the environment, because a chaotically economical development it is going to ruin the life conditions with non recoverable repercussions in time.

Sustainable development, the concept that clearly define that it must establish the present necessities without compromising the ability of future generations to satisfy their own needs, represent the only way to progress.

Also, there are many opinions that this concept, of sustainable development is a utopia, that this concept can not be imposed to transition and poor countries, because of their impossibility to apply and respect these principles.

So, it is necessary a stagnation of economical development if we do not want to affect the environment.

The outstanding results in area of materials science and engineering from the last 10 years, on the basis of developing non polluting technologies and constant re-using of scraps is creating the premises to affirm that the materials science and engineering development permit the discovery of non polluting technologies, that are using non conventional fuels, ecological technologies for scraps reusing.

These facts are contributing to realise an effective economical increasing on the basis of sustainable development.

2. Discussions

Economical development on industrial basis it is strictly connected with development of materials engineering, environmental protection and its resources because of using the minerals resources (bringing out, working out, processing) in industrial processes that are producing industrial gases that have a high degree of pollution, and affects the environment.

For decreasing these negative aspects, the materials obtaining and processing technologies must concentrate on reducing the consumptions of materials and energy, on decreasing the technological losses and minerals resources and on minimizing of polluting emissions and scraps.

In highly developed countries it was imposed a legislation regarding pollution, a legislation that is needed to be applied in our country, too. These laws are referring at the designing in the same time with the destruction (at the end of the life-cycle) of technologies or products. This project of designing (with the project of destruction) must contain elements and possibilities of recovery of some parts of the initial project.

The implementation of non polluting or with a low degree of polluting technologies (ecological technologies) are very expansive and need important material resources. The economical agents, in their majority, do not have enough capital and financial assets to apply these technologies, so authorities must interfere to support these initiatives to introduce the non polluting technologies and to minimize the negative effect of industrial activity over environment.

The chaotically industrial development, massive forest land clearings, water courses deviations, brutal modifications of eco systems, intense exploitation of natural deposits are important risk factors that can not be avoided.

It is a very wrong thesis that sustains the issue according to this is the price we have to pay for welfare increasing.

For underlining the importance of some economical and industrial category as a subject of sustainable development, in assuring environmental quality conditions, these have the eco suffix. Eco-material and eco-product represent, in this context, categories that have an ecological performance, as:

- to respect the norms of environmental quality, product norms and emissions norms;
- to have a high degree of recyclability to justify big expanses for storing or neutralization.

It can be said, at this moment, that the eco suffix is old, because in the present time we must rapport us not only at ecological matters, also at the matters that satisfied the model of sustainable development.

In this context we must operate with notions as sustainable material or durable material.

It may say that a sustainable material, processed in a sustainable industry is the result of an industrial process characterised through:

- have eco material characteristics and it is, also an performant material;
- have the substitution of diverse assets: natural, economical, human etc;
- metallurgical processes and technologies are transforming into social engineering;

- represents the success of scientifically and technological progress, in industrial globalization conditions;
- integration of environmental engineering in scientific sciences, as part of socio – economical theory.

From industrial metallic materials area an important place have steel. In this context, we can say that, in the present, steel can be considered as a sustainable material, made in a sustainable syderurgy.

The arguments for sustaining this idea are:

- steel is and will be the principal metallic vector for developing high research areas, with direct implications in life quality;
- syderurgy represents an auto-performant area through increasing the technical and scientific assets. Often, the assets in this area are underestimated, because the innovations are known, strictly by the specialists and producers. The work from materials engineering is find in developing of materials industries;
- the syderurgy have a process of translating the quality of material giver to industrial systems giver;
- steel evolution is based on industrial fitness, defined as the way found by an industrial area stays always in actual trend.

Industrial fitness represents the procedure in which an industrial area stays young, for its workers. This is not a biological age issue; it is the expression of an interior attitude. To be always young in industrial sciences means not to be finished ever, to continue improving the development.

3. Conclusions

For our country, that is in a full process of European integration , the phenomena's and processes which take place at international level, represents a chance to integrate us in this process without going through precursory levels.

Materials Science represents a science in full evolution in concordance with the necessities of a modern society. Without modern materials and without European integration we can not conceive a society development at the needed level.

In our region we put accent on regional development especially by education at the level of technical high – degree education. Therefore, after the right training of human capital, we can introduce modern and competitive engineering in order to produce modern materials through advanced technologies.

In conclusion, to this area, of materials science and engineering it is assigned the mission to find technical and technological solutions for reducing the negative aspects of other activities, for reducing the environmental pollution and to contribute with scientifically researches to invigorate the polluted areas.

REFERENCES

- 1 T.Rusu, L.Moldovan, SE Avram (2003) Managementul activitatilor pentru protectia mediului, Ed. Mediamira, Cluj Napoca
- 2 A. Nicolae (2004) Dezvoltare durabila in siderurgie prin valorificarea materialelor secundare, Ed. Printech, Bucuresti.
- 3 M.Bordea (2006). Consideratii si cercetari privind informatizarea proceselor metalurgice din unele aggregate moderne pentru elaborarea otelurilor, teza de doctorat, Cluj Napoca.
- 4 A.Dima, AA Minea (2004) Durable development – way to progress, welfare and european integration, Buletinul IPI,trom XL, Iasi

Received 12 december 2005

¹Gh. Asachi” Technical University of Iasi, Romania

²Tutora School, Tutora, Iasi

**STIINTA SI INGINERIA MATERIALELOR, DOMENIU DEFINITORIU AL UNEI
DEZVOLTARI DURABILE**

REZUMAT: Această lucrare prezintă importanța domeniului Știința și Ingineria Materialelor în dezvoltarea durabilă a unei regiuni. Se poate spune că, în acest moment, denumirea tehnologiilor specifice ingineriei materialelor cu prefixul eco este depășită, deoarece în prezent trebuie să ne raportăm nu numai la rigorile de natură ecologică, ci în special la cele de dezvoltare durabilă.

TECHNOLOGY TRANSFER IN ADVANCED MATERIALS IN ROMANIA: A KEY ISSUE FOR SUSTAINABLE DEVELOPMENT

BY

ROBERT RADU PITICESCU¹

ABSTRACT. *The technology transfer of advanced materials including nanomaterials is of crucial importance for the sustainable development of many industrial branches from textiles and home appliances to high tech applications in microelectronics, sensors, actuators or medicine. Synthesis of nanopowders (metallic, ceramic, semiconductors composites or hybrid inorganic/organic) and their processing to advanced materials is accompanied by a number of changes in chemical or physical properties that require a close cooperation between the research and industry for their successful transfer into innovative high added value products. Some examples of technologies ready to be transferred from the recent portfolio of National Institute for Non-ferrous and Rare Metals are presented.*

KEY WORDS: *advanced materials ,nanopowders, technology transfer.*

1. SYNTHESIS OF ADVANCED MATERIALS IN THE NATIONAL R&D INSTITUTE FOR NON-FERROUS AND RARE METALS.

National is a strategic institute with about 40 years of activity in the field of non-ferrous metallurgy, material science and engineering. The basic activity consists in the elaboration of studies, research works, technology transfer, consulting as well as small tonnage production developed in the following main fields:

Metallurgy and environment protection: new technologies for obtaining non-ferrous and rare metals, hydrometallurgical technologies, recycling of Non-ferrous and Rare Metals, technologies for environment protection.

New and Advance Materials: special alloys:non-ferrous Powder Metallurgy, biomaterials (metallic, ceramic and composites), metallic, ceramic and composite coatings; nanomaterials; modeling and optimization of synthesis processes.

The main equipment for research activities and technological services existing are: hydrometallurgical laboratory plant; electron beam furnace, electric furnaces, induction furnaces, laboratory plant for electrolysis of metals, laboratory for sol-gel colloidal synthesis of ceramics and composite powders, autoclaves for hydrothermal synthesis of nanopowders, hydrothermal/electrochemical system for thin film nanostructured films, laboratory for chemical analysis, XRD, TDA and TG, microstructural characterization.

2. CENTER FOR TECHNOLOGY TRANSFER OF ADVANCED MATERIALS

During last years, following the participation of the institute in more NATO Science for Peace, European Projects (in the frame of 5th and 6th Programmes) a significant number of new materials and technologies have been made available for both national market and European partners. The transfer of these technologies became of high importance in order to improve the competitiveness of the Institute. With the support of National Programme INFRATECH starting with 2004 it was started the Centre for Technology Transfer for Advanced Materials (CTT AVANMAT). The centre is located inside the headquarter of the National R&D Institute for Non-ferrous and Rare Metals and has as strategic partners the Romanian Chamber for Trade and Industry with main idea of a wide dissemination of knowledge toward SMEs and National R&D Institute for Microtechnologies for future implementation of some advanced materials toward high tech environment.

The mission of the centre consists in:

- Rapid technological transfer and implementation of new technologies toward SMEs;
- Identify market requirements for new technologies, services and products in the field of advanced biocompatible and smart metallic, ceramic and composite materials;
- Consultancy and expertise in the field of advanced materials ;
- Participation in elaboration of prognoses in the field;
- Improving industrial training for personnel working in the field of advanced materials;
- Encouraging specialized studies for students, masters, PhD students;
- Consultancy for SMEs and companies in the elaboration and participation in national and European R&D projects;
- Support for SMEs in implementation of European standards for materials.

3. TECHNOLOGICAL OFFER

Some examples of technologies available in the portfolio of CTT AVANMAT are given below:

- **New metal/ceramic nanocomposites with designed composition and phase distribution for special applications.**

A chemical sol-gel colloidal process starting from inorganic precursors has been developed to produce nanostructured composite powders consisting of a metallic core (stainless steel, Ni, magnetic alloys) and a thin nanostructured ceramic shell was developed. Figure 1 presents the special morphology of these powders. This was developed in the frame of an European CRAFT project. The processing of these powders may be done by conventional pressing and sintering in controlled atmosphere, plasma spraying as well as other advanced techniques such as microinjection molding. As a function of the nature of components the applications may vary from high corrosion resistant coatings to magnetic microsensors and even substrates for implants.

- **Technology for the hydrothermal synthesis of nanostructured ceramic powders.**

Low reactions temperatures specific to hydrothermal synthesis of nanopowders avoid problems related to the volatilisation of components and stress induced defects, produces nanocrystalline powders due to uniformity of nucleation and growth and it is economically accessible for SMEs due to the lower costs for energy, instrumentation and precursors. The time required for one-step synthesis process and energy consuming is lower for the hydrothermal processes due to the fact that mixing and milling steps used in traditional ceramic technology are not necessary.

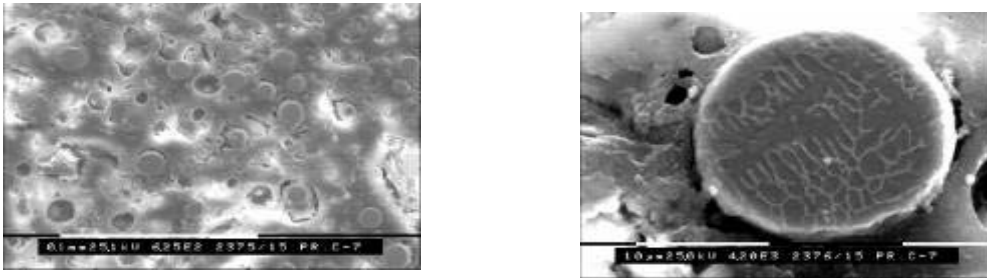


Figure 1. SEM for composite stainless steel core/alumina shell particles, calcined in Ar atmosphere

Technologies for a large range of ceramic nanopowders have been optimised, such as: - barium titanate (BT) and lead zirconate titanate (PZT) (resulting from an European PHARE Project for Technology Transfer and Quality Management and a project in the National Programme for New and Advanced Materials, Micro and Nanotechnologies). These powders can be processed into dense sintered pellets used as substrates in piezoelectric device applications (figure 2).

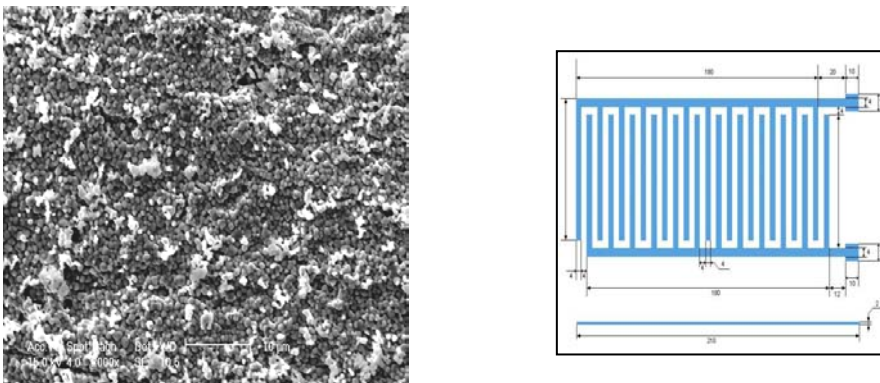


Figure 2. SEM image of PZT sintered pellet and design of piezoelectric sensor system

- yttria-doped zirconia/alumina nanocomposite powders that could be processed via different methods (tape-casting, hot pressing) for mechanical pressure sensors with higher sensitivity (applications resulting from a NATO Science for Peace Project).

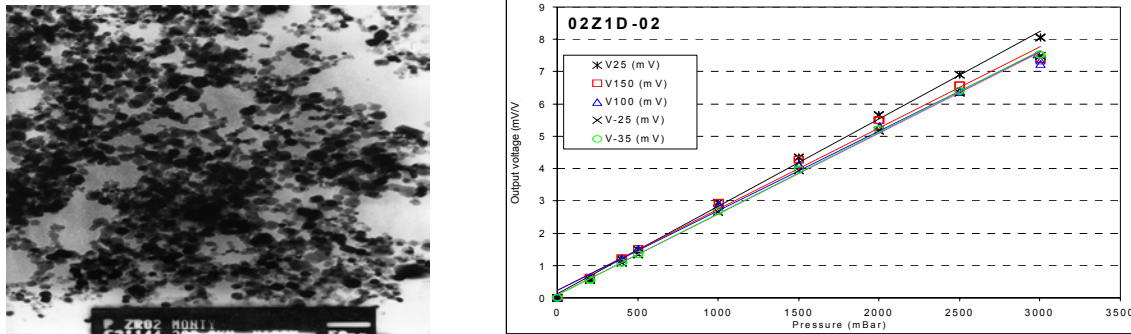


Figure 3. TEM image of Y₂O₃-ZrO₂ nanopowders obtained by hydrothermal method and the signal output of the mechanical pressure sensor obtained by processing of these nanopowders

- hybrid composite nanopowders based on hydroxyapatite and functionalized polymers were synthesized in-situ at temperatures below 150⁰C resulting in powders with high specific surface area and enhanced properties for biomedical applications (table 1). The original process has been developed in the frame of an project financed by the National Programme for New and Advanced Materials, Micro and Nanotechnologies. It opens new fields of applications in the field of tissue engineering as materials with enhanced biocompatibility (figure 4).

Table 1. Main characteristics of hybrid hydroxyapatite/polymer nanopowders

Characteristics	Commercial hydroxyapatite	Hydrothermal synthesized hydroxyapatite	Hydroxyapatite/ maleic acid copolymer hybrid nanopowders
Specific surface, m ² /g	39	59.48	148.59
Picnometric density, g/cm ³	3.02	3.03	2.93
Particle size, nm	33	33.27	14.4

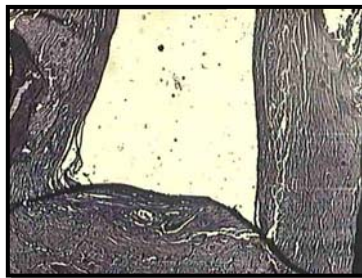


Figure 4. Visual aspect of hybrid hydroxyapatite/polymer nanopowders obtained by hydrothermal method and its behavior during in-vivo tests

- **Technological services**

We can offer also services for characterization of metallic, ceramic and composite materials (main elements, impurities, C, N and O content, XRD, SEM, complex thermal analysis), compressibility tests for a wide range of metallic, ceramic and composite powders as well as other tests required for implementation of advanced materials into different fields of applications.

Received December, 15 2005

¹Center of Technological transfer for Advanced Materials

TRANSFERUL TECHNOLOGIC IN DOMENIUL MATERIALELOR AVANSATE IN ROMANIA: UN DOMENIU KEY CHEIE PENTRU DEZVOLTAREA DURABILA

REZUMAT. Transferul tehnologic in domeniul materialelor avansate inclusiv nanomaterialele are o importanta cruciala in dezvoltarea durabila a majoritatii ramurilor industriale de la textile si bunuri de larga folosinta la aplicatii “ high tech” in microelectronica, senzori, actuatori sau medicina. Sinteza nanopulberilor (metalice, ceramice, semiconductori, composite sau hibride anorganic/organic) si procesarea lor la materiale avansate este insotita de un numar de modificari ale proprietatilor chimice si fizice ce necesita o cooperare stransa intre cercetare si industrie pentru a asigura succesul transferului tehnologic in produse cu valoare adaugata ridicata. In lucrare se prezinta cateva exemple. de tehnologii ce pot fi transferate din protofoilul recent al Institutului National de C-D pentru Metale Neferoase si Rare.

THE STUDY OF SANDS FROM THE REGION VĂLENI THE VALLEY FÂNTÂNELE (HUȘI)

BY

NASTACA TIMOFTE¹, BOGDAN NICOLAU¹

ABSTRACT: *On the outskirts of the locality Văleni (Huși), from the perimeter of Pădureni, there is an important accumulation of sand on a high profile of 30-40 m laying on a surface of 2 km.*

The analysed sand in the region Fântânele belongs to the superior Chersonian, being divided into three distinct levels:

- *the superior level, composed of very thin granular sands, with a high levigating component of 6,07%;*
- *the medium level, composed of thin sand, with a medium levigating component on a profile of 1,72%*
- *the inferior level, composed of very thin sands, with a high levigating component of 7,39%*

The sand in the region Fântânele developed in a deltaic environment, with a mineralogical content, consisting of quartz (65 – 85%), muscovite (5 – 10%), opaque minerals (1 – 3%) and iron oxydes of the goethite - limonite type.

KEYWORDS: *Văleni (Huși), granular sands, mineralogical*

1. INTRODUCTION

South from the town Huși, in the superior basin of the Elan river (affluent of Prut), in the hills of Lohan, an important accumulation of sand develops. To the Elan` springs there are several affluents of this river, which, by erosion, have opened excellent massive horizons of great dimensions of sand, with thin intercalations of gritstones and clays. The best opening than 2 km long, can be found along the valley Fântânele, which in the region of its springs opens the sands. The Valley Fântânele goes through the village Văleni (Huși), and then it flows into the Elan river.

2. THE GEOLOGY OF THE REGION

The examined perimeter comprises sarmatian formations belonging to the Chersonian.

In his doctoral dissertation Jeanrenauld (1958) divided the Chersonian from south of Huși in two unities:

- The inferior unity, with small mactres;
- The superior unity, in seaside facies , lacking in fossils.

The superior unity, which comprises the sands examined by us, facies deltaic develops, without mactres.

North from the village Văleni, (ancient Șchiopeni), the Valley Fântânele opens the succession of sands that totalizes 80 – 90 m thickness (fig. 1). Excellent openings appear in the almost vertical slopes of the canion of sand which the Valley Fântânele

digged through erosion. In this profile, the Chersonian begins with an horizon of 5 m of bluish clays. At the entrance in the canion, going upstream, there follow 10 – 12 m of sand with crossed structure and microconglomerates with clay pebbles. Then there are reddish sands, weakly ferruginous (4 m thick), out of which we have gathered samples 5 and 6. It follows a level of sandy clays and clayey sands (9 m thick), out of which we have gathered. Then, on a thickness of 10 m, there are sands with fragments of *Planorbis*. The following 10 m thickness consist of sands that contain small concretions. To the superior part of the profile from the Valley Fântânele there is compact sand, with a thickness of 40 m. In these sands, there are lenticular quartz gritstones and trovants.

Thickness	Lithological column	Number of samples	Type of rock
	10	Massive sands with trovants and lenticular gritstones strata	
	9	Trovants sands	
	8	Trovants sands	
	7	Bluish clays and sands	
	6	Breccia with clay pebbles	
	5	Ferruginous sands	
	4	Massive sands with crossed structure	
	3	Microconglomerates with clay pebbles	
	2	Clays and silthites	
	1	Sandy clays	

Fig. 1. The lithological column of sands of Văleni (Huși) in the outcrop from the stream Fântânele.

3. THE GRANULOMETRIC COMPOSITION

We have analysed granulometric 18 samples of sand, collected in the following way:

1. From the profile of the riverbad and from the slopes of the Valley Fântânele: samples V, F-14, F-12, F-2;
2. From the quarry of sand from the village Leoști, Pădureni (Huși): samples IV, V.

In the Table 1 are presented the results of the granulometric analyse expressed in granulometric fractions, separated through sifting. The results are given in grams and percents of weight remained on each sieve. We have calculated also the

cumulative which we expressed in percents remained on the sieve and in percents passed through the sieve.

Table1. Granulometric composition of the sands from the region Văleni, Valley Fântânele (Huși)

Sample V	Sieve	Remained on the sieve		Cumulative	
	mm	Grams	Grams %	Remained %	Passed %
Total mass = 50 g Left on the server = 1.320 Losses = 0.379	1.00	0.25	0.5	0.5	99.5
	0.63	0.47	0.94	1.44	98.56
	0.5	0.56	1.12	2.56	97.44
	0.4	0.61	1.22	3.78	98.22
	0.315	0.74	1.48	5.22	94.74
	0.25	1.99	3.98	9.24	90.76
	0.2	9.66	17.32	26.56	73.44
	0.16	0.66	1.32	27.88	72.12
	0.1	31.87	63.74	91.62	8.38
	0.063	2.49	4.98	96.6	3.4

Sample F-14	Sieve	Remained on the sieve		Cumulative	
	mm	Grams	Grams %	Remained %	Passed %
Total mass = 50 g Left on the server = 0.97 Losses = 0.490	1.00	0.14	0.28	0.28	99.72
	0.63	0.29	0.56	0.84	99.16
	0.5	0.22	0.44	1.28	98.72
	0.4	0.34	0.68	1.96	98.04
	0.315	0.53	1.06	3.02	96.08
	0.25	1.18	2.38	5.38	94.62
	0.2	6.85	13.7	19.08	80.92
	0.16	16.84	33.68	52.76	47.24
	0.1	18.97	37.94	90.7	9.3
	0.063	3.19	6.38	97.08	2.92

Sample F-12	Sieve	Remained on the sieve		Cumulative	
	mm	Grams	Grams %	Remained %	Passed %
Total mass = 50 g Left on the server = 0.97 Losses = 0.490	1.00	0.62	1.24	1.24	87.76
	0.63	0.62	1.24	2.48	97.52
	0.5	0.54	1.08	3.56	96.44
	0.4	0.23	0.46	4.02	95.98
	0.315	0.42	0.84	4.86	95.14
	0.25	3.42	6.84	11.7	88.3
	0.2	16.65	33.3	45	55
	0.16	14.65	29.3	74.3	25.7
	0.1	10.55	21.1	95.4	4.6
	0.063	1.55	3.1	98.5	1.5

Sample F-4	Sieve	Remained on the sieve		Cumulative	
	mm	Grams	Grams %	Remained %	Passed %
Total mass = 50 g Left on the server = 1.93 Losses = 1.4	1.00	9.1	18.2	18.2	81.8
	0.63	2.74	5.48	23.68	76.32
	0.5	1.22	2.44	26.12	73.88
	0.4	1.43	2.86	28.98	71.02
	0.315	2.16	4.32	33.3	66.7
	0.25	2.16	4.32	37.62	62.38
	0.2	5.16	10.32	47.94	52.06
	0.16	6.03	12.06	60	40

	0.1	11.33	22.66	82.66	17.34
	0.063	5.34	10.66	93.34	6.66

Sample F-2	Sieve	Remained on the sieve		Cumulative	
	mm	Grams	Grams %	Remained %	Passed %
Total mass = 50 g Left on the server = 0.960 Losses = 0.460	1.00	5.34	10.68	10.68	89.32
	0.63	1.66	3.32	14	86
	0.5	0.58	1.16	15.16	84.84
	0.4	0.654	1.3	16.46	83.54
	0.315	0.98	1.84	18.3	81.7
	0.25	2.369	4.76	23.06	76.94
	0.2	5.94	11.88	34.94	65.06
	0.16	8.54	4.9	39.84	60.16
	0.1	25.96	51.92	91.76	8.24
	0.063	2.84	5.68	97.44	2.56

Sample IV	Sieve	Remained on the sieve		Cumulative	
	mm	Grams	Grams %	Remained %	Passed %
Total mass = 50 g Left on the server = 0.960 Losses = 0.460	1.00	0.06	0.12	0.12	99.88
	0.63	0.04	0.08	0.2	99.8
	0.5	0.03	0.06	0.26	99.74
	0.4	0.03	0.06	0.32	99.68
	0.315	0.14	0.28	0.6	99.4
	0.25	0.29	0.58	1.18	98.82
	0.2	3.36	8.72	7.9	92.1
	0.16	1.83	3.66	11.56	88.44
	0.1	32.96	65.92	77.48	22.52
	0.063	7.8	15.9	93.08	6.92

Based on these results we have built histograms, frequency curves and cumulative curves for all the samples. On the basis of these curves we have calculated the average, the standard deviation, the asymmetry, the graphic sharpness, the modified sharpness and the sorting coefficient S_0 .

The obtained results allow the division of the column of sand in three different levels:

- The superior level (samples V and F-2 to F-4), composed of very thin granular sands;
- The medium level (samples F-12 and F-14) which consists of thin sand;
- The inferior level (samples 5) composed of very thin sands.

The analysed sands show in the field a strong crossed stratification specific to the deltaic sands.

We have used the granulometric parameters calculated in order to built binary graphics of covariation of the pairs of parameters. On this basis we could determine the environments of sedimentation. The results are the following:

- Samples F-12, F-14, IV, V are part of the category eolian sands (from the dunes);
- Samples F-2, F-4, are sands of marine beach (Fig. 2).

4. THE LEVIGATING COMPONENT

The levigating component has been determined by washing, stirring, leaching and sedimentation. We have used a mechanic agitator with the speed of 300 rotations /

minute, with 20 mm long palettes, and with the angle of adjustment of 30 - 35°. The results are presented in the figure 2. The levigating component varies between 0,53% and 18,12% with the average of profile of 4,16%.

Table 2. Levigating component and the environment of sedimentation of the sands from the region Văleni – Valley, Fântânele (Huși).

The analysed samples	Levigating component		Environment of sedimentation
	%	Average on the profile	
V	18.12	4.16	Dune sand
IV	6.9		Dune sand
F-2	1.60		Marine beach sand
F-4	3.86		Marine beach sand
F-12	0.88		Dune sand
F-14	1.94		Dune sand

The mineralogic composition

The microscopic analyse and with the binocular magnifying glass of the samples of sand showed the presence in the samples of the following minerals (Fig. 3):

- Quartz, in the form of isometric granules or easily elongated and fragments of quartz and quartzite crystals;
- Lune spar, in the form of rounded granules and fragments of limestones;
- The muscovite, in the form of white grey thin papers, sometimes with hexagonal outline;
- Opaque minerals, in small quantities, consisting of pyrites and magnetite.

The quartz and lune spar granules are often covered with a film of goethite and haematite.

Table 3. The mineralogical composition of the sands from the region Văleni – Valley, Fântânele (Huși)

Number of sample	Minerals limits of variation, (%)				
	Quartz	Lune spar	Muscovite	Clayey minerals	Opaque minerals
V	65-75	10-15	5-10	10-17	1-3
IV	70-80	10-15	5-10	5-7	1-3
III	70-80	10-15	5-10	3-5	1-3
II	70-80	10-15	5-10	5-7	1-3
I	80-85	5-10	5-10	1-2	1-3
F-2	76-80	10-15	5-10	1-2	3-5
F-4	75-80	5-10	5-10	3-5	1-3
F-5	80-85	5-10	5-10	1-2	1-3
F-6	75-85	5-10	1-3	1-2	3-5
F-7	70-75	10-15	5-10	3-5	3-5
F-8	80-85	5-10	5-10	1-3	1-3
F-12	70-75	10-15	5-10	1-2	3-5
F-14	70-75	10-15	5-10	2-3	1-3
9	65-75	5-10	5-7	10-15	1-3
8	75-80	5-10	5-10	5-10	1-3
6	80-85	10-15	5-10	3-5	1-3
5	80-85	5-10	5-10	2-3	1-3

5. CONCLUSIONS

1. On the northern outskirts of the locality Văleni (Huși), from the perimeter of Pădureni, in the minor riverbed and in the slopes of the Fântânele stream, there is

an important accumulation of sands, well open in the quarry of Leoști and on the stream Fântânele.

2. The natural opening from the valley Fântânele is impressive by the following characteristics:
 - A) the excellent development of the profile in canyon, with vertical walls 30 – 40 m high, which we prefer to call for the first time cansand; B) the alternation of the sequences of sand with deltaic pseudoconglomerates lens; C) the sand shows a strong crossed stratification, typical for the delta; D) the cansand spar in the formation of sand is 2 km long and has vertical walls 30 – 40 m high.
3. The sands from the region Fântânele (Huși) are specific to the facies deltaic, without mactres, from the chersonian of the Moldavian Platform.
4. The sands from the region Fântânele (Huși) belong to the superior Chersonian, being equivalent in the geological column of the Moldavian Platform to the sands of Păun (Iași)
5. The stream Fântânele opens, by erosion, a succession of sand, silthite and clays of about 80-90 m thickness.
6. The sand analysed in the region Fântânele can be divided into three distinct levels:
 - A. the superior level (samples I- IV and F-2, F-4), composed of very thin granular sands, with a high levigating component, of 6,07%; B. the medium level (samples F-5, F-12 and F-14), composed of thin sand, with a levigating component, average on the profile of 1,72 %; C. the inferior level (samples 5, 6, 8 and 9), composed of very thin sands, with a high levigating component of 7, 39%;
7. The sands from the region Fântânele are made of the following minerals:
 - A. quartz (65 – 85%); B. lunc spar (5 – 15%); C. muscovite (5 – 10%); D. opaque minerals (1 – 3%);
8. Consisting of pyrites, magnetite and haematite. The red sand contains iron oxydes of the goethite - limonite type; The sands from the region Fântânele (Huși) developed in a deltaic geological environment.

REFERENCES

1. Brânzilă M. (1983): Contribuții la studiul nisipurilor cuarțoase de Bârnova din perimetrul localității Răducăneni. Conferința națională de turnătorie 26-27 mai Iași
2. Grasu C., Petreuş I, Brânzilă M. (1987) Associations des minéraux lourds dans le sable de Șcheia (plate forme Moldoava). Anal St. Univ. Al.I Cuza, II b Geol-Geogr XXXIII, Iasi
3. Ionesii L (1994): geologia unităților de platformă și a orogenului Nord-Dobrogean, ed. Tehnica, Bucuresti
4. Ionesii L, Petrus I si Ionesii Bica (1977): Studiul geologic si petrografic al nisipurilor si argilelor volhinienne din bazinul Somuzului Mare si al argilelor

Received January, 10 2006

¹Technical University "Gh. Asachi" Iasi

STUDIUL NISIPULUI DIN ZONA VĂLENI VALEA FÂNTÂNELE (HUȘI)

REZUMAT: La poalele localitatii Valeni (Husi), in perimetrul zonei Padureni, exista o importanta acumulare de nisip cu un profil inalt, in strat de 30-40 m, pe o suprafata de 2 km.

Nisipul analizat din zona Fantanele apartine Chersonianului superior, existand in trei nivele diferite:

- nivelul superior, alcatuit din nisip granular foarte fin, cu componenta levigabila inalta de 6,07%;

-
- nivelul mediu, alcătuit din nisip fin, cu componenta levigabilă medie de 1,72%;
 - nivelul inferior, compus din nisip foarte fin, cu componenta levigabilă înaltă de 7,39%.
- Nisipul din regiunea Fantanele s-a dezvoltat în mediu deltaic, cu conținut mineralogic, constând din cuarț (65-85), muscovite (5 – 10%), minerale opace (1-3%) și oxizi de fier de tipul goetit și limonit.

HYDROTHERMAL PROCEDURES: A NEW METHOD IN THE ENVIRONMENTAL DEVELOPMENT OF NANOMATERIALS

BY

ROXANA MIOARA PITICESCU¹, R. R. PITICESCU¹, E. VASILE²

ABSTRACT. Earth is a closed system and the energy and heat losses should be minimized to protect its biosphere, lithosphere, atmosphere and hydrosphere. In this purpose an increasing number of scientists focused their efforts toward new materials less harmful for the humans and new environmental friendly processes for their fabrication.. Well known and established techniques like CVD, MOCVD, sputtering, MBE and other spraying techniques require high energy consumption and require special means to avoid environmental problems. Soft solution (or soft chemical) processing like hydrothermal-electrochemical methods, inspired by the nature, have a great potential in the development of morphology-controlled nanomaterials for a wide range of applications, from opto/microelectronics to automotive, catalysis and biomaterials for implants. The main advantages come from their low energy consumption (low temperatures in one-step process), reduced environmental impact, versatility in production of many new materials in any shape and size. The paper presents a literature survey on the hydrothermal/electrochemical procedures for obtaining of perovskite powders and thin films and also some original results about the synthesis of Nb-doped PZT and BST materials using these methods.

KEY WORDS: hydrothermal synthesis, nanopowders, thin films, PZT, BST

1. INTRODUCTION

In the 1960s Feynman proposed to explore nanoscale size in different scientific disciplines, but the term nanotechnology was introduced for the first time in 1974 by Taniguchi. In 1980s Drexler popularized the term “nanotechnology” and introduced the concept of “molecular manufacturing” [1]. Starting from 1985 together with the discovery of C₆₀ the scientists were more and more interested in the field of nanomaterials. Development in computing power and materials modelling coupled with advances in characterisation techniques (AFM-atomic force microscopy, STM-scanning tunnelling microscopy) and synthesis routes are important factors that have enabled the designing of nanomaterials for specific application [2]. Today, nanotechnology is a frequently used term but it is no consensus regarding the limit of the nanodomain. Nanomaterials link together these two fields: nanosciences and nanotechnology. The properties of materials at nanoscale (1nm to 250 nm according to [2]; 1nm to 100 nm according to [1]) are governed by surface properties due to the large surface area. The variations of nanostructured microstructure can affect the macroscopic properties such as: electronic, optical, magnetic, chemical, mechanical and electrical properties. For nanomaterials it is expected the increase of some properties, such as: electrical conductivity of ceramics nanocomposites, electrical

resistivity of metals, magnetic coercivity, hardness and strength of metals and their alloys, luminescent efficiency of semiconductors.

It is well known that the size range below 100 nm is of greatest interest for the scientific community and represents the greatest application potential. Nanomaterials could be polymers, metals and ceramics. Nanoparticles can have different morphologies: spheres, flakes, platelets, tubes, rods and dendritic structures.

Nanoparticles can be manufactured by four generic routes: wet chemical, mechanical, form-in-place and gas phase synthesis [2]. Wet chemical procedures include: sol-gel methods, hydrothermal techniques and precipitation processes. Mechanical processes include grinding, milling and mechanical alloying techniques. Form-in-place processes include lithography, vacuum deposition techniques (CVD, PVD), spray coatings. Gas phase synthesis includes flame pyrolysis, electro-explosion, laser ablation, high temperature evaporation, plasma synthesis techniques.

The aim of the paper is to present hydrothermal electrochemical procedures an environmentally friendly method to produce nanomaterials. Some original results about the synthesis of Nb doped PZT and BST materials using these methods will be also presented.

2. BRIEF SURVEY ON HYDROTHERMAL ELECTROCHEMICAL TECHNIQUE

The first publication on hydrothermal synthesis of ceramics dated from the middle of the 19th century [3]. At the beginning the geologists tried to simulate in the laboratory natural hydrothermal phenomena occurring in the Earth's crust. The development of pressure engineering vessel in the 19th century determined the enhancing of researches in the field of hydrothermal synthesis in Germany, France, Italy and Switzerland. In the 20th century the main centres for studying and development of the hydrothermal techniques were in USA, Russia and Japan. In the 20th century hydrothermal synthesis was clearly identified as an important technology for material synthesis mainly for single crystal growth [3]. Due to the severe conditions required for the single crystal growth in the hydrothermal conditions (supercritical conditions), the commercialisation was very difficult. In the recent years the interest in commercialisation of the hydrothermal methods enhanced in part due to the possibilities to obtain a large family of materials under mild conditions (temperature <350°C, pressure < 100 MPa) [3]. Riman [3] defined hydrothermal synthesis as a process that utilises single or heterogeneous phase reactions at temperatures > 25°C and elevated pressures > 100 kPa to crystallise ceramic materials directly from solutions. The pressure is the vapour pressure above the solution at the hydrothermal parameters namely temperature, composition and concentration of the precursor solutions. Some additives are used: mineralising agent (organic / inorganic) to control pH and to promote solubility and other agents (organic / inorganic) to control the morphology or to promote the particle dispersion. A significant number of powders and films can be obtained in hydrothermal conditions at temperatures in the range 25-200°C and pressures <1.5 MPa. This hydrothermal synthesis breakthrough made it more interesting for the industry.

Some advantages of the hydrothermal synthesis are presented below:

- Hydrothermal synthesis is an environmentally friendly procedure due to the fact that it takes place at lower temperatures and pressures closely to the living conditions

on Earth. Other processes require higher temperatures and higher/lower pressures and therefore they are considered environmentally stressed (see figure 1) [4]. Low reactions temperatures avoid problems related to the volatilisation of components and stress induced defects;

- The rate and uniformity of nucleation, growth and aging can be controlled;
- Powders, fibers, single crystals, monolithic bodies, coatings on metals, polymers, and ceramics can be prepared;
- The costs for energy, instrumentation and precursors are lower. According to [4] a large quantity of energy is necessary to create melt, vapour, gas, plasma comparing to the formation of an aqueous solution at the same temperature. The time and energy consuming is lower for the hydrothermal processes due to the fact that mixing and milling steps are not necessary.
- Hydrothermal processes can be combined with electrochemical, mechanical, microwave techniques. Hydrothermal electrochemical synthesis is a soft solution processing (SSP) [4] which allows in situ fabrication of shaped, sized, oriented ceramic materials without firing, sintering or melting steps.

The increasing interest in hydrothermal synthesis is illustrated by the growing of number of scientific papers. In figure 1 is presented the estimated evolution of scientific papers on hydrothermal and hydrothermal electrochemical synthesis based on our own literature survey.

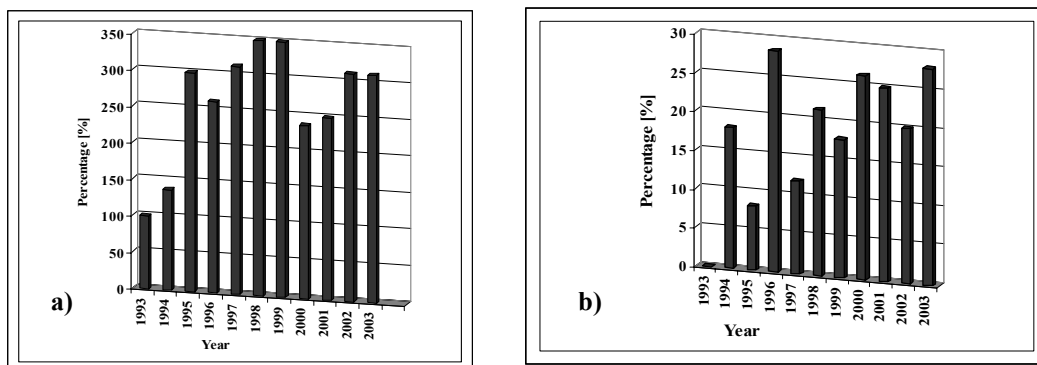


Figure 1. Scientific papers on hydrothermal synthesis (a) and hydrothermal electrochemical deposition processes (b)

In the last years hydrothermal methods were intensively studied and were applied to obtain nanomaterials: powders, thin/thick films, nanorods, fibers, nanotubes. Some of the recent examples are presented below: nanotubes arrays of barium titanate (BT) and barium strontium titanate (BST) were synthesised under hydrothermal conditions taking oxidised titania nanotubes as templates [5]; submicron, spherical $\text{Ba}_{0.75}\text{Sr}_{0.25}\text{TiO}_3$ powders were prepared by microwave-hydrothermal route using potassium titanyl oxalate, barium and strontium titanates as precursors; the mineralising agent was potassium hydroxide [6]; barium titanate powders were obtained by hydrothermal route starting from barium hydroxide and anatase [7]; thin films based on BST were grown on titanium electrodes in aqueous solutions by hydrothermal-electrochemical method starting from barium and strontium hydroxides deposited on anodised titanium [8]; thin or thick ferroelectric films (PZT for example) were obtained by electrophoretic deposition using a trifunctional additive [9]; PZT thin films were obtained by a hydrothermal method [10, 11]; α - Fe_2O_3 nanoparticle were

synthesised in hydrothermal conditions in aqueous organic microemulsion under mild conditions [12]; alkali-metal titanates [13] and single crystalline spinal cobalt ferrite nanorods [14] were also synthesised in hydrothermal conditions; indium hydroxide nanocubes (around 70nm length) have been prepared by a hydrothermal synthesis [15].

3. ORIGINAL RESULTS

When a synthesis technology of different materials is transferred to an end user some activities related to the environment protection have to be considered namely: identifying and characterisation of the wastage source, determination their environmental impact, management of the fabrication wastages getting together and storage, management of the fabrication wastages recovery. The Directive 96/61/EC regarding the provenience and integrated control of the contamination has to be taking into account. Our experimental laboratory work was organised following both the environmental impact of the hydrothermal synthesis and the obtaining of the nanostructured materials by this technique.

3.1. PZT powders and thin/thick films

Lead zirconate titanate based powders and thin/thick films were synthesised in hydrothermal conditions starting from soluble salts of Pb(II), Zr(IV) and Ti(IV). The synthesis procedure is described elsewhere [16, 17]. The impact of synthesis parameters on the environment with respect to the regulations is presented in table 1. The environmental impact can be reduced by using a continuous flow hydrothermal process.

Table 1. Experimental values for some ions after hydrothermal synthesis

Product	Cations concentration	Anion concentration
Mother liquour	Pb= 0.001-0.012 g/L (mean 0.01 g/L) Ti <0.005 g/L Zr<0,005 g/L K ⁺ =17,5-24,37 g/L (mean 21.4 g/L)	NO ₃ ⁻ mean 14,26 g/L Cl ⁻ mean 16,8 g/L
Washing solution, 1 st step	Pb= 0.007-0.012 g/L (mean 0.036 g/L) Ti <0.005 g/L Zr<0,005 g/L K ⁺ mean 4.00 g/L	NO ₃ ⁻ mean 4.34g/L Cl ⁻ mean 3.00 g/L
Washing solution, 2 nd step	Pb mean < 0.0002 g/L Ti <0.005 g/L Zr<0,005 g/L K ⁺ mean 0,48 g/L	NO ₃ ⁻ mean 0.93 g/L Cl mean 0,31 g/L
PZT powder	According to desired molar formula	
Gases from drying	Pb under limit of detection. May contain nitrates	

The remained lead amount in solution after hydrothermal treatment decreases with synthesis time. If the synthesis time is higher than 6 hours redissolution reaction can take place. PbZr_{1-x}Ti_xO₃ powders (x=0.52; 0.57) were obtained in hydrothermal conditions (different temperatures, pH and synthesis time). The powders composition was determined by quantitative chemical analysis (inductively coupled plasma and direct coupled plasma) and powders phase composition was investigated by XR diffraction [16]. Dried powders morphology was determined by transmission electron microscopy. Small quantities of these powders were immersed in isopropyl alcohol,

the suspension being ultrasonically homogenised. Some examples of the transmission electron microscopy images for PZT powders synthesised in hydrothermal conditions (high alkaline pH, 200°C, 1 hour) are presented in figure 2.

Thin PZT films with the composition $\text{PbZr}_{0.52}\text{Ti}_{0.48}\text{O}_3$ were deposited on titanium or platinum by a hydrothermal –electrochemical procedure from soluble salts of titanium, zirconium and lead. The mineralising agent was potassium hydroxide.

The films deposition was performed in a CORTEST Teflon autoclave endowed with working electrode, counter electrode and reference electrode. The deposition system was computer controlled using a potentiostat - galvanostat PGZ 100 Radiometer and VOLTALAB software. The films microstructure was investigated by scanning electron microscopy (Phillips 515 scanning electron microscope) and by transmission electron microscopy (Phillips TEM CM30 endowed with EDAX).



Figure 2. TEMBF of dried $\text{PbZr}_{0.52}\text{Ti}_{0.48}\text{O}_3$ (a) and $\text{Pb}(\text{Zr}_{0.52}\text{Ti}_{0.48})_{0.975}\text{Nb}_{0.025}\text{O}_3$ (b)

Some examples of TEM images are presented in figures 3a to 3c . The investigation by TEM showed the existence of the nanoclusters with crystalline structures. In figure 3a TEM BF image relieves nanometric clusters (30 nm) linked in twiggly chains. TEM BF image presented shows that in sample are also present very small clusters (3-5 nm). Energy dispersive XR microanalysis showed for both type of nanoclusters the presence of Pb, Zr and Ti. Electron diffraction image (SAED) (figure 3c) associated to the micro area from figure 3b relieves the polycrystalline structure of the nanoclusters. The inter-planar distances corresponding to the diffraction arches are 2.89 Å; 2.1 Å; 1.65 Å; 1.30 Å which correspond to a crystalline planes family of tetragonal PZT.

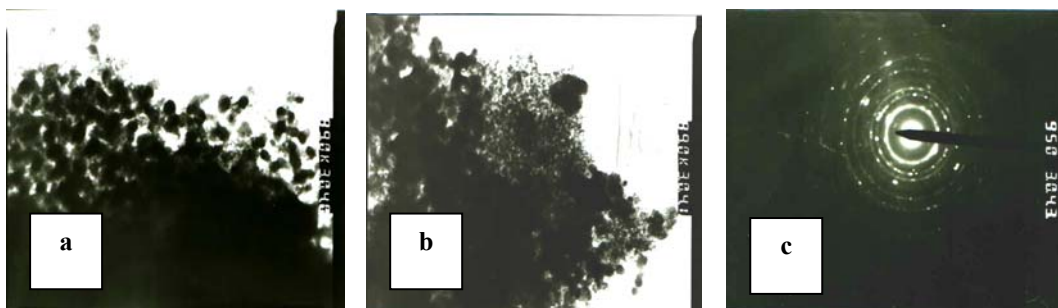


Figure 3. a) and b) TEM BF image (x 89000); c) SAED image associated to b)

3.2. Barium strontium titanate powders and sintered pellets

Barium strontium titanate powders were synthesised in hydrothermal conditions in alkaline media, at 200°C and different time. The powders composition was determined by quantitative chemical analysis (inductively coupled plasma and direct coupled plasma).

The powders morphology and microstructure was investigated by transmission electron microscopy in bright field (TEMBF), electron diffraction (SAED) and high resolution transmission electron microscopy (HRTEM) using electronic microscope Philips CM 12 with a resolution of 2Å. Some examples of TEMBF and HRTEM images for BST powders and sintered BST pellets are presented in figures 4a and 4b.

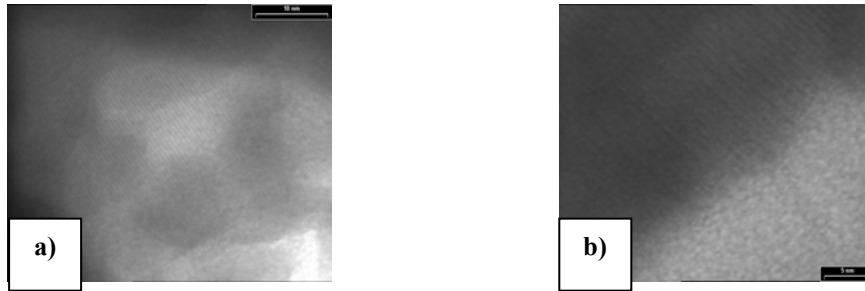


Figure 4. Transmission electron microscope analysis: a) HRTEM image of the sintered BST pellet; b) a crystallite with ferroelectric nanodomains (from sintered BST pellet)

REFERENCES

- [1] J.Schoonman, Solid State Ionics, **135** (2000), 5-19
- [2] Michael J.Pitkethy, Nanotoday, December 2004
- [3] R.E.Riman, Ann. Chim. Sci. Mat., **27(6)** (2002), 16-36
- [4] M.Yoshimura and W.Suchanek, Solid State Ionics, **98** (1997), 197-208
- [5] Jianlig Zhao, Xiaohui Wang, Renzheng Chen and Longtu Li, Materials Letters (2005) available on line, in press
- [6] S.B.Deshpande, Y.B.Khollam, S.V.Bhoraskar, S.K.Date, S.R. Sainkar, H.S.Potdar, Materials Letters, **59** (2005) 293-296
- [7] Lai Qi, Burtrand I.Lee, Prerak Badheka, Dang-Hyok Yoon, William D.Samuels, Gregory J.Exarhos, J.Eur. Ceram.Soc., **24** (2004), 3553-3557
- [8] Seema Agarwal and G.L. Sharma, Sensors and Actuators, **B 85** (2002), 205-211
- [9] Patent US 2001002681
- [10] Patent EP 1020937
- [11] Patent EP 1039559
- [12] S.Giri, S.Samanta, S.Maji, S.Ganguli and A.Bhaumik, J.Magnetism and Magnetic Mat., **285** (2004) 296-302
- [13] Dong-Seok Seo, Hwan Kim and Jong-Kook Lee, J.Cryst. Growth, available on line, in press
- [14] G.B.Ji, S.L.Tang, S.K.Ren, F.M.Zhang, B.X.Gu and Y.W.Du, J.Cryst. Growth, **270** (2004), 156-161
- [15] Hongliang Zhu, Yong Wang, Naiyan Wang, Ye Li, Jun Yang, Materials Letters, **58** (2004), 2631-2634
- [16] Roxana M.Piticescu, Ana Maria Moisin, Dragos Taloi, Viorel Badilita, Iuliana Soare, J. Eur. Ceram. Soc., **24** (2004), 931-935
- [17] Roxana M.Piticescu, Liliana Mitoseriu, Massimo Viviani, Victor Moagar Poladian, J. Eur. Ceram. Soc. (in press)

Received December, 15 2005

¹Center of Technological transfer for Advanced Materials
²Metav C.D. S.A

PROCEDEELE HIDROTHERMALE: METODE NOI ECOLOGICE IN DEZVOLTAREA NANOMATERIALELOR

REZUMAT Pamantul este un sistem inchis in care pierderile energetice si termice trebuiesc minimalizate pentru protectia biosferei, litosferii si hidrosferei. In acest scop un numar tot mai mare de cercetatori isi concentreaza eforturile spre noi materiale mai putin daunatoare sanatatii si fabricarii lor prin tehnologii ecologice. Tehnologiile cunoscute cum ar fi CVD, MOCVD, pulverizarea si tehnicile de spraiere au un consum energetic ridicat si necesita masuri speciale de protectia mediului ambiant. Metodele chimice soft in solutii ca de ex. metodele hidrotermal-electrochimice, inspirate din natura, au un impact ridicat in dezvoltarea nanomaterialelor cu morfologie controlata pentru un domeniu larg de aplicatii de la opto si microelectronica la industria auto, cataliza si materiale pentru implanturi. Principalele avantaje sunt: consumul energetic redus (temperaturi joase si procese in tr-o singura etapa) impact redus asupra mediului, versatilitate in productia unor materiale noi si avansate in orice forma si marime. Lucrarea prezinta o trecere in revista a procedeelor hidrotermal/electrochimice de obtinere de pulberi si filme perovskitice si cateva rezultate originale despre sinteza materialelor de PZT dopate cu Nb si BST..

STUDIES REFFERING TO THE EFFECT OF THERMIC TREATMENT, OF CLASSIFICATION THROUGH THE PRECIPITATION OF ALUMINIUM ALLOYS THAT ARE CAST IN THE PISTONS OF TERMIC MOTORS

BY

SPOREA I.¹ MANDEK FR.¹ BORDEASU I.¹ STOICAN
C.¹ SPOREA M.¹

ABSTRACT: The paper presents the results of the tests in order to determine the effects of the thermic treatments applied to the aluminium alloys that function at higher temperatures in the equilibrium diagram in comparison with the line „solvus”, that is an alloy element (referring to the thermic motors pistons). Key words: alloys, aluminium, pistons, thermic treatments.

KEYWORDS: aliaje, Al, pistoane, motoare termice.

1. INTRODUCTION

The 20-th century, considered also the speed century, led to the discovery of some technical solutions, in which the pistons of the thermic motors must fully satisfy the requires of the society, as: a high refraction [7], a reduced thermic dilatation coefficient [2][11], a good processing through splinting [14], acceptable casting features [12], high mechanical features [1], [4] and so on.

The best aluminium alloys to meet these requirements were found to be the alloys that contain as alloy elements: Si, Cu, Mg, Ni, and a lot of other alloy elements

It is known, that most of the above elements dissolve in aluminium, making a solid substance ($ss\alpha$), which in certain conditions of cooling, after casting or after a thermo-mechanic treatment or violent cooling, may become supersaturated substance in the alloys and as a result the alloy gets mechanic properties (hardness and breaking resistance), and it is superior than the state in equilibrium of slow cooling.

Based on the thermic treatments (T.T), applied to the aluminium alloys, cast or reformed plastically called: steeling and recovering, putting into solution, hardening through precipitation (or dispersion) natural or artificial ageing, it may be obtained mechanical properties 50% higher in comparison with those untreated thermically (N) [13], in alloys that form $ss\alpha$ of Al (Cu, Mg, Zn, etc).

Knowing the good effect of hardening through precipitation, the special literature recommends practical applications of aluminium alloys that are hardened (usually hardaluminium).

2. THE STABILITY OF T.T. EFFECT OF ALUMINIUM ALLOYS CAST IN THERMIC MOTOR PISTONS

The benefic effects of T.T. applied to aluminium alloys refer to the using of surrounding temperature while the pistons of thermic motors functioning, reach the temperature higher than 300 [1],[5]. So it is necessary the making of T.T. of disperse durification recommended by the bibliography [1],[4].

The aluminium alloys used to cast the pistons of thermic motors with firing through a spark, contain as main alloy elements Si and Cu. These elements react the best to the asked requirements: good mechanical and cast properties, reduced thermic dilatation coefficient and high refraction, etc.

One of these alloys is also the alloy ATSI 5 Cu 7 Mg Ni (Fe) upon which there were experimental a lot of attempts in order to relieve the T.T. effect after the cast and to state them during the functioning.

The alloy had the chemical composition: Si=4,8%; Cu=5,11; Mg=0,53; Fe=0,53; Mg=0,34, rest Al, and it was elaborated in an oven with indirect flame (iron cast creuzet) and test tubes were obtain in the oven (concordant STAS 200-61). The test tubes were put to T.T. of durification through precipitation as: heating above Solvus line (400) for 10'/mm diameter, and cooled in water; and a part that was not treated thermically (N). The test tubes were tried: breaking resistance R_m , hardening HB, alloys A (table 1). The results of the mechanical tests as 20°.

Table 1

the state of alloy	R_m [daN/M]	HB[daN/mm]	Alloy A[%]
Treated Thermically(T.T)	32,00	137	0,30
Untreated (N)	21,00	105	1,00

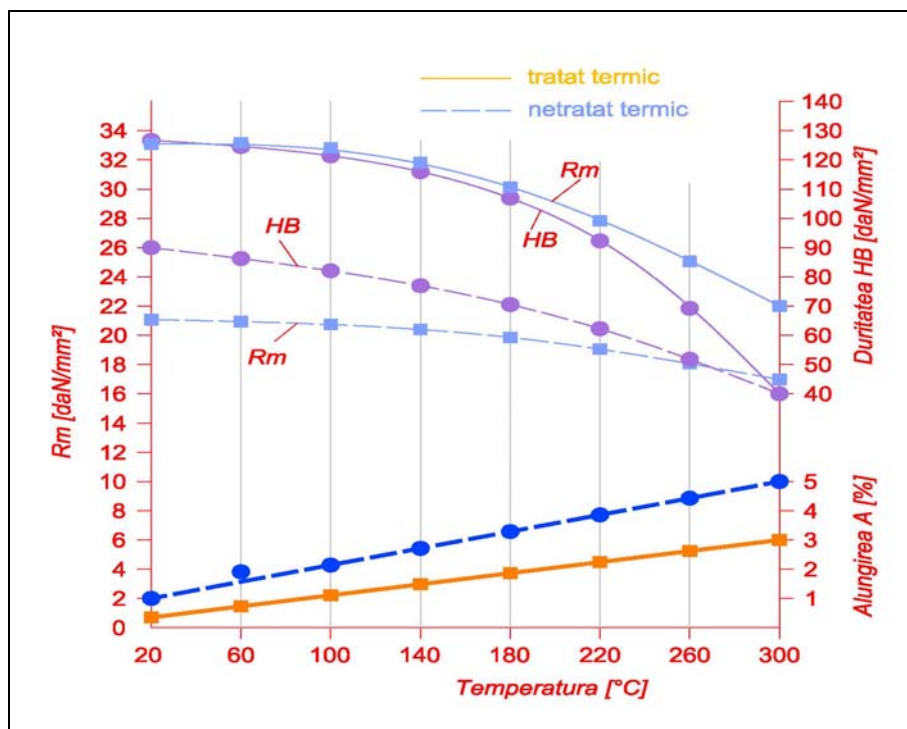


Figure 1. The influence of the heating temperature upon the properties of the aluminium alloys T.T. and N.

Then the test T.T. and N werw put to a continuous heating (picture 1), till the temperature of 300, measuring some properties at some temperature levels:60;100;140;180;220;260; and 300.

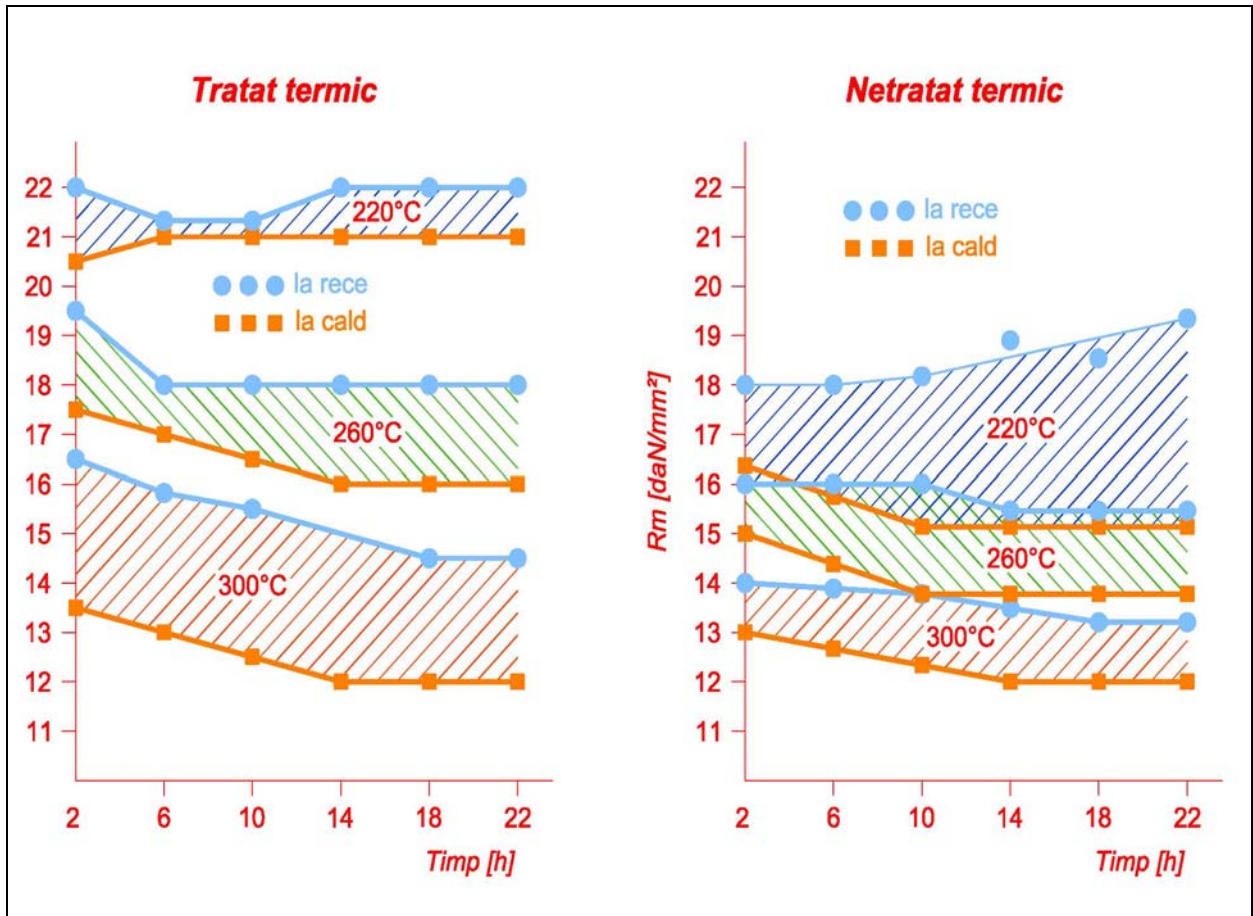


Figure 2. The influence of the heating temperatures and of keeping time upon R_m and T.T and N alloys.

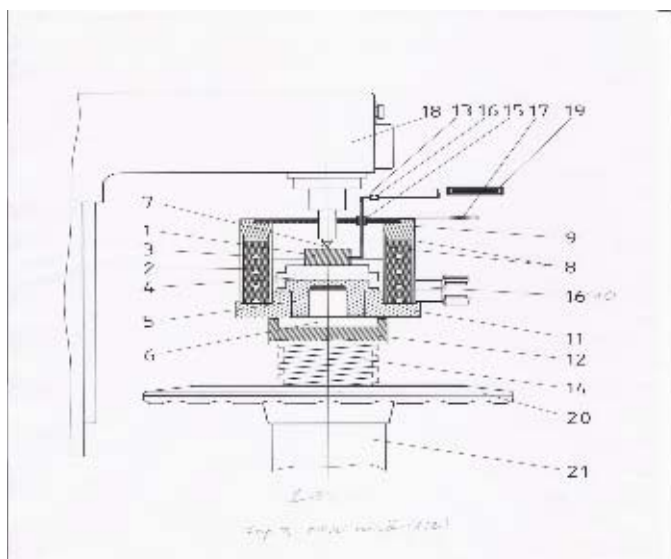


Figure 3. The equipment for determining the hardness in hot atmosphere of T.T and N alloys in which: 1-test; 2,4,5,6,7,12,14,18,20,21 - elements of device Brinell; 3,8,9,10,11,17 – elements of hot device ; 13,15,16,19 – elementes of the measuring temperatures plant

Because the pistons of thermic motors are put to the wearing out (at hot and cold temperatures, at different humidity), it is necessary to know also the hard values that the T.T and N alloys obtain, knowing that hardness influences the most the state of wearing out (and also the structures of alloy).

In order to find out the hardness, it was used a heating equipment that was built on device Brinell (picture 3). The result of the measures are presented in picture 4.

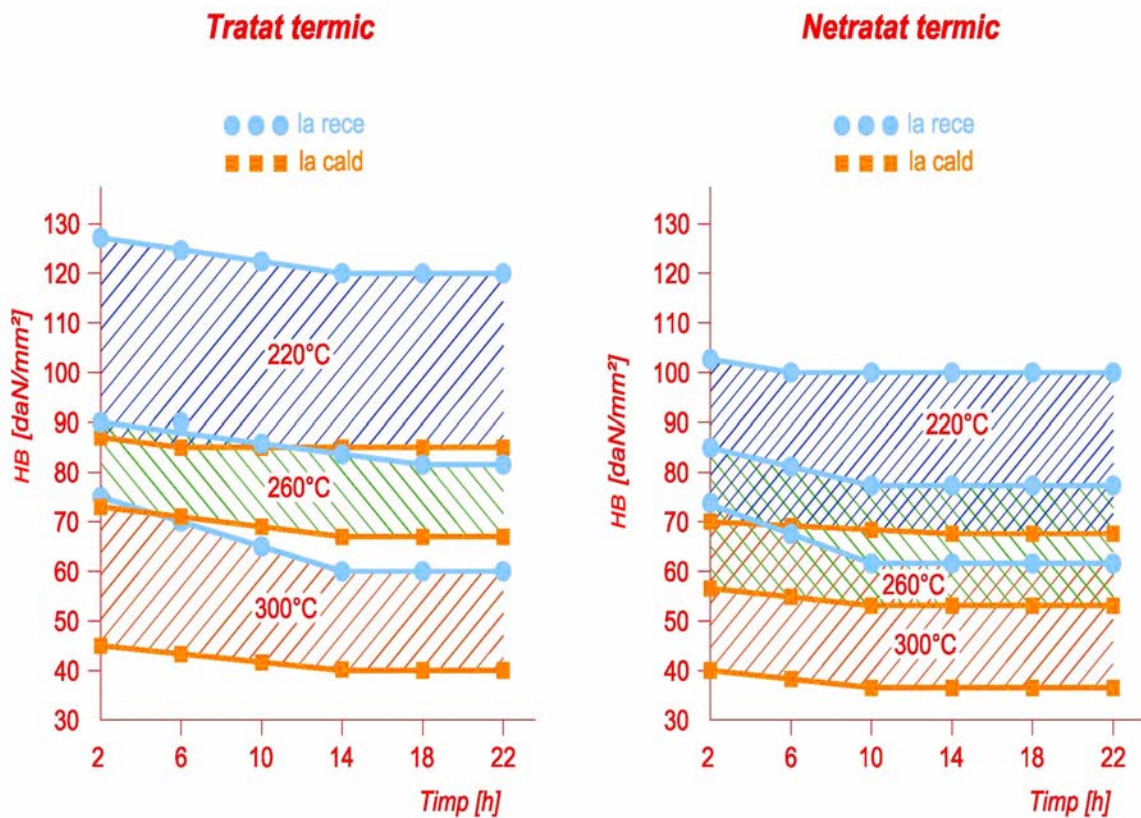


Figure 4. Temperatures and the heating temperatures until stabilisation of value HB.

3. CONCLUSIONS

From the tests of determining the properties of $ATSi_5Cu_7 + MgNi(Fe)$ treated thermally and centreated, for the casting of the pistons of thermic motors with firing through spark was shown that:

3.1. The thermic treatment of hardening through precipitation, the treatment that wants to obtain some maximum mechanical properties based on a solid solution supersaturated by Ea in Al, it is proved to be useless, because of the following phenomena

3.2. The pistons of thermic motors, during functioning, pass over the SOLVUS CURVE temperature (the solubility curve in a solid state of Ea in Al), and the obtained effect through T.T is annuled.

3.3. The annulment of the obtained effects after T.T, of hardness through precipitation, depends on temperature and on the maintaing time at this temperature (functioning of the thermic motor, time, speed e.t.c.).

3.4. Between the breaking resistance at pushing and the hardness of the tested alloys exists a close link. That is why, in future may be done only experiments of hardness in relation with the behaviours of alloys, because they are simpler, more comfortable, cheaper and easier to do.

3.5. Because on the pistons, the temperature obtained during functioning is different, it is supposed that the top of the T.T piston will resist better to working out (especially if it is not a greasing part), and we shall have less lack of gases in the oil bath (a cleaner oil and consumed; e.t.c.)

REFERENCES

1. Apostolescu, N., Băgață, N., – Motoare cu ardere internă E.D.P.Buc.1967,pg.51
2. Bagiu, L., Sporea, I., – Cercetări teoretice și experimentale asupra pistoanelor motoarelor cu combustie internă. BSt.TIPT-șoara, Tom 7 (21) 1962.
3. Bagiu, L., Sporea, I., – Cercetări teoretice și experimentale cu privire la înlocuirea aliajelor pentru pistoanele motoarelor cu combustie internă BSt.TIPT-șoara, Tom 7 (21) 1962.
4. Bagiu, L., – Metode de calcul a proporției constituenților și fazelor aliajelor neferoase polinare.Rezumatul Tezei de Doctorat. I.P. „Tr. V” Timișoara 1971.
5. Bănărescu, M. - Motoare cu ardere internă. E.T., Buc 1967.
6. Domșa, A., Chișu, A., Treborius, I., – Pistoane, ETB, 1961, pg.11-80.
7. Kolobnev, I.F., – Jaroprocinosti liteinâh aliuminievâh splavov Moskva „Metallurgia” 1973, pg.21-42.
8. Mandek, Fr., ș.a. – Influența modificării aliajului ATSi12CuMgNi asupra proprietăților pistoanelor tip Dacia.Anal. of the Univ. of Oradea, vol III (XIII), 2004, Fascicle of MTE.
9. Mandek, Fr., ș.a. – Încercări practice de folosire a aliajelor de Al modificate turnate în pistoane.Univ.Tehnică Cluj-Napoca, TSMA 2004.
10. Mandek, Fr., Sporea, I., Bordeășu, I., Sporea-Iacob, I., Marta, C-tin. – Influența sistemului de turnare asupra caracteristicilor bilelor turnate din oțel austenitic manganos T120CrMn130.Analele Univ. „Aurel Vlaicu” Arad, 2002.
11. Sporea, I., - Influența temperaturii de încălzire și a timpului de menținere asupra valorilor coef. BST 8 (22), 1963, Fasc. 2.
12. Sporea, I., ș.a. – Asupra eficacității modificării aliajelor de tip silumin. BSTIPT, Tom 22 (36), Fasc. 1., 1997.
13. Sporea, I., ș.a. – Studii privind stabilitatea efectului de T.T la piesele turnate din AA. Metalurgia, 19 (1967), Nr. 1, Buc. Pg. 11-15.
14. Sporea, O., Ghiță, M.,Sporea, I. – Vlianie vibrații na serohovatasti poverhnasti pri obrabotve ciugunov. TAP. Nr. 3-4 Penza 1997, Rassia, pg.109-110.

Received january, 11 2005

¹POLITEHNICA University, Timișoara

**STUDII REFERITOARE LA EFECTUL TRATAMENTULUI TERMIC AL CLASIFICARII
PRECIPITARII COMPLETE A ALIAJELOR DE AL TURNATE IN PISTOANELE
MOTOARELOR TERMICE.**

REZUMAT: Lucrarea prezinta rezultatele testelor in ordinea determinarii efectelor tratamentelor aplicate aliajelor din Al realizate la temperaturi ridicate in diagrama "solvus" care este un element de aliaj (referitor la pistoanele motoarelor termice)

CHANGES OF THE MECHANICAL CHARACTERISTICS OF HIGH RESISTANCE WIRES DRAWN IN ULTRASONIC FIELD

BY

SUSAN MIHAI¹, ILIESCU VIOREL², DUMITRAȘ PETRU³

***ABSTRACT:** The changes of the mechanical characteristics of some high resistance wires, drawn in ultrasonic field while the die is located into the oscillation maximum of the waves and actuated parallel to the drawing direction, have been mainly determined by the work – hardening decrease caused by the “surface effect of ultrasonics” as a consequence of the fractional regime of plastic deformation.*

***KEYWORDS:** mechanical characteristics, hardening, ultrasonic*

1. INTRODUCTION

The drawing of high resistance wires in ultrasonic field represents one of the modern technologies of plastic working of metals, besides other techniques that use directional flows of magnetic, light, electric and so on energies.

Ultrasonic or ultra – acoustic waves represent a variety of elastic waves with the frequency ranging between 16.000 and 10^{10} Hz [1].

The area of the elastic medium in vibratory state, which lodges the ultrasonic waves, is denominated as “ultrasonic field”.

As in the case of other plastic working technologies of metals, at wire drawing in ultrasonic field high – energy ultrasonics are used. This ultrasonics, when propagating through an elastic medium such as a metal, undergo a damping effect which depends upon time.

For high resistance wire drawing, it is recommended that the deformation focus is located in the oscillation maximum of the waves while the tool is actuated parallel to the drawing direction [2]. Under these conditions, as compared to classic wire drawing a sensible reduction of the drawing force is obtained due to the “surface effect of ultrasonics”. This effect is explained by means of the “mechanism of frictional force reversion”, illustrated in Fig. 1 [2].

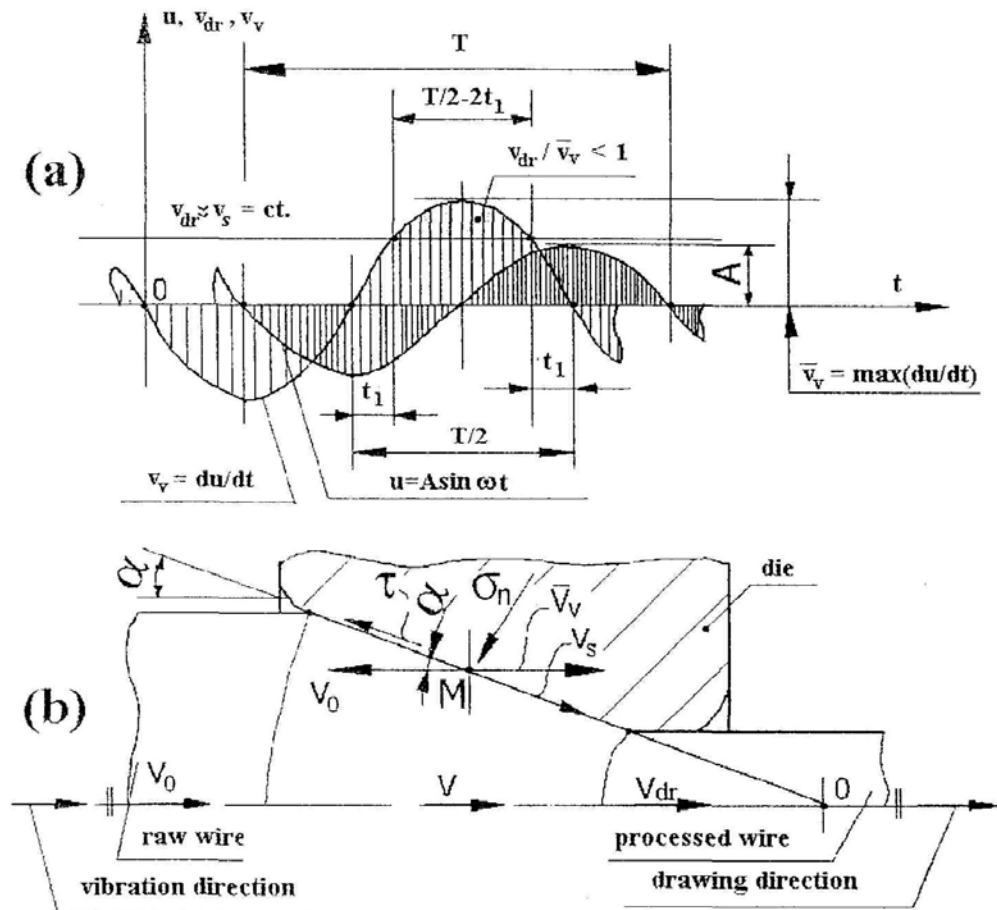


Figure 1. Principle scheme of technology wires drawn in ultrasonic field: (a) –variation in time of wave displacement (u), drawing rate (v_{dr}) and vibration rate (v_v); (b) -proper scheme: σ_r – normal stress in any given point M , τ – shear stress on metal-tool interface; v_s – slip rate of metal during drawing; v_v – maximum vibration rate of the die; α – semiangle of deformation cone; v_0 – initial rate (raw wire); v_{dr} – final drawing rate (processed wire); A – oscilation amplitude.

Conical convergent die were used with a cylindrical calibration zone of the processed wire. Any given point M , from the deformation zone, takes part to notions: a feed motion with v_s rate along the generator of the deformation care and a vibratory motion with v_v rate. The resulting vector of relative rate (after composing the two rate vectors) will change the displacement sense of point M as follows: during $T/2-2t_1$ its displacement sense will coincide with that of the metal and during $T/2+2t_1$ the displacement will be done in contrary sense. This suposition explains, in fact, the “reversion mechanism of average friction force” at the metal – tool contact, assuming a Coulomb – type friction [3].

2.EXPERIMENTAL TEST AND RESULTS

The experiment have been carried out at a laboratory level on wires made of RUL 1V/STAS 11250-89 steel-grade with the chemical composition in Table 1.

Table 1. Chemical composition of RUL 1V steel - grade in wt. % according to STAS 11250 – 89

C	Mn	Si	Cr	S	P	Mo	Ni, Cu
1,10	0,40	0,30	1,50	0,02	0,02	0,08	0,2

The wire drawing installation, with hydraulic control, is equipped with a UZG 2-4M ultrasonic generator, that functions in conjunction with magnetostrictive transducers at the resonance frequency of 17500 Hz, and includes standard force concentrators of the type PMS 15A-18.

The oscillating system is of the “closed” type being designated according to “ $n \cdot \lambda / 2$ ”. The die is located in the oscillation maximum of the waves and actuated parallel to the drawing direction, as shown in fig. 2.

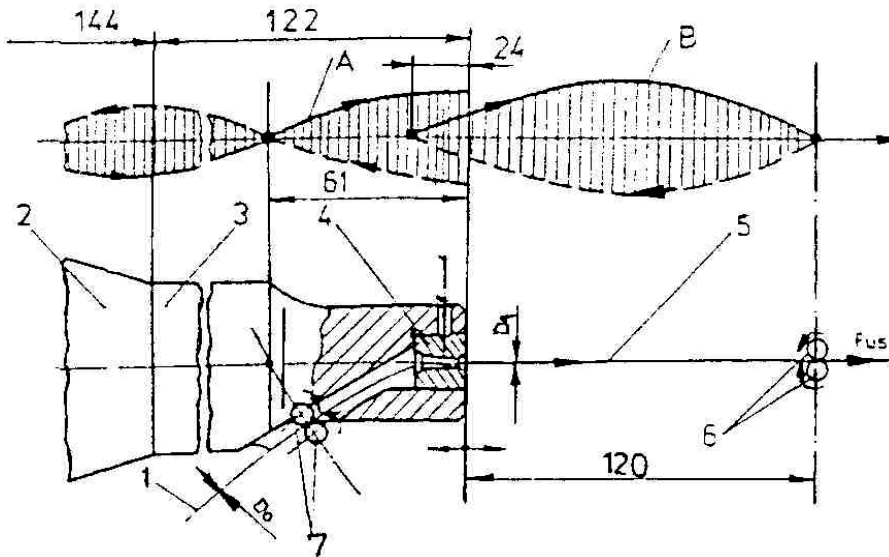


Figure 2. Schematic structure of the oscillation system [4]: 1 – raw wire; 2 – PMS15A-18 force concentrator; 3 – cylindrical step concentrator (for work); 4 – die; 5 – drawn wire; 6,7 – reflectors of ultra-acoustic energy: A – oscillation of the work concentrator; B – oscillation of the wire.

The wavelength is determined as:

$$\lambda = \frac{c}{f} \quad (1)$$

where: c is the propagation rate of ultrasonics within the given medium and f is the resonance frequency.

Closing the oscillation system is accomplished by means of the reflectors of ultra-acoustic energy, located at certain well-defined distances [4] in order to obtain a stable system of stationary within the wire.

The work concentrator is made from a titanium-based alloy, BT 3 (90% Ti, 6% Al and 4% V with $\rho = 4,42 \text{ Kg/dm}^3$), resisting at ultrasonic fatigue.

For drawing the RUL 1V wires, both with and without ultrasonics, WC-Co metallic carbides dies are used. These dies have the opening semiangle $\alpha = 8^\circ$ and achieve a total 41% cross-section reduction (determined between two applied heat treatments for structure restoring) if soap powder is used as a lubricant. The degrees of cross-section reduction are determined for pass with:

$$\delta_i = 1 - \left(\frac{D_i}{D_{i-1}} \right)^2 \quad (2)$$

and for the whole operation (the total degree of section reduction) with:

$$\delta_{\text{tot}} = 1 - \left(\frac{D_i}{D_0} \right)^2 \quad (3)$$

The raw wires, with an initial diameter $D_0 = 3,85$ mm, are in annealed condition, being properly prepared for drawing. The efficiency of ultrasonic drawing is emphasized by:

$$\Delta F = \frac{F_0 - F_{us}}{F_0} \cdot 100 [\%] \quad (4)$$

where: F_0 is the drawing force for classic wire drawing and F_{us} is the force used at ultrasonic field wire drawing. The experimental determination of the force, either with and without ultrasonics was accomplished by means of a tensiometric dose of the type DT-106.000 and a tensiometric bridge, type N 2314. In order to better emphasize force fluctuations they were recorders as a function of time by means of plotter, type Recorder XY-Endim 620.02. This, the stability of the system of stationary wares within the wire could be checked out by means of the force constancy at ultrasonic field wire drawing.

The technologic, ultrasonic and force parameters. Used within the experiments, are listed in Table 2.

The mechanical resistance parameters have been determined on long specimens, according to STAS 6951-80. From each of the wires either with or without ultrasonics, three samples have been taken.

The tensile mechanical characteristics, namely: ultimate strength (R_m), technical flow strength ($R_{p0.2}$) and ultimate strain (A_{100}), have been determined from the recorder stress-strain curves. For a more accurate determination, the tensile curves have been plotted by using an extensometer. The values listed in Table 3 have been obtained as an average of three tests.

Table 2. Ultra-acoustic, tehnologic and force parameters used for experiments.

Symbol of the drawing series	Drawing course	Ultra-acoustic parameters			Tehnologic parameters					Force parameters		
		f [Hz]	A [μ m]	\bar{v}_v [m/s]	δ_i [%]	δ_{tot} [%]	α [$^\circ$]	v_{dr} [m/s]	v_{dr} / \bar{v}_v	F_0 [N]	F_{us} [N]	ΔF [N]
I/1	3,58 \rightarrow 3,60	17500	28	3,0	14	14	8	0,03	0,01	1280	866	32,34
I/2	3,60 \rightarrow 3,45				10	21				1350	1053	22,00
I/3	3,45 \rightarrow 3,30				10	28				1225	812	33,71
I/4	3,30 \rightarrow 3,20				8	32				982	708	27,90
I/5	3,20 \rightarrow 3,10				8	36				950	613	35,47
I/6	3,10 \rightarrow 3,00				8	41				882	530	40,00

Table 3. Values of tensile mechanical characteristics, obtained as an average of three tests.

Symbol of the drawing series	Drawing course	Wire drawing stresses		Mechanical characteristics							
				Classic wire drawing				Ultrasonic wire drawing			
I	D ₀ →D ₁ [mm]	σ _{to} [MPa]	σ _{tus} [Mpa]	R _m [MPa]	R _{p0,2} [MPa]	A ₁₀₀ [%]	HV _{0,1} -	R _m [MPa]	R _{p0,2} [MPa]	A ₁₀₀ [%]	HV _{0,1} -
0	3,85	-	-	630	475	18,0	179	630	475	18,0	179
I/1	3,58 →	127	83	935	855	14,2	230	905	811	15,0	215
I/2	3,60	146	113	1025	998	12,2	250	1003	939	13,0	234
I/3	3,60 →	144	95	1110	1080	10,4	275	1090	1045	11,8	249
I/4	3,45	123	88	1170	1145	9,5	288	1152	1117	11,0	268
I/5	3,45 →	126	81	1245	1225	9,0	298	1230	1201	10,0	284
I/6	3,30	125	75	1335	1319	8,5	304	1323	1302	9,0	292
	3,30 →										
	3,20										
	3,20 →										
	3,10										
	3,10 →										
	3,00										

The tensile tests have been carried out on an EU-40 – type machine, with a drawing speed of 20 mm/min, according to prescriptions found in STAS 6951-80. The mechanical characteristics have been calculated according to STAS 200-87. Besides the three above-mentioned tensile mechanical characteristics, table 3 also contains the average values of HV0.1 Vickers microhardness, determined according to STAS 7057-78, by means of a PMT-3 microhardness tester.

The maximum value of the oscillation (vibration) rate of the tool is determined with the relationship:

$$V_v = 2\pi f \cdot A \quad (5)$$

where: f - is resonance frequency and A is the oscillation amplitude of the tool. The wire drawing stresses are determined during the drawing processes, carried out both with and without ultrasonics, as the ratio between the force value and the drawn wires' cross-sections.

3.CONCLUSIONS

The changes of the mechanical characteristics, during the drawing of RUL 1V wire field with the die located in the oscillation maximum of the waves and actuated parallel to the drawing direction, have been mainly determined by the “surface effect of ultrasonics” that is by diminution of the “friction force at metal-tool contact.”

During a complete oscillation period of the tool, the plastic deformation of the metal occurs only for the duration of $T/2+2t_1$ (when a certain amount of ultra-acoustic energy is introduced within the wire) since on the $T/2 - 2t_1$ time interval metal-tool contact surfaces are separated.

Actually, under such circumstances, plastic deformation is produced by impulses (fractionally) causing a decrease of the wire drawing force on the drawing series, a stabilization of the plastic deformation process, a work-hardening decrease and a diminution of the cold working non-uniformity. All these effects induce changes of the

mechanical characteristics, generally illustrating an increase of plasticity, at the wires drawn in ultrasonic field.

Thus, the possibility to increase both the deformation degree and the safety level of plastic deformation may be foreseen.

REFERENCES

- [1] Drăgan, Ov. ș.a, - *Ultrasunete de mari energii*. Editura Academiei, București, 1983
- [2] Severdenro, V.P. ș.a - *Ultrazvuk și plasticinosti*. Nauka i Tehnika, Minsk, 1976
- [3] Susan, M ș.a, - *The metal-tool contact friction at the ultrasonic vibration drawing of ball-bearing Steel wires*. Rev. Metal, madrid 35 (1999). Pp.379 – 383.
- [4] Susan, M., - *Cercetări privind trefilarea sârmelor din oțeluri de rulmenți în câmp ultrasonor*. Teză de doctorat, Universitatea Tehnică “Gh. Asachi”, Iași, 1996.

Received January, 3 2006

¹ *Technical University “Gh. Asachi” Iasi*

² *Cablero SA Iasi*

³ *Technical Academy, Rep. Moldova*

MODIFICARI ALE CARACTERISTICILOR MECANICE PENTRU SARME DE INALTA REZISTENTA TREFILATE IN CAMP ULTRASONOR

REZUMAT. Modificarea caracteristicilor mecanice pentru sarmele de inalta rezistenta mecanica trefilate in camp ultrasonor cu filiera situata in maximul oscilatiei undelor si activata paralel cu directia tragerii, sunt determinate in special de reducerea ecruisarii cauzata de “efectul de suprafata al ultrasunetelor”, respectiv de regimul fractionat al deformarii plastice.

CONSIDERATIONS CONCERNING THE METAL-PLUG CONTACT FRICTION AT THE PIPES DRAWING WITH ULTRASONIC VIBRATIONS

BY

OMER MOHAMED ABBALLA MOHAMED¹, ADRIAN DIMA¹

ABSTRACT: *At tube drawing, on sustained plug, ultra-acoustically actuated by means of longitudinal oscillations, a decrease of the drawing force has been obtained due to the “surface effect of ultrasonics”. The decrease of the average frictional force at the metal-plug contact is discussed by means of the magnitude of the φ coefficient, expressed as a function of the v_{tr} / v_v ratio, which offers sufficient design data for the new tube drawing technology.*

KEYWORDS: *friction, ultrasonic vibration, frictional force*

1. INTRODUCTION

The tubes made from some hardly cold-workable metallic materials cannot be deformed by conventional drawing, due to the extremely high frictional forces and stresses, which are developed, causing both micro and macrocracks in the cold worked tube.

By means of tube cold-drawing with ultra-acoustic actuation, most of the drawbacks of classic working are avoided due to the volume and/or surface effects of high-energy ultrasonics. For ultrasonic field drawing, either the die or the sustained plug can be actuated or even several schemes of combined ultra-acoustic actuation can be applied [1].

Die-actuation is recommended when a special quality is required for the drawn tubes external surface while plug-actuation is applied in the cases which involve particular case for internal surface.

In the case of tube drawing on ultra-acoustically-actuated, sustained plug (the Sonodraw system), besides the technical applicability ease, the ultra-acoustic energy transfer is provided inside the tube, where deformation efforts are extremely high [2].

The decrease of the force for ultrasonic drawing as compared to classic technology, is mostly based on the „surface effect of ultrasonics”, technically materialized by the frictional force reduction at the metal-pug contact (the Coulomb-type friction being admitted), Figure 1.

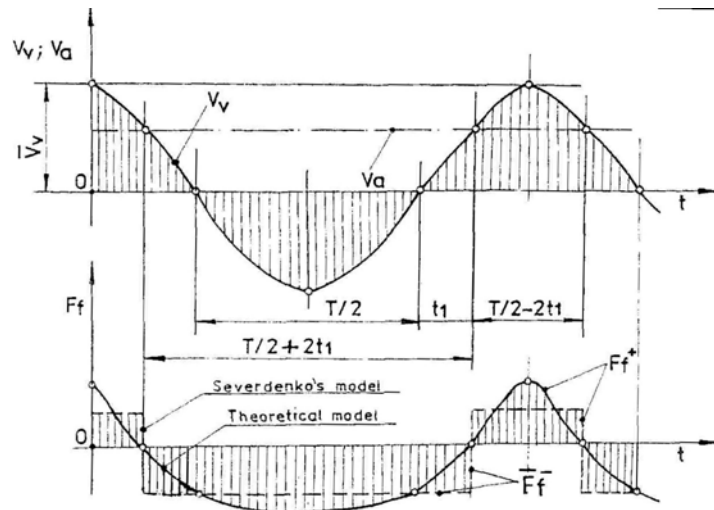


Figure 1. Variations of the oscillations and the feed rates (v_v and v_a , respectively) and of the frictional force, during a complete oscillation period).

At plug-actuation, with longitudinal ultra-acoustic oscillation, any A' point from the B-B₁ contact surface of the plug Figure 2 takes part at two movements. Firstly there is a feed movement along plug's generator, with a V_a rate and secondly there is an oscillation (vibration) movement, with a V_v rate.

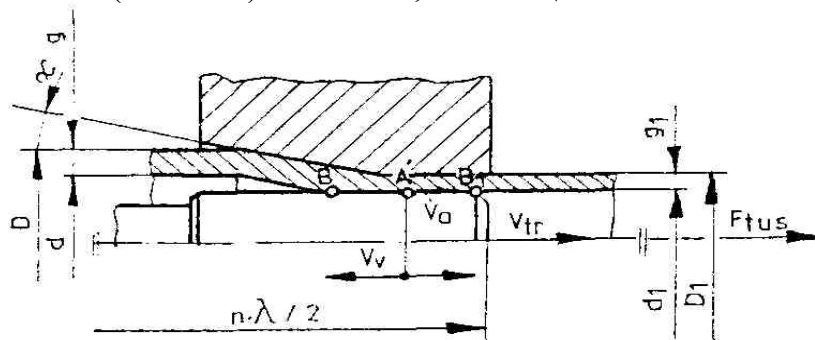


Figure 2. Scheme for tube drawing on sustained plug, ultra-acoustically-actuated by means of longitudinal oscillations.

When the oscillation rate of the plug is higher than the feed rate, $v_v > v_a$, the total vector of the relative rate of A' point, on the B-B₁ contact surface, will change its sense. Thus, during a part of the oscillation period, the total relative rate of point A' will coincide with the metal's displacement along plug's generator while during the other part, it will have a contrary sense.

When $v_v < v_a$, the vector of the total relative rate will always coincide with the metal's displacement sense.

Nosal and Rimsa [1] consider that for $v_v > v_a$ the frictional force contributes to metal's displacement, thus reducing the value of the total drawing force while for $v_v < v_a$ no reduction of the drawing force occurs.

From Figure 1 it is noticeable that during $T/2 - 2t_1$ the frictional force is positive and during $T/2 + 2t_1$ it is negative (F_f), at the level of a complete oscillation period.

The ratio designated by φ represents a coefficient that emphasizes the diminution of the average frictional force at the metal-plug contact, in the A' point. Its value is [1;3]:

$$\varphi = \frac{(T/2 + 2t_1) + (T/2 - 2t_1)}{(T/2 + 2t_1) - (T/2 - 2t_1)} \quad (1)$$

If the oscillations' displacement is considered according to the movement law: $u = A \cdot \sin \omega \cdot t$ (2)

The oscillation rate (v_v) may be determined as:

$$v_v = du / dt = A\omega \cos \omega \cdot t \quad (3)$$

The maximum value of the oscillation rate (\bar{v}_v) is obtained for $\cos \omega \cdot t_1 = 1$; its value is: $\bar{v}_v = A\omega = 2\pi f \cdot A$ (4)

From the relationship (3) and (4) it follows that:

$$v_v = \bar{v}_v \cos \frac{2\pi}{T} t_1 \quad (5)$$

If the feed and oscillation rates are equal $v_v = v_a$, t_1 results as:

$$t_1 = \frac{T}{2\pi} \arccos \frac{v_a}{v_v} \quad (6)$$

By replacing t_1 and T in the relationship (1), the coefficient φ becomes:

$$\varphi = \frac{\pi}{2} \cdot \frac{1}{\arccos \frac{v_a}{v_v}} \quad (7)$$

In order to obtain a reduction of friction upon the entire metal-plug contact surface it is necessary to replace the value of the feed rate in point A' by the value of the average displacement rate of the metal, determined between the start and the finish points of the metal-plug contact surface.

By applying the equation of the metal flow continuity it follows that:

$$S_B v_B = S_{B1} v_{B1} = S_{B1} v_{tr} \quad (8)$$

$$\text{Which leads to: } v_B = v_{tr} \frac{S_{B1}}{S_B} \quad (9)$$

Since the tubes subjected to ultra-acoustically-actuated cold drawing have much less wall-thickness, as compared to their diameters [2]:

$$\frac{g}{D} = \frac{1}{10} \dots \frac{1}{200} \quad (10)$$

Based on the above considerations, from equation (9) it follows that:

$$v_B = v_{tr} \frac{g_1}{g} \cos \alpha \quad (11)$$

where: g and g_1 represent the wall-thickness for the raw and the drawn tubes, respectively; v_{tr} – drawing rate; α – opening semiangle of the die. Therefore, the average displacement rate of the metal, on its contact surface with the plug, becomes:

$$v_m = \frac{v_B + v_{tr}}{2} = \frac{v_{tr}}{2} \left(\frac{g_1}{g} \cos \alpha + 1 \right) \quad (12)$$

By replacing the mean rate value obtained from (12) in the relationship (7) and by considering the low-value of the $\omega \cdot t_1$ product, the coefficient φ becomes:

$$\varphi = \pi \frac{v_v}{v_{tr}} \frac{1}{\frac{g_1}{g} \cos \alpha + 1} \quad (13)$$

Based on the logical scheme illustrated in Figure 3, the variation of φ , that emphasizes the decrease of the average drawing force at the metal – plug contact (in the

conditions: $\alpha = 8^\circ$, $f = 18000\text{Hz}$, $g/g_1 = 1,07$ and $\lambda_i = 1,2$), is determined as a function of the v_v/v_{tr} ratio.

For qualitative evaluation of the influence that the friction reduction, on the metal – plug contact, exerts on the total drawing force, simplified relationship introduced by A. Gavrilenco can be used [1]:

$$F_t = F_d + F_f = F_d(1 + \mu \text{ctg} \alpha) \quad (14)$$

Where: F_d is the proper deformation force; F_f – the frictional force, μ - the friction coefficient and α has the above mentioned significance.

For tube drawings on a sustained plug, ultra – acoustically – actuated with longitudinal oscillations, the relationship (14) changes to:

$$F_{ms} = F_d \left(1 + \frac{\mu \text{ctg} \alpha}{\varphi}\right) \quad (15)$$

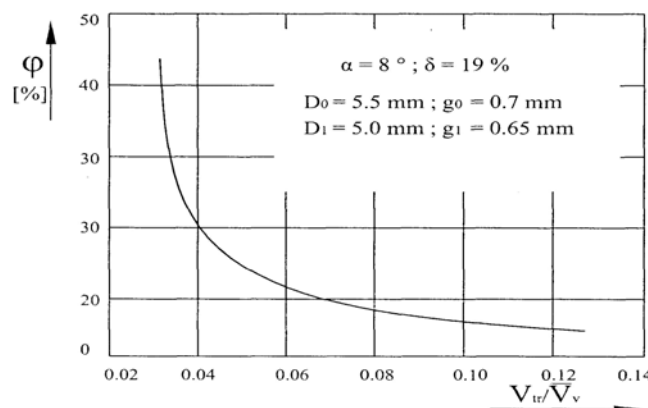


Figure 3. Variations of the coefficient φ as a function of the v_{tr}/v_v .

3. CONCLUSIONS

In this case of tube drawings on a sustained plug, ultra – acoustically – actuated with longitudinal oscillations (according to the Sonodraw system) it is firstly recommended to plot the graphical variation of the coefficient as a function of the ratio between the drawings and the oscillation rates, $\varphi = f(v_{tr}/\bar{v}_v)$. The φ coefficient will emphasize, thus, the average frictional force seduction on the metal – plug contact.

Blendes the concrete technology drawings conditions with this occasion some direct information can be obtained on the ultra – acoustic parameters, as well, due to relationship (4): $\bar{v}_v = 2\pi f A$ (where f is the resonance frequency and A is the amplitude of plug oscillation).

REFERENCES

- [1] Severdenko, V.P.; s.a.; *Prokatka; volocenie ultrazvokom Nauka i Tehnika*, Minsk, 1970
- [2] Drăgan, Ov. ș.a. *Ultrasunete de mari energii*. Editura Academiei, București 1983
- [3] Susan, M. ș.a., *The metal – tool contact friction at the ultrasonic drawing of ball – bearing steel wires*. Rev. Metal, Madrid 35 (1999), pp. 379...383.

Received December, 2006

¹ Technical University "Gh. Asachi" Iasi

**CONSIDERATII PRIVIND FRECARA DE CONTACT METAL-DOP
LA TRAGEREA TEVILOR CU VIBRATII ULTRASONICE**

REZUMAT: La tragerea țevilor pe dop susținut și activat ultraacustic, cu oscilații longitudinale, se obține reducerea forței de tragere pe baza „efectului de suprafață al ultrasunetelor”. Reducerea forței medii de frecare la contactul metal – dop este pusă în discuție, prin mărirea coeficientului φ , ca o funcție de raportul v_{tr}/v_v – care prezintă suficiente informații de proiectare a noii tehnologii de tragere a țevilor.

—

CONSIDERATION CONCERNING THE OUTPUT PARAMETERS OF THE CO₂ LASER

BY

ONOFREI ROXANA IOANA¹, NEGURA CRISTINA¹

ABSTRACT: *Laser had a big impact in manufacturing industries. In this paper we present two types of measurement with gas laser. We utilized a laser that uses carbon dioxide for cooling. The laser utilizes a gas source with close circuit. We realized two types of measurements: in the first case we studied the variation of the thermodynamic tension and in the second case we followed the variation of the temperature. For the first experiment we use a chromium-aluminum thermocouple which was put in a metallic piece, the thermocouple is connected to the DT 830 B measure device. In the second experiment to measure the temperature we used a thermocouple from the DT 9208A measure device box. The results pointed different values for different conditions of measurement.*

KEYWORDS: *laser beam, measurement, thermocouple*

1. INTRODUCTION

Laser is an acronym for Light Amplification by Stimulated Emission of Radiation. Laser creates an intense coherent beam of light when atoms or molecules in a gas, liquid or solid medium, force an incoming mix of wavelengths (or colors) of light to work in phase, or, at the same wavelength. Laser light is analogous to a loud, single-pitch note, while normal white light is analogous to audio static on a radio.

Einstein can be considered as the *father* of the laser. 80 years ago he postulated photons and stimulated emission and won the Nobel Prize for related research on the photoelectric effect. This section discusses the historical evolution from microwave lasers to optical lasers and finally to x-ray lasers and lasers discovered in space.

The CO₂ laser (carbon dioxide laser) is a laser based on a gas mixture as the gain medium, which contains carbon dioxide (CO₂), helium (He), nitrogen (N₂), and possibly some hydrogen (H₂), water vapors, and/or xenon (Xe).. Nitrogen molecules are excited by the discharge into a metastable vibration level and transfer their excitation energy to the CO₂ molecules when colliding with them. Helium serves to depopulate the lower laser level and to remove the heat. Other constituents such as hydrogen or water vapors can help (particularly in sealed tube lasers) to re-oxidize carbon monoxide (formed in the discharge) to carbon dioxide.

The major types of CO₂ lasers are:

- sealed tube or no-flow lasers for low powers
- axial flow lasers
- fast transverse flow lasers (for multi-kW continuous-wave output powers)

- transverse excited atmosphere (TEA) lasers with very high (about atmospheric) gas pressure and a series of electrodes and gas inlets along the tube (for pulsed mode only, suitable for multi-kW average powers)
- high power slab lasers, with the gas in a gap between a pair of planar water-cooled RF electrodes
- gas dynamic CO₂ lasers for multi-MW powers (e.g. for anti-missile weapons), where the energy is not provided by a gas discharge but by a chemical reaction in a kind of rocket engine

The concepts differ mainly in the technique of heat extraction, but also in the used gas pressure and electrode geometry. In low power sealed tube lasers (used e.g. for laser marking), waste heat is transported to the tube walls by diffusion or a slow gas flow. The beam quality can be very high. High power CO₂ lasers utilize fast forced gas convection, which may be in the axial direction or in transverse direction (for highest powers).

CO₂ lasers are widely used for material processing, e.g. cutting and welding (with multi-kW powers) and for laser marking (with lower powers), but also in laser surgery and for range finding. Compared to solid state lasers with similar output powers, they are usually cheaper, but have a lower potential for very strong focusing, remote welding, and short pulse generation. Also, beam delivery can be a problem, since there are no optical fibers for high power 10- μ m laser beams.

Due to their high powers and high drive voltages, CO₂ lasers raise serious issues of laser safety. However, their long operation wavelength makes them relatively eye-safe at lower intensities.

2. EXPERIMENTAL CONDITIONS AND RESULTS

In this paper we present two types of measurement with gas laser. We utilized a laser that uses carbon dioxide for cooling. This laser belongs to The Non-conventional Technology Laboratory of The Machine Manufacturing Faculty. The laser was made by The Physical, Laser, Plasma and Radiation Institute, Bucharest.

Due de fact that the active medium is carbon dioxide, the wave length of the laser beam radiation is $\lambda=10,6 \mu\text{m}$, that means the laser works in infrared field. The laser source can offer 35 W maximum powers in direct current. Two sources of electrical discharges are available, each of them have the intensity between 5-25 μa . The cooling system of the laser is made by a water circuit with a debit of 2-3 l/min. Considering the existing conditions in the laboratory we tried to realize different experiments to the better knowledge of this laser.

How do we use the laser :

- checking the laser beam shutter to be Off;
- set the cooling water system and control the water debit coming out from the cooling system (optimum debit 2-3 l/min);
- set ON the self fuse from the posterior control panel, checking the state of the high tension switch that generate the discharges in the laser tube;
- connect to the network supply with alternating monophasic current 220V;
- mark the working area with laser and take the safety measures;
- set left switcher: ON; on the measuring device will be indicated the current in the discharge tube;

- the current adjustment allows the continue check of the power between 1-10W (for a single discharge);
- activate the second discharge part (the switcher from the right part of the frontal panel);
- with the two discharges activated at the maximum current (25mA) the maximum power transmitted by the laser is 35W;
- for technical applications at the outlet of the laser is assembled detachable focusing head. The focusing head has a 90° reflection mirror of the laser beam which is emitted and focused by a KCL lens, the focus distance is 7cm;
- when working with the laser beam will be insured a gas flow through the protection device of the focusing lens and put ON the shutter of the laser beam.



Fig.1 The laser equipment

The laser positioned on a drilling machine base with the possibility of vertical movement. We realized two types of measurements: in the first case we studied the variation of the thermodynamic tension and in the second case we followed the variation of the temperature.

For the first experiment we use a chromium-aluminum thermocouple which was put in a metallic piece, the thermocouple is connected to the DT 830 B measure device. In order to measure the variation of thermo-electromotive tension, on the two perpendicular directions, we used a moveable table to which we attached two comparators. All this assembly was fixed on a wooden table with four cylinders. The supports of the two comparators were fixed on the wooden table with some weights.

The working area of the laser was limited by a ceramic flat, 8mm thickness, in which we realized a conical whole so that the laser beam will fall directly on the thermocouple without reflecting on the metallic surface towards the operator. The positioning of the thermocouple in the center of the ceramic flat was easy to realize because the thermocouple was on the top of the cutting tool and pointed out.

Also to protect the operator a glass screen was mounted on a moveable table and the operator had to wear goggles. We used a sheet of paper that covered the ceramic flat to view the laser beam position.

To have a bench-mark, we searched the maximum value that the tension can reach to, both on horizontal and vertical direction; we found the maximum value of 1,9 mV and the minimum value 0,3mm. Then we moved the table from 0,1mm to 0,1 mm, on both directions, to the maximum value and back to the minimum one and we obtained the values pointed out in tab. no.1.

Table no.1. The variation of the thermo-electromotive tension

No. experiment	1	2	3	4	5	6	7	8	9	10	11	12	13	14
Distance, mm	0	0.1	0.2	0.3	0.4	0.5	0.6	0.7	0.8	0.9	1.0	1.1	1.2	1.3
T.E.M, mV	0.3	0.3	0.3	0.3	0.3	0.3	0.4	0.4	0.4	0.4	0.5	0.5	0.5	0.6
No. experiment	15	16	17	18	19	20	21	22	23	24	25	26	27	28
Distance, mm	1.4	1.5	1.6	1.7	1.8	1.9	2.0	2.1	2.2	2.3	2.4	2.5	2.6	2.7
T.E.M, mV	0.7	0.8	1.0	1.1	1.2	1.3	1.4	1.4	1.4	1.5	1.5	1.7	1.8	1.9

Using a computer program elaborated in T.C.M. faculty, we established an empirical model for the values in table no.1:

$$U=0.1846 + 0.78479a - 1.0336a_2 + 0.43326a_3 \quad (1)$$

$$\text{The Gauss sum for this mathematical model is } S = 6,6379 \times 10^{-3} \quad (2)$$

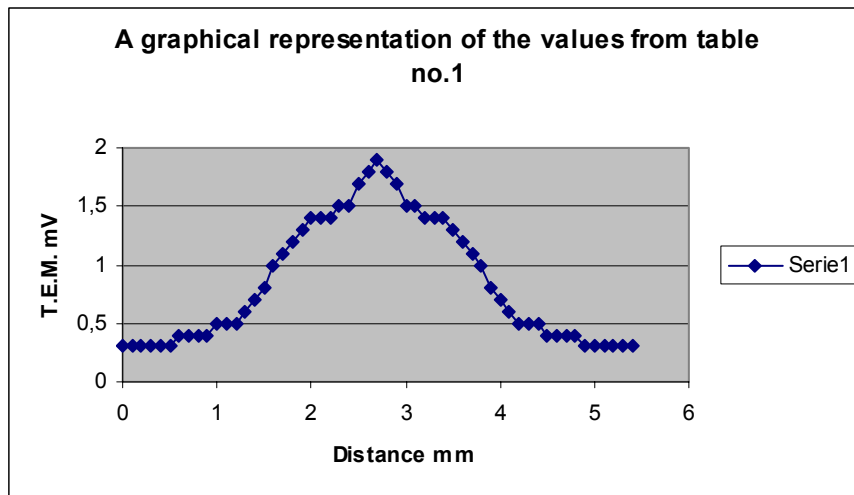


Fig.2. A graphical representation of the values from table no.1

For the second experiment we used a thermocouple from the measure device case DT 9208A. We used the same ceramic flat with a little conical hole so that the laser beam will fall directly on the thermocouple without reflecting on the metallic surface towards the operator. A bit difficult this time was to centre the thermocouple in the ceramic flat because the thermocouple was thinner and not fitted on the cutting tool. This assembly was put on a movable table of which we attached two comparators. The magnetic supports of the two comparators were fixed on the metallic

table. In this case we also used a sheet of paper that covered the ceramic flat to view the laser beam position.

Also to have a bench-mark, we searched the maximum temperature that can be touched and we found a maximum of 108°C and a minimum of 34°C, measuring from 0,5 to 0,5mm. The results are pointed out in the table no.2.

Table no.2 Temperatures values

No. experiment	1	2	3	4	5	6	7	8	9	10
Distance, mm	0	0.05	0.1	0.15	0.2	0.25	0.3	0.35	0.4	0.45
Temperature, °C	85	83	81	79	73	67	59	53	51	49
No. experiment	11	12	13	14	15	16	17	18	19	20
Distance, mm	0.5	0.55	0.6	0.65	0.7	0.75	0.8	0.85	0.9	0.95
Temperature, °C	48	47	46	45	44	43	37	36	35	34

The mathematical model for these experimental results is:

$$U=88.65842 + (-105,9283)a + 51.03657a^2 \quad (3)$$

$$\text{For this mathematical model is } S=8.83117 \quad (4)$$

Table no.3.Variations of the temperature with the distance to the laser beam axe

No. experiment	1	2	3	4	5	6	7	8	9	10
Distance, mm	0	0.05	0.1	0.15	0.2	0.25	0.3	0.35	0.4	0.45
Temperature, °C	74	72	71	67	65	64	63	61	59	58
No. experiment	11	12	13	14	15	16	17	18	19	20
Distance, mm	0.5	0.55	0.6	0.65	0.7	0.75	0.8	0.85	0.9	0.95
Temperature, °C	57	55	53	52	51	49	47	45	44	42

The mathematical model for these experimental results is:

$$U=75.378-37.604A+5.1944A^2 \quad (5)$$

$$\text{The Gauss sum is } S=0.4471 \quad (6)$$

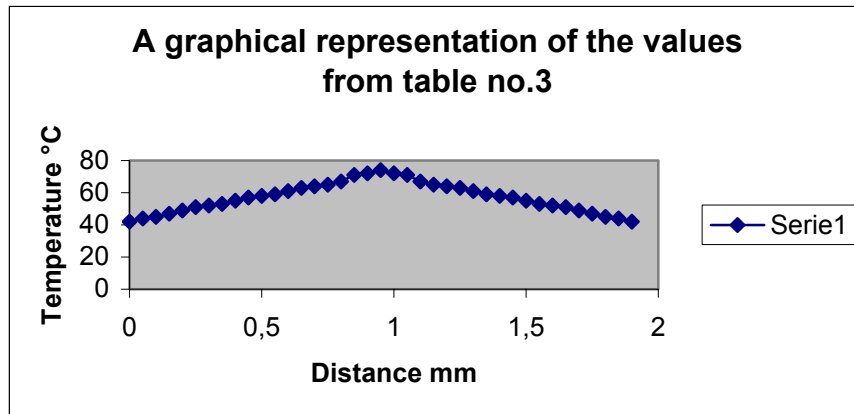


Fig.4. A graphical representation of the values from table no.3

Considering that the obtained values do not point the exact temperature that can be reached, we tried another method by bonding the thermocouple on a ceramic flat with abrasive surface and covering the reflection area with a sheet of paper. With this assembly we made measurements for different distances between the thermocouple and the laser spot area. The obtained values are:

- at 1 cm, the maximum value is 102°C;
- at 2 cm, the maximum value is 85°C;
- at 2,5 cm, the maximum value is 74°C;
- at 5 cm, the maximum value is 88°C;

For X axis starting with 102°C, the maximum temperature, we obtained 82°C, the minimum temperature, by measuring from 5 to 5 mm and for Y axis from 92°C to 52°C.

3. CONCLUSIONS

One of the conclusions we reached to, is that when the gas debit is low the temperatures are high, but the absence of the gas leads to deterioration of the lens.

Another explanations for the fact that the temperatures are low is that the radius of laser beam is 0,4 mm comparing with the radius of the warm welding of the thermocouple that is 1mm, the heat of the laser beam being spreaded in all warm welding area of the thermocouple.

Improvement solutions:

- Another method to protect the lens (besides compressed air);
- Using a warm welding with the same area as the laser beam;
- Using a numerical command table;

REFERENCE:

1. Slatineanu, L., *Non traditional technologies in Machine Manufacturing*, Chisinau, Publishing house Tehnica-Info, 2000;
2. ****Using instructions for the CO₂ laser The Physical*, Laser, Plasma and Radiation Institute, Bucharest;
3. Cretu, Gh., *Bases of experimental research*, Laboratory Guide;
4. Dumitras, D., *Gas laser*, Publishing house Academy R.S.R., 1982;

Received december, 19 2005

¹Technical University Gh. Asachi Iasi

CERCETĂRI PRIVIND EVALUAREA UNOR PARAMETRI DE IEȘIRE AI LASERULUI CU CO₂

REZUMAT: Laserul a avut un impact foarte mare asupra industriei. În această lucrare, vom prezenta doua tipuri de măsurători cu ajutorul laserului cu gaz. Am utilizat un laser care folosește CO₂ pentru răcire. Laserul folosește o sursă de gaz cu circuit închis. Am făcut două tipuri de măsurători: în primul caz am studiat variația tensiunii termodinamice iar în al doilea caz am urmărit variația temperaturii. Pentru primul experiment am folosit un termocupul de cromel-alumel care era introdus într-o piesă metalică termocuplul fiind legat la un aparat de măsurat de tip DT 830B. În al doilea experiment am folosit pentru a măsura temperatura, un termocuplu existent în trusa aparatului de măsură de tip DT 9208A. Deasemenea, termocuplul a fost pus într-un cuțit dispunând de canal. Rezultatele au arătat că pentru diferite condiții de lucru se obțin valori diferite.

**MODERNISATION TRENDS IN THE COLD ROLLING AND
CONSIDERATIONS CONCERNING THE DETERMINATION OF THE
OPTIMUM COLD ROLLING FORCE**

BY

**MIHAI ALEXANDRU¹, GHEORGHE BADARAU², LIVIU RUSU¹, VASILICA MIRON¹,
ROMICA MANEA¹**

***ABSTRACT:** The paper presents modern way to get cold rolling products, and also presents a mathematical model of the process, combined whit a Bland and Ford model for determination a optimum of the cold rolling force.*

***KEY WORDS:** rolling force, optimization, mathematical model*

1. INTRODUCTION

In the cold rolling profile manufacturing, in the last decay, it was seen an interesting behavior of the market. So, small enterprises appeared having one or two products in the production of which they are completely specialized. From the point of view of the quality and price of the products these enterprises are competitive becoming a real threat for the big rolling mills.

In these circumstances appeared some technical reactions that we will present in this paper.

2. MODERN PREOCCUPATIONS CONCERNING THE DIRECTIONS OF MODERNIZATION AND THE TRENDS OF DEVELOPMENT IN THE FIELD OF COLD ROLLING.

In the present paper, after analyzing a great number of specialty publications, we draw the conclusions that the main directions in which the specialists and researches work do not imply the construction of new rolling units but the modernization of the existing ones.

The modernization of the Sakai rolling mill can be included in this current. This modernization started in 1989 by the introduction of the forth cage beside the three existing ones (3TM) and it continued with the introduction of the continuous decapation line (2CP). Once these modifications made there were achieved important technological modifications too. The aim of these important modifications is the enhancing of the productivity, quality improvement and diversifying of the products. The scheme of positioning of the modernized line is shown in the next figure.

The steel producers have introduced cages having six cylinders in height and cooling units, both having a good capacity of shape control. Sometimes these systems can be combined. The same type of methods gave satisfaction at the Nagoya Works at the number 3 rolling mill.

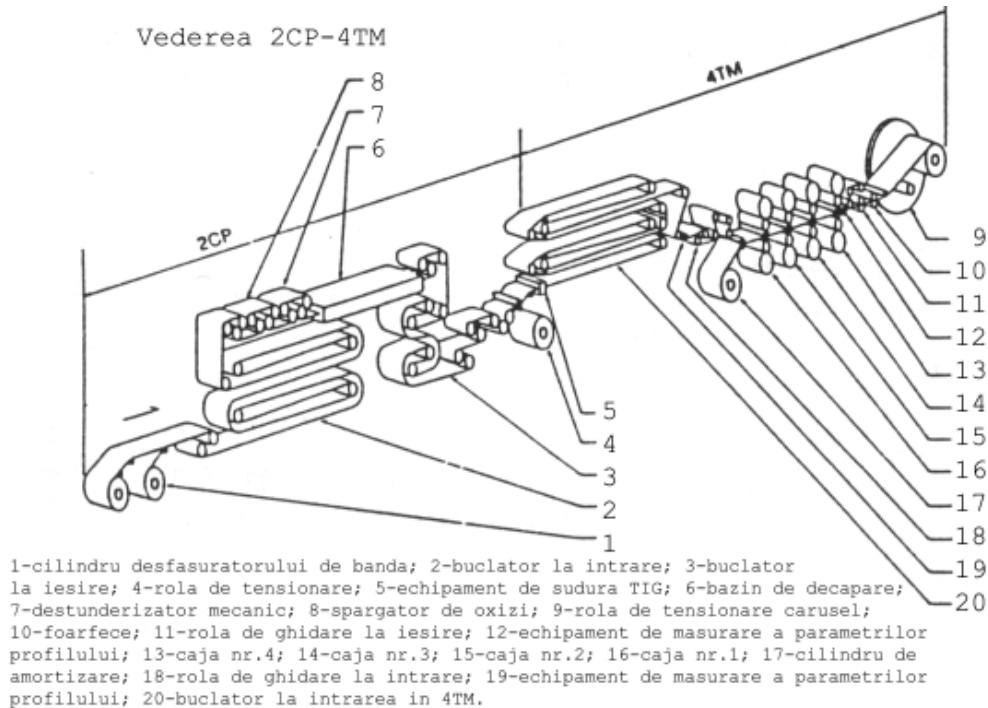


Fig. 1 The scheme of principle of the assembly 2CP – 4TM

- 1 - cylinder of the strip developer; 2 - entrance loop maker; 3 - exit loop maker; 4 – tensioning roll; 5 – TIG welding equipment; 6 – decapation tank; 7 – mechanical cleaner; 8 – oxides breaker; 9 – tensioning carousel roll; 10 – scissors; 11 – guiding roll; 12 – profilmeter; 13 – cage no.4; 14 – cage no. 3; 15 – cage no. 2; 16 – cage no. 1; 17 – shock absorber cylinder ; 18 – guiding roll; 19 – profilmeter; 20 – loop maker at the 4TM entrance.

Solving with the finite element method enables the determination of the forming limit e in each finite element of the part. The strip between the tensions represents the general law of Hook's for homogenous and isotropic materials.

Using the relation of the cold forming force and the optimum value of the forming limit determined by the theory of plastic instability one obtains the optimum values of the tension. The optimum value of the forming force must satisfy the following conditions: $Opt_x(x); x \in E^n$

$$h_j(x) = 0 \quad j=1, 1$$

$$g_j(x) \leq 0 \quad j=j+1, m$$

x is the vector of variables

Optimization is being achieved in the following stages :

- a point $P_1 (x_{i,1}) \quad i= 1, n$ is chosen in the space having n dimensions in which we define this function;
- the value of a size is being taken, knowing that the accuracy of estimations is proportional with $1/a$;
- $P_i (x_{i,j}) \quad j= 2, n+1$ is determined in the condition that the distance between two established points is constant and equal with a ;

-we calculate $f(P_1) \dots f(P_{n+i})$ and then we determine the most unfavorable value:

$$X_i^{(N)} = \left(\frac{2}{n} \left(\sum_{j=1}^{n+1} x_i^{(j)} - x_i^{(R)} \right) \right) - x_i^{(R)}$$

where: $x_i^{(N)}$ is the coordinate of the new point;

$x_i^{(R)}$ is the coordinate of the rejection point that gives the worst value for f .

For the optimization of the parameters of the rolling process we have calculated in an analytical way the deformation forces, in which all the expressions that are constant were introduced as they are and the other were calculated using the dependency relations.

After a complex research we came along with a relation having the shape below. The relation is being derived from the Bland and Ford model adapted for the cold rolling and using an original program.

$$P = \frac{\pi \cdot E_C \left(\sqrt{\delta + \delta_1 + \delta_2} + \sqrt{\delta_2} \right)^2 \cdot \left(\delta - R \arccos^2 \left(1 - \frac{\delta}{2R} \right) \right)}{16R(1 - \nu^2) \arccos^2 \left(1 - \frac{\delta}{2R} \right)}$$

We could do in this particular manner a comparison between the experimental values and the ones obtained in the analytical way for the rolling force on width unit remarking a good correlation of the mathematical model Bland and Ford with the programmed experiment.

Valorizing the experimental results we determined the functions of variation and the regression equations that correlate the cold plastic deformation process of the profile with the compression test.

The figure below presents the experimental point as well as the variation polynomial curve associated.

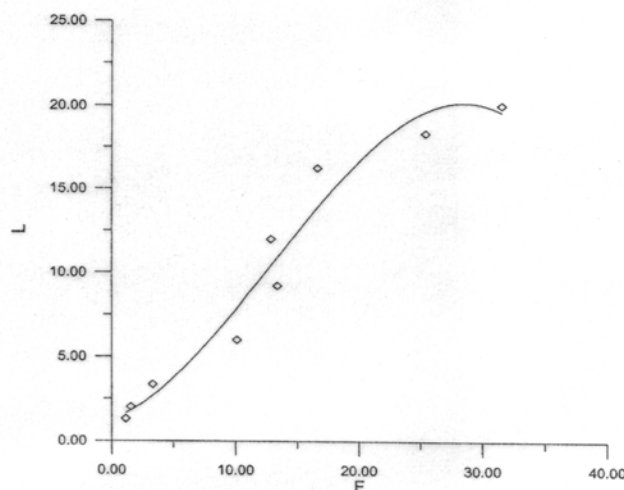


Figure 2 Experimental point as well as the variation polynomial curve associated.

3. CONCLUSION

Both the regression equation and the maximum of the function assures that the nine points are representatives for the chosen domain. The theoretical curve based on the experimental dates comprises the phenomenon, demonstrating the correspondence in the study field, expressing the close interdependency between the linear sizes variation and the deformation force.

REFERENCES

1. **Huisman, R.L., Galma, M.E., Bruinsma, H.**- The application of a Mathematical Model Based on Physical Relations for an On Line Preset Model for Cold Rolling, The Science and Technology of Flat Rolling, vol. 2, Deauville, France, 1987, pp.35-42;
2. **Zhou Guo Yng**- Calculul forțelor de laminare în cazul laminării la rece, Neue Hutte, Germania, vol 35, nr.9, 1990, pp.331-335;
3. **Trillo, C.T.** – Controlul procesului la laminorul la rece de la Novi Ligure, Associazione Italiana di Metallurgia, Centro Lavorazioni Plastiche, 1981, pp.206-224;
4. **Alexandru, M.** – Cercetări experimentale, interpretarea rezultatelor și contribuții fundamentale –aplicative privind îmbunătățirea parametrilor constructivi și funcționali ai unei linii de laminare la rece-referatul 3, Universitatea Tehnică „Gh. Asachi”, Facultatea SIM, Iași 1997;
5. **Alexandru, M.** – The Mathematical Model Based on Plastic Instability Theory of Roll Forming Force – Buletinul Institutul Politehnic Iași, secțiunea Știința și Ingineria Materialelor, Tomul XLII (XLVI), Lucrările celui de-al Doilea Congres Internațional, 27-31 mai Iași 1997
6. **Alexandru M.** – Contribuții teoretice privind îmbunătățirea parametrilor constructivi și funcționali ai unei linii de laminare la rece – Teza de doctorat, Iași 2004

Received December, 21, 2006

¹*High School “Stefan Procopiu” Iași*
²*Technical University “Gh. Asachi ” Iași*

TENDINTE DE MODERNIZARE ÎN LAMINAREA LA RECE ȘI CONSIDERĂȚII PRIVIND DETERMINAREA OPTIMĂ A FORȚEI DE LAMINARE

REZUMAT: Lucrarea prezintă metode moderne de obținere a produselor laminate; de asemenea prezintă un model matematic al procesului combinat cu modelul Bland and Ford pentru determinarea forței optime de deformare la laminarea la rece.

IDENTIFICATION AND MEASUREMENT OF QUALITY PARAMETERS FROM RESIDUAL WATER, WHO ARE SPECIFIED TO TECHNOLOGICAL PROCESS OF THERMAL ZINC PLATING, FOR SOLVE BY EFFICIENCY WAY, THE CHEMICAL (SEWAGE) TREATMENT PROCESS, WITH STRAIGHT IMPLICATION TO THE ENVIRONMENT.

BY

**VASILE DIA¹, MIHAI ALEXANDRU², MARIA COJOCARA³, DOINA HINCUI²,
GHEORGHITA BADARAU⁴**

***ABSTRACT:** The paper present some of the biggest polluting factor who are found in the sewage industrial waters from the zinc plating process, some ways to reduce that factors, and some solution to make a nonpolluting future.*

***KEY WORDS:** zinc plating process, sewage waters*

1.INTRODUCTION

Quality and quantity characteristicals of sewage industrial waters

Establishing the origin and quality characteristicals of sewage industrial waters, required the knowledge of the industrial process for a better design work for purification stations. Sow, we must know the origin of principals affluent to define purification way. If we want to reduce the debit of sewage industrial waters, we must use new technology. The principals bad substance of sewage industrial waters are organically substance (CBO₅), suspension substance, toxically substance, and hard metals. Sewage industrial waters may contained organically substance (CBO₅) who have a harmful effect in the good way sense of a better function for purification stations, because the oxygen it is necessary for aerobiosis process (aerobiosis bacteria's), who oxides the organically substance. The suspension substances (base crude oil, different kind of oil) make hard the absorption of the oxygen by the surface of the water, and auto filtration, blocking-up the filters for water filtration. That kind a substance are deposit to the bottom of the receiver, and blocked the filtration process.

Hard metals (Pb, Cu, Zn, Cr) have a toxically action for aquamarine organism, make worsen any process of filtration. CCO₅ and CCO, azotical and phosphorical salts (nutrients) make maritime algae to grow faster. But, in the last years, technological process are using new toxically substance who are hard to determinated: nitrochlorbenzen, phitopharmaceutical, etc.

In sewage industrial waters are impose different maximal concentration (mg/l) for ammonium (NH₄), ammonia (NH₃), azotates (NO₃), NO₂, CO₂, Ca, cyanides (CN), free chlorine (Cl₂), chlorides (Cl), hydrogen ions (pH), tri valence Cr, hex valence Cr, Cu, anion abluent, carbolate, sulfurated hydrogen (H₂S), Hg, O₂, Na, sulphates (SO₄), Zn, bacillite.

For organically substance we define consumption of biochemical oxygen (CBO₅), and consumption of chemical oxygen (CCO), the last by the method who use CCOMn or CCOCr.

Effectiveness, the filtration of sewage industrial waters degree, are calculated with relation:

$$\beta = ((M-m)/M) 100$$

M= initial substance concentration, m= after filtration concentration

Because the industrial contaminants are refers at the organically loading, defined based by CBO₅, and at impurity suspensions, it is necessary to define a indicator who reunited these dates. So, it is use "equivalents inhabitants", who defined some of the principal characteristics of pollution, in present case CBO₅, and suspensions, if we use same units measures.

Because sewage industrial waters have different debits and different concentration in time, beyond purification stations it is necessary to make the equalizing for sewage industrial water, but after pre-purification stations who are for cleaning away nondissolving contaminant.

2. CHEMICAL QUALITATIVE INDICATORS OF SEWAGE INDUSTRIAL WATERS WHO ARE IMPOSED BY THE STANDARDS

Sewage industrial waters collect in the combined storm and sanitary sewer network, or in the purification stations are make in the condition imposed by the annex 2 of NTPA-002/2002. Before are evacuated in the naturals receptors, sewage industrial waters will be constrained to a secondary filtration, to respect the normative (table 1).

Table 1

Nr. crt.	Quality indicator	UM	Demands conf. NTPA 002/2002	
			Admisibile value	Analizing methods
1	Temperature	°C	40	-
2	Concentratio of hydrogen ions (pH)	unit pH	6,5 – 8,5	SR ISO 10523-97
3	Suspensions particules	mg/dm ³	350	STAS 6953-81
4	Biochimichal oxygen consume at five days (CBO ₅)	mg O ₂ /dm ³	300	STAS 6560-82 SR ISO 5815/98
5	Chimichal oxygen consume – bicromat of K method (CCOCr)	mg O ₂ /dm ³	500	SR ISO 6060/96
6	(NH ₄ ⁺)	mg/dm ³	30	STAS 8683-70
7	(P)	mg/dm ³	5.0	STAS 10064-75
8	(CN)	mg/dm ³	1.0	SR ISO 6703/1-98
9	(S ₂ ⁻)	mg/dm ³	1.0	SR ISO 10530-97
10	(SO ₃ ²⁻)	mg/dm ³	2	STAS 7661-89
11	(SO ₄ ²⁻)	mg/dm ³	600	STAS 8601-70

12	Water vapors mixed whit fenols (C6H5OH)	mg/dm3	30	STAS 7167-92
13	Exctractible substance mixed whit organical solvents	mg/dm3	30	SR 7587-96
14	Sintetiquals active anion abluent	mg/dm3	25	SR ISO 7875/1.2-96
15	(Pb2+)	mg/dm3	0.5	STAS 8637-79
16	(Cd2+)	mg/dm3	0.3	SR ISO 5961/93
17	(Cr3+)	mg/dm3	-	-
18	(Cr3+ + Cr6+)	mg/dm3	1.5	STAS 7884-91
19	(Cr6+)	mg/dm3	0.2	STAS 7884-91 SR ISO 11083-98
20	(Cu2+)	mg/dm3	0.2	STAS 7795-90
21	(Ni2+)	mg/dm3	1.0	STAS 7987-67
22	(Zn2+)	mg/dm3	1.0	STAS 8314-87
23	(Mn2+)	mg/dm3	2.0	SR 8662/1-96 SR ISO 6633-96
24	Free rezidual Cl (Cl ₂)	mg/dm3	0.5	STAS 6364-78

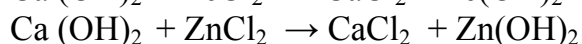
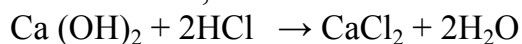
3. IDENTIFICATION AND MEASUREMENT OF CHEMICAL INDICES OF SEWAGE INDUSTRIAL WATERS WHO RESULTS AT TECHNOLOGICAL PROCESS OF THERMAL ZINC PLATING

Depending of specificall activity made, sewage industrial waters can be characterized by much many indicator than we find in the table 1. The study must shows, also, quality and quantity methods of analyzing, but also the adequate technology for water filtrated and there are approval by the central publican authority.

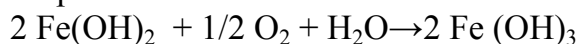
Inside the thermal zinc plating workshop are used acid based on water solution, basically, cromical, which are contained some toxically and aggressive components. These solutions, are consumed because the chemical process of the surface the tubes.

In the same time, they are finish the basic components and are get rich in contaminants who make to became inactive. After some time, it is necessary to exhaust these big quantities of depletion solutions. Because they are priority acid, first of all, we must treat them whit an neutralization substance.

Acids-alkaline depletion solutions are reverse first of all in the neutralizing collectors from the sewage industrial waters filter station, whit the washing waters from the technological process of surface tube preparing. For a better results are used milk caustic lime, the reaction been:



CaCl₂ and ZnCl₂ are deposit whit high speed, but Fe(OH)₂ are deposit very hard, because this big solubility. For a quick deposit, we do a barbotage whit air who mixed and the depletion solutions whit milk caustic lime for speeding velocity of reaction.



After neutralization, waters from the collectors are pump over in centrifugal settling tank where sludge are purificated and separated.

Precious information are obtained after physical- chemical analyzed of a slam (sludge) who are result after chemical treatments process. As we aspect, the slam is composed most of CaCl_2 , ZnCl_2 , $\text{Fe}(\text{OH})_2$, $\text{Fe}(\text{OH})_3$. We are take assay from sewage industrial waters and from the slam by different places: neutralization collectors, settling tank, slam, water from evacuation channel, and we make analysis.



Fig. 1 Neutralization collectors



Fig. 2 Centrifugal settling tank

In fig. 3 it's shows slam assay from the settling tank who present trace of $\text{Fe}(\text{OH})_2$ (green trace), so, the aerate of the neutralization bath it not was made right. That thing will cause the exceed

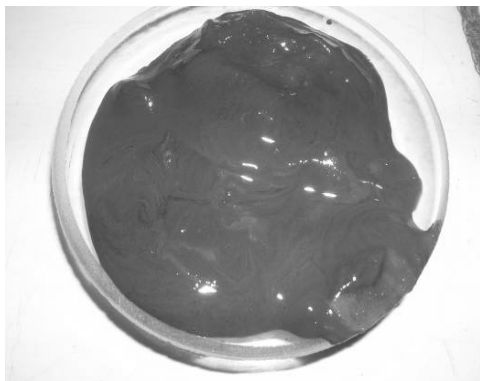


Fig. 3 Slam assay taked from settling tank



Fig. 4 Slam assay taked from settling tank after separation

value for the quality indicator Fe^{2+} . In fig. 4 are shows a assay of settling tank and who was separated by gravitation whit water. That slam still have a big quantity of water, and he must be centrifuged. To find best solutions for water filtration who are results from zinc plating, was made a physical-chemical and granulometrical analyze to the contraries who was find in the water.



Fig. 5 Mesh wire for granulometrical measures

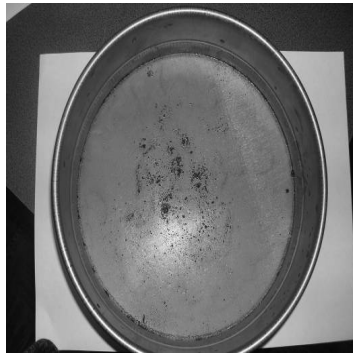


Fig. 6 Contraries stopped whit 35µm mesh wire

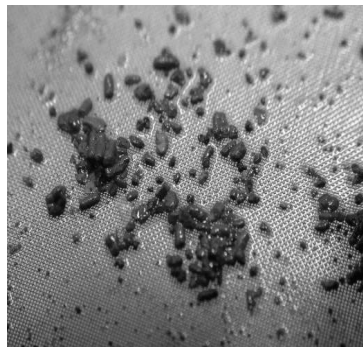


Fig.7 Macro aspect of contraries(0.035mm)



Fig. 8 Particle of Zn(OH)₂ obtained with 100 mesh wire. Contraries are $\approx 650 \mu\text{m}$

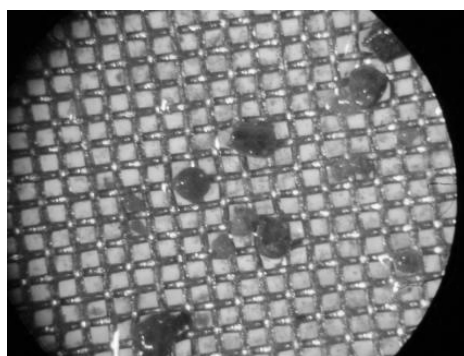


Fig. 9 Particle of Fe (OH)₃ and CaCl₂ with size 100-130 μm

In table 2 are shows quality indices of sewage industrial waters who results at technological process of thermal zinc plating, and same value who are obtained in 2005 (medium and maximum value). As we shows, exceeded from value are : pH, contraries, chloride, and at hard metal Fe and Zn.

Table 2

Nr. crt	Sewage water quality indicator	U.M.	Medium value /2005	Maximum value/2005	Maximal value admissible NTPA 002/2002+ Contract RAJAC
1	pH	unit. pH	7,66	4,5	6.5-8.5
2	contraries	mg/dm ³	212	657	300
3	extractible substances	mg/dm ³	5,9	23	30
4	Zn	mg/dm ³	21,3	151,8	1
5	Fe	mg/dm ³	8,6	150	5
6	CBO ₅	mg/dm ³	18.46	27	300
7	CCo-Cr	mg/dm ³	60.48	124	500
8	NH ₄	mg/dm ³	11.33	28,5	30
9	Cr	mg/dm ³	0.34	1,3	1.5
10	chloride	mg/dm ³	287.32	427	300
11	fixed waste	mg/dm ³	675	1391	1000

4. SOLUTION REGARDS REDUCING THE POLLUTION OF THE SEWAGE INDUSTRIAL WATERS WHO ARE SPILLED IN CENTRAL CITY CHANNEL.

Possible alternative for removing and recuperating of the toxically organical compounds from sewage industrial waters are:

- Oil separating machine
- Flocculation for organical colloidal
- Floating for contraries who are bigger than 1
- Settling whit chemical precipitation
- Complete oxidation and reduction using air and O₂
- Filtrating with small volume of water
- Neutralizing, when must spilled solution who have pH=6-8, using solution like calcium hydroxide

If we look carefully in the tables, we seen, making a comparetion whit NTPA 002/2002, that:

- Are some accidental exceeded to the pH at the assays who was collected at a zinc plating section
- Continual exceeded in Zn and Fe in assays from collector
- High concentration in chloride and fixed residue exceeded in the collector

If the exceeded of the pH value it is a accident, caused by a technological indiscipline, worst problems are in mater whit Fe and specially Zn.

5. CONCLUSION

Possible solution to reduce ionic Zn concentration are to neutralizing in excess water until rich a 8.5-9 value of pH, when are take place precipitation of Zn(OH)₂. That sing precipitating the Zn and that can be separated in the separator. Other more efficient way, but much expensive, are to coagulate and flocculate, method which presume removing some particle by sedimentation (coagulation) and destabilization by absorbing some big molecule of polymers who forming bridges between particle.(flocculation) Are being used for the colloidal particle. Of course, the best way to reduce water pollution by zinc plating is to change all actually technology whit non polluting technology, or whit an smaller grade of pollution. That thing means very big investition because implies to change some equipments, and a new design for a filtration station.

REFERENCES

1. Epurarea apelor uzate industriale (vol. 1), Coordonator Mircea Negulescu, Ed. Tehnica, Bucuresti, 1987
2. Epurarea apelor uzate industriale (vol. 2). Coordonator Mircea Negulescu. ed. Tehnica, Bucuresti, 1989
3. **Varduca Aurel.** Monitoringul integrat al calitatii apelor. Ed. H.G.A., Bucuresti, 1999
4. **Varduca Aurel.** Protectia calitatii apelor. Ed. H.G.A., Bucuresti, 2000
5. Water Resources. Environmental Planning, Management and Development. Editor Asit K. Biswas. McGraw – Hill, 1997
6. **Grigg Neil S.** Water Resources Management: Principles, regulations and cases. McGraw – Hill, 1996.
7. Sustainable Water Management in the Baltic Sea Basin. Book 2. Water Use and Management. Editor Larss-Christer Lundin, Uppsala University, 2000
8. **Tobolcea V., Ungureanu D.** Managementul apelor uzate. Partea I. Iasi:, 1993

9. **Lidia-Maria Vaicum.** Epurarea apelor uzate cu namol activ. Bazele biochimice. Editura Academiei RSR, Bucuresti, 1981
10. **Robesen D. s. a.** Tehnologii, instalatii si echipamente pentru epurarea apei. Ed. Tehnica, bucuresti, 2000
11. **W.W. Eckenfelder Jr., J.C. Musterman.** Activated Sludge Treatment of Industrial Wasterwater Technomic Publishing. Co. Inc., 1995, 281 p.

Received January, 10 2006

¹*S.C. Mitall Steel S.A.*

²*High School "Stefan Procopiu" Iasi*

³*High School Valeni Vaslui*

⁴*Technical University "Gh. Asachi" Iasi*

**IDENTIFICAREA SI MĂSURAREA PARAMETRILOR DE CALITATE DIN APELE
UZATE, SPECIFICE PROCESULUI TEHNOLOGIC DE ZINCARE TERMICĂ A ȚEVILOR,
ÎN VEDEREA SOLUȚIONĂRII EFICIENȚEI PROCESULUI DE EPURARE A APELOR
UZATE, CU IMPLICAȚII DIRECTE ASUPRA PROTECȚIEI MEDIULUI INCONJURĂTOR**

REZUMAT: Lucrarea prezinta citiva din cei mai mari factori poluanti care se gasesc in apele uzate provenite de la procesul de zincare a tevilor, citeva cai de reducere a lor, si solutii pentru un viitor nepoluant.

RESEARCHES ABOUT THE SUSTAINABLE DEVELOPMENT AND HOT – DIP GALVANIZING

BY

VASILICA MIRON¹, DOINA HINCUI², CONSTANTIN ALEXANDRU³, VASILE DIA⁴, MARIA
COJOCARU⁵

ABSTRACT: *SD is the right approach for a responsible industry. It is also measurable in terms of the improvement in the quality of life (social), the number of jobs created (economic), and the level of care given to the water, air, and Earth (environmental). Now, whole industries and companies are regularly graded for their commitment to SD.*

KEY WORDS: *sustainable development, hot dip galvanizing, zinc coating*

1. INTRODUCTION

What is Sustainable Development? Sustainable Development (SD) is the social, economic, and environmental commitment to build a future that is more prosperous, more just, and more secure. It involves business growth and development that balances near-term interests with the protection of the interests of future generations. Investment decisions in the industry and companies are made as a result of these grades.

Zinc metal has a number of characteristics that make it well-suited for use as a coating for protecting iron and steel products from corrosion. Its excellent corrosion resistance in most environments accounts for its successful use as a protective coating on a variety of products and in many exposure conditions.

The excellent field performance of zinc coatings results from their ability to form dense, adherent corrosion product films and a rate of corrosion considerably below that of ferrous materials, some 10 to 100 times slower, depending upon the environment. While a fresh zinc surface is quite reactive when exposed to the atmosphere, a thin film of corrosion products develops rapidly, greatly reducing the rate of further corrosion.

In addition to creating a barrier between steel and the environment, zinc also has the ability to cathodically protect the base metal. Zinc, being anodic to iron and steel, will preferentially corrode and protect the iron or steel against rusting when the coating is damaged. A number of different types of zinc coatings are commercially available, each of which has unique characteristics.

These characteristics not only affect applicability but also the relative economics and expected service life. The method of processing, adhesion to the base

metal, protection afforded at corners, edges and threads, hardness, coating density and thickness can vary greatly from one type of zinc coating to another.

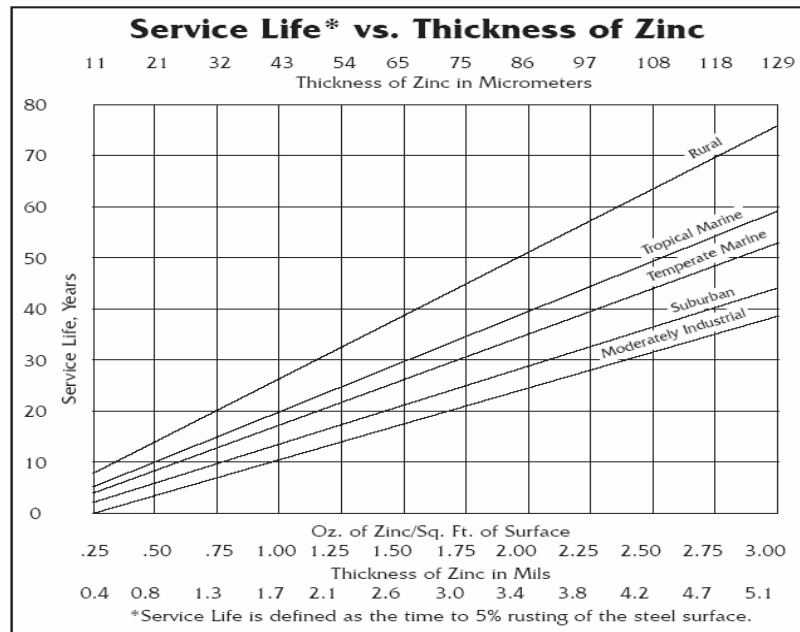


Figure 1 Service life to first maintenance (5% red rust) of iron and steel based on the zinc coating thickness and the environment.

Each of the major types of zinc coatings, applied by batch hot-dip galvanizing, continuous sheet galvanizing, electro galvanizing, zinc plating, mechanically plating, zinc spraying and zinc painting, are discussed here as a practical aid to the specialist who must assess and select zinc coatings for corrosion protection.

2. BATCH HOT-DIP GALVANIZING.

The hot-dip galvanizing process, also known as “batch” galvanizing, produces a zinc coating on iron and steel products by immersion of the material in a bath of molten zinc metal. The steel to be coated is first cleaned to remove all oils, greases, soils, mill scale and rust. The cleaning cycle usually consists of a degreasing step, followed by acid pickling to remove scale and rust, and fluxing to apply a protective surface to inhibit oxidation of the steel before dipping in the molten zinc.

Fluxing can be accomplished by pre-fluxing in a solution of zinc ammonium chloride (dry process), or by use of a molten flux blanket on the zinc bath surface (wet process) Materials to be hot-dip galvanized may range in size from small parts such as nuts, bolts and nails, to very large structural shapes.

The upper limit is restricted by the size of available zinc baths and material handling capabilities. Molten zinc baths 60 feet long and six feet deep are common in North America. By double-dipping or progressive dipping (immersing one portion of the product and then the other), the maximum size that can be accommodated in the zinc bath is increased substantially, to near double bath length or depth.

Since the material is immersed in molten zinc, the zinc can flow into recesses and other areas difficult to access, allowing all areas of even the most complex shapes to be thoroughly coated and protected against corrosion.

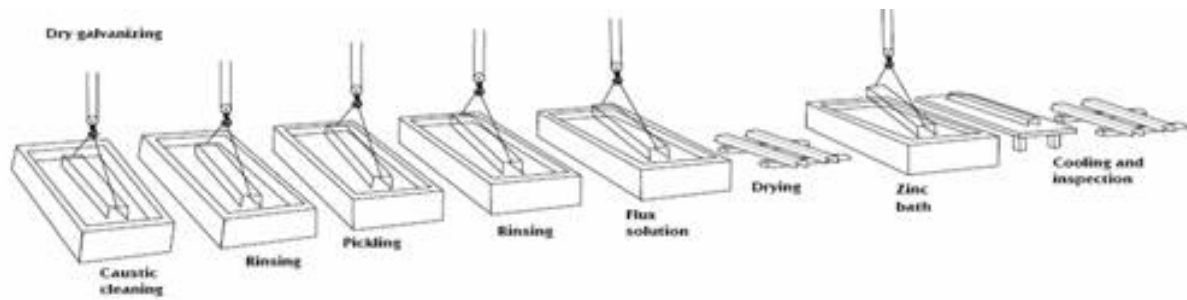


Figure 2 Dry process of the hot dip galvanizing

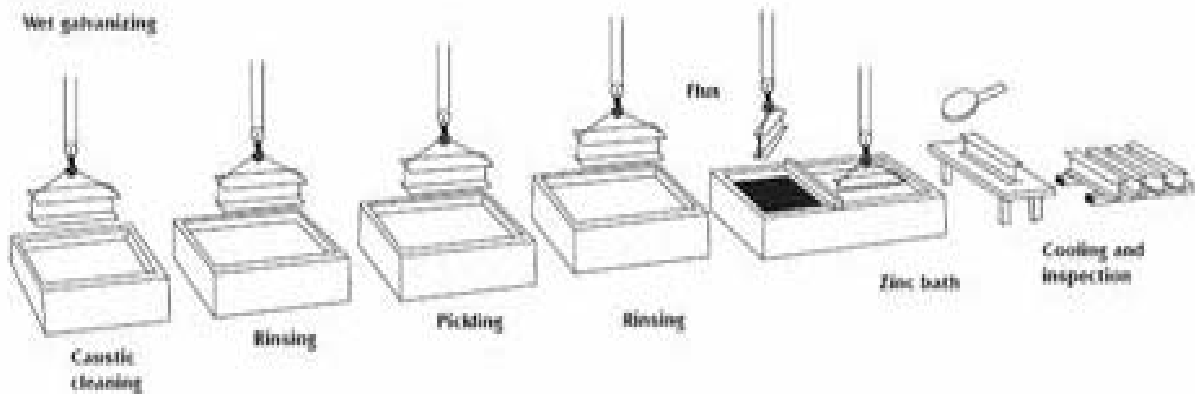


Figure 3 Wet process of the hot dip galvanizing

3. CHARACTERISING OF ZINC COATING

The batch hot-dip galvanized coating consists of a series of zinc-iron alloy layers with a surface layer of zinc. The coating is unique in that it is metallurgical bonded to the steel substrate, with the coating integral to the steel. The strength of the bond, measured in the range of several thousand psi, results in a very tightly adherent coating. Batch hot-dip galvanizing produces thick coatings.

The standard coating thickness requirement is 2 oz/ft² (600 g/m²), 3.3 mils (85 μ m). Thicknesses of 6 to 8 mils (150-200 μ m) on structural steels are common.

For most steels, the coating thickness obtained is relatively insensitive to processing variables. Heavier coating thicknesses can be obtained by abrasive blast cleaning of the steel prior to galvanizing. Coating thickness is proportional to coating weight, with 1 oz of zinc/ft² (320 g/m²) of surface equal to 1.7 mil (43 μ m) thickness.

The zinc-iron alloys that make up the coating have hardness values that approach or exceed those of the most commonly galvanized structural steels, offering excellent abrasion resistance for applications such as stairs and walkways.

The zinc-iron alloy layers are actually harder than the base steel. The coating is generally uniform on all surfaces.

Edges, corners and threads have coatings at least as thick, or thicker than, on flat surfaces providing excellent protection at these critical points. The pure zinc layer

and the zinc-iron alloy layers are anodic to steel, providing sacrificial protection in the event the coating is scratched.

This ensures that the steel exposed as a result of damage to the hot-dip coating will not rust as long as there is sufficient coating on the surface of the steel.

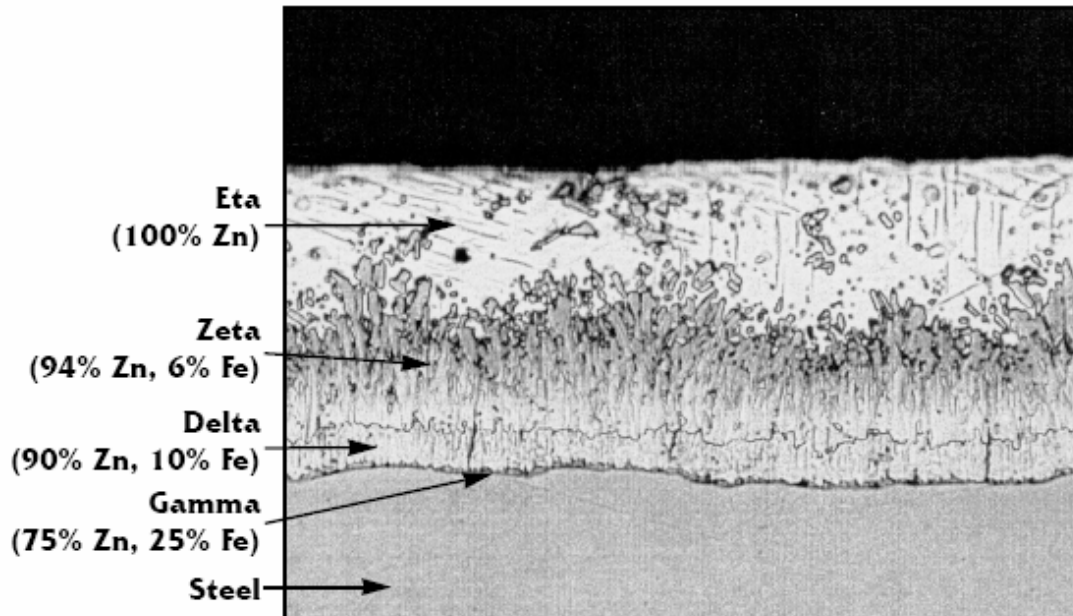


Figure 4. Photomicrograph of batch hot-dip galvanized coating

Coating Thickness vs. Coating Weight.

The usual criterion for determining the expected service life of zinc coatings is thickness: the thicker the coating, the longer the service life. This is an acceptable criterion when comparing zinc coatings produced by the same process .

When comparing zinc coatings produced by different processes, the thickness criterion cannot be used without considering the amount of available zinc per unit volume. It is also important to keep in mind various ASTM or other specifications as they relate to coating weight or thickness, and reduce the coating requirements to a common denominator prior to making a comparison of different zinc coatings.

While the coating densities for some of the different types of zinc coatings are nearly identical, others differ considerably. The coating densities, in terms of thickness required to equal 1 oz. of zinc/ft² of surface, are:

- Hot-dip galvanizing 1.7 mils (43 μ m)
(batch or continuous),
- electro galvanizing, zinc plating
- Zinc spraying (Metallizing) 1.9 mils (48 μ m)
- Mechanical plating 2.2 mils (55 μ m)
- Zinc-rich paint 3-6 mils (75-150 μ m)

Each of these thicknesses, representing the same weight per unit area of zinc, would be expected to provide equivalent service life; i.e. 1.7 mils of hot-dip galvanized would give about the same service life as 2.2 mils of mechanical plating or 3-6 mils (depending on the paint formulation) of zinc rich paint.

It is also important to remember that for all continuous galvanized sheet materials, including electro galvanized, the coating weight is given in weight per unit area of sheet. To obtain the amount of zinc per unit area of surface, the weight given must be divided in two, assuming equal distribution on both sides.

For example, an ASTM A 653 Class G90 sheet contains 0.90 oz. zinc/ft.² of sheet or about 0.45 oz./ft.² on a surface. A G210 (2.10 oz/ft.²) sheet would have to be specified to obtain about 1 oz/ft² on each side of the sheet.

4. ECONOMIC CONSIDERATIONS.

Selection from the wide range of coatings available for steel will normally depend on the suitability of the coating for the intended use and the economics of the protective system. Factors that affect the economics for a particular application include:

1. Initial cost of the coating;
2. Coating life to first maintenance;
3. Cost of maintenance;
4. Hidden costs, such as accessibility of the site, production loss due to maintenance re-coating, and rising wages for labor-intensive coatings, such as metal spraying and painting.

The choice of the most economical system cannot be precise, because neither the timing nor the cost of future maintenance can be accurately predicted. In addition, depreciation of capital investment, tax relief for investment and maintenance cost and the time value of money must be considered and can change over time.

Sustainable HDG Steel Project Applications

Hot-dip galvanized steel is used in several different types of project applications. From bridges and buildings to power and recreational applications, hot-dip galvanized steel is used to fight corrosion. The following applications identify the numerous ways that hot-dip galvanized steel can be used to provide a sustainable future.

These wind turbine electrical generators were entirely constructed using hot-dip galvanized steel. The tower structures are fabricated of three components measuring from three to four feet in diameter, with heights as tall as 72 feet. The hot-dip galvanized coating covers the turbine nacelle, access platform, and miscellaneous steel. There are more than 7,000 turbines located in the Altamont Pass area, and a recent inspection of the project revealed the galvanized coating still exhibited the traditional coating appearance.



Figure 5

Texas Motor Speedway is the second-largest sports facility in the country and the third largest in the world. Hot-dip galvanizing was chosen for several reasons, including low maintenance costs, increased safety, cost effectiveness, and aesthetic appeal. In addition to the structural steel, the bracings, handrails and fixtures were also galvanized.



Figure 6

This 90 by 1,500-foot structure heralds a new generation of piers at the Norfolk Naval Base, serving as a model for the rehabilitation or replacement of all the base's piers within the next 25 years. Its innovative design incorporates precast concrete pile caps, slabs, and edge beams protected by aesthetically pleasing hot-dip galvanized fenders and corner bolsters. The canopy structure is part of the 35th Street bridge that crosses over a major expressway in Chicago and connects the Chicago White Sox baseball park with the internationally renowned Illinois Institute of Technology. Eighty-six tons of hot-dip galvanized steel were used to support the fiberglass roof panels of the canopy. The selection of hot-dip galvanized coating was made easy by the desire to have a simplistic uniform coating that could withstand the substantial level of road salts used during snowy winters.

REFERENCES

1. Sustainable Water Management in the Baltic Sea Basin. Book 2. Water Use and Management. Editor Larss-Christer Lundin, Uppsala University, 2000
2. Water Resources. Environmental Planning, Management and Development. Editor AsitK. Biswas.

McGraw–Hill, 1997

3. W.W. Eckenfelder Jr., J.C. Musterman. Activated Sludge Treatment of Industrial Wasterwater

Received January, 11 2006

¹ *Technical University “Gh. Asachi ” Iasi,*
² *High School “Stefan Procopiu” Iasi,*
³ *Informatical High School “Grigore Moisil” Iasi,*
⁴ *S.C. “Mittal Steel” Iasi,*
⁵ *High School Valeni Vaslui*

CERCETARI DESPRE DEZVOLTAREA DURABILA SI DESPRE GALVANIZAREA PATRUNSA

REZUMAT: Dezvoltarea durabila este maniera cea mai potrivita de abordare pentru o industrie bine pusa la punct. Se poate, de asemea, masura in termeni precum nivelul calitatii vietii (social), numarul de locuri de munca create (economic) si nivelul de responsabilitate fata de poluarea aerului si apei si solului (ecologic). Astazi, anumitor ramuri ale industriei, precum si unui numar de companii li se acorda note care atesta implicarea lor in dezvoltarea durabila.

SOME ADVANCED MATERIALS AND TECHNOLOGIES FOR ELECTRONICS

BY

DUMITRU MNERIE¹, GABRIELA-VICTORIA ANGHEL¹

ABSTRACT: *Advanced Materials is the top in the materials sciences, with the highest independently assessed impact factor of any professional. In general, advanced materials can be: semiconductors; linear and non-linear optical materials; glasses; photoactive materials; laser materials; luminescent, photo chromic and electro chromic materials; ceramics including high temperature superconductors; magnetic materials; low dimensional solids; polymer encapsulates; biological materials; electro-rheological fluids; liquid crystals; chemically modified electrodes; resists; metallic conductors. For the future of electronics it must be to develop the continuum research about electroceramics.*

KEY WORDS: *material, electronics, technologies, electroceramics, nonoparticules*

1. INTRODUCTION

The complexity of microelectronics integrated circuits continues to increase while the size of the products. There are many firms who support the electronics industry, through making better electronic materials as well as by providing:

- materials development,
- systems engineering,
- synthesis,
- processing,
- testing services.

Hybrid microelectronics applications often require substrates and packages with desired tailored electrical and thermal properties. It meets these needs by preparing custom powders and parts. Hot pressing is particularly effective in preparing electronic substrates and packages. Additionally, it makes:

- special thick-film
- pastes
- additives for improved
 - electrical,
 - thermal
 - mechanical properties of microelectronics polymers.

Now are many firms who support the electronics industry, through making better electronic materials as well as by providing materials development, systems

engineering, synthesis, processing, and testing services. For example, it is development projects to make materials with desired electrical and thermal properties. In addition, it measures electrical and thermal properties of materials using some test and measurement equipment.

Some engineers are deeply involved in creating novel materials and processes with the objective of finding real-world applications for these technologies.

Advanced Materials for Electronics aims to provide a forum for the exchange of knowledge of those materials - inorganic, organic, polymeric and biological - whose focus of interest is the emerging discipline of Information Technology in its broadest sense. Its purpose is to bring about the integration and interaction of the science and technology of advanced materials whose scope includes:

2. FUTURE FOR NANOMATERIALS

Current efforts are focused on exquisitely responsive materials for sensor applications, electro-optic materials for electronics and communication applications, and special composites for strong, lightweight materials and corrosion-resistant coatings. Sensor applications range from the detection of explosives at unprecedented levels of sensitivity, sensing of chemical warfare agents and toxic industrial chemicals through the use of highly selective chromo-pores, and the detection of organisms of concern in biological warfare, medical diagnostics, and food safety via a variety of probes and reagents.

In the field of electro-optic materials, the focus has been on finding practical applications for discoveries made by our scientists in collaboration with others. For example, it is exploiting the unique optical properties of micro-spheres and fiber coatings to control the flow of light within chemical sensors and optical fiber networks. In last time it has developed a new class of low-dielectric constant organic polymers for integrated circuit manufacture that promise-enhanced speed.

Current work with nano-particles is focused on the photo-luminescent properties of these materials for use in light-emitting diodes, radiation dosimeters, and medical imaging agents. We are also exploiting the physical properties of nano-materials, and carbon nano-tubes in particular, for the development of extremely strong, lightweight composites. Another nano-particle-based composite with great potential for widespread use is a new class of environmentally friendly corrosion-resistant coatings being developed for the Air Force.



Figure 1. – Different forms of raw material for material electronics.

Also it is using nano-materials to construct a matrix for tissue engineering, and current development efforts in this area promise to open entirely new opportunities in culturing artificial tissue. Finally, in the early-stage exploration of other applications for nano-materials, it is including shaped nano-particles and nano-wires.

Nowhere is the ability to produce new materials more crucial than in the electronics industry. Indeed, semiconductor device manufacturers pioneered many of the materials and processes now having an important impact in other industries. Materials used to process semiconductors and printed circuit boards as well as advances in areas such as diamond films and conductive polymers will shape the electronics industry in the coming years.

2. SOME EXAMPLES

Advanced semiconductor and circuit board manufacturing requires a long list of specialized and high purity materials.

For example, some new interesting subjects are:

- Ultra-pure materials for the semiconductor industry
- Advanced glasses and glass ceramics
- Rare earths
- Advanced ceramics, fine and nano-ceramic powders
- Optical coatings
- Magnetic materials
- Diamond
- Electronic polymers
- Sol gel
- Carbon products: fiber, foams and composites
- Switch able ferroelectric, electro-chromic and optical materials
- Iron and iron-oxide powders
- Nano-structured materials: electronic, magnetic and optoelectronic
- Plastics
- Semiconductor materials
- Nano-materials
- Doping materials for semiconductors.



Figure 2. Mitsubishi's Electronic materials.

For example Mitsubishi Materials can supply sputtering targets for the following applications: LSI, Magnetic Disk and Head, Magneto-Optical Disk, Optical Disk, Superconducting Thin Film, Protective Film and Precious Metal.

Table 1.

	<i>Application</i>	<i>Comments</i>
1	Large Scale Integration	Types = Al, Mo, W, Mo-Si, W-Si, Ti-Si, Ti, Ti-W, TiN all with 5N purity
2	Magnetic Disk & Head	Types = Co-Cr, Co-Ni, Ni-Fe, Permalloy, Supermalloy all with 3N purity; Cr with 2N8/3N5/4N5 purity; Co-Ta-Zr, Co-Nb-Zr ($\pm 5\%$ of each composition); Sendust (Fe-Al-Si) with any composition
3	Magneto-Optical Disk	Types = Tb-Fe, Tb-Fe-Co, Tb-Gd-Fe-Co, Nd-Dy-Fe-Co with negotiable composition
4	Optical Disk	Types = Te, Se, Sb, Te Alloy, Se Alloy, Sb Alloy, In-Alloy with negotiable composition ... more than 100 different compositions produced. Alloy elements are controlled within $\pm 0.5\%$.
5	Superconducting Thin Film	Types = La-Sr-Cu-O, Y-Ba-Cu-O, Bi-Sr-Ca-Cu-O; 3N purity; any composition is available
6	Protective Film	Types = SiO ₂ (5N purity) and Sialon (Si-Al-O-N)
7	Precious Metal	Types = Au (3N/4N/5N purity); Au-Si, Au-Ge, Au-Sn (4N purity) any composition available; Ag, Pd, Pt (3N/4N purity)

Mitsubishi Materials Corp. (MMC) is a provider of specially purified Pb and solders alloys. Low alpha materials are products whose alpha-ray counts have been reduced to approximately 1/100 ~ 1/1000 of their normal values. Alpha-ray emission is a known cause of soft errors in sensitive semiconductor memories.

MMC's production facility includes a special refining line, which removes significant amounts of "trace" materials and produce a very pure grade of Pb and Sn. Low alpha solder products from MMC have been used in the Japanese semiconductor industry for over 10 years. Since the beginning, MMC has retained statistical data on alpha measurements to provide analysis of lot-to-lot consistency and superiority over standard materials. Below is a comparison of lead products CPH (Alpha-ray counts per hour).

(cph/ cm²) – Table2.

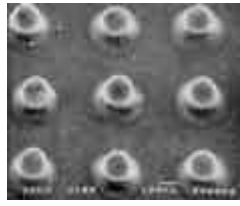
	LA		ULA		SULA	
	<i>Spec.</i>	<i>Actual</i>	<i>Spec.</i>	<i>Actual</i>	<i>Spec.</i>	<i>Actual</i>
Pb-Sn series	<1.0	0.3 ²	<0.02	0.01	-	-
Lead-Free	-	-	<0.01	0.005	<0.005	0.001

Low alpha solders in a variety of forms including foil, paste, liquid and balls. Lead free products are also available.

Special paste



Printability



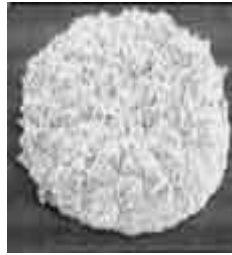
After re-flow

MMC's low alpha soldering paste is made with fine particles and has excellent printability. After re-flow the solder forms perfect bumps. The solder pastes is available in standard Pb-Sn and also lead free formulations.

Liquid



Bump from MMC solution



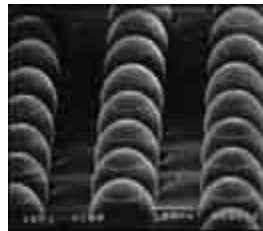
Conventional solution

Low alpha solder solution for flip chip use. The solution will create ideal bumps for the flip chip, being perfectly round in shape with a flat top as can be seen in the photos on the left.

Balls



LA/ULA solder balls



After mounting

Low alpha solder balls in various diameters from 0.10mm to 0.30mm, with very tight tolerances. The balls can be made in Pb-Sn, Sn-Ag or other formulations.

Gold Bonding Wire

With the continuing trend toward smaller circuits, we have continued in developing new types of wire to meet customer's requirements such as low loop, long loop, and higher strength fine wire. Magnetic garnet single crystals are used for the optical isolators that suppress or redirect backscattered or back-reflected laser light in optical communications. Optical waveguide are important devices that handle the divergence and convergence of signals sent through optical fibers in optical communications.

Anti-ferroelectric Liquid Crystal is a novel LC materials characterized by high-speed response and wide viewing angle. The LCD applied AFLC is capable of displaying complete moving images.

Electroceramic materials excel for many reasons.



Figure 3. Gold Bonding Wire.

Enormous strides have been made in microprocessor speed and memory density during the past few decades, but comparable developments in sensors and actuators have, in many cases, lagged considerably.

Many such devices remain bulky, consume substantial power, do not readily interface with electronics, and respond sluggishly. The effective integration of functional electroceramic materials into microelectronic and micro-electromechanical (MEMS) technologies remains a key challenge for this field.

The ability to harvest the benefits of miniaturization, low power, integration, and the ability to fabricate large arrays, will, however, pay major dividends in performance, versatility, speed, and reduced costs.

To appreciate the versatility of electroceramics and their potential use in smart systems, we summarize some of the key properties most commonly associated with sensing and actuating functions. For example, piezoelectrics such as $\text{Pb}(\text{Zr}_{1-x}\text{Ti}_x)\text{O}_3$ (PZT) are used to detect mechanical displacement electrically and inversely to induce mechanical displacements by applying electric fields.

Solid electrolytes, such as $\text{Zr}_{1-x}\text{Y}_x\text{O}_{2-x/2}$ (YSZ), are used potentiometrically to monitor the chemical state (oxygen activity) of an environment or to modify that state by electrochemically pumping oxygen into that environment. These and other examples that relate to transduction between electrical, optical, magnetic, and thermal forms of energy are summarized in Table 1.

Typical materials and applications are included in this table.

Table 3.

<i>Energy Transduction</i>	<i>Materials</i>	<i>Applications</i>
Electrical mechanical	$\text{Pb}(\text{Zr}_{1-x}\text{Ti}_x)\text{O}_3$ (PZT)	Positioner, optical tuner
Mechanical electrical		Igniter
Electrical chemical	$\text{Zr}_{1-x}\text{Y}_x\text{O}_{2-x/2}$ (YSZ),	Oxygen pump
Chemical electrical	SnO_2	Gas sensor
Electrical optical	LiNbO_3	Electro-optic modulator

Optical electrical	GaN	Light detector
Electrical magnetic	AB ₂ O ₄ spinel: A,B = Mn, Zn	Write head
Magnetic electrical	La _{1-x} Ca _x MnO ₃	Read head
Electrical thermal	SiC	Resistive heater
Thermal electrical	AB ₂ O ₄ spinel: A,B = Mn, Ni, Fe, Co, Cu	NTCR thermistor
	BaTiO ₃ perovskite	PTCR thermistor

In the microelectronics industry, *piezoelectric motors* or stacks enable mask positioning in the submicron range.

Similar positioning systems are used in electron microscopy and *atomic force microscopy* (AFM) to control stage movements of 10–100 nm.

In AFM, for example, the position of the micro-cantilever beam relative to the substrate is detected optically by reflecting a laser beam off the micro-cantilever beam and measuring its movement by using position-sensitive photo-detectors.

Thus, the feedback loop involves an optical sensor, computer, and piezoelectric actuator.

3. CONCLUSIONS

These examples about advanced materials are at the base of other new materials, and the nanoscience can be offers

Consumer applications include *camera lens controllers* and video camera stabilizers.

Auto-focus camera lenses now contain built-in piezoelectric ultrasonic motors.

These motors operate in a feedback mode and reposition the optical components in the lens to achieve fast and accurate auto-focusing.

Some manufacturers use piezoelectric sensors to sense *video camera vibrations*. Two piezoelectric velocity sensors respond to the camera's movement along its vertical and horizontal axes.

The sensors control motors that realign a prism that bends the light to compensate for vibrations.

In each period there are many transformations of the strategies, thus about some advanced materials and technologies for electronics can be show many interesting things, and about these applications.

REFERENCES

- [1]. Haertling, G.H. in *Ceramic Materials for Electronics*, R.C. Buchanan, ed., Marcel Dekker, NY, 1991. pp. 129–202.
- [2]. Hill, D.C. and H.L. Tuller, in *Ceramic Materials for Electronics*, 2nd ed., R.C. Buchanan, ed., Marcel Dekker, NY, 1991, pp. 249–347.

- [3]. Kuwabara, M., in *Additivies and Interfaces in Electronic Ceramics*, M.F. Yan and A.H. Heuer, eds., *Advances in Ceramics*, Vol. 7, American Ceramic Society, Columbus, OH, 1983, p. 128.
- [4]. Mnerie, D., *Electroceramic materials*, - Răduță, A., Nicoară, M., Berta, Laura, Firu, Carmen, *Advanced materials*, Ed. Orizonturi Universitare, Timișoara, 2002, pp.203-230.
- [5]. Moulson, A.J. and J.M. Herbert, *Electroceramics Materials, Properties, Applications*. Chapman and Hall, 1990.
- [6]. Tuller, H., *Encyclopedia of Smart Materials*, Massachusetts Institute of Technology, Cambridge, M.A. Ytshak Avrahami, Massachusetts Institute of Technology, Article Online Posting Date: July 15, 2002.

Received december, 15 2005

¹POLITEHNICA University, Timișoara, Faculty of Mechanics

CATEVA MATERIALE SI TEHNOLOGII AVANSATE DESTINATE ELECTRONICII

REZUMAT. Materialele avansate sunt in atentia stiintei materialelor, cu un factor mare de impact pentru orice domeniu de activitate.

In general, materialele avansate pot fi: semiconductori, materiale optice, (liniare si non-liniare), sticle, materiale fotoactive, materiale pentru laser, materiale luminescente, materiale foto-cromatice si electro-cromatice, ceramicile, care includ semiconductoare rezistente la temperaturi inalte, materiale magnetice, solide de dimensiuni mici, polimeri, materiale biologice, fluide electro-reologice, cristale lichide, electrozi modificati chimic, rezistente, conductori metalici.

Lucrarea prezinta cateva aspecte ale prezentului si perspectivei de dezvoltare a electroceramicelor.

THE EFFECT OF COOLING BELOW 0°C ON STRUCTURE AND HARDNESS OF BEARING STEELS

BY

ADRIAN ALEXANDRU¹, SORIN IACOB STRUGARU¹, IOAN ALEXANDRU¹,
MIRELA GHEORGHIAN²

ABSTRACT: *The paper presents the influence of thermal treatments at temperature below 0°C on phasic composition and hardness of bearings steels 100Cr6 and 100CrMnSi6-4 SREN ISO 683-17: 2002, the equivalents of steels RUL 1 and RUL 2 – STAS 1456-89.*

After application of these thermal treatments, the quantity of residual austenite decreases, the submicronic dimensional carbides density increases and the hardness increases with positive influences above durability of bearings.

KEYWORDS: *bearings steel, thermal treatment below 0°C, residual austenite*

1. INTRODUCTION

The construction of bearings is confronting at this moment with new demands concerning the dimensional stability, noise level and durability. All of these are ensured by the presence of a small quantity of residual austenite, of a very fine carbides and a fine martensite in important quantity. The structure which presents such conditions it may be obtained only by application of some unconventional processing: quenching below 0°C, quenching in ultrasonic or magnetic field, thermo-mechanical treatments etc.

These qualities of final structure cannot be obtained only if the initial structure obtained after the thermal treatment of normalising and annealing (800°C/3h, cooling and maintaining at 700-720°C/4h; slow cooling in oven) is formed by fine and homogeneous globular perlite.

The parameters of classic quenching and tempering and the quantity of residual austenite depending on initial structure of 100Cr6 and CrMnSi6-4 bearing steel are presented in table 1.

We can say that by classic thermal treatments the smallest quantities of residual austenite (11.3÷13.6%) are obtained after the application of some variants of thermal treatments V or VI which ensures in structure the fine and homogeneous globular pearlite.

Continuously cooling in oil at -30°C or -60°C results a phasic constitution optimum for the properties of exploitation of bearings.

The bearings treated below 0°C it sale with attractive prices thanks to the destination of devices or machines which contains rotating organs. Such destinations may be the device and machines which must ensure the security of humans in trains, plains, spaceships; devices which works in polar zones etc.

Table 1

Steel	Initial state	Lamellar pearlite (I)	Fine globular pearlite (II)	Partial unglobulizate pearlite (III)	Inhomogeneous globular pearlite (IV)	Homogene globular pearlite (V)	Fine globular pearlite normalized (VI)	
100Cr6	Quenching	Admitted interval ($^{\circ}\text{C}$)	820-830	810-860	810-830	810-850	810-835	810-840
		Optim interval ($^{\circ}\text{C}$)	-	810-840	-	-	820-830	820-830
		Maintaining time (min)	15	15-30	15-30	15-30	15-30	15-30
	2h($^{\circ}\text{C}$)Tempering	180-200	180-200	180-200	180-200	180-200	180-200	
	Corresponding AR (2h at 180°C after tempering) (%)	16.6-17	11.6-15.2	13-14.2	11.5-14.4	11.3-13	12-15.5	
CrMnSi6-4	Quenching	Admitted interval ($^{\circ}\text{C}$)	800-830	800-850	-	-	810-840	800-830
		Optim interval ($^{\circ}\text{C}$)	-	820-830	-	-	-	-
		Maintaining time (min)	15-20	15-20	-	-	15-20	15-20
	2h($^{\circ}\text{C}$)Tempering	180-200	180-200	-	-	180-200	180-200	
	Corresponding AR (2h at 180°C after tempering) (%)	18.8-20	17-20	-	-	15.6-19.2	13.2-17	

Technical literature in this domain appreciate that the implementation of thermal treatment below 0°C processing will increase the cost price with 13%, but this increase is covered by the demands of the market.

2. EXPERIMENTAL PROGRAMME

The research were made on rings of bearings by two alloyed steels for bearings with chemical composition determinate which is presented in table 2.

Table 2

Chemical composition (%)								
Steel (SR EN ISO 683-17)	C	Si	Mn	P	S	Cr	Mo	Others
100Cr6	0.93	0.15	0.25	0.025	0.015	1.35	Max.0.1	Al

	1.05	0.35	0.45			1.6		Max.0.05
determination	0.98	0.30	0.36	0.018	0.014	1.45	-	
100CrMnSi6-4	0.93-	0.45-	1.00-			1.40-		-
determination	1.05	0.75	1.20	0.025	0.015	1.65	Max.0.1	
	1.00	0.51	1.15	0.015	0.010	1.48	-	

The bearings elements were thermally treated by the variants given in table 3.

Table 3

Thermal treatments variants	Technological parameters
A	Quenching at 840 ⁰ C in oil at 60 ⁰ C, tempering at 190 ⁰ C/3h
B	Quenching at 840 ⁰ C in oil at 60 ⁰ C, cooling at -30 ⁰ C, tempering at 170 ⁰ C 1.5 h
C	Quenching at 840 ⁰ C in oil at 60 ⁰ C, cooling at -60 ⁰ C, tempering at 170 ⁰ C 1.5 h

The samples thermal treated by these variants were investigated by optical microscopy X rays diffraction and Rockwell hardness determination.

3. EXPERIMENTAL RESULTS

Microscopically researches were made on an optical microscope Neophote 21 at 500:1 magnification after the attack with natal 3% reactive.

The structure of the researched bearings steels after the primar thermal treatment of normalizing and globulization annealing is presented in figure 1, a,b were can be observed the globular pearlite which is fine and homogene in the two steel.

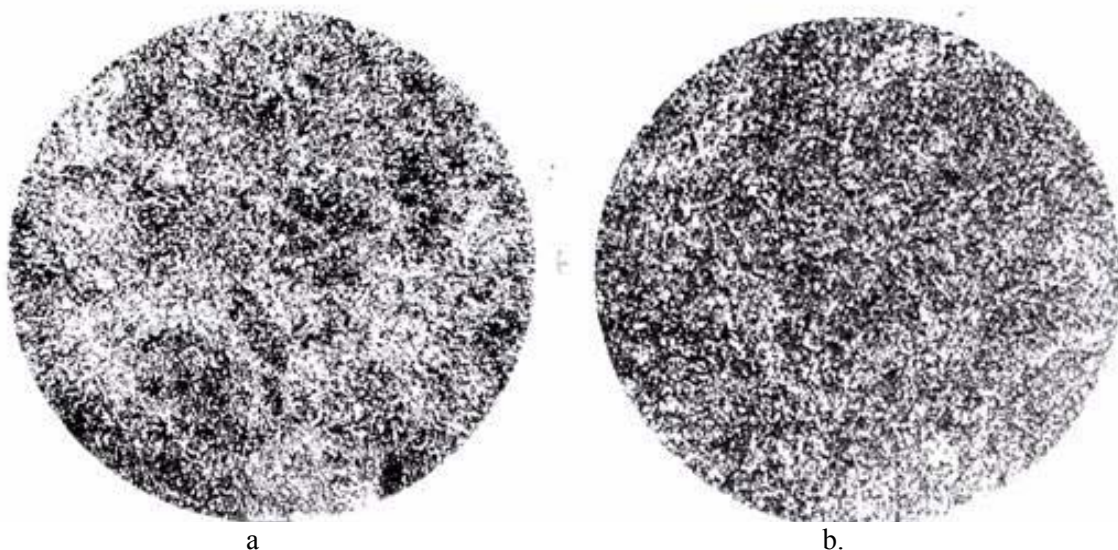


Fig. 1. The structure of 100Cr6(a) and 100CrMnS6-4 (b) after the globulization annealing (500:1)

The bearings steels structures after classic quenching and tempering (A variant) is formed by martensite very fine, residual austenite and carbides, as is presented in figure 2, a, b.

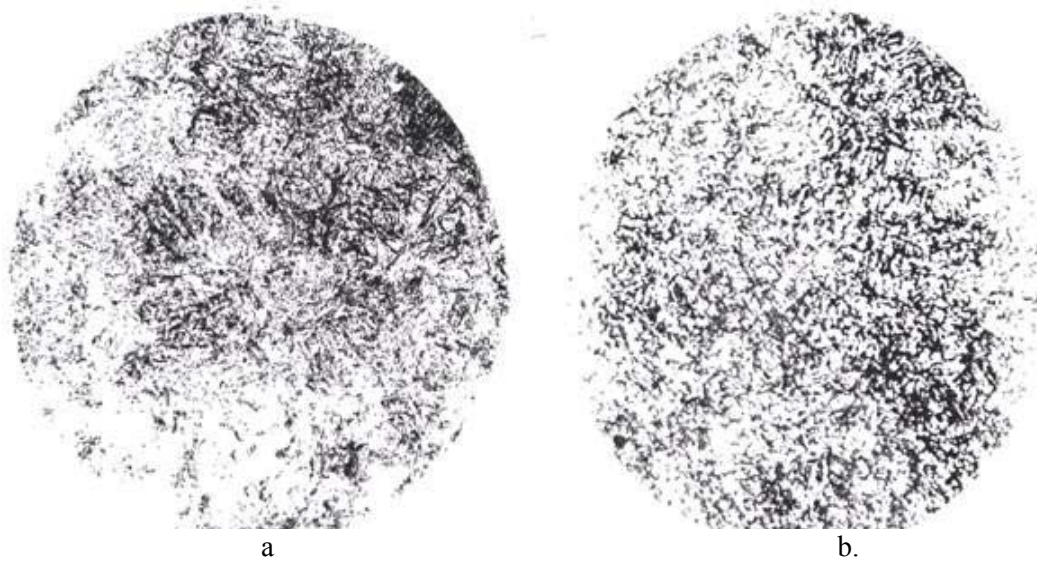


Fig. 2. The structure of 100Cr6(a) and 100CrMnS6-4 (b) after quenching in oil and tempering 500:1

The structures of bearings steels after cooling at -30°C and -60°C and tempered at 170°C are formed by very fine martensite, small quantities of residual austenite and carbides with small dimensions as is presented in fig. 3 a, b and 4 a,b.

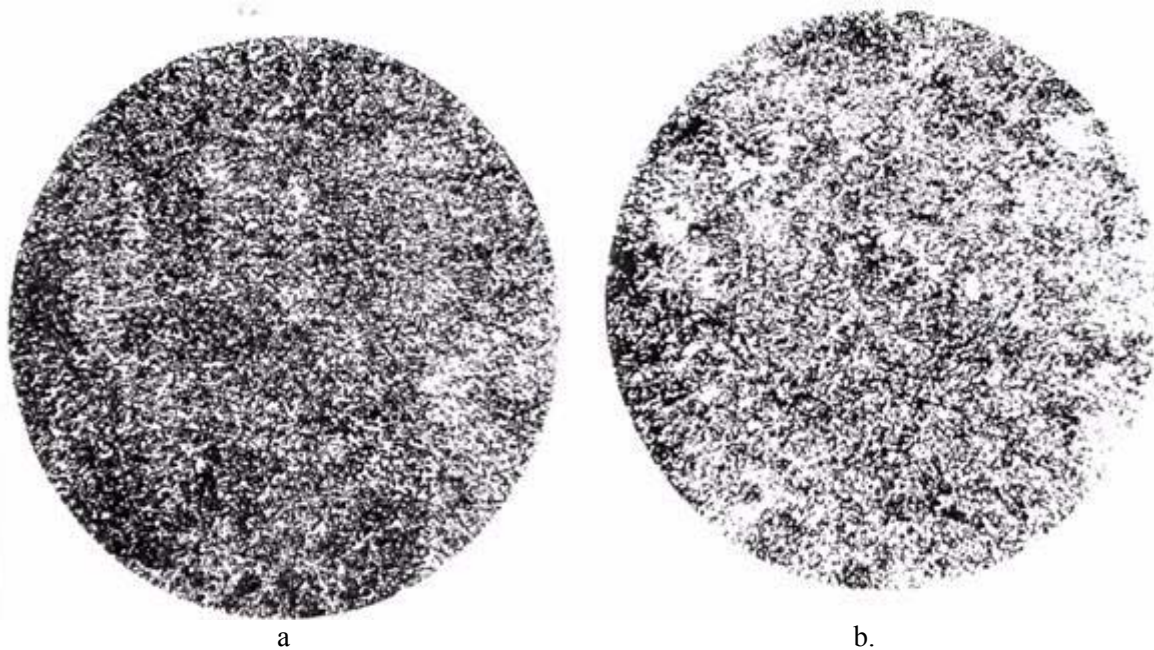


Fig. 3. The structure of 100Cr6(a) and 100CrMnS6-4 (b) after cooling at -30° and tempering 500:1

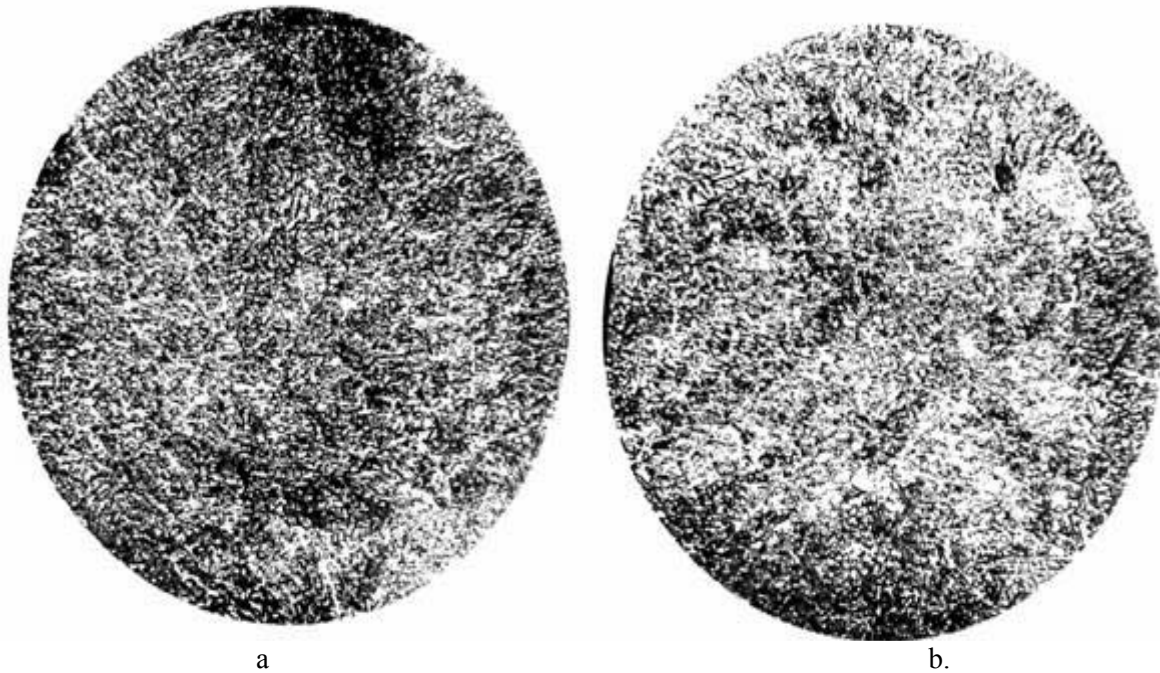


Fig. 4. The structure of 100Cr6(a) and 100CrMnSi6-4 (b) after cooling at -60°C and tempering 500:1

The value of hardness and quantities of residual austenite (AR) diffractographic determined on the bearings steels are presented in table 4.

Table 4

Steel	Quenching					Tempering			
	Heat temp. ($^{\circ}\text{C}$)	Time (min.)	Cooling Temp./ Maintain temp. ($^{\circ}\text{C}$)	HRC	AR(%)	Heat temp. ($^{\circ}\text{C}$)	Maintain Time (min)	HRC	AR (%)
100 Cr 6 (RUL 1)	840	30'	oil 60°	63	16.5	190	3 h	61	9.85
	840	30'	$-30^{\circ}/30^{\circ}$	64	7.38	170	1.5 h	63.5	6.28
	840	30'	$-60^{\circ}/30^{\circ}$	66	6.13	170	1.5 h	64	4.08
100CrMnSi6-4 (RUL 2)	840	30'	oil 60°	63	20.98	180	3 h	62	17.80
	840	30'	$-30^{\circ}/30^{\circ}$	65	12.8	170	1.5 h	64	7.13
	840	30'	$-60^{\circ}/30^{\circ}$	66	10.18	170	1.5 h	64	6.74

It see that with the increasing of cooling temperature at -30°C and -60°C the quantity of residual austenite decrease from 9.85%, at 6.38%, respective 4.08% for the 100Cr6 steel and from 17.8% at 7.13% respective 6.74 for 100CrMnSi6-4 steel and the hardness increase from 61 HRC at 64 HRC.

4. CONCLUSIONS

By application of thermal treatments at temperatures below 0°C in the bearings steels takes place important phasic modifications - decrease the quantity of residual austenite, increase the density and uniformity of the small dimensional carbides (0.001 mm).

These structural modifications determine the increase of hardness and in the end the increase of bearings fiability.

REFERENCES

1. Gary Jeff – Cryogenic Treatment of Steel. University of Texas of Austin, Department of Mechanical Engineering, Spring, 1999.
2. Carlson Earl – Cold Treating and Cryogenic Treatment of Steel. ASM Handbook, vol. 4, Heat Treating, 1991.
3. Alexandru Ioan, Balancea Vasile- Effect of Cryogenic Cooling on Residual Stresses, Substructure, cap. 26, Handbook of Residual Stresses and Distortion of Steel, U.S.A., 2002.

Received January, 11 2006

*¹Technical University “Gh. Asachi” Iasi;
²Bacau University*

EFFECTUL RACIRII LA TEMPERATURI SUB 0⁰C ASUPRA STRUCTURII SI DURITATII OTELURILOR PENTRU RULMENTI

REZUMAT: Lucrarea prezinta influenta tratamentelor termice la temperaturi sub 0⁰C asupra compozitiei fazice si duritatii otelurilor de rulmenti 100Cr6 si 100CrMnSi6-4 SR EN ISO 683-17 :2002 echivalentul otelurilor RUL 1 si RUL 2 – STAS 1456-89.

In urma aplicarii acestor tratamente termice cantitatea de austenita reziduala scade, densitatea carburilor cu dimensiuni submicronice creste si duritatea se mareste cu efecte pozitive asupra durabilitatii rulmentilor.

**THE STUDY OF DEGRADATION THROUGH AGEING OF THE
THERMORESISTENT STEELS 13CRMO4-5 USED IN THE TUBULATURE
OF THE LIVE STEAM IN THERMO-ELECTRIC POWER STATIONS**

BY

**ALEXANDRU IOAN¹, ALEXANDRU ADRIAN¹, IACOB STRUGARIU SORIN¹, BACIU
MARIA¹**

***ABSTRACT:** The paper deals with the stage of thermoresistent steels 13CrMo4-5 degradation, as a result of utilization in exploitation at 565 °C for 10⁵ hours in the tubulature of live steam, in Borzesti thermo-electric power station. The structural analysis and mechanical tests are made comparatively with the delivery conditions and with the values prescribed in standards. It has been found that the steel exploitation at work temperature did affect neither the structure nor the mechanical properties*

***KEYWORDS:** thermoresistent steel, live steam ducts, ageing process.*

1. INTRODUCTION:

The thermoresistent steels are carbon steels or allied with manganese, chrome-molybdenum, silicon-manganese or vanadium-molybdenum-chrome, realized in shape of tubular and flat products, and used in the -20...+640 °C temperature range, corresponding to the technical requirements imposed and supervised by ISCIR.

The main utilization characteristics are the mechanical resistance and the tenacity. Great importance for these steels has the influence that they have over the main utilization characteristics, the aggressive environment actions, the mechanical tensions, the temperature and the time.

The mechanical resistance depends mainly on alloying degree with chrome and molybdenum, and on the applied thermal treatment. The increase of mechanical resistance is possible through the alloying of ferrite, in presence of fine dispersed carbides, especially Mo₂C precipitated at 450...600 °C and through the decrease of ferrite amount in the structure. The resistance to rupture of these steels is between 400 and 640 N/mm².

The flow limit is 175...590 N/mm² at ambient temperature and decrease at 100...200 N/mm² when the assay temperature rise until 450...500 °C. This assay temperature becomes important if the steels are used at moderate temperatures or short periods, when the creep does not interpose. At higher temperatures or exploitation periods, when the creep interpose, keeping the resistance and the flow limit at the utilization values depends on steels structural stability, especially determined by the resistance opposed at the molybdenum carbides, chrome-molybdenum carbides and

molybdenum-vanadium-wolfram carbides.

The steels tenacity has higher values, to avoid the fragile fracture during a long exploitation at high temperatures (370...600 °C). The warm brittleness of the steels allied with molybdenum or molybdenum-chrome is caused by the hardening of metallic matrix through precipitation with carbides of type M_2C . The brittleness appears especially in the thermal influenced area of the weld or at the ex-austenitic grains boundary, where the compounds rich in carbon precipitate or where impurities segregate. The brittleness is produced at temperatures below the creep appearance temperatures, when is named reversion creep and determines the decrease of the resilience with 25%, and at the creep appearance temperatures (the creep brittleness), when produces both the decrease of brittleness and the elongation at creep rupture.

2. THE RESEARCH METHOD

The researched steel is a thermoresistent steel used for under pressure equipments, with the mark: 13CrMo4-5 – SREN 10028: 1996, respectively 12MoCr22 – SMG 2883-88. The steel results from a tube section, which worked at 565 °C temperature and at 28 Barr pressure. The test-bar has been subdued at the investigations prescribed through ISCIR C29-82 standards: the compositional analysis, the micrographic analysis in longitudinal and transversal section, the mechanical tests – the breaking resistance (R_m), the flow limit ($R_{p0.2}$), the elongation (A_5), the constriction (Z), Brinell hardness.

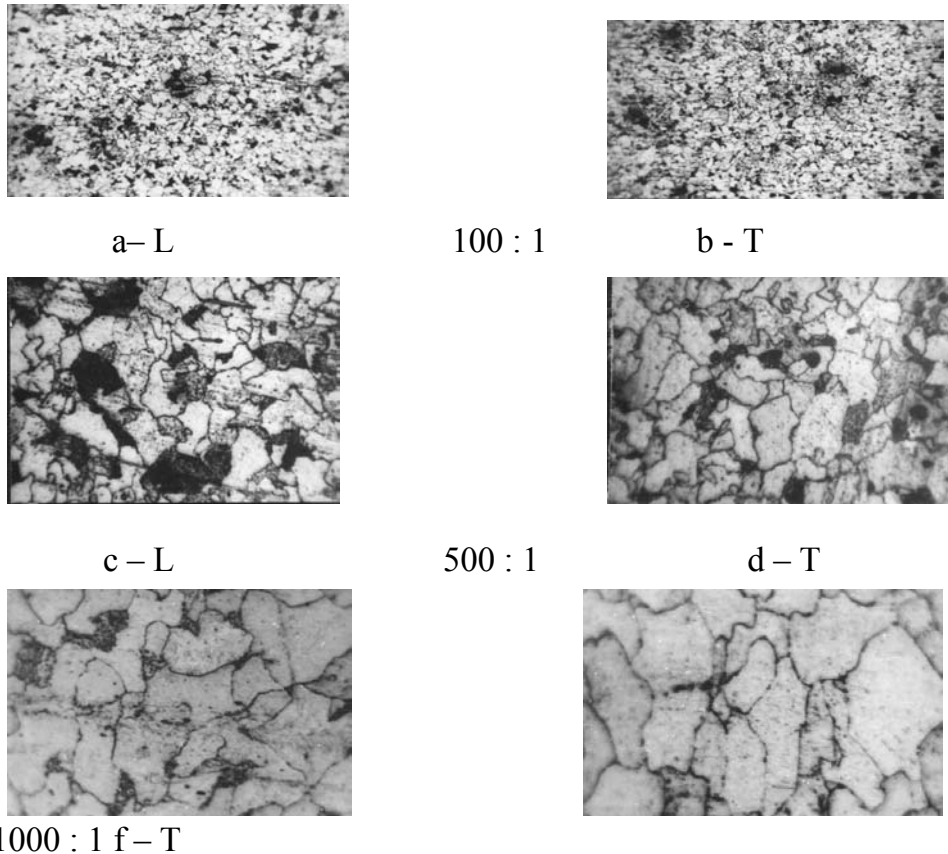
Experimental results: The chemical analysis, spectrographically determined, is presented in table 1 and frames the steel in mark 13CrMo4-5.

Table 1

Source	Chemical composition, %									
	C	Si	Mn	Cr	Ni	Mo	V	Cu	S	P
Test-bar	0.11	0.25	0.6	2.1	0.1	0.95	0.2	0.15	0.027	0.027
prescribed	<u>0.08</u> 0.15	<u>0.15</u> 0.5	<u>0.3</u> 0.6	<u>4.0</u> 6.0	-	<u>0.9</u> 1.1	-	-	0.03	0.035

The micrographic analysis: Is made on transversal and longitudinal surfaces, on an optical microscope Neophat 21 at: 100:1, 500:1 and 1000:1 magnification, after chemical attack with nital 3%, with the purpose of pointing out the carbides precipitation process at the grains boundaries.

The analyzed steel presents a ferrite-perlite polyhedral structure, with a reduced amount of perlite, with grains uniform as size (8/9 score). There are not pointed out decarburizations or small precipitations of chrome and molybdenum carbides. The amount of insular or intergranular carbides is reduced (which are pointed out only at 1000:1 magnification), figure 1a, b, c, d, e, f. From the structural point of view, the steel used at 565 °C temperature at 28 Barr pressure and for 10^5 hours, is not deteriorated. *Mechanical tests* are made on normal test-bars, subdued from the tube wall thickness, on longitudinal and transversal direction at 20 °C, 510 °C, 540 °C, 565 °C, and 580 °C temperatures.



e – L 1000 : 1 f – T

Figure 1. The micrographics of 13CrMo4-5 steel used at 565°C for 10⁵ hours.

The mechanical resistance values (R_m), elongation (A_5), flow limits ($R_{p0.2}$), constriction (Z), resilience (KCU), Brinell hardness (HB), are presented in table 2 and the variation of these properties with the test temperature is presented in figure 2.

Table 2.

Characteristic	Section	Work temperature, °C				
		20	510	540	565	580
R_m , daN/mm ²	T	50.9	45.45	38.11	36.9	34.94
	L	50.08	40.96	36.96	35.3	34.6
$R_{p0.2}$, daN/mm ²	T	34.02	31.36	30.86	30.45	26.3
	L	39.21	30.44	29.32	26.06	26.02
A_5 , %	T	25.4	26.0	27.1	26.8	27.0
	L	25.1	26.8	26.0	27.1	27.4
Z , %	T	65.05	67.17	77.41	81.2	83.95
	L	78.11	81.95	84.2	86.3	87.61
HB	T	164.75	162.27	141.24	119.16	115.38
	L	173.06	157.42	140.26	115.34	102.05
KCU, daJ/cm ²	T	16.7	14.2	11.9	11.3	10.4
	L	34.6	24.7	23.4	21.5	18.1

It has been ascertained that the values of mechanical properties determined at 20 °C temperature are superior to the values indicated in standards, and once with the increase of test temperature, the values of resistance properties (R_m , $R_{p0.2}$, HB, KCU) decrease continuously, and the tenacity properties (A_5 , Z) increase continuously. It results that the variations of mechanical properties with the temperature is framed into the general behavior of the thermoresistent mild-allied steels.

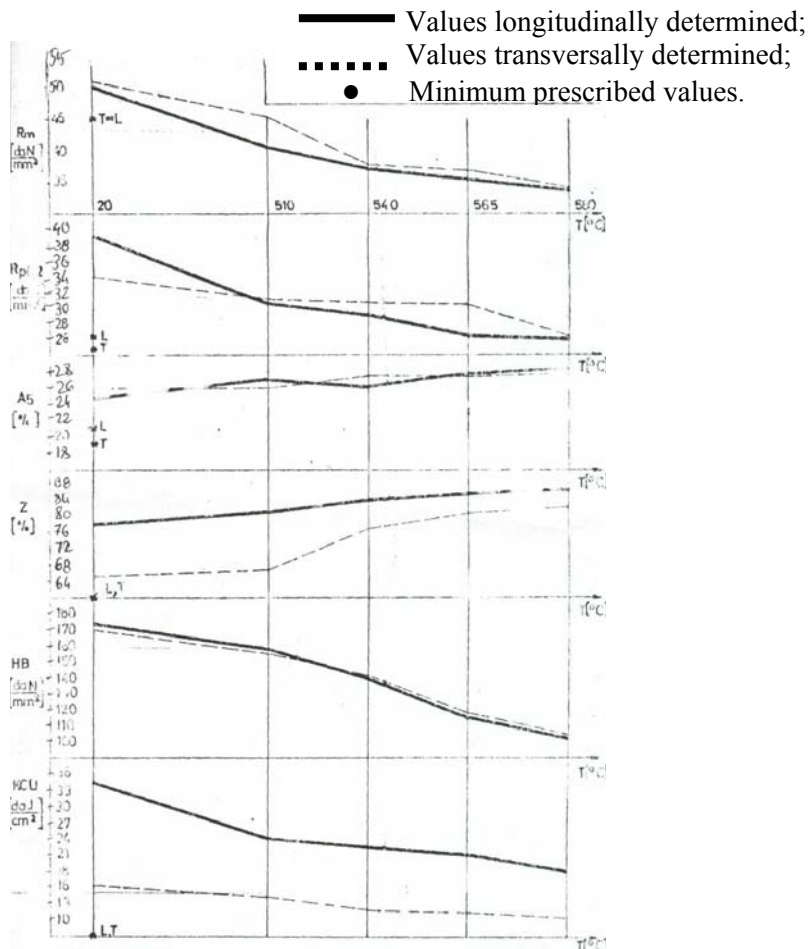


Figure 2. The mechanical properties variation with the test temperature.

3. CONCLUSIONS

The researches pointed-out the fact that the thermoresistent mild-allied steel 13CrMo4-5 SREN 10028: 1996, exploited in live steam ducts in thermo-electrical power stations at 565°C temperature, 28 Barr pressure and for 10^5 hours, is not degraded from the structural point of view and from the mechanical properties values point of view, and the fact that the steel could be maintained in exploitation.

REFERENCES:

1. **Baciu C-tin, Alexandru Ioan** – “Știința materialelor metalice”, E.D.P. București, 1996.
2. **Alexandru Ioan, s.a.** – “Alegerea și utilizarea materialelor metalice”, E.D.P. București, 1997.
3. **Baciu C-tin, Alexandru Ioan** – “Studii asupra stadiului transformărilor structurale ale materialelor tubulaturii de abur la cazane din termocentrale”, Comitet de cercetare, 1990.

Received January, 10 2006

¹Technical University “Gh. Asachi” – Iasi.

STUDIUL DEGRADĂRII PRIN ÎMBĂTRÂNIRE A OTELULUI TERMOREZISTENT 13CRMO4-5 FOLOSIT ÎN TUBULATURA DE ABUR VIU A TERMOCENTRALELOR ELECTRICE

REZUMAT: Lucrarea tratează stadiul degradării oțelului termorezistent 13CrMo4-5 în urma utilizării în exploatare la 565°C timp de 10^5 ore în tubulatura de abur viu în termocentrala electrică de la

Borzesti. Analizele structurale si incercarile mecanice s-au facut comparative cu starea de livrare a otelului si cu valorile prescrise de standarde. S-a constatat ca exploatarea otelului la temperatura de lucru nu a afectat nici structura si nici proprietatile mecanice.

DÉVELOPPEMENT DURABLE DES SYSTÈMES DE PRODUCTION. L'INTÉGRATION DE L'ERGONOMIE ET DE LA PREVENTION DANS UN PROJET DE CONCEPTION D'UNE ALUMINERIE

PAR

CONSTANTIN BACIU¹, IOAN ALEXANDRU¹, SILVIA GEORGESCU¹

RÉSUMÉ: *Cet étude a été réalisée afin de reconstituer l'activité d'un ergonome qui, de concert avec deux spécialistes en prévention, a mis en place une démarche originale pour intégrer l'ergonomie et la santé-sécurité (SST) dans un projet de construction d'une aluminerie. Les cinq stratégies d'intervention identifiées ont permis aux spécialistes d'influencer la conception des situations de travail, d'éliminer un grand nombre de risques à la source et de concevoir le programme de prévention avant le démarrage de l'usine..*

MOTS CLÉS: *développement durable; ergonomie de conception; ergonomie et prévention, sécurité et santé du travail (SST).*

1. INTRODUCTION

L'idée que le développement durable des systèmes de production passe, entre autres, par l'intégration de l'ergonomie et de la SST dans toutes les phases de leur conception est admise en ergonomie depuis plus de vingt ans. Mais les moyens de réaliser et réussir une telle intégration restent à développer. La recherche peut y contribuer en produisant des connaissances sur les stratégies et les outils utilisés dans des situations concrètes par des praticiens. Celle présentée ici se situe dans cette lignée.

Elle a consisté à reconstituer l'activité de l'ergonome qui, de concert avec deux spécialistes en prévention, a été impliquée dans le projet de conception d'une aluminerie et à tirer des enseignements généraux de cette étude de cas, entre autres, en matière de gestion des projets et des organisations.

2. MÉTHODOLOGIE

La recherche a bénéficié des acquis d'un programme plus large qui, par la modélisation des pratiques d'ergonomes et de spécialistes en prévention oeuvrant en correction comme en conception, vise entre autres à améliorer leurs outils d'intervention et leur contexte de travail. À ce jour, cinq recherches ont été réalisées dans le cadre de ce programme (Lamonde, Beaufort, & Richard, 2002). Des généralisations ont été dégagées de chacune en mettant à profit la littérature sur la pratique professionnelle, l'intervention et la conduite de projet (ingénierie simultanée, sociotechnique, *Total Quality Management*, ergonomie de conception). Des recherches du même type sont menées dans des disciplines variées comme l'architecture,

l'éducation, l'urbanisme et l'ingénierie.

En ce qui a trait à l'étude présentée ici, elle couvre les phases du projet allant du préconcept à l'ingénierie détaillée (graphique 1). L'activité des trois intervenants a été reconstituée *a posteriori* à partir de 37½ heures d'entretiens enregistrés et retranscrits réalisés avec eux et avec six de leurs interlocuteurs dont les chefs des équipes projet et exploitation (décrites plus loin). Ces entretiens ont été menés suivant une méthodologie inspirée du courant théorique de l'action située : nous avons cherché à documenter la signification des actions et des communications des intervenants de leur point de vue, ici et maintenant. Une démarche analytico-régressive a permis d'identifier leurs stratégies, des structures significatives autour desquelles s'organise la cohérence de leurs actions. Les résultats de l'analyse de l'activité ont été validés par les intervenants, comme il est d'usage de le faire en ergonomie.

1996		1997	1998	1999	2000	2001-2002
Préconcept	Concept	Ingénierie préliminaire	Ingénierie détaillée	Appels d'offre et construction	Vérifications pré-opérationnelles	Démarrage

Graphique 1: Phases du projet avec, en gris, celles couvertes par l'étude

3. RÉSULTATS

Le travail des intervenants, déterminé par les caractéristiques tant du projet que de l'entreprise, a permis d'obtenir des résultats à la fois positifs et négatifs. Un des cinq stratégies mises en œuvre est détaillée afin d'illustrer comment les éléments de contexte favorables et défavorables à la prise en compte de la SST et de l'ergonomie dans la conception ont été identifiés.

Le contexte de travail de l'ergonome et des deux spécialistes en prévention

La conception de l'aluminerie exigeait d'innover techniquement, mais aussi de concevoir une usine respectant les valeurs fondamentales de l'entreprise en matière d'ergonomie, de SST, de protection de l'environnement et de gestion des ressources humaines. Une équipe projet et une équipe exploitation ont conduit les travaux, en invitant entre autres les spécialistes en ergonomie et en SST dont l'activité a été étudiée.

L'équipe projet et de conception

Au préconcept, le directeur du projet a nommé son équipe: neuf responsables décisionnels du processus d'ingénierie d'un secteur de l'usine (centre d'électrolyse, des anodes, de coulée, etc.) et un spécialiste en environnement, hygiène industrielle et sécurité, pour les influencer. Il devait faire respecter le budget temps du projet, formaliser les spécifications techniques et piloter l'ingénierie réalisée à l'externe. Au cours des phases étudiées, des liens contractuels ont été établis avec 7 firmes externes pour répondre aux besoins en ingénierie, en architecture et en gérance du projet. Deux millions d'heures d'ingénierie ont été nécessaires et de 700 à 1000 concepteurs (ingénieurs, techniciens, etc.) ont travaillé à la définition détaillée de l'usine.

L'équipe exploitation

Fait remarquable, le directeur de la future usine a été nommé en même temps que le chef de projet afin d'influencer la conception.

Pour ce faire:

- 1) il s'est adjoint les services d'un ergonome au préconcept;

2) du préconcept à 50% de l'ingénierie préliminaire, il a créé un groupe témoin par sous-secteur de la future usine, chacun réunissant des utilisateurs (ingénieurs, techniciens, etc.) des usines existantes, afin de tirer profit de leur expérience;

3) il a nommé un préventionniste, à 50% de l'ingénierie détaillée pour voir à ce que les choix de conception facilitent la gestion de la prévention dans la future usine ;

4) à l'ingénierie détaillée, il a constitué la future équipe de direction (groupes de pilotage) pour qu'elle «apprenne» la nouvelle usine pendant sa conception, un rôle qui l'a aussi poussé à questionner et à influencer l'équipe projet.

Des outils et des compétences disponibles au départ

Au démarrage du projet es intervenants disposaient:

1) d'une politique d'entreprise plaçant les enjeux d'ergonomie et de SST au premier plan;

2) d'une méthodologie de conduite des projets obligeant la tenue de revues critiques SST par les concepteurs afin d'identifier les risques, en mettant à contribution, au besoin, le personnel d'exploitation et des spécialistes (en SST, en ergonomie, etc.);

3) d'un processus de pré qualification des entrepreneurs réservant le droit de soumissionner à ceux qui respectent certains critères relatifs, notamment, à l'ergonomie et à la SST et donc d'un bassin d'entrepreneurs de la région connaissant les pratiques de l'entreprise dans ces domaines;

4) d'un bassin d'ingénieurs, de techniciens et autres, oeuvrant dans les usines en exploitation et ayant reçu des formations de base en ergonomie et en SST et travaillé en collaboration avec des spécialistes de ces domaines.

Les résultats positifs et négatifs obtenus

Les intervenants ont contribué à diminuer de beaucoup la présence de risques dans les milieux de travail. En effet, leur travail a mené à l'identification de 3108 risques majeurs, dont 2051 ont été éliminés et 497 ont été diminués au stade de l'ingénierie. De plus, la gestion des 1057 risques résiduels a pu être planifiée dans le programme de prévention avant le démarrage de la nouvelle usine. Ils ont par ailleurs contribué à améliorer le processus global d'ingénierie.

Ainsi, une banque de données sur les risques identifiés a aussi été conçue pour aider l'équipe exploitation à retrouver à tout moment les plans d'ingénierie. De plus, tout en aidant à identifier des risques, l'ergonome a ciblé des équipements non nécessaires aux opérations.

Cependant, des gains plus importants auraient pu être obtenus puisque:

1) 1057 risques, pourtant identifiés au stade de l'ingénierie, n'ont pas été éliminés et devront de ce fait être gérés pendant tout le cycle de vie de l'usine;

2) les risques mineurs n'ont pas été traités;

3) la conception de certaines parties de l'usine n'a pu être suivie;

4) des risques n'ont été identifiés qu'au démarrage de l'usine;

5) les problèmes d'utilisation générant de l'inefficacité sans pour autant générer des risques SST n'ont pas été systématiquement identifiés, l'ergonomie ayant été utilisée comme une technique d'identification des risques SST, ce qu'elle n'est pas.

L'activité des trois intervenants

Ces résultats sont liés à la mise en place de quatre principaux moyens (graphique 2):

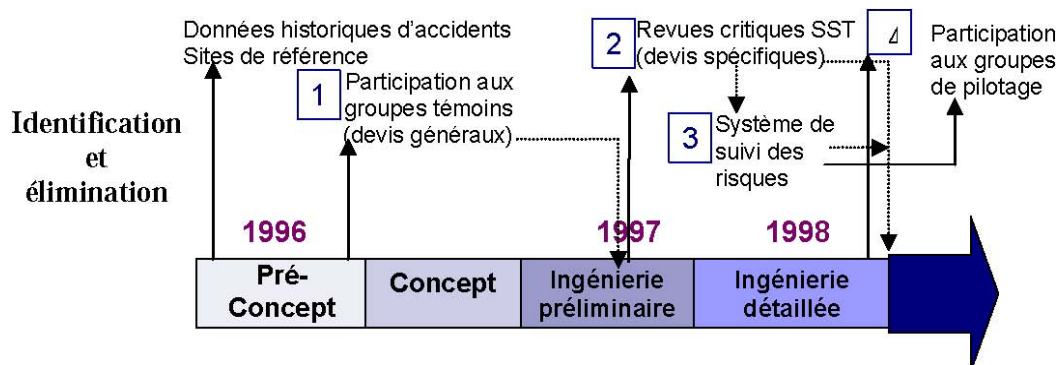
1) le recours à des données d'accidents et à des études ergonomiques (données des usines en exploitation et visites de sites de référence) pour alimenter les réflexions

des groupes témoins et influencer les devis généraux;

2) l'insertion dans la programmation du projet et la réalisation de revues critiques pour influencer les devis spécifiques;

3) la conception d'un système de suivi des risques pour assurer la réalisation effective des modifications et pour préparer le programme de prévention avant le démarrage de l'usine;

4) la participation aux groupes de pilotage pour continuer d'influencer la conception après l'ingénierie détaillée.



Graphique 2 : Tâches effectuées pour identifier et éliminer les risques en cours de conception

Derrière ces outils concrets se cachent cinq principales stratégies d'intégration déployées tout au long du projet: avancer pas à pas; s'ajuster aux exigences de l'ingénierie; légitimer les actions en SST et en ergonomie; mettre les choix de conception à l'épreuve de la logique d'utilisation; et construire une mémoire de leurs actions.

Ces stratégies sont détaillées dans Lamonde, Beaufort, & Richard (2002); une brève illustration est proposée ici.

«S'ajuster aux exigences de l'ingénierie» comprend trois stratégies plus fines dont une consiste à réaliser un arbitrage constant entre faire soi-même, voire avoir recours à plus spécialisé que soi, et déléguer à des nonspecialistes ayant une formation de base. Deux déterminants de cette façon de faire (et des résultats obtenus) peuvent être soulignés. D'abord, ce dosage a été possible parce que les deux types de compétences étaient disponibles. Tel que mentionné, depuis vingt ans, les intervenants avaient multiplié les activités de transfert de leur savoir-faire à l'interne et aux firmes de la région ; les formations et outils d'intervention simples ainsi développés ont servi à initier les concepteurs des nouvelles firmes externes. Avec 700 à 1000 concepteurs impliqués, les trois spécialistes ne pouvaient traiter tous les aspects SST et ergonomie. Ce dosage leur a permis de s'investir là où ils avaient le plus de valeur ajoutée et d'influencer les choix de conception même en leur absence. Cependant, l'expertise en prévention et en ergonomie avait jusque là été peu formalisée dans l'entreprise : la culture prédominante en était une de prise en charge par les non-spécialistes. Cela a donné lieu à une programmation de projet supportant mal la multidisciplinarité : seule était prévue la réalisation de revues critiques. Les intervenants ont perdu beaucoup de temps en cours de conception à structurer la coopération avec les concepteurs, du temps qui aurait pu être dédié à des interventions «à valeur ajoutée directe».

4. LES RECOMMANDATIONS FORMULÉES À L'ENTREPRISE

Pour donner les moyens aux spécialistes en prévention et aux ergonomes d'agir plus efficacement dans les projets futurs et dans l'organisation, les recommandations formulées concernent:

- 1) le développement d'une démarche de conception réellement multidisciplinaire;
- 2) la façon de doser expertise et transfert entre les spécialistes en SST et en ergonomie d'une part et les non-spécialistes initiés à ces domaines d'autre part, mais également entre les spécialistes en prévention et les ergonomes;
- 3) l'intégration de la SST et de l'ergonomie quand la conception est réalisée à l'externe; et enfin;
- 4) la façon de structurer l'amélioration continue de la conduite de projet.

5. CONCLUSIONS

Cette étude de cas illustre l'ampleur de la valeur économique ajoutée de l'intégration de l'ergonomie et de la SST en conception. De plus, elle a permis de dégager des principes directeurs généralisables à d'autres situations, capables de soutenir les ergonomes et les spécialistes en prévention dans leurs efforts de structuration d'une stratégie d'intégration de leur discipline respective dans les organisations et les projets.

Ils abordent en effet des questions comme:

- l'importance d'une stratégie offensive consistant à «prendre le train» de tendances convergentes comme celles liées à la performance globale, aux programmes à valeur ajoutée (PVA), au développement durable, à l'ingénierie simultanée et au *Total Quality Management*;
- l'arrimage stratégique à assurer entre les activités en correction et en conception («l'ergonomie de conception» ne peut être pensée en marge, voire en opposition à, «l'ergonomie de correction»);
- la gestion équilibrée des interventions «de premiers soins» et en expertise, y compris entre ergonomes et spécialistes en prévention (un élément important à l'heure où, en France, ergonomes et spécialistes en prévention envisagent une collaboration plus étroite);
- les marges de manœuvre qu'il est possible d'aller chercher en favorisant et en infiltrant les activités de «mémoire de projet»

REFERENCES

1. Daniellou, F., *Ergonomie et démarche de conception dans les industries de processus continu: quelques étapes clé. Le travail humain*, 51, pp. 185-194, 1988
2. Bossard, P., Chanchevrier, C., Leclair, P., *Ingénierie concourante, de la technique au social*, pp. 39-55, Edition Economica, Paris, 1997
3. Lamonde, F., *L'intervention ergonomique, un regard sur la pratique professionnelle*, Les éditions Octarès, Toulouse, 2000
4. Lamonde, F., Beaufort, P., Richard, J.G., *La pratique d'intervention en santé – sécurité et en ergonomie dans des projets de conception. Étude d'un cas de conception d'une usine*, Rapport no. R318, IRSST (www.irsst.qc.ca), Montréal, 2002
5. Maillebouis, M., Vasconcellos, M.D., *Un nouveau regard sur l'action éducative: l'analyse des pratiques professionnelles. Perspectives documentaires en éducation*, 41, pp. 35-67, 1997
6. Schön, D.A., *The reflexive Practitioner: How Professionals Think in Action*, Basic Books, New York, 1983

7. Vinck, D., *Ingénieurs au quotidien, ethnographie de l'activité de conception et d'innovation*, Presses Universitaires de Grenoble, 1999

Reçu janvier, 10 2006

¹Université technique "Gh. Asachi" Iași

**DEZVOLTAREA DURABILA A SISTEMELOR DE PRODUCTIE.
INTEGRAREA ERGONOMIEI SI PREVENTIEI ÎN CADRUL UNUI PROIECT DE
CONCEPTIE A UNEI TURNATORII DE ALUMINIU**

REZUMAT: Acest studiu a fost realizat în vederea reconstituirii activitatii unui specialist în ergonomie care, împreună cu specialiști în prevenire, a conceput un sistem original pentru integrarea ergonomiei, securitatii și sanatații în munca în cadrul unui proiect de construcție a unei turnatorii de aluminiu. Strategiile de intervenție identificate au permis specialistilor să influențeze concepția locurilor de munca, să elimine un număr important de riscuri la sursă și să conceapă un program de prevenire înainte de demararea investiției.

APPLICATION OF THE RULE OF MIXTURE, PARALLEL TENSILE TEST AND IMAGE ANALYSIS METHOD FOR DETERMINATION OF THE WELD METAL PROPERTIES IN THE CASE OF TAILOR WELDED BLANKS

BY

G.BRABIE¹, B. CHIRITA¹, C. CHIRILA¹

ABSTRACT: *The quality of a weld in the tailor welded blank is very important for the success of the forming operation. The mechanical properties of the weld metal can be determined by applying different methods, such as: parallel test, normal test, microhardness test etc. The present paper investigates the mechanical properties of the weld metal in a tailor welded sheet made by joining similar metals. The investigation was performed by applying the microhardness and parallel tests in conjunction with the rule of mixture. The analysis of the behaviour of tailor welded blanks by examining the strain variation during tensile parallel test of tailor welded sheets applying the image analysis method is also presented in the paper.*

KEYWORDS: *weld metal properties, parallel test, rule of mixture, image analysis, strain distribution*

1. INTRODUCTION

A tailor welded blank consists of two or more sheets that are welded together to make a single blank prior to forming (Fig. 1). These sheets can be identical, or they can be of different thickness, mechanical properties, or surface coatings. The blanks are either joined by mash seam welding or by laser beam welding, electron-beam welding, and induction welding.

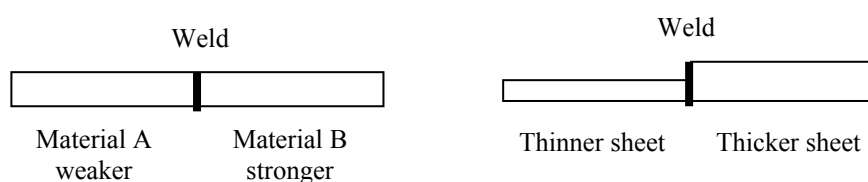


Fig. 1 Tailored blanks

The quality of the weld in the tailor welded blank is very important for the successful of the forming operation. Physical testing of the weld metal is very important to determine the behaviour of the TWB during forming. Generally, for a steel TWB the basic metal has significantly lower yield strength and tensile strength and hence higher ductility than the weld metal.[1], [2] The mechanical properties of the weld metal can be determined by applying different methods, such as: parallel test, normal test, microhardness test etc. The present paper investigates the mechanical properties of the weld metal in a tailor welded sheet by applying the microhardness

and parallel tensile tests in conjunction with the rule of mixture, and by analysing the strain variation during parallel tensile test using the image analysis method

2. DETERMINATION OF WELD METAL PROPERTIES FROM PARALLEL TEST

To extract the weld metal properties, a parallel test can be done in conjunction with the “*rule of mixture*”. According to this rule, the stress-strain tensile test must be performed using specimens cut from basic materials and from TWB. The following relation gives the total load applied on specimen:

$$F = \sigma_1 A_1 + \sigma_2 A_2 + \sigma_w A_w, \quad (1)$$

where: σ_1, σ_2 are the stresses corresponding to the areas of the basic materials; σ_w is the average stress corresponding to the weld area; A_1, A_2 and A_w are the cross section areas of the basic and weld metal, respectively. The longitudinal strains are assumed to be constant across the TWB specimen, so that:

$$\varepsilon_1 = \varepsilon_2 = \varepsilon_w. \quad (2)$$

Based on the Ludwik-Hollomon equation, the relation (1) takes the following form:

$$F = (K_1 \varepsilon_1^{n_1}) A_1 + (K_2 \varepsilon_2^{n_2}) A_2 + \sigma_w A_w. \quad (3)$$

From relation (3) the average stress will result as follows:

$$\sigma_w = \frac{F - (K_1 \varepsilon_1^{n_1}) A_1 - (K_2 \varepsilon_2^{n_2}) A_2}{A_w}. \quad (4)$$

By taking into account the assumption (2), equation (4) can be rewritten as:

$$\sigma_w = \frac{F - (K_1 \varepsilon_w^{n_1}) A_1 - (K_2 \varepsilon_w^{n_2}) A_2}{A_w}, \quad (5)$$

equation that defines the stress-strain relation for the weld metal. In the conditions when the basic materials are the same and the sheets have the same thickness, the following parameters of the materials and sheets will have equal values:

$$K_1 = K_2 = K, n_1 = n_2 = n, A_1 = A_2 = A.$$

Hence, the equation (5) can be rearranged as follows:

$$\sigma_w = \frac{F - 2(K \varepsilon_w^n) A}{A_w} = \frac{F - (K \varepsilon_w^n)(A_t - A_w)}{A_w}, \quad (6)$$

where the cross section area of the basic materials was replaced by $A = (A_t - A_w)/2$. The area A_w of the weld metal cross-section can be obtained using the following methods: the direct measurement of the weld width; the measurement of a metallographic section; the determination of micro hardness profiles. [3], [4]

The parallel test was performed in the frame of laboratories from LMecA – ESIA Annecy, France on an INSTRON-5569 Tensile Testing Machine. Standard specimens were used in the test. The specimens were made from TWBs and obtained by joining the same metals: SPE 220BH and FEPO 5MB. The width of the weld was determined on a microhardness profilometer. The results concerning the weld metal properties obtained from the parallel test were compared with the results obtained from the image analysis.

The obtained results have been presented as follows: Hardness variation on the width of the specimens in Figure 2, Estimated values of A_w area in Table 1, True stress

– strain curves for the weld metals in Figures 3 and 4.

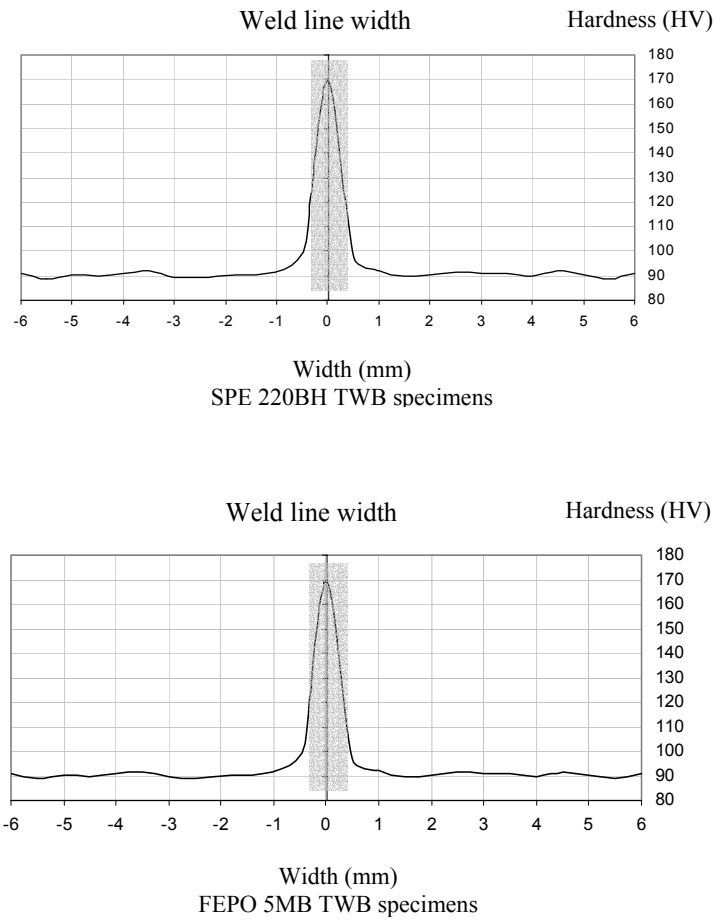


Figure 2 - Hardness variation on the width of the specimens

Table 1. Estimated values of A_w area

TWBs	Sheet thickness (mm)	Width estimating method	Width value (mm)	A_w area (mm)
TWBs made in SPE 220BH steel sheets	0,7	Direct measurement	0,64	0,448
		Hardness measurement		
TWBs made in FEPO 5MB steel sheets	0,75	Direct measurement	0,65	0,4875
		Hardness measurement		

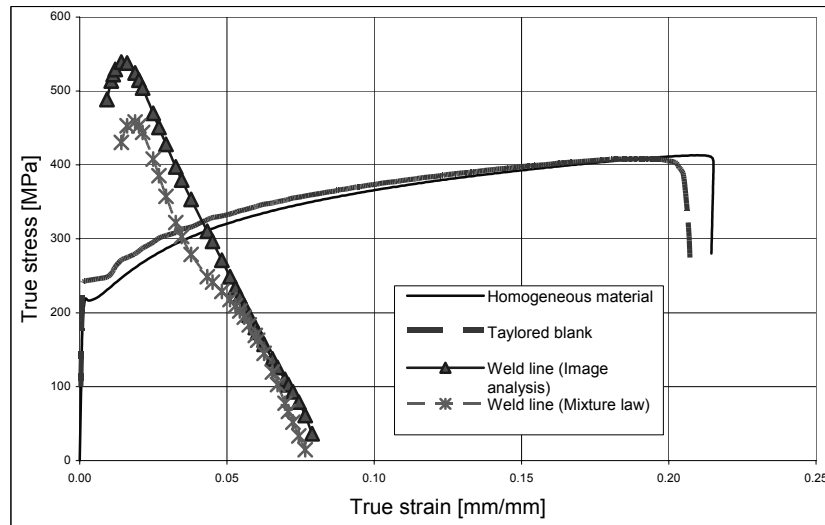


Figure 3 - True stress – strain curves for the weld metal for TWB - SPE 220BH TWB specimens

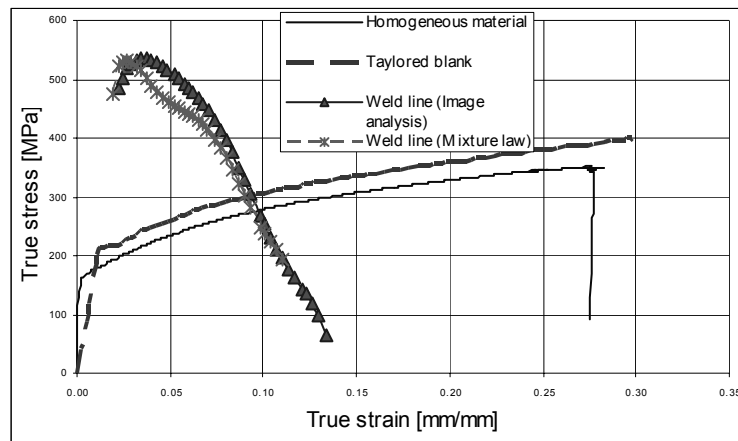
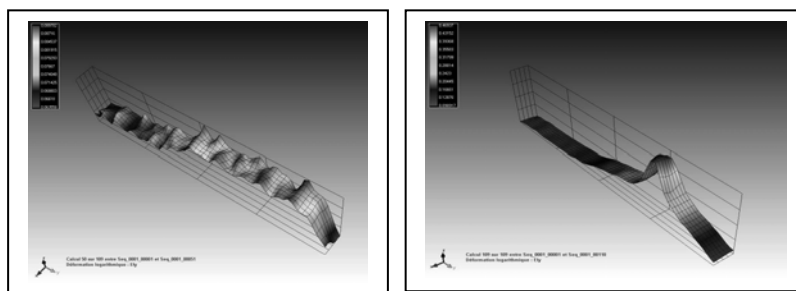


Figure 4 - True stress – strain curves for the weld metal for TWB - FEPO 5MB TWB specimens

3. DETERMINATION OF STRAIN VARIATION DURING THE TENSILE TEST OF TWB SHEETS BY USING THE IMAGE ANALYSIS METHOD

The tests were performed on an INSTRON-5569 Tensile Testing Machine. The parallel tensile test was applied and standard specimens were used. The strain measurement was performed based on the method of image analysis using a Hamamatsu C4742-95 digital video camera. The specimens were prepared using as basic materials in TWB the SPE 220BH steel sheet. Each test was repeated three times in the same experimental conditions and using the same type of specimen. The processing of the experimental results was performed using a SEPT-D LMECA – version 0.5.0.15 software.

The obtained results have been presented as follows: Strain variations in parallel test - from test half stage till fracture - TWB made in SPE 220 BH steel in Figure 5, Parallel tested specimens: zone of necking and fracture in Figure 6.



Strain variation on specimen length

Figure 5 Strain variations in parallel test - from the initial stage of the test till fracture - TWB made in SPE 220 BH steel

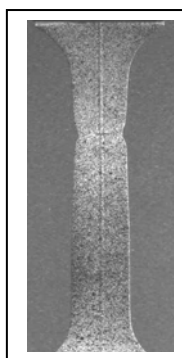


Figure 6 Parallel tested specimens: zone of necking and fracture

4. CONCLUSIONS

Concerning the mechanical properties of weld metal:

In the case of parallel test, for both TWBs, the strains of the weld metal in elastic region could not be determined. For the plastic region both methods – low of mixture and image analysis - lead to approximately the same result.

The tensile strength of the weld metal is 1.6 times bigger than that of the base material in the case of TWBs made in SPE 220BH and 1.3 times bigger in the case of TWBs made in FEPO 5MB.

Concerning the strains distribution:

By analyzing the graphs which represent the strain variation on the basis of the analysis of images (Figure 5), the following aspects were notified:

- the strains variation on the specimen thickness presents a smaller intensity on the weld line in comparison with the matrix one.
- the strains on the specimen length are uniformly distributed on the matrix and weld

metal till necking stage; the fracture will occur first in the weld metal as can be seen in Figure 6.

-the strains on the specimen width are mainly located in the matrix, the weld metal presenting only small strains.

General conclusions:

Basing on the hardness variation at the transverse section of a specimen and on the strain variation at the specimen width, it can be concluded that the analysis of TWB mechanical properties should only take into account the behaviour of base materials and weld materials whereas the heat affected zone (HAZ) does not seem to have any influence.

Based on the uniform strain distribution at the width, thickness and length of a specimen, the assumption that the longitudinal strains are constant across the TWB specimen applied in the rule of mixture can be considered as correct. Hence, we can conclude that for the determination of weld metal properties the application of the parallel test in conjunction with rule of mixture is beneficial for the accuracy of results.

Acknowledgments. This research was performed with the financial support of the European Commission.

REFERENCES:

- [1] Tailor welded blank design and manufacturing manual, <http://www.a-sp.org>
- [2] Annual book of ASTM Standards, 1990
- [3] Lee J.K, Chun B.K. Numerical investigation of TWB forming and springback, Simulation of Mat. Proc. Theory, pp. 729-734, 2001
- [4] Abdullah K., a.o., Tensile testing for weld deformation properties in similar gage TWBs using the rule of mixture, J. of Mat. Proc. Tech., 112 (2001), pp 91-97

Received December, 20 2005

¹*University of Bacau*

**APLICATII ALE METODELOR DE ANALIZA A IMAGINILOR, MIXTURII SI
TENSIUNILOR PARALELE IN DETERMINAREA PROPRIETATILOR METALELOR
SUDATE, IN CAZUL ARBORILOR**

REZUMAT: Calitatea sudurii in cazul arborilor obtinuti prin sudura este foarte importanta pentru succesul operatiei de fabricare a acestora. Proprietatile mecanice ale imbinarilor sudate pot fi determinate prin aplicarea diferitelor metode de incercare, cum ar fi: metoda paralelelor, testul normal, teste de microduritate etc. In lucrarea de fata se investigheaza proprietatile mecanice ale sudurilor prin metode combinate.

SUPERFICIAL HARDENING OF TOOLS THROUGH SUCCESSIVE ALLOYING

BY

ANIȘOARA CORĂBIERU¹, IOAN ALEXANDRU², ȘTEFAN VELICU³, PETRICĂ CORĂBIERU¹, IOAN VRABIE¹, SANDU BUTNARU⁴

ABSTRACT. *Superficial hardening through zonal structural modifications method is formed from two main phases:*

-successive alloying - direct achieved from casting through interaction of the liquid steel with the alloying layers which are deposited on the casting form walls. These alloy layers were obtained using alloying pastes which contain graphite, FeV, FeMo, FeCr, electrolytic Ni, diluent and binders;

-zonal heating process through contact – it is made on a simple installation using treatment cyclograms, which were established before, depending on the material of the tools which are treated, composition and structure of the superficial layers obtained after the first phase .

KEYWORDS: *Successive alloying, zonal heating processes*

1. INTRODUCTION

Superficial hardening through zonal structural modifications is a modern manufacturing method for the achievement of tools with soft and tenacious core and hard superficial layers, which are resistant at all loading.

The thickness of the superficial layer is usual small comparative with the base material which assumes the majority of loading during the tools working. Comparative with the usual versions the tools manufacturing through ASPHZC method assures a substantial reduction of the costs and all special properties of the work surfaces are respected. All this reasons justifies the growth of industry interest for the using of superficial hardened tools like a characteristic of the modern economical development.

The efficiency of tools manufacturing through successive alloying and hardening through subsequent heating treatments of the superficial layers is determined by the knowledge of phenomenons which are during deposition and alloying and using of all technical indications for the achievement of high quality tools. The growth interest of the businessmen from industry for the tools is determined by the economical and technical advantages, which became very important because the working parameters from advanced industries must be improved [2].

The ASPHZC method will be used for the achievement of different types of tools from metallurgy, electrotechnics, manufacturing of machinery, etc. The tools which can be manufactured through ASPHZC method are necessary in any technological process. The manufacturing of high quality tools depends on constructive conception and

material selection. The high developed countries use tools especially in manufacturing of machines for energetic and chemical industries, because it assure materials savings and an increased durability.

2. SUGGESTED TECHNICAL SOLUTION – SUCCESSIVE ALLOYING AND ZONAL HEATING PROCESSING BY CONTACT

The suggested process for manufacturing of tools is new because it is obtained through successive alloying and zonal heating processing by contact [1].

ASPHZC method is formed from two main phases:

- successive alloying - direct achieved from casting through interaction of the liquid steel with the alloying layers, which are deposited on the casting form walls. These alloy layers were obtained using alloying pastes which contain graphite, FeV, FeMo, FeCr, electrolytic Ni, diluent and binders;
- zonal heating process through contact – it is made on a simple installation using treatment cyclograms, before established, depending on the material of the tools which are treated, composition and structure of the superficial layers obtained after the first phase.

2.1. Successive alloying AS

The successive alloying replace the classic version of manufacturing for the tools from alloy steels with a more simplified version like phases and technological operations; it is based on casted steels that are cured in liquid phase through a new method which can be achieved on the installations from firms with metallurgic profile. This method offers the advantage that the steel has a low manufacturing price and the high mechanical-physical characteristics are obtained through the diffusion of the carbide alloy elements (V, W, Cr) from the alloy pastes which are deposited on the cast form cavity surface for the tool. The durability of the tools, which are obtained through ASPHZC, is comparative with the durability obtained through classic versions, respectively from alloy steels through one-piece method.

The science purpose is to obtain tools with a superficial layer which is resistant at composed loading: contact pressure, compression, wear, endurance and heating-mechanical composed alternative shocks.

After ASPHZC process, the low alloy steel obtains mechanical and physical characteristics in the superficial layer like a high - alloy tool steel. The technology of superficial successive alloying in liquid phase consists in the covering of the cast form cavities surface with a paste that is formed from carbide alloy powders, which allows the diffusion of carbide elements in the tools superficial layer through casting [1].

Through this method it will be obtained the microalloying of tools working surface on a superficial layer depth of maximum 5 mm and the keeping of the tool core which is formed from a steel or low alloy steel metallic matrix. The growth of tool-working

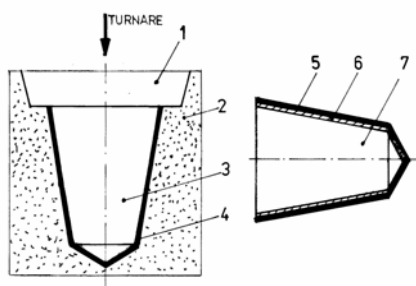


Fig.1 The principle scheme of the AS - superficial successive alloying - direct from the tool casting. 1. Casting feeder cavity; 2. Casting form; 3. Casting form cavity; 4. Alloying paste layer; 5. Successive alloying superficial layer; 6. Transition intermediate layer; 7. Tool core.

zone hardening will make with keeping of a high-tenacity, which represents an accumulator of stresses from manufacturing. The method principle is described in fig.1.

The performances which are obtained through AS are comparative with the results obtained through the casting of high alloy steels

2.2. The zonal heating processing by contact (PHZC)

The zonal heating processing by contact consists in using of Joule-Lenz effect which is produced by continuous or alternative current of 50 Hz frequency through the contact resistance from pressing of a copper electrode roll on the tool surface. The heat quantity is distributed between roll and tool, but the superficial layer absorbs the most important part of heat. In a very short time a volume from the tool superficial layer arrives the austenite range. The current density proportional decreases with the square of distance to the core of processed tool. The heating of tool superficial layer is a gradual heating in spiral and the majority of tools have a cylinder shape or cylinder portions. This method has the following particularities:

- the appearance of a cold superficial layer (fig. 2a);
- the forming of auto-tempered strips in spiral (fig. 2b).

The temperature that must be maintained for the roll and superficial layer is 450°C and so the heat is continuous send to the tool core and roll [3].

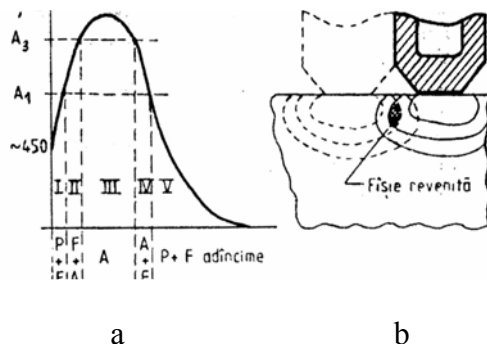


Fig. 2 The temperature variation in the tool superficial layer depth

a – zones which appear in the superficial layer at heating; b – the mode how appear the auto-tempered strips in spiral after cooling.

The temperature in the depth of tool superficial layer varies after a diagram which has five zones: - zone I under-heated (under A_1); - zone II intercritical heated; - zone III: heated over A_3 ; - zone IV intercritical heated; - zone V temperature under A_1 . Because there are these five heating zones the hardened structure is non uniform and it has three distinct portions:

- section I with initial structure (zone I and zone V);
- section II - incomplete hardened (zone II and zone IV);
- section III - complete hardened (zone III).

The existence of zone I represents an advantage because it is avoided the overheating, but it is a disadvantage the necessity of processing for removing of zone I and zone II which are soft.

The auto-tempered strips appear because the roll creates a thermal field which partial overlaps over the already hardened strips. ASPHZC can be used especially for the manufacturing of tools which have cylindrical shapes or cylindrical sections; the results are comparatively with the tools, which are obtained through the classic version: one-piece from high alloy steels.

The method novelty consists in the following aspects:

-in the first phase it is achieved ,direct from casting, the successive alloying (AS) of the tools active superficial layers; the tools superficial layers are enriched with alloy elements Cr, Ni, V, Mo while the carbon content grows until 0,6%;

-in the second phase it is achieved the zonal heating process by contact (PHZC) which consists in two phenomenons:

- the martensite hardening (structural transformation of phase); it is obtained a hard martensite-sorbite structure;
- the forming of the hard chemical compounds in the superficial layer: hard carbides of Cr, Ni, V, Mo (chemical transformations).

3. ANALYSIS OF THE LABORATORY EXPERIMENTS RESULTS

The laboratory experiments which consisted in hardness tests, chemical and metallic analysis were made on 12 samples. The laboratory experiments results are presented in table 1.

Table 1. Laboratory experiments results

Sample notation	Carbon content	Carbon content layer ,%			Core layer HRC	Core hardening HRC	Layer depth mm
		on	1,5 mm depth	2,5 mm depth			
P1	0,2	0,4	0,3	0,25	50	35	2,5
P2	0,2	0,56	0,4	0,3	55	30	3
P3	0,2	0,5	0,4	0,25	50	35	2,5
P4	0,22	0,58	0,45	0,35	55	30	3
P5	0,22	0,6	0,4	0,3	60	30	3
P6	0,22	0,55	0,42	0,25	55	30	2,5
P7	0,25	0,61	0,43	0,32	60	30	3
P8	0,25	0,56	0,38	0,24	50	35	2,5
P9	0,25	0,62	0,45	0,35	60	30	3
P10	0,26	0,61	0,43	0,32	60	30	3
P11	0,26	0,6	0,4	0,33	60	38	3
P12	0,26	0,61	0,43	0,37	60	38	3,5

For the tests achievement were casted in the induction furnace four hotmetal charges from low alloy steel which are presented in table 2

Table 2 Chemical composition

No charge	Mass kg	Chemical composition %								
		C	Mn	Si	P	S	Mo	Cr	Ni	V
1	80	0,2	1	0,17	0,05	0,05	0,1	0,4	0,2	0,2
2	80	0,22	1,4	0,2	0,04	0,04	0,1	0,3	0,3	0,2
3	80	0,25	1,2	0,2	0,04	0,04	0,05	0,2	0,2	0,1
4	80	0,26	1,3	0,17	0,04	0,04	0,05	0,2	0,3	0,2

Examples of micro-structural observations of some test samples are presented in fig. 3÷5.

Sample 1 – charge no.1- carbon from core: 0,2%; - carbon from superficial layer: 0,4%; - carbon at depth of 1,5 mm: 0,3%; - carbon at depth of 2,5mm: 0,25%; - superficial layer depth: 2,5mm; - layer

hardening: 50 HRC; - core hardening: 35 HRC; - geometrical configuration: $\varnothing 50\text{mm}$; - L= 200mm; - casting version:I; - paste type: A; - PHZC

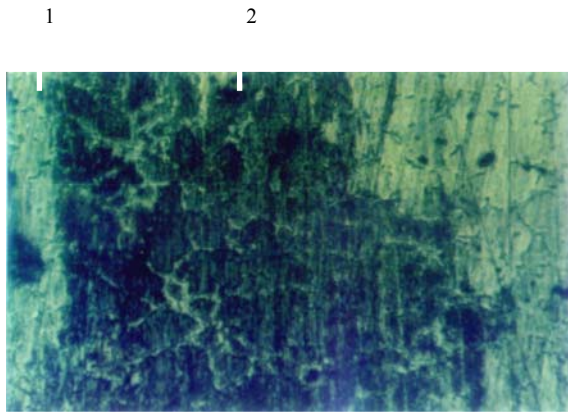


Fig. 3. Sample 1 micrograph from charge 1, paste A, version 1 PHZC. 1- superficial layer (martensite structure with complex carbides, acicular cementite);2- transition zone (transition sorbite-pearlite structure); 3 – core (gross ferrite+pearlite).

version: 1;

- structure: nital 2,5% attack, 100:1

Sample 2 – charge no.1- carbon from core: 0,2%; - carbon from superficial layer: 0,56%; - carbon at depth of 1,5 mm: 0,4%; - carbon at depth of 2,5mm: 0,35%; - superficial layer depth: 3mm; - layer hardening: 55 HRC; - core hardening: 30 HRC; - geometrical configuration: $\varnothing 50\text{mm}$; - L= 200mm; - casting version:I; - paste type: A; - PHZC version: 1; - structure: nital 2,5% attack, 100:1

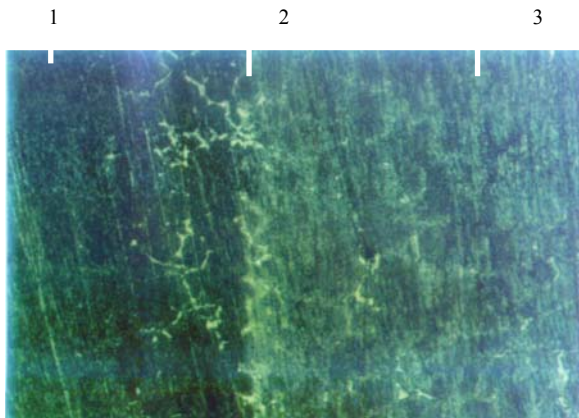


Fig. 4. Sample 2 micrograph from charge 1, paste A, version 1 PHZC. 1-superficial layer (martensite structure with complex carbides, acicular cementite); homogeneous layer with adequate depth; 2- transition zone (transition sorbite-pearlite structure); 3 – core (gross ferrite+pearlite).

Sample 3 – charge no.1- carbon from core: 0,2%; - carbon from superficial layer: 0,5%; - carbon at depth of 1,5 mm: 0,4%; - carbon at depth of 2,5mm: 0,25%; - superficial layer depth: 2,5mm; - layer hardening: 50 HRC; - core hardening: 35 HRC; - geometrical configuration: $\varnothing 50\text{mm}$; - L= 200mm; - casting version:I; - paste type: A; - PHZC version: 1; - structure: nital 2,5% attack, 100:1

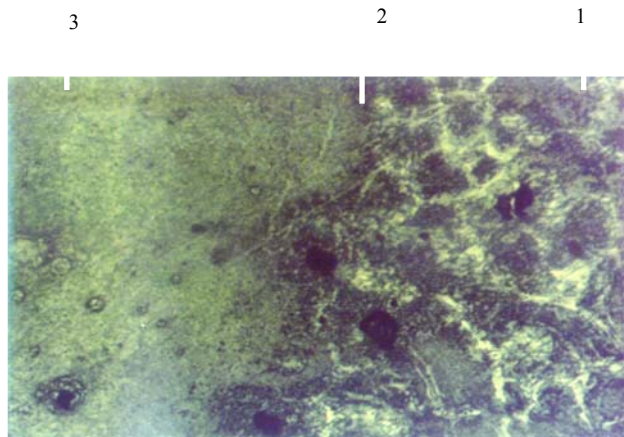


Fig. 6. Sample 4 micrograph from charge 2, paste A, version 1 PHZC.1- superficial layer (martensite structure with complex carbides, acicular cementite); homogeneous and dense layer with penetration on depth;2-transition zone (transition sorbite-pearlite structure); 3 – core (gross ferrite + crowds of zonal pearlite).

4. CONCLUSIONS

- The sample were casted in three casting versions: Version I – forms with semicircular transversal section; Version II – forms with semicircular core; Version III – forms with type I core;
- PHZC were executed on a PHZC installation and it were used two versions:
Version PHZC 1: - process temperature = 850° C; - heating speed = 250 ° C/s; - I = 600A/mm; - $D_1 = 90A/cm^2$; - maintenance temperature = 450° C;
Version PHZC 2 : - process temperature = 900° C; - heating speed = 300 ° C/s; - I = 700A/mm; - $D_1 = 100A/cm^2$; - maintenance temperature = 450° C;
- After experiments it were obtained the following optimal values for every technological parameter: Carbon content in core: minim 0,2%; maximal 0,26%; Carbon content in superficial layer: minim 0,4%; maximal 0,62%; Carbon content at 1,5mm depth: minim 0,3%; maximal 0,45%; Carbon content at 2,5mm depth: minim 0,25%; maximal 0,37%; Superficial layer hardening: minim 50 HRC; maximal 60 HRC; Core hardening: minim 30HRC; maximal 38 HRC; Superficial layer depth: minim 2,5mm; maximal 3,5mm; Casting temperature: minim 1150° C; maximal 1600° C; Temperature in superficial layer during PHZC process: minim 850° C; maximal 900° C; Heating speed during PHZC process: minim 250° C/s; maximal 300° C/s; Electric current intensity/roll breadth during PHZC process: minim 600A/mm; maximal 700A/mm; Current density in superficial layer during PHZC process: minim 90A/cm²; maximal 100A/cm²; Layer heating depth: minim 4mm; maximal 5mm; Maintenance temperature of superficial layer during PHZC process: 450° C.
- The best results for the technological parameters were obtained when it were used the following: casting version no.II – forms with semicircular cores; casting version no. III – forms with type I cores; C paste type : graphite + FeV + FeMo + FeCr + electrolytic Ni; PHZC version no.2

REFERENCES

- 1) P.Corăbieru, A.Corăbieru, I.Alexandru, I.Vrabie - Buletinul Institutului Politehnic Iași, Tomul LI (LV) Fasc.3 Secția Știința și Ingineria materialelor (2005), p. 83
- 2) D. Bunea., R.Șaban., V.Toma , D.Gheorghe , M. Brânzei – Alegerea și Tratamentele Termice ale Materialelor Metalice – Editura Didactică și Pedagogică R.A. București, (1996), p.213
- 3) A.Corăbieru, P.Corăbieru, I.Vrabie, D.Ciobănică – Revista de Ecologie Industrială nr. III-IV (2004), p. 60

Received december, 20 2005

¹*PRESUM PROIECT Sh. C. Iași, România*

²*Technical University Gh. Asachi, Iași, România*

³*Technical University POLITEHNICA, București, România*

⁴*B.M.T. Sh.C. Iași România*

DURIFICAREA SUPERFICIALĂ A SCULELOR PRIN ALIERI SUCESIVE

REZUMAT. Metoda de durificare superficială a sculelor prin alieri succesive este formată din două faze:

- alieri succesive - realizate direct din turnare prin interacțiunea oțelului lichid cu straturile de aliere depuse pe pereții formei. Straturile de aliere depuse s-au obținut folosindu-se paste de aliere având în compoziție grafit, FeV, FeMo, FeCr, Ni electrolitic, diluant și elemente de liere;
- prelucrarea termică zonală prin contact -se efectuează pe o instalație relativ simplă utilizându-se ciclograme de tratament dinainte stabilite în funcție de materialul sculelor de calibrare și pneumatice tratate și de compoziția și structura straturilor superficiale obținute în urma primei faze.

EXPERIMENTS REGARDING THE CASTING OF BIMETALLIC CYLINDERS WITH SMOOTH BARREL ROLL

BY

PETRICĂ CORĂBIERU¹, CRISTIAN PREDESCU², ANIȘOARA CORĂBIERU¹, SANDU
BUTNARU³

ABSTRACT: *The assembling between the main components (support-barrel roll) was made by indirect casting of a steel joint body between support and barrel-roll. Also we checked technological parameters of casting for the steel joint body.*

The experimental methodology consists in casting of steel bodies which assure the filling of the clearance between support and barrel roll or between support and mould. This clearance is technological made for the joint through diffusion and local welding (the precompression and compression forces created by the steel contraction during crystallization and solidification of the steel joint body between the main components).

The assembly method by indirect casting between support and barrel roll was experimented in three versions.

KEYWORDS: *casting bimetallic cylinders, barrel roll*

1. INTRODUCTION

Assembly process between support and barrel roll by casting must be analysed through the thermal phenomenous which are during the casting of the steel in the clearance between support and barrel roll until the cooling of the whole assembly.

The experiments werw made on samples of support with cylindrical shape with diameters between 30 and 180 mm and on samples of barrel roll which werw forged and casted with diameters between 100 and 300 mm. The samples had the mass between 15-40 Kg and were fabricated from plain carbon steel and low-alloy steel.

The assembling between the main components (support-barrel roll) was made by indirect casting of a steel joint body between support and barrel roll. Also we checked the technological parameters of casting for the steel joint body. The experiments werw made at S.C. FORTUS S.A. IAȘI în the Steel Foundry.

In all experiments we checked the main technological parameters for casting and also we followed same technological aspects regarding the heat change and the interaction between the casted steel and support respective the barrel roll which influenced the joint quality. After the experiments we determined that the following parameters had a small influence on the joint quality: surfaces roughness and the type of antioxygen flux layer from the contact surfaces with liquid steel.

Also it was necessary to check the next parameters: the quantity of steel for washing, the dilatation and contraction coefficients of the steels from assembly

(determined by the cooling conditions and the quantity of casted steel). The researches were made for finding a technology of assembling, in industrial conditions, between support and barrel roll.

2. EXPERIMENTS REGARDING THE ASSEMBLING OF PROFILED SUPPORT AND PROFILED BARREL ROLL-BY INDIRECT CASTING-VERSION II

At this version the support and barrel roll have longitudinal and cross chanalls. So the contact surfaces between casted joint body and the main components (support and barrel roll) became bigger (about 2 times like version I) and this implies the growing of the precompression force between the main components which result from the contraction of the steel from the casted joint body. The main consequence is the growing of the joint rigidity.

For the experiments it were used supports and barrel rolls fabricated from the following steel marks: OL37, OL60, OLC45, OSC7 and 12MoCr22. It were used three geometrical shapes of the clearance between support and barrel roll and we present in the next figure.

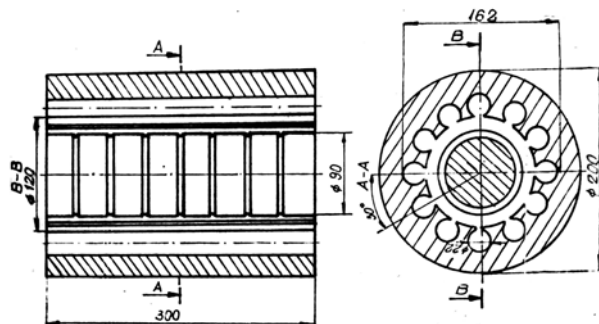


Fig.1 Experimental technological scheme for assembling profiled cylindrical support-profiled barrel roll (the longitudinal chanalls have the same length with the barrel roll lenyht) by casting-version II-1

Table 1 Experimental technological parameters at assembling of profiled support and profiled barrel roll by indirect casting exterior diameters: 100-300 mm.

No	Ratio: barrel roll width /support width	Assembly: barrel roll-support according version			Preheating temperature °C		Casting temperature °C	Ratio: quantity of steel for recirculation/quantity of steel from casted joint body	Observations
		II-1	II-2	II-3	tăblie	Ax			
1	0,25	X			400	300	1550	1	oft-grade assembling
2	0,30		X		450	350	1550	2	oft-grade assembling
3	0,35		X		450	350	1560	2	sufficient assembling
4	0,40		X		450	350	1580	2	sufficient assembling
5	0,45			X	600	500	1570	2	normal assembly
6	0,50			X	600	500	1600	4	normal assembly
7	0,55			X	600	500	1600	3	normal assembly
8	0,60	X			600	500	1600	3	cross cracks on the casted joint body

9	0,65	X			650	550	1600	5	cross cracks on the casted joint body
---	------	---	--	--	-----	-----	------	---	---------------------------------------

According with the results presented in table 1 the best results were obtained in the following conditions:

- the assembling is made with version II-3;
- the ratio barrel roll width/support width has values of $0,45 \div 0,55$;
- the heating temperature of support and barrel roll is between $500 \div 600^{\circ}\text{C}$ (under A_{c1});
- casting temperature of the steel is between $1570 \div 1600^{\circ}\text{C}$;
- the quantity of steel for recirculation is minimum there times bigger like the quantity of steel for casted joint body.

3. EXPERIMENTAL METHOD FOR ASSEMBLING OF SUPPORT-CASTED BARREL ROLL - VERSION III

This version consists in using of a metallic mould where is put and centered the support. The barrel roll is fabricated through the casting of the liquid steel in the clearance between support and mould; the solidification of the steel starts from the mould to the center of support.

During the experiments we followed to find an optimal ratio between casted barrel roll width and support width according to the mechanical stresses of the assembly. We determine the next conclusions:

- for small values of the barrel roll width we obtained low mechanical characteristics of the jointing and when we exceeded the optimal values it were created elongation tensions (fissures at the exterior surface of the barrel roll);
- the admissible deformation of the steel from barrel roll and support must be smaller like the proper deformation from elasticity limit.

The admissible deformation is estimated through the following parameters: elasticity limit, long-time creep strength and fracture strength. The rigidity of the cased assembly is also influenced by the geometrical shape of the support. The correlation between the ratio casted barrel roll width/support width and the metallurgical parameters was experimental determined and this results are presented in table no.2.

Table 2 Technological parameters of the barrel roll/support assemblies with exterior diameter between 100-300 mm.

No.	Ratio: barrel roll width/forging support width	Assembly: barrel roll-support according version			Preheating temperature $^{\circ}\text{C}$	Casting temperature $^{\circ}\text{C}$	Ratio: quantity of steel for recirculation/ quantity of steel from casted joint body	Observations
		III-1	III-2	III-3				
1	0,15			X	200	1520	1	un adequate assembly
2	0,20	X			300	1550	1,5	adequate assembly medium
3	0,25		X		500	1580	2	adequate assembly
4	0,30		X		600	1600	2,5	adequate assembly

5	0,35			X	600	1600	3	adequate assembly
6	0,40	X			600	1600	2,5	un adequate assembly
7	0,45		X		600	1600	3	un adequate assembly

The conclusion is that the best results were obtained in the following conditions:

- ratio between casted barrel roll width and support width must have values of $0,25 \div 0,35$;
- heating temperature of the support: $500 \div 600^{\circ}\text{C}$;
- steel temperature at casting: $1580 \div 1600^{\circ}\text{C}$;
- quantity of steel for recirculation must be twice or more like the quantity of steel for casting of the barrel roll.

The geometrical shapes of the support which was used during the experiments from this version are presented in figure no.2.

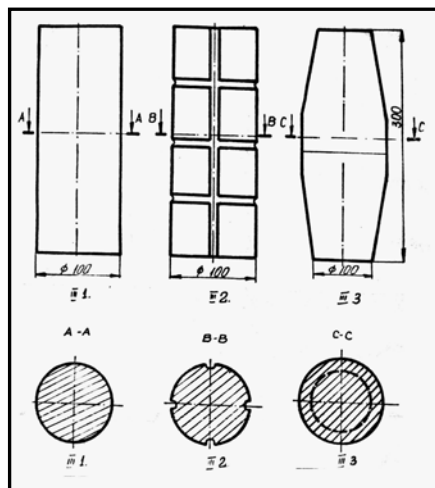


Fig. 2 Geometrical shapes of the supports which were used in support barrel roll assembling: Version III-1 cylindrical support; III-2 cylindrical support with from longitudinal chanalls wich are equidistant disposed; III-3 double taper support

4. METALLOGRAPH RESEARCH OF THE SUPPORT-CASTED BARREL ROLL ASSEMBLIES

The metallograf research meant macrograph and micrograph analysis of support-casted barrel rolls assemblies samples according to three experimental procedures: version I; support-smooth barrel roll; version II: support-casted barrel roll.

In macrographs and micrographs of the samples it were pointed out the dimensions and geometrical shape of the support and the common phases of transition from support-casted body and casted body barrel roll.

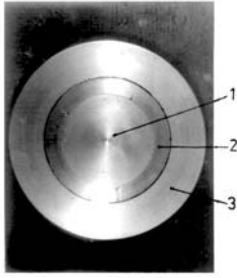


Fig.3 Macrography in cross section of support-smooth barrel roll sample-version I

1- support from rolled hypoeutectoid steel; 2- joint casted body from T20Mn14; 3- barrel roll from rolled alloy steel

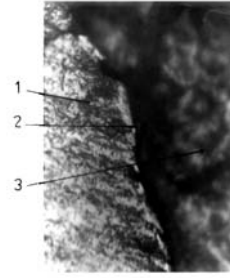


Fig.4 Microstructura of the transition zone support-joint casted body T20Mn14, version I, x400, nital attack 2%

1-support:ferite-pearlite structure of normalizing; 2-transition zone: support joint casted body (oxides layer at common interface); 3- joint casted body-ferite-pearlite structure of casting

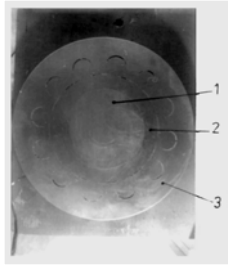


Fig.5 Macrography in cross section $D_{max} = 300$ mm-version II

1- support from rolled hypoeutectoid steel; 2- joint casted body from T20Mn14; 3- profiled barrel roll with axial rolls from rolled alloy steel

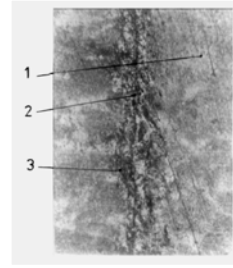


Fig.6 Microstructura of the transition zone support-joint casted body T20Mn14, version II, x200, nital attack 2%

1-support:ferite-pearlite structure of normalizing; 2-transition zone: support joint casted body (slight smelting and pearlite concentration); 3- joint casted body-ferite-pearlite structure of casting

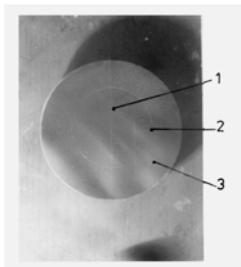


Fig.7 Macrography in cross section $D_{max} = 102$ mm-version III

1- support rolled hypoeutectoid steel; 2- interface; 3- casted barrel roll

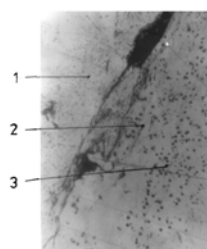


Fig.8 Microstructura of the transition support-casted barrel roll (alloy hypoeutectoid steel) version III, x400, nital attack 2%

1-support:ferite-pearlite structure of normalizing; 2-transition zone support -casted barrel roll (inclusions of pearlite on ferite-pearlite background, oxides in common interface); 3 casted barrel roll

5. CONCLUSIONS

the best experimental results were obtained with version II-3, which assures a good rigidity; it is proposed for experiments in industry;

-version II-2 doesn't assure the elimination of the clearance between support and barrel roll;

-version I-1 doesn't assure a good stability in axial direction and also it is necessary a mechanical work of the topped support;

-version III-3 assures a good axial stability but it doesn't assure a good rigidity; it is difficult the mechanical work and also it is difficult to make a heat treatment because the clamping values (the casted barrel roll contraction on support) are in a restricted interval (0,9÷2,49 mm) which is difficult to control;

-version III-2 assures a good rigidity because the axial and cross contact surfaces have smelting and slight diffusion zones which imply low tangential and radial stresses in barrel roll and it at joint surface; the cross channels from support and barrel roll permit bending stresses of the assembly; it is possible the heat treatment for the assembly and this version is proposed for experiments in industry;

-version III-1 assures a good dimensional stability, but it has the metallurgical problems from version III-3;

-the experimental samples which were obtained at version I had a clearance between barrel roll and casted body and a oxides layer between casted body and support.

REFERENCES

1. Corăbieru Petrică, Corăbieru Anișoara, Curecheriu Petru- Bimetale fabricate prin imersie și centrifugare verticală. Editura Tehnypress, Iași, 2004, ISBN 973-702-048-0.
2. Corăbieru Anișoara, Corăbieru Petrică – Cilindri bimetaliți fabricați prin asamblări ax- tăblie din turnare. Editura Tehnypress, Iași, 2004, ISBN 973-702-020-0.
3. Corăbieru A., Corăbieru P., Vrabie I., Bugeac D.,- Experimentări privind fabricarea cilindrilor bimetaliți prin asamblări ax-tăblie din turnare, Revista de Ecologie industrială, nr. III-IV 2004, pag.46-59, Editor: Oficiul de Informare documentară pentru industrie, cercetare, management, ISSN 1224-3183.
4. Corăbieru P., Alexandru I, Corăbieru A., Alexandru A.- Contribuții privind obținerea și caracterizarea unor asamblări bimetalițe ax- tăblie prin turnare, Conferința națională- Turnătoria, de la rigoarea tehnicii la artă, ARTCAST 2004- ediția a-II-a, Galați 14-15 mai 2004, Editura Academica, pag. 243-250, ISBN 973-8316-43-X.

Received december, 20 2005

¹*PRESUM PROIECT Sh. C. Iași, România*

²*Technical University POLITEHNICA, București, România*

³*FORTUS Sh.C. Iași România*

EXPERIMENTĂRI PRIVIND FABRICAREA CILINDRILOR BIMETALICI PRIN ASAMBLĂRI AX-TĂBLIE DIN TURNARE

REZUMAT. Asamblarea celor două componente de bază (ax-tăblie) s-a făcut prin turnare indirectă (între ax și tăblie) și verificarea parametrilor tehnologici de turnare a unui corp de legătură din oțel. Metodologia experimentală constă în turnarea unor corpuri din oțel care să asigure umplerea interstițiului ax-tăblie și ax-cochiă. Acest interstițiu este tehnologic creat în scopul îmbinării prin difuzie și sudare locală (datorită forțelor de prestângere și strângere create de contracția oțelului în timpul cristalizării și solidificării între componentele de bază ax-tăblie. Metoda de asamblare prin turnare ax-tăblie a fost experimentată în 3 variante.

CO-FeTi COMPOSITE MATERIAL WITH SOFT MAGNETIC PROPERTIES

BY

ELENA DRUGESCU¹, LUCICA BALINT¹, SIMION BALINT¹

ABSTRACT, *This composite material was obtained in the likeness of film through electrochemical deposit, which has a dendritic structure, a perpendicular texture to the electrodeposition plan support. Cobaltul is a chemical element which crystallize in the hexagonal system, what assures to obtain uniaxiale anisotropy in the layer deposited. Thus established alone direction of easy magnetization, comed on the hexagon axis. The experimental researches distinguish the appearance metalografic of dendrites developed perpendicular, to parallel kathode among themselves (photo 1) and magnetic soft property of Co-FeTi films after thermochemical treatment in reducing atmosphere of hydrogen in mixture with the argon to temperature of 200⁰C, 350⁰C, 1050⁰C and 1150⁰C.*

KEY WORDS: *composite, magnetic, induction, coercivity, treatment.*

1. INTRODUCTION

Composite materials consist of a metallic or non-metallic matrix (of organic or inorganic nature) in which case particles or small fibers are dispersed.

The dispersion phase can take place in any aggregation status.

Composite materials can be deposited on metallic or non-metallic substrates through different procedures; after taking away the support, coating with special properties in comparison with the base material are obtained.

This paper presents results obtained through electrochemical deposition of a composite material with superior magnetic properties.

Cobalt was chosen as matrix for the composite material because it has a hexagonal crystallographic structure, with only one direction of light magnetization, which together with a perpendicular dendritic increases on the support, ensures the existence of single axial magnetic anisotropies.

Iron-cobalt alloys near the echiatomic composition are technologically important because of their high saturation magnetization, low magnetocrystalline anisotropy, and associated high permeability. The high saturation values, high curie points, high permeability, and low coercivity obtainable in these materials have made them suitable for transformer core materials requiring high flux densities. High saturation values allow for miniaturization where weight or size savings are important, such as in air electric generators. These alloys are also used for receiver coils, switching and storage cores, high temperature components, as diaphragms in telephone hands because of the high incremental permeability over a wide induction range and to a limited extent for magnetostrictiv transducers for sonar.

The temperature of treatment is analyzing of phase diagrams. Iron and cobalt form a complete series of disordered f.c.c. solid solution γ , at elevated temperatures. At low temperatures the b.c.c. solid solution α , exist above 730°C up to $\sim 75\% \text{Co}$. The α b.c.c. solid solution near equiatomic composition undergo below 730°C an atomic ordering to the CsCl structure tip α_1 , and this order-disorder transformation plays an important role in determining the magnetic properties of these materials. This materials tend to be brittle because of the ordering of a α phase and the presence of trace amounts of carbon, hydrogen and oxygen. Consequently, the magnetic properties attainable are sensitive to heat treatment and purity of the alloys.

Experimental research has shown some magnetic hysteresis curves with very low values for the coercitive magnetic field.

2. EXPERIMENTAL INVESTIGATION

Composite coats were obtained with different thicknesses, on steel tin with surface special prepared for the exfoliation of the coat.

The electrodepositing of cobalt was performed with an electrolyte made of 86 % cobalt sulphate, and 14 % cobalt chloride, with $\text{pH}\sim 5$ and the current density of $100\text{-}650\text{a/m}^2$.

The ferrotitanium powder of dimensions smaller than $10\mu\text{m}$ was introduced in the electrolyte and was stirred during the electro deposition. The deposited material was exfoliated from its substrate and was treated for 30 minutes at 200°C , 1050°C , 1150°C and 350°C , 1050°C , 1150°C , in argon and hydrogen atmosphere.

Many experiments have been conducted and led to the establishing of the optimal parameters for the material to present the requested properties.

3. RESULTS AND DISCUSSION

The quality of the ferrotitanium composite coatings in cobalt matrix was compared to electrodeposited coatings of pure cobalt through macrostructural analysis, the distribution of the disperse phase in cobalt matrix and the magnetic hysteresis curve.

3.1. Microstructural analysis

Through microstructural analysis, the increase of the cobalt crystals was pointed out and dendrites developed parallel with each other and on perpendicular direction of the support (photo 1).

Electrodepositing method, practical on various bases, materials, results in better characteristics than those of components do and shortage materials savings do. The trade of thin layers resulting from electrolysis, their structure and depend on the surface state of basis material, deposition current density, electrolyte's pH, electrolyte's temperature and the stirring, for homogenization of ion concentration in the cathodic film and in the bath solution.

Electrodepositing operational factors have been determined experimentally so to obtain fine grain structure in the deposit layer and, consequently, good mechanical and magnetic characteristics.

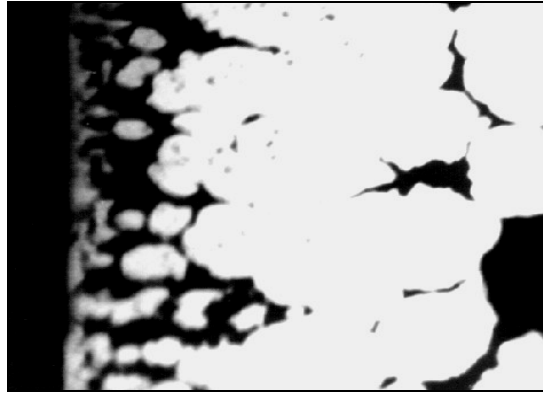


Photo 1. Dendrites developed parallel with each other on perpendicular direction of the support (200x).

3.2. Experimental results and their interpretation

As basis material for electrodepositing were used steel sheet samples, with the chemical composition: 0,05 %C; 0,26 %Mn; 0,02%Si; 0,012 %P; 0,015 %S; 0,039 %Al; and Fe. The layers were obtained consequent to several operations given below, in schemes 1 and 2.

Scheme 1:

Polishing→Washing→Organic solvent degreasing→Washing→Chemical degreasing→Washing→Chemical pickling→Washing→Greasing with oil→Assembling in the electrolyser.

Scheme 2:

Assembling of steel sheets at the cathode→Assembling of graphite anode→Filling of electrolyser with electrolyte→Dosage of ferrotitanium powder in electrolyte→Stirring of bath solution→Electrodepositing→Washing→Loading in the heat treatment furnace

Organic solvent degreasing to dissolve saponifiable and nonsaponifiable fats was made at temperature through immersion in benzene.

Alkali degreasing solution had the following composition: 30-50 g/l Na_2CO_3 ; 5-10 g/l Na_2SiO_3 . The working temperature was 70-80 °C, the holding time about 10 min. hot water washing followed.

Surface pickling is always consequent to degreasing so as to remove oxide layers from metallic surfaces treated with acid solutions, resulting water soluble salts. The composition of chemical pickling solution was 100 ml H_2SO_4 , time 10-30 sec. Flushing and drying followed.

The sheets prepared for electrodeposition were assembled at the cathode of the electrolyser varied between 135 and 615 A/m^2 .

The layers were tested with regard to grain size variation and Vickers microhardness, related to current density increasement, as well as adherence of layers to basis material.

The composite film so obtained was treatments of small and high temperature for analysis magnetic properties.

The treatments were carried out in a tight closed precinct, where a mixture of ases of argon and hydrogen (1/3) was introduced for protection respectively for

reducing the impurities typical of electrodeposition which affect the magnetic properties.

The treatment against fragility eased the detachment of the films from the support material. Treatment parameters are presented in Table 1

The samples microstructures are presented in Photos 2 and 3, following a treatment at 200⁰C respectively 350⁰C, in Photo 4 following a treatment at 1050⁰C and Photo 5 following a treatment at 1500⁰C.

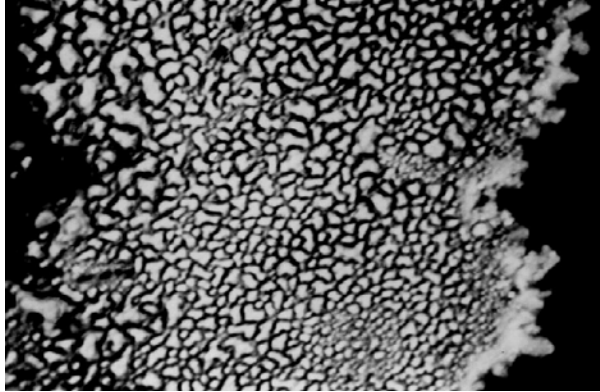


Photo 2. Sample microstructure nr.1, after treatment at 200⁰C (left: support-right: the dendritic crests) (x200).

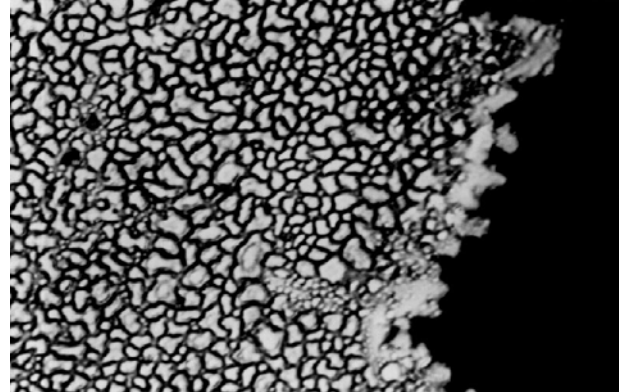


Photo 3. Sample microstructure nr.2, after treatment of 350⁰C temperature, (x200).

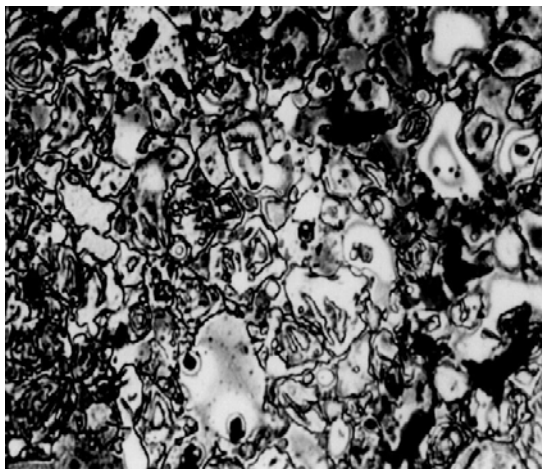


Photo 4. Sample microstructure nr.3, after treatment of 1050⁰C, temperature (x200).



Photo 5. Sample microstructure nr.3, after treatment of 1150⁰C, temperature (x200).

Table 1.

Nr. Sample	Thickness of films [μm]	Treatment	Temperature [°C]	Observations
1	35,5	unbreakable	200	Mat dark gray
2	35,5	unbreakable	350	Mat dark gray
3	35,5	thermal treatment	1050	Silvery white, metallic gloss
4	35,5	thermal treatment	1150	Silvery white, metallic gloss
5	56,9	unbreakable	200	Mat dark gray

6	56,9	unbreakable	350	Mat dark gray
7	56,9	thermal treatment	1050	Silvery white, metallic gloss
8	56,9	thermal treatment	1150	Silvery white, metallic gloss

The samples were subjected to magnetic analysis on a Ferro-tester, for 0.5x120mm. The values that were obtained were introduced in Table 2

Table 2.

Nr. Sample	Temperature [°C]	Surface, [mm ²]	Remanent induction, B _r [T]	Saturation induction, B _s [T]	Coercivity force, H _c [A/m]
1	200	5	-	0,240	12
1	1050	5	0,21	0,480	1736,7
1	1150	5	0,06	0,210	1603,1
2	200	1	0,23	0,600	-
2	1050	1	0,9	2,100	1335,9
2	1150	1	0,75	2,250	1870,3
5	350	5	0,01	0,255	53,4
5	1050	5	0,26	0,645	1603,1
5	1150	5	0,06	0,390	1335,9
6	350	1	0,23	1,200	26,7
6	1050	1	1,13	1,800	2137,5
6	1150	1	0,75	2,400	1870,3

Table 3.

Nr. Sample	Temperature [°C]	Surface, [mm ²]	Remanent induction, B _r [T]	Saturation induction, B _s [T]	Coercivity force, H _c [A/m]
1	200	5	-	0,240	12
1	1050	5	0,21	0,480	1736,7
1	1150	5	0,06	0,210	1603,1
2	200	1	0,23	0,600	-
2	1050	1	0,9	2,100	1335,9
2	1150	1	0,75	2,250	1870,3
5	350	5	0,01	0,255	53,4
5	1050	5	0,26	0,645	1603,1
5	1150	5	0,06	0,390	1335,9
6	350	1	0,23	1,200	26,7
6	1050	1	1,13	1,800	2137,5
6	1150	1	0,75	2,400	1870,3

The results above mentioned, emphasizes the fact that the film's thickness does not influence the magnetic characteristics, but does influence the current density used to obtain the films.

In Figure 1 are presented the variations of the coercitive field with the treatment temperature for samples 1 and 5. It can be seen that the coercitive field reaches a maximum at 1050⁰C, and very low values at 200⁰C for sample 1.

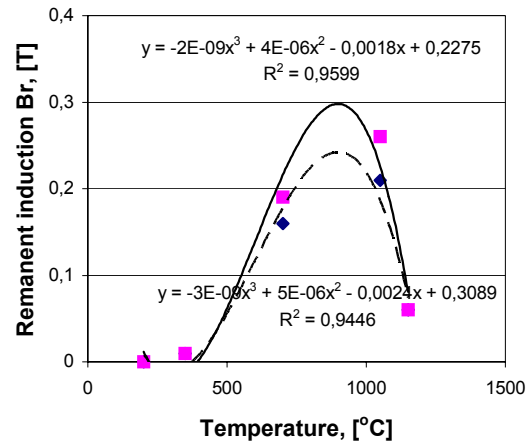


Figure 1. The variation of the coercive field with the treatment temperature

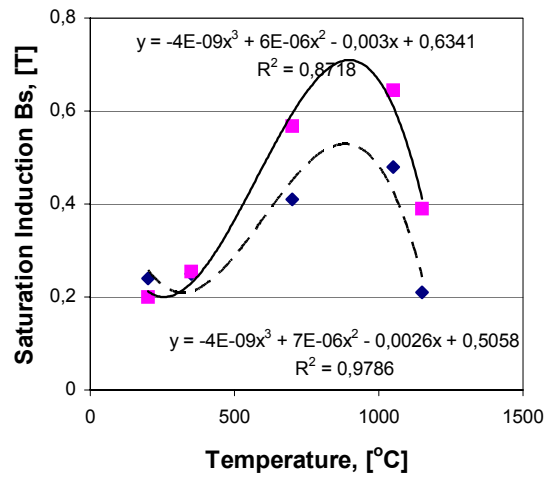


Figure 2. The variation of the remanent induction with the treatment temperature

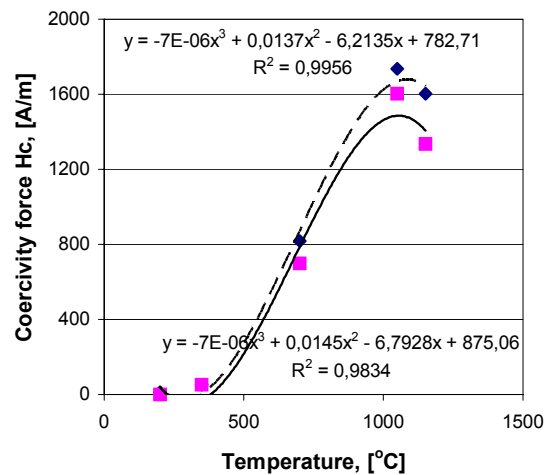


Figure 3. The variation of saturation induction with the treatment temperature

4. CONCLUSIONS

The ferrotitan composite films in cobalt matrix obtained at current densities of 135 and 615 A/m², are very dense, the interdendritic areas disappear almost completely and the surface of the deposition is very smooth, with few singular systems especially when 615A/m² current density is used.

The spread phase which is made of ~1µm ferrotitanium particles is evenly distributed inside the granules as well as on their edges.

The thermal treatment against fragility must be carried out after the electrolysis process, in order to eliminate the specific impurities.

The thermal treatment was carried out in protection atmosphere because of the advanced instability of cobalt in air at temperatures higher than 200⁰C.

After the thermal treatment the samples are silvery gray colored, without any oxides.

After thermal treatment at 1150⁰C the ferrotitanium particles can no longer be distinguished and areas of microdiffusion appear where initially ferrotitanium particles were.

The composite films obtained at a current density of 615 A/m² have better soft magnetic properties than those obtained at 135A/m².

The thermal treatment against fragility at ~200⁰C leads to lower coercitive forces than the one carried out at 350⁰C.

The increase of temperature contributes to the increase of magnetic hardness of the material reaching a maximum at ~1050⁰C

REFERENCES

1. O. Mitoşeriu, E. Drugescu, “*Straturi subţiri de tip compozit cu matrice metalică*”, Simposiom – Academia Română, Bucureşti 1994, vol. Tech. Spec., p. 349-356;
2. G.Y. Chin, J.H. Wernick, *Soft Magnetic Metallic Materials*;
3. F. Potecaşu, E. Drugescu, “*Aspecte structurale ale depunerilor compozite*”, vol. 1, p. 212-215, 1998;
4. I.D.Bursuc, N.D. Suliţanu, “*Proprietăţi magnetice ale straturilor subţiri*”, Editura tehnică, Bucureşti 1991, p. 430-437.
- 5.L. Balint, Drugescu E. s.a., “*Research on the Composite Coats with Uniaxial Magnetic Anisotropy Perpendicular on the Coat Plane*”, Analele Universităţii « Dunărea de Jos » din Galaţi, fascicula IX, 1997.

Received January, 10 2006

¹University “Dunărea de Jos”, Galaţi,

COMPOZIT DE CO-FeTi CU PROPRIETĂŢI MAGNETICE MOI

REZUMAT. Acest compozit a fost obţinut sub formă de pelicule prin depunere electrochimică, rezultând o structură dendritică, texturată perpendicular pe planul suportului electrodepunerii (a catodului). Cobaltul este un element chimic care cristalizează în sistemul hexagonal, ceea ce asigură

obținerea unei anizotropii uniaxiale în stratul depus. Astfel se stabilește singura direcție de magnetizare ușoară, dată de axa hexagonului.

Cercetările experimentale evidențiază aspectul metalografic al dendritelor dezvoltate perpendicular pe catod, paralele între ele (photo 1) și proprietățile magnetice ale peliculei compozitului Co-FeTi tratat termochimic în atmosferă reductoare de hidrogen în amestec cu argon la temperaturi de 200°C, 350°C, 1050°C and 1150°C.

THE CREEP BEHAVIOUR AT 500°C FOR THE STEEL 41MoCr11

BY

DUMITRU MIHAI¹, MIHAI STEFAN¹, GHEORGHE BADARAU¹

ABSTRACT: *The paper shows the determination of the family of creep curves by an original method for the steel 41MoCr11.*

KEYWORDS: *creep behaviour, steel, low alloyed*

1. INTRODUCTION

The use of steels at the construction of some installations from the energetic industry, operated for a long time at high temperatures, imposes the handling of their behaviour in creep conditions. For designing, achieving and operating in safety conditions of such installations there are necessary a great number of experimental tests. A special importance have the long duration mechanical tests, the traction creep testing being the most used. A large spreading have the low alloyed steels, in these steels, Mo and V are being introduced for enhancing the creep behaviour and Cr for enhancing the oxidation resistance.

2. METHODOLOGY FOR ESTABLISHING THE FUNCTION OF A FAMILY OF CREEP CURVES

For describing the evolution in time of the accumulation of plastic deformation at the constant temperature and constant tension it is proposed a function as follows:

$$\varepsilon_{plastic}(t) = Q.t + M(1 - e^{N.t}) \quad (1)$$

in which :

$\varepsilon_{plastic}$ -is the specific plastic deformation;

t - time;

Q,M,N coefficients that depend on material, tension and temperature.

The values of the coefficients Q,M,N can be determined on the basis of experimental results, by applying the method of least squares. For this purpose it was used a calculus program. Making creep test for several initial tensions σ_i (at least four), one can obtain the functions:

$$\varepsilon_{i\,plastic}(t) = Q_i.t + M_i(1 - e^{N_i.t}) \quad (2)$$

In view of establishing a function for th creep family curves one extrapolates the results obtained for the coefficients Q_i, M_i, N_i .

$$\varepsilon_{plastic}(t) = Q.t + M(1 - e^{-N.t})$$

This relation represents the equation of a surface generated by the creep curves at the T temperature. By developing in a MacLaurin series:

$$e^{-N.t} = 1 - \frac{N.t}{1!} + \frac{(N.t)^2}{2!} - \frac{(N.t)^3}{3!} + \dots + \frac{(-1)^n}{n!}(N.t)^n + R_n \quad (3)$$

$$\varepsilon_{plastic}(t) = A_0 + A_1.t + A_2.t^2 + A_3.t^3 + A_4.t^4 + A_5.t^5 + A_6.t^6 + A_7.t^7 \quad (4)$$

The specific plastic deformation can be computed with the relations (1) and (4), from the graphs it results they are convergent.

The determination of the function of the family of creep curves for the steel 41MoCr11 at 500 °C

The chemical composition of the studied steel, determined by the spectral method with a Quantovac type equipment is shown in table 1.

Table 1. The chemical composition of the steel 41MoCr11

41MoCr11	C %	Si %	Mn %	Cr %	Mo %
STAS 791-80	0,38-0,45	0,17-0,37	0,40-0,80	0,90-1,30	0,15-0,25
Sample	0,42	0,36	0,75	1,28	0,21

For determining the mechanical characteristics there have been made traction tests at the temperatures of 20 °C and 500 °C. The tests were made according to the prescriptions from the standards SR EN 10002-1994 for tests at the environment temperature and SR EN 10002-5 - 1995 for high temperature tests. The results are given in table 2.

Table 2 mechanical properties in given testing conditions

Material	Temperature [°C]	R _{p02} [MPa]	R _m [MPa]	A _{11,3} [%]
41MoCr11	20	850	1000	15
	500	625	810	28

For the creep tests there were used samples having the shape and the sizes foreseen in STAS 6596-81 and there were conducted on a MF –300 installation.

The heating of the sample was achieved by using an electric furnace, the temperature being measured with the three thermocouples Pt – PtRh. The maintaining and the regulation of the temperature were done with an electronic regulator that ensures the nominal testing temperature with an accuracy of $\pm 2^{\circ}C$ during thye whole testing period.

The measurement of deformations (elongations) was done with a mechanic extensometer that ensures a precision of 1µm. there were done creep tests at the following tensions 200 MPa, 300 MPa , 350 MPa and 400 Mpa. The results of these tests are shown in figures1,2,3,4. One can see that the creep speed enhances very much at tensions overcoming 400 MPa.

The tests made at the tensions 430 MPa and 500 MPa were done until breaking. The breaking elongations A_n and the creep necking Z , as well as the duration until breaking t_R are given in table 3.

Table 3 the breaking elongation A_n , the creep necking Z and the duration until breaking t_R

Tension [MPa]	T_R [min]	A_n [%]	Z [%]
430	310	28	75
500	29	19	61

The following creep curves were obtained:

- for $\sigma = 200MPa$

$$\varepsilon_{plastic}(t) = \beta(t) = \theta(t) \quad ; \quad \varepsilon_{plastic}(t) = o(t);$$

$$y := \left(\begin{array}{c} \text{ORIGIN} \equiv 1 \\ 0 \\ 0.821 \cdot 10^{-3} \\ 1.087 \cdot 10^{-3} \\ 1.421 \cdot 10^{-3} \\ 1.48 \cdot 10^{-3} \\ 1.521 \cdot 10^{-3} \\ 1.795 \cdot 10^{-3} \\ 1.8125 \cdot 10^{-3} \\ 1.9713 \cdot 10^{-3} \\ 2.0231 \cdot 10^{-3} \\ 2.2415 \cdot 10^{-3} \\ 2.261 \cdot 10^{-3} \\ 2.4265 \cdot 10^{-3} \end{array} \right)$$

$$x := \begin{pmatrix} 0 \\ 0.833 \\ 1.66 \\ 2.5 \\ 3.33 \\ 4.166 \\ 5 \\ 5.83 \\ 6.66 \\ 7.5 \\ 8.33 \\ 9.66 \\ 10 \end{pmatrix}$$

$$n := \text{length}(x)$$

$$m := 7$$

$$i := 1..n$$

$$k := 1..2 \cdot m + 1$$

$$s_k := \sum_i [(x_i)^{k-1}]$$

$$k := 1..m + 1$$

$$b_k := \sum_i y_i \cdot [(x_i)^{k-1}]$$

$$j := 1..m + 1$$

$$i := 1..m + 1$$

$$a_{i,j} := s_{i+j-1}$$

$$c := a^{-1} \cdot b$$

$$c = \begin{pmatrix} 1.987 \times 10^{-6} \\ 1.492 \times 10^{-3} \\ -8.627 \times 10^{-4} \\ 3.287 \times 10^{-4} \\ -7.57 \times 10^{-5} \\ 1.009 \times 10^{-5} \\ -7.084 \times 10^{-7} \\ 2.012 \times 10^{-8} \end{pmatrix}$$

$$w(t) := 2.012 \cdot 10^{-8} \cdot t^7 - 7.084 \cdot 10^{-7} \cdot t^6 + 1.009 \cdot 10^{-5} \cdot t^5 - 7.57 \cdot 10^{-5} \cdot t^4$$

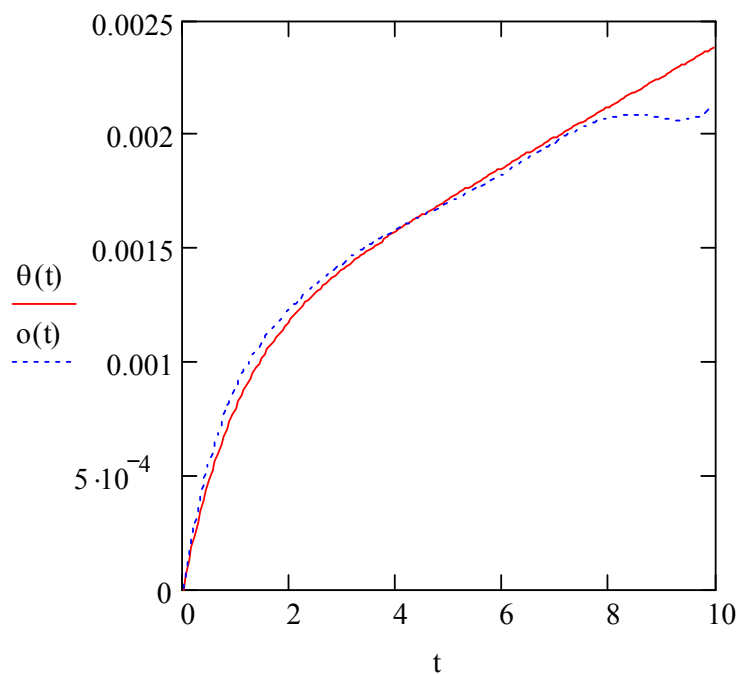
$$n(t) := 3.287 \cdot 10^{-4} \cdot t^3 - 8.627 \cdot 10^{-4} \cdot t^2 + 1.492 \cdot 10^{-3} \cdot t + 1.987 \cdot 10^{-6}$$

$$o(t) := w(t) + n(t)$$

$$t := 0, 0.05467 \dots 10$$

$$\theta(t) := 1.32793903026957 \cdot 10^{-4} \cdot t + 1.06157320381208 \cdot (10^{-3}) (1 - e^{-Ct})$$

$$C := 1.25258096215274$$



- for $\sigma = 300MPa$

$$\varepsilon_{plastic}(t) = \beta(t) = \theta(t) \quad ; \quad \varepsilon_{plastic}(t) = o(t);$$

```
ORIGIN ≡ 1
(
  0
  2.4352 · 10-3
  2.9121 · 10-3
  3.6214 · 10-3
  4.3125 · 10-3
  4.7231 · 10-3
  5.4628 · 10-3
  5.8137 · 10-3
  6.5270 · 10-3
  6.8521 · 10-3
  7.781 · 10-3
  8.1 · 10-3
  8.614 · 10-3
)
y :=

(
  0
  0.833
  1.66
  2.5
  3.33
  4.166
  5
  5.83
  6.66
  7.5
  8.33
  9.66
  10
)
x :=

n := length(x)
```

$$\begin{aligned}
m &:= 7 \\
i &:= 1..n \\
k &:= 1..2 \cdot m + 1 \\
s_k &:= \sum_i [(x_i)^{k-1}] \\
k &:= 1..m + 1 \\
b_k &:= \sum_i y_i \cdot [(x_i)^{k-1}] \\
j &:= 1..m + 1 \\
i &:= 1..m + 1 \\
a_{i,j} &:= s_{i+j-1} \\
c &:= a^{-1} \cdot b \\
c &= \begin{pmatrix} 5.64 \times 10^{-6} \\ 5.515 \times 10^{-3} \\ -4.637 \times 10^{-3} \\ 2.154 \times 10^{-3} \\ -5.309 \times 10^{-4} \\ 7.094 \times 10^{-5} \\ -4.847 \times 10^{-6} \\ 1.325 \times 10^{-7} \end{pmatrix}
\end{aligned}$$

$$w(t) := 1.325 \cdot 10^{-7} \cdot t^7 - 4.847 \cdot 10^{-6} \cdot t^6 + 7.094 \cdot 10^{-5} \cdot t^5 - 5.309 \cdot 10^{-4} \cdot t^4$$

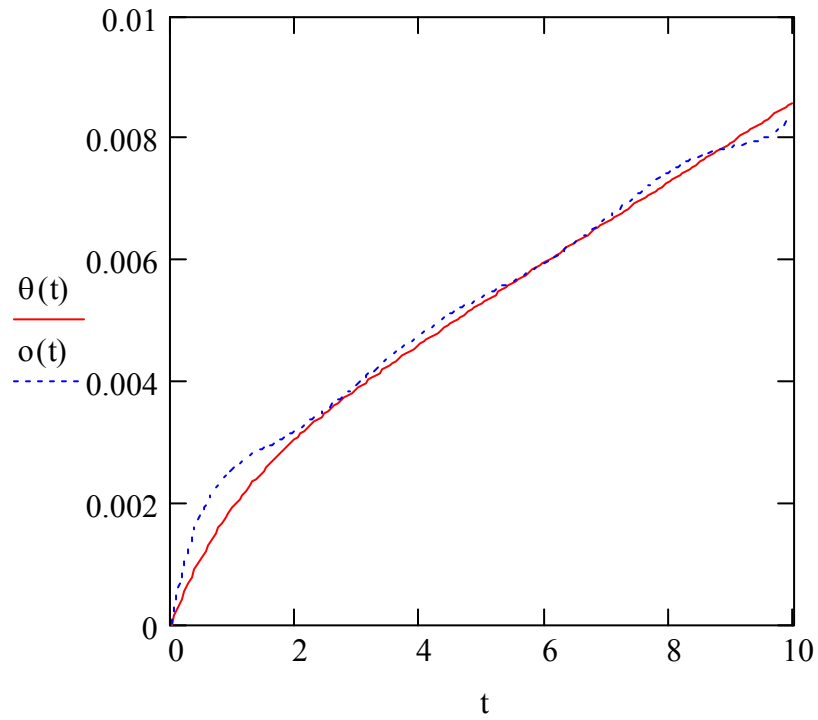
$$n(t) := 2.154 \cdot 10^{-3} \cdot t^3 - 4.637 \cdot 10^{-3} \cdot t^2 + 5.515 \cdot 10^{-3} \cdot t + 5.64 \cdot 10^{-6}$$

$$o(t) := w(t) + n(t)$$

$$t := 0, 0.05467..10$$

$$\theta(t) := 6.5925429177144 \cdot 10^{-4} \cdot t + 2.01360146952748 \cdot (10^{-3}) (1 - e^{-Ct})$$

$$C := 3.06300691220006$$



- for $\sigma = 350MPa$

$$\varepsilon_{plastic}(t) = \beta(t) = \theta(t) \quad ; \quad \varepsilon_{plastic}(t) = o(t);$$

ORIGIN \equiv 1

$$y := \begin{pmatrix} 0 \\ 3.81 \cdot 10^{-3} \\ 4.921 \cdot 10^{-3} \\ 6.413 \cdot 10^{-3} \\ 7.01 \cdot 10^{-3} \\ 7.706 \cdot 10^{-3} \\ 8.820 \cdot 10^{-3} \\ 9.921 \cdot 10^{-3} \\ 10.62 \cdot 10^{-3} \\ 11.35 \cdot 10^{-3} \\ 12.93 \cdot 10^{-3} \\ 13.91 \cdot 10^{-3} \\ 14.851 \cdot 10^{-3} \end{pmatrix}$$

$$x := \begin{pmatrix} 0 \\ 0.833 \\ 1.66 \\ 2.5 \\ 3.33 \\ 4.166 \\ 5 \\ 5.83 \\ 6.66 \\ 7.5 \\ 8.33 \\ 9.66 \\ 10 \end{pmatrix}$$

$$n := \text{length}(x)$$

$$m := 7$$

$$i := 1..n$$

$$\begin{aligned}
 k &:= 1..2 \cdot m + 1 \\
 s_k &:= \sum_i \left[(x_i)^{k-1} \right] \\
 k &:= 1..m + 1 \\
 b_k &:= \sum_i y_i \cdot \left[(x_i)^{k-1} \right] \\
 j &:= 1..m + 1 \\
 i &:= 1..m + 1 \\
 a_{i,j} &:= s_{i+j-1} \\
 c &:= a^{-1} \cdot b \\
 c &= \begin{pmatrix} 1.055 \times 10^{-5} \\ 7.272 \times 10^{-3} \\ -4.662 \times 10^{-3} \\ 1.864 \times 10^{-3} \\ -4.23 \times 10^{-4} \\ 5.428 \times 10^{-5} \\ -3.649 \times 10^{-6} \\ 9.955 \times 10^{-8} \end{pmatrix}
 \end{aligned}$$

$$w(t) := 9.955 \cdot 10^{-8} \cdot t^7 - 3.649 \cdot 10^{-6} \cdot t^6 + 5.428 \cdot 10^{-5} \cdot t^5 - 4.23 \cdot 10^{-4} \cdot t^4$$

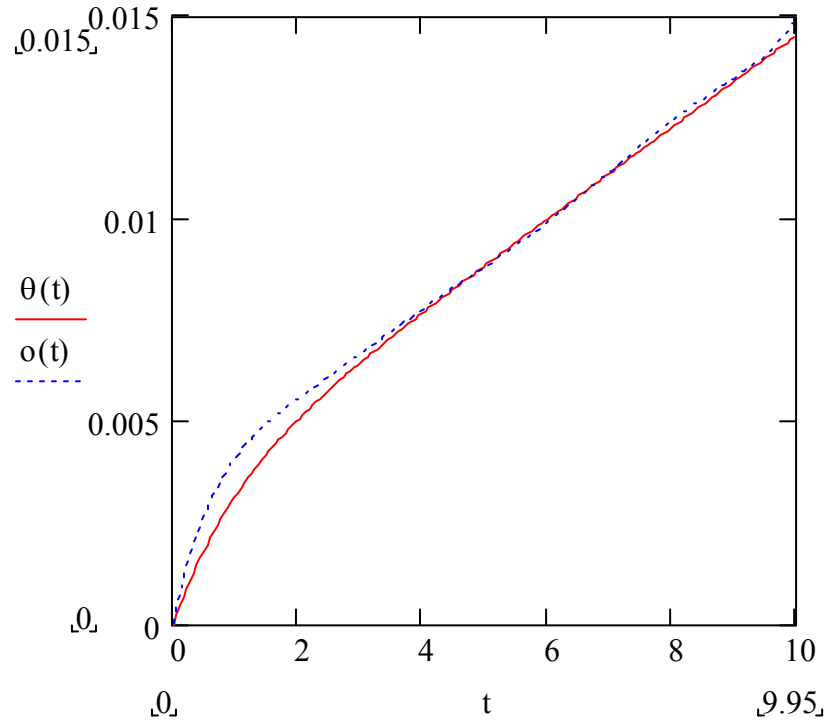
$$n(t) := 1.864 \cdot 10^{-3} \cdot t^3 - 4.662 \cdot 10^{-3} \cdot t^2 + 7.272 \cdot 10^{-3} \cdot t + 1.055 \cdot 10^{-5}$$

$$o(t) := w(t) + n(t)$$

$$t := 0, 0.05467..10$$

$$\theta(t) := 1.13170467981006 \cdot 10^{-3} \cdot t + 3.21400684929937 \cdot (10^{-3}) (1 - e^{-Ct})$$

$$C := 2.62122833108804$$



- for $\sigma = 400MPa$

$$\varepsilon_{plastic}(t) = \beta(t) = \theta(t) \quad ; \quad \varepsilon_{plastic}(t) = o(t);$$

$$y := \begin{pmatrix} \text{ORIGIN} \equiv 1 \\ 0 \\ 5.214 \cdot 10^{-3} \\ 7.041 \cdot 10^{-3} \\ 8.402 \cdot 10^{-3} \\ 9.921 \cdot 10^{-3} \\ 10.625 \cdot 10^{-3} \\ 12.431 \cdot 10^{-3} \\ 13.924 \cdot 10^{-3} \\ 14.921 \cdot 10^{-3} \\ 16.241 \cdot 10^{-3} \\ 17.925 \cdot 10^{-3} \\ 19.423 \cdot 10^{-3} \\ 20.324 \cdot 10^{-3} \end{pmatrix}$$

$$x := \begin{pmatrix} 0 \\ 0.833 \\ 1.66 \\ 2.5 \\ 3.33 \\ 4.166 \\ 5 \\ 5.83 \\ 6.66 \\ 7.5 \\ 8.33 \\ 9.66 \\ 10 \end{pmatrix}$$

$$n := \text{length}(x)$$

$$m := 7$$

$$i := 1..n$$

$$k := 1..2 \cdot m + 1$$

$$s_k := \sum_i [(x_i)^{k-1}]$$

$$k := 1..m + 1$$

$$b_k := \sum_i y_i \cdot [(x_i)^{k-1}]$$

$$j := 1..m + 1$$

$$i := 1..m + 1$$

$$a_{i,j} := s_{i+j-1}$$

$$c := a^{-1} \cdot b$$

$$c = \begin{pmatrix} 4.567 \times 10^{-6} \\ 0.01 \\ -6.372 \times 10^{-3} \\ 2.445 \times 10^{-3} \\ -5.267 \times 10^{-4} \\ 6.426 \times 10^{-5} \\ -4.136 \times 10^{-6} \\ 1.088 \times 10^{-7} \end{pmatrix}$$

$$w(t) := 1.088 \cdot 10^{-7} \cdot t^7 - 4.136 \cdot 10^{-6} \cdot t^6 + 6.426 \cdot 10^{-5} \cdot t^5 - 5.267 \cdot 10^{-4} \cdot t^4$$

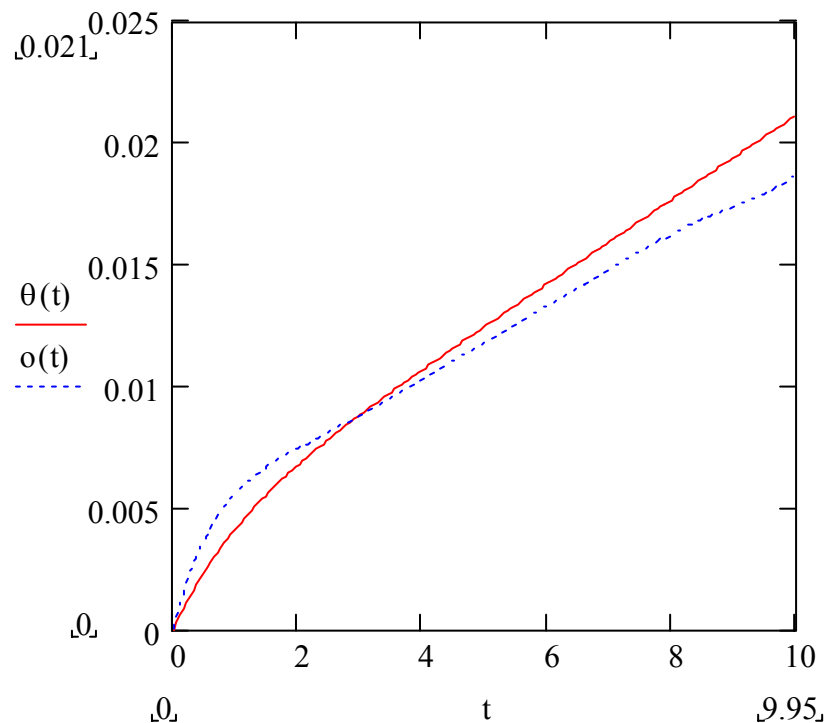
$$n(t) := 2.445 \cdot 10^{-3} \cdot t^3 - 6.372 \cdot 10^{-3} \cdot t^2 + 0.01 \cdot t + 4.567 \cdot 10^{-6}$$

$$o(t) := w(t) + n(t)$$

$$t := 0, 0.05467.. 10$$

$$\theta(t) := 1.73580760087601 \cdot 10^{-3} \cdot t + 3.81593841256878 \cdot (10^{-3})(1 - e^{-Ct})$$

$$C := 5.46247097039668$$



3. CONCLUSIONS

The methodology shown is especially useful for establishing a function of the family of creep curves at a certain temperature, by making a restrained number of tests.

Having in view the lack of experimental data referring to the creep behaviour of the

mild alloyed steels it is necessary to extend it to other steel brands and temperatures recommended for thermal power plants.

REFERENCES

1. Constantinescu, A., Rotenstein, B., Lascu-Simion, N., Fluajul metalelor, Editura Tehnica, Bucuresti, 1970
2. Mocanu, D.R., s.a., Incercarea materialelor, vol.1, Editura tehnica, Bucuresti, 1982
3. Vernon, J., testing of materials, McMillan, London, 1992
4. Mihai, D., Influence of the exposure temperature and time on some pipe steels used for live stream transport, European Journal of Mechanical and Environmental Engineering, vol. 46, nr.3, 2001, p185, Bruxelles, Belgia
5. Mihai, D., Fiabilitatea conductelor din otel 15123, utilizate la transportul aburului viu in termocentrale, Cercetari metalurgice si de noi materiale, vol. IX, nr.3, 2001.

Received January, 2006

*¹Faculty of Materials Science and Engineering,
Technical University "Gh.Asachi" Iasi*

COMPORTAREA LA FLUAJ LA 500 °C A OTELULUI 41MOCR11

REZUMAT Lucrarea prezinta determinarea familiei curbelor de fluaj aentru otelul 41MoCr11 printr-o metoda originala.

EXPERIMENTAL PROGRAMMING IN MATERIALS SCIENCE

BY

PETRICĂ VIZUREANU¹

***ABSTRACT.** The main stage in solving an optimization problem is finding the performance function (the target function) of the analyzed process. In most of the real problems the process's efficiency is appreciated not through an indicator but through more. In this situation it is necessary to peak one of this indicators, the most complete or the most representative and finally check the way in which the optimum solution corresponds from the other indicators point of view.*

***KEYWORDS:** materials science, computer, experimental programming*

1. INTRODUCTION

In all technical and economical fields being familiar with the technological processes and facts of all kind is based on processing and improving the information obtained after performing some tests.

In the context of the contemporary technical and scientific revolution, in which our country is profoundly involved, a special attention is granted to the qualitative increase, the diversification and the improvement of the material production.

The special task that is put in front of our industry in the actual stage can be at a higher qualitative level and entirely solved only through a scientifically approach and an optimum management of the technological processes.

By using science as a productive force, people work is moving towards reasoning and taking decisions, operational work being gradually taken by machineries and automatic equipment.

For reasoning and taking decisions, in the management of a process, science puts at our disposal necessary means as patterns – physical and mathematical – able to reach at any change in the working conditions.

Taking into consideration that researching on physical patterns has important shortcomings, like long standing of researching involving a higher consumption of intellectual activity and the impossibility to cover economical factors, the actual purpose in managing technological processes is the use of the mathematical patterns on a large scale. These patterns reproduce the process studied using some functional

relations and they allow finding most favorable conditions to work duly and spending less money than using physical patterns.

The experiment has always served as a way of knowing the reality, being a good criterion to verify the hypothesis and theories. For a long time, it has been thought that choosing the experiments' strategy and materializing it are determined by the experience and tester's intuition, Mathematics being used only at processing the results.

The rapid growth of experiments research volume has led in the centre of attention the problem of experiments efficient growth. The appearance of electronic computers has allowed the realization of such experimental schemes that contribute to the output's sensitive increase in research

In this content appeared the mathematical theory of the experiment as part of it (within the fragment of it) the experiment's organization. The experiment is programmed according to a determined plan which is perfect from the algorithm's point of view referring to the factor's modification. Realizing the experiment provides a complex influence concerning variable conditions of the researched object.

The variety of the purposes is followed in research; generate a multitude of experimental programs. The mathematical experiments theory places in hand a series of necessary concepts to achieve the research's goals.

Generally, experimental research is realized without a very well determined logic, without programming the laborious experiments and without establishing from the very beginning and with accuracy what there is to do and where to aim it. Many times, those experiment something new. Do so as to obtain what they want and not what they must obtain.

Processing the experimental data trough statistic methods presumes having a very good general knowledge.

The leading process is an informational process based on a methodology that must cover:

- collecting and preparing the information about the state of the object that is managed;
- processing the obtained information to get to the necessary decision;
- sending forth the execution for the leading decisions.

The systems can be studied through different methods. No matter what method is used to the base of these theories stands the "modeling concept".

Modeling is the studying method of the technological processes where the experiment is on a certain object and not on the original.

2. THE STAGES OF SOLVING AND OPTIMISATION OF THE PROBLEM

The main stages that must be followed to solve and optimise a problem are:

1 – By *gathering the information referring to the studied process*, we understand the gathering of statistic data and information that describe the specific process.

2 – *The elaboration of the mathematical model*. The mathematical model of a process defines as being the equation's and inequation's system capable to describe correctly the interdependences between the process's variables.

The mathematical models of the technological processes are of two kinds:

- theoretical models, obtained on the basis of some determined relations between the elements of the process; and on the relations that make the models equations;

- statistical models obtained by the statistic processing of the experimental data.

The elaboration of the mathematical model includes the next principal stages:

- the formulation of the model is made in four stages:
- establishing the model's purpose;
- the determination of the modeled process;
- establishing the process's parameters;
- the determination of the model's necessary type.
- establishing the performance function. The performance function is a unique univocal and objective criterion, through which the efficiency of the technological process is estimate (the economical criterion).
- establishing the equations of the mathematical model is done trough theoretical and empirical methods in other words through verified theoretical methods and completed through empirical methods (statistical and mathematical).

3 – *The examination of the mathematical model*. Verifying the model contains the next stages:

- analyzing the errors on the model's equation;
- simulating the process on a computer;
- trying the model on an "on-line" computer.

4 – *The determination of the optimum solution*. Finding the optimum solution is made through the determination of some values of the independent variables, so that the best value for the performance function is obtained. Through the best value of the performance function it is understood, from case to case, its maximum or minimum value.

5 – *the application of the optimum solution*. Applying the optimum solution consists in exploiting it in normal conditions and observing its behavior in process of the realized optimization.

3. CONCLUSION

The enhancing of the volume of experimental research had brought into attention the problem of enhancing of the experiment efficiency. The introduction of electronic computers enabled the achieving of such schemes of testing to contribute at the sensible growing of the efficiency in research. In this context the mathematical theory of experiment was developed and in it the experiment programming. The experiments are being programmed according a determined plan, previously established, optimum from the point of view of the algorithm of modification of factors, its achievement ensuring a complex influence on the variable state of the researched object.

REFERENCES

1. J. T. Nosek, "The Case for Collaborative Programming," in *Communications of the ACM*, vol. 41 no. 3, 1998, pp. 105-108.
 2. D. O. Case and G. M. Higgins, "How Can We Investigate Citation Behavior? A Study of Reasons for Citing Literature in Communication," *J. American Society for Information Science*, 51(7), pp. 635-645, 2000.
 3. Titu M, Oprean C – "Tehnici si metode in conducerea proceselor tehnologice", Editura Universitatii Lucian Blaga din Sibiu, 2001.
- * * * - "Computer and Information Science Papers CiteSeer Publications Research Index" <http://citeseer.ist.psu.edu/cis>, 2004.

Received January 10, 2006

¹TECHNICAL UNIVERSITY IASI

PROGRAMAREA EXPERIMENTULUI ÎN ȘTIINȚA MATERIALELOR

REZUMAT. Etapa esentiala în rezolvarea unei probleme de optimizare este alegerea functiei de performanta (functia obiectiv) a procesului analizat. În cele mai multe probleme reale, eficienta procesului este apreciata nu printr-un singur indicator, ci prin mai multi. Într-o asemenea situatie este necesar sa se aleaga unii dintre acestia, cel mai complet sau cel mai reprezentativ si sa se verifice în final modul în care solutia optima corespunde din punctul de vedere al celorlalti indicatori.

**SOME ASPECTS REGARDING THE INFLUENCE OF THE
THERMOMAGNETIC TREATMENTS ON THE HARDNESS
NUMBER OF STEELS AND THE SUPERFICIAL LAYERS
NITRIDED EVOLUTION DURING WEAR PROCESS**

BY

PAPADATU CARMEN-PENELOPI¹

***ABSTRACT:** Two types of steels subjected to a nitriding thermo-chemical treatment after thermomagnetic treatments. The structural aspects into superficial layer of these steels are studied during friction process by using of an Amsler machine, taking two sliding degrees, different contact pressures and testing time. I tried to determine the durability of these materials, the surface structure evolution at different tests after thermomagnetic treatments.*

***KEYWORDS:** thermo-magnetic treatments, wear process, durability*

1. Introduction

Overlapping a magnetic field on Conventional heat treatments (the hardening and the recovery processes - the improvement process), the energy of magnetic field interferes in global energy balance of solid stage transformation. This magnetic field changes (thermodynamic changes), the transformations mechanism and cinetics – obtaining the thermomagnetic treatment.

In the end, it can be obtained the change of the mechanical properties and the change of structure configuration for these materials. Interciding with a surface treatment (thermo-chemical treatment) like nitriding with plasma (ionic nitriding), the resistance to wear increase (8) and the resistance to corrosion too.

In this paper, it was made the balance- sheet looking at the advantages/disadvantages between: classic improvement plus ionic nitriding and the improvement in different regimes of magnetic field (continuous or alternative current), different cooling regimes and ionic nitriding.

Until 1932, the martensitic structure of steels – after hardening process, it was considered the principal materials for the magnets (6). Minkievici, Stark and Zaimovski, Erahtin, Komar and Tarasov studied roentgenographic, these alloys.

They demonstrated that, the optimal magnetic properties are a consequence of their variable structure-that appear in the initials processes stages by order.

Because variable structure, the materials has individuals micro-volumes of different phases. Each of these micro-volumes of ferromagnetic phase, has a spontaneous magnetization and a marked magnetic anisotropy (a single axes by light magnetization). These micro-volumes are isolated magnetic layers, un-magnetic layers

or, easily magnetic layers. Result, a big coercitive force which depends by the grain size and the temperature.

For the stable magnetic texture making, are preferred two methods:

- a). The cooling regime in outside magnetic field - thermo-magnetic treatment;
- b). The cooling regime based on overlap to unilateral elastic tensions - Thermo-mechanic treatment.

2. Experimental tests

I considered two few alloy steels, for improvement treatments, useful in metallurgical industry: 42MoCr11 (code V) and, 38MoCrAl09 (code R). These materials are presented in table 1.

Table 1: The chemical composition

Steel grade	C(%)	Mn(%)	Si(%)	P(%)	S(%)	Cr(%)	Cu(%)	Mo(%)	Al(%)
42MoCr11 (code V)	0,38- 0,45	0,60- 0,90	0,17- 0,37	Max. 0,03	0,02- 0,04	0,90- 1,20	Max 0,30	0,15- 0,30	0,02
38MoCrAl09 (code R)	0,35- 0,42	0,30- 0,60	0,20- 0,45	Max. 0,03	0,02- 0,035	1,35- 1,65	Max 0,30	0,15- 0,25	0,70- 1,10

The heat and thermo-chemical treatments applied are:

t_1 = Martensitic hardening process (at 850 °C for code V and 920°C – for code R) and high recovery (at 580°C –for code V and 620°C – for code R)), without magnetic field (classic treatment: $H=0$). $T1 = t_1$ + ionic nitriding (at 530°C);

t_2 = Complete martensitic hardening process in weak alternative magnetic field (cooling in water) and high recovery process (just cooling in water, in strong alternative magnetic field – $H=1300$ A/m). $T2 = t_2$ and ionic nitriding;

t_3 = hardening process (cooling in water, in strong alternative magnetic field) and high recovery process (cooling in water, in strong alternative magnetic field – more then 1300 A/m). $T3 = t_3$ and ionic nitriding;

t_4 = hardening process (cooling in water in strong continuous magnetic field) and high recovery process (cooling in water in strong continuous magnetic field). $T4 = t_4$ and ionic nitriding.

$T_5 = t_1$ + laser nitriding ($t = 5$ ms);

$T_6 = t_1$ + laser nitriding ($t = 5$ ms);

$T_7 = t_4$ + laser nitriding ($t = 5$ ms);

$T_8 = t_3$ + laser nitriding ($t = 5$ ms).

The usual methodology for the machinery parts study (roller wheel) useful in the metallurgical industry, presents the theoretic contact like a point (point contact) or, a line (linear contact).

On Amsler machines (7), I tried to determine the durability of rolls, the surface structure evolution at differents tests. Not must be neglect the other factories which influence the wear process: the geometric forms at contact machinery parts (roll on roll, roll on ring), the technological parameters (the surface quality, the heat treatments,) or, the exploitation conditions (the sollicitation temperature – for example).

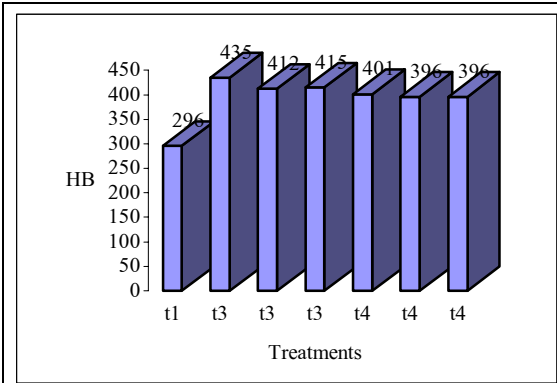


Figure 1: The influence of the magnetic field applied on the hardness number, for code V (42MoCr11)

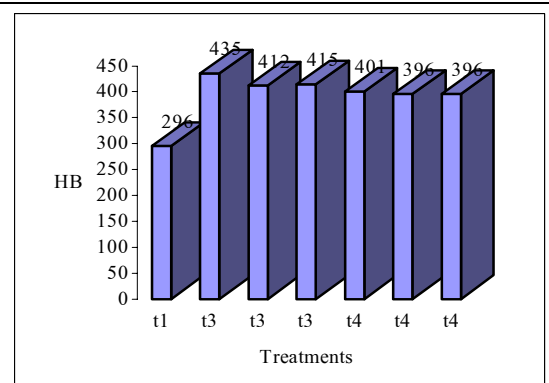


Figure 2: The influence of the magnetic field applied on the hardness number, for code R (38MoCrAl09)

It were submissive at wear process on Amsler machine from University “Dunarea de Jos” of Galati –Romania, rolls with different diameters and, different materials (code V, code R) which suffered different regimes like: $T_1, T_2, T_3, T_4, T_5, T_6, T_7, T_8$. The forces Q_i are variable from a roller to another one, and the wear process period, is variable too.

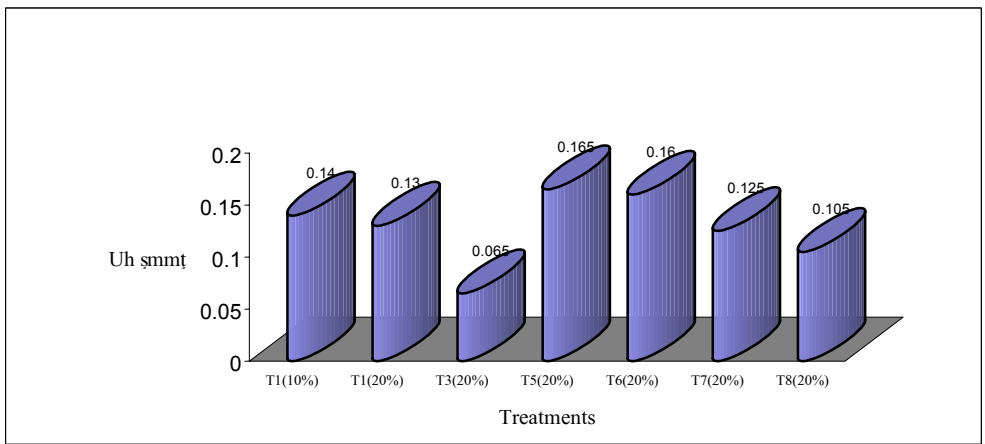


Figure 3: The worn-out layer depth evolution as a function by the treatments applied for 38MoCrAl09 (code R) steel grade

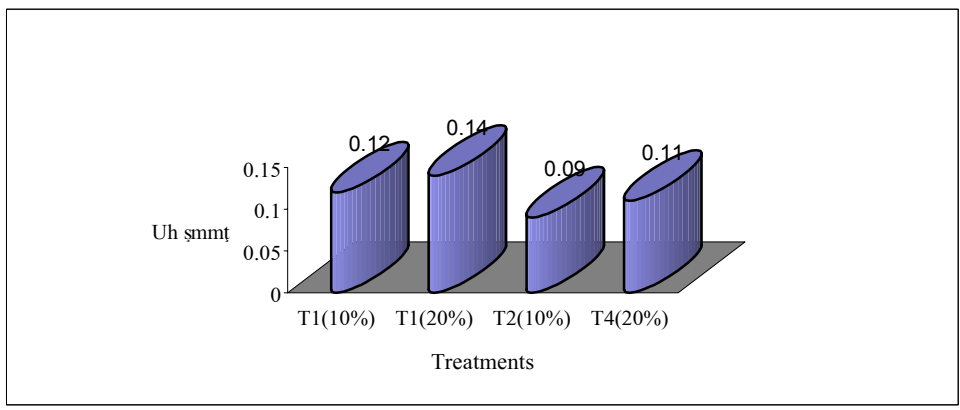


Figure 4: The worn-out layer depth evolution as a function by the treatments applied for 42MoCr11 (code V) steel grade

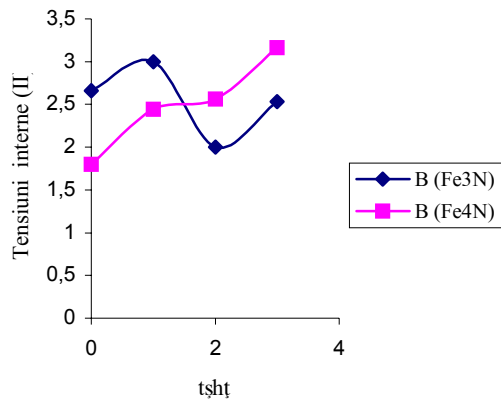


Fig.5 : The evolution of internal tensions (II) function by period, during wear process, for two phases: Fe3N and Fe4N (T1, 75 daN, 10%,Code V)

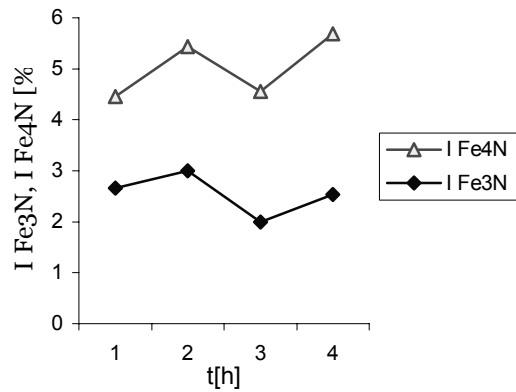


Fig.6: The phases distribution on the depth nitriding layer at different wear process stages (T1, 75 daN, 10%, Code V)

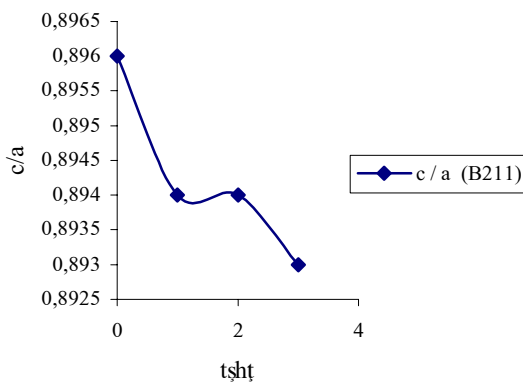


Fig.7: The degree of tetragonality evolution, for martensite phase (T1, 75 daN, 10%, Code V)

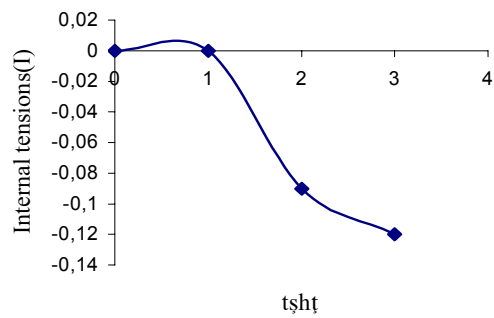


Fig.8: The deviation of diffraction line(220) position (which corresponding to internal tensions I), function by the wear process period (T1, 75 daN, 10%, Code V)

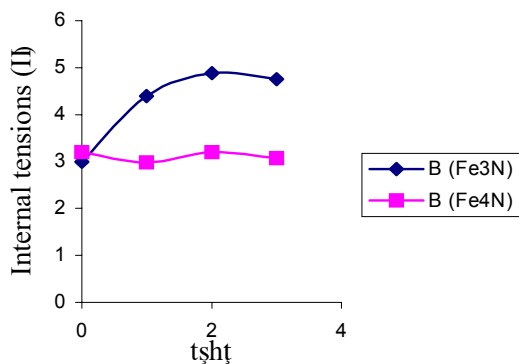


Fig 9: The B(Fe3N) and B (Fe4N) variation function by the wear off length (T1, 75 daN, 10%, Code R)

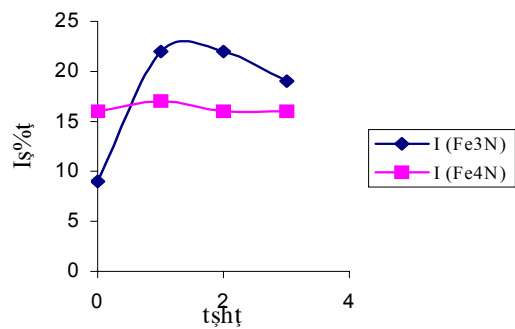


Fig.10: The phases distribution on the depth nitriding layer at different wear process stages (T1, 75 daN, 10%, Code R)

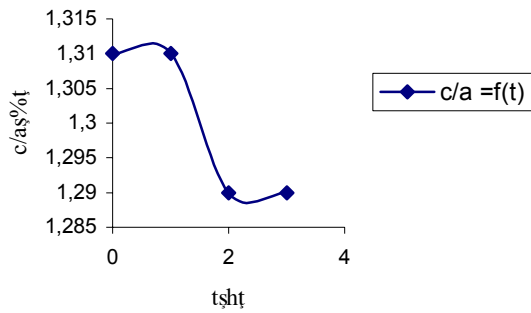


Fig.11: The degree of tetragonality evolution, for martensite phase (T1, 75 daN, 10%, Code R)

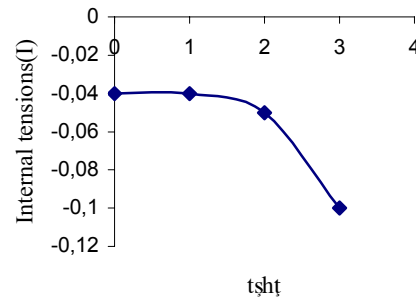


Fig.12: The deviation of diffraction line (211) position (which corresponding to internal tensions I), function by the wear process period (T1, 75 daN, 10%, Code R)

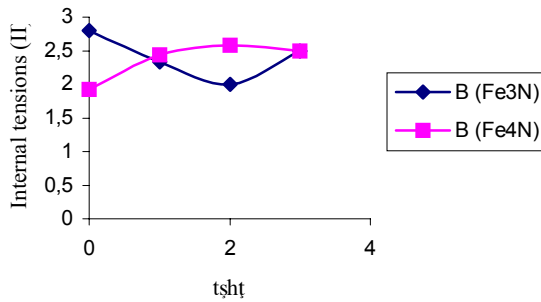


Fig.13: The evolution of internal stress (II) function by wear process period, for Fe3N phase and Fe4N phase (T2, 75 daN, 10%, Code V)

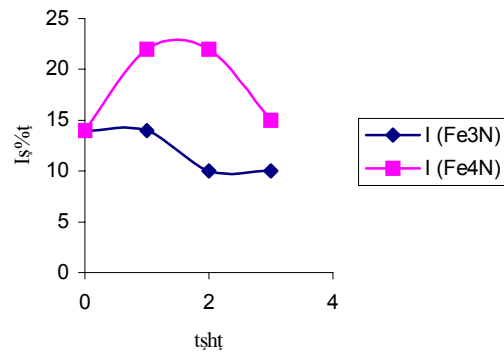


Fig.14: The phases distribution on the depth nitriding layer at different wear process stages (T2, 75 daN, 10%, Code V)

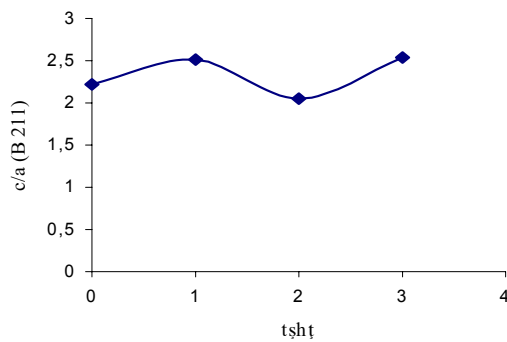


Fig.15: The degree of tetragonality evolution, for martensite phase, during the wear process (T2, 75 daN, 10%, Code V)

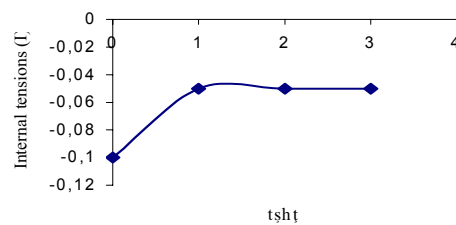


Fig. 16: The deviation of diffraction line (220) position function by the wear process period (T2, 75 daN, 10%, Code V)

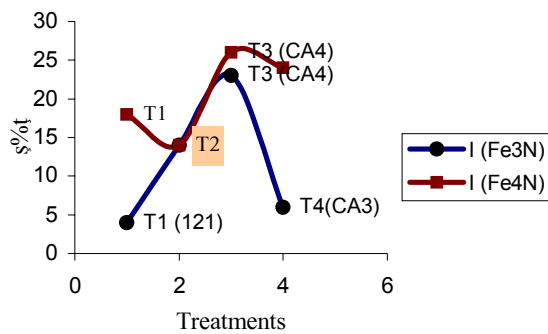


Fig. 17: The phases distribution on the depth nitriding layer function by the treatments applied, before wear tests (code V)

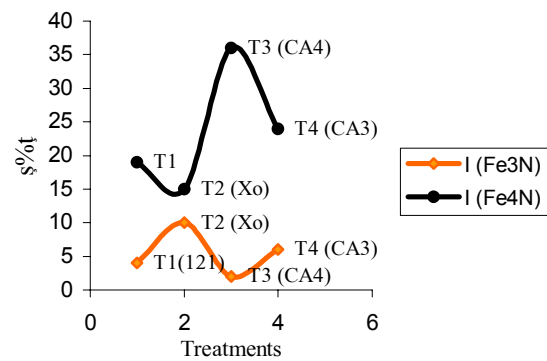


Fig.18: The phases distribution on the depth nitriding layer function by the treatments applied, before wear tests (code R)

3. Conclusions

The worn-out layer depth decrease and the hardness number of steels increase for the thermomagnetic treatments case. This study may be considered like a fundamental research as it shows the necessity to perform typical studies for each kind of material and each kind of thermal or thermochemical treatment applied.

REFERENCES

- (1) Crudu I., Gheorghies C., , *Incerarea materialelor*, Editura Tehnica, Bucuresti; 1986
- (2) Crudu I. s.a., *Structural modification in the superficial layer of the material in wear and fatigue processes* », Nagoya, Japan; 1990,
- (3) Gheorghies C., Crudu I., - *A Cybernetic Structural Model Applied to the Study of Friction Process*”, NORDTRIB 2000, 11-14 IUNIE Porvoo, Finland;
- (4) Gheorghies C., *Modificari structurale in procese de uzura si oboseala*, Ed. Tehnica, Bucuresti
- (5) Drugescu, E.- Teza de Doctorat;
- (6) Vonsovski: *Teoria moderna a magnetismului*, Editura Tehnica, Bucuresti, 1956, pag.311;
- (7) Stefanescu, I., s.a.-”*Organe de masini*”, Indrumar de laborator, Editura Fundatiei Unioversitare “Dunarea de Jos” din Galati, 2002
- (8) Papadatu, C., Stefanescu, I.: -*Experimental study on the behaviour of some non-conventional treated steels during friction process* », Analele Universitatii “Dunarea de Jos” din Galati, Fasc.VIII-Tribology, 2004.
- (9): Papadatu, C.-P., Stefanescu, I. :, An overview of researches regarding the change of mechanical characteristics by thermomagnetic treatment”-ROTRIB2003-Galati;

Received January, 11 2006

¹“Dunarea de Jos”University of Galati

ASPECTE PRIVIND INFLUENTA TRATAMENTELOR TERMOMAGNETICE ASUPRA DURITATII OTELURILOR SI EVOLUTIA STRATURILOR SUPERFICIALE NITRURATE, IN TIMPUL FUNCTIONARII

REZUMAT: Au fost studiate doua oteluri nitrurate (ionic sau , cu laser) dupa aplicarea tratamentului termomagnetic volumic. Aspectele stratului superficial sunt studiate in timpul procesului de uzura prin frecare, acest proces de uzura efectuandu-se pe un stand Amsler, lund in considerare doua grade de alunecare si sarcini de solicitare diferite. S-a incercat sa se determine durabilitatea acestor oteluri, urmarind evolutia straturilor superficiale la diferite solicitari, straturi obtinute prin tratament termochimic aplicat dupa tratament termomagnetic volumic.